Faculty of Aerospace Engineering

Effects of Wind and Trajectory Uncertainty in a 4D Trajectory Management Interface

Bringing 4D Air Traffic Control Closer To Reality

M. M. Ottenhoff

26 February 2020

Delft University of Technology

Challenge the future

Effects of Wind and Trajectory Uncertainty in a 4D Trajectory Management Interface

Bringing 4D Air Traffic Control Closer To Reality

Master of Science Thesis

For obtaining the degree of Master of Science in Aerospace Engineering
at Delft University of Technology

M. M. Ottenhoff

26 February 2020

Faculty of Aerospace Engineering · Delft University of Technology

Delft University of Technology

Delft University Of Technology
Department Of
Control and Simulation

The undersigned hereby certify that they have read and recommend to the Faculty of Aerospace Engineering for acceptance a thesis entitled **"Effects of Wind and Trajectory Uncertainty in a 4D Trajectory Management Interface"** by **M. M. Ottenhoff** in partial fulfillment of the requirements for the degree of **Master of Science**.

Dated: 26 February 2020

Professor: ____________________
prof.dr.ir. M. Mulder

Supervisor: ____________________
dr.ir. C. Borst

Readers: ____________________
dr.ir. O. A. Sharpans'kykh

____
dhr. F. Dijkstra

Preface

Before the reader lies the product used in the assessment of my Master Thesis Project conducted at the faculty of Aerospace Engineering, Delft University of Technology. This project was done in collaboration with LVNL as part of the Centre of Excellence, funded by the Knowledge & Development Centre.

This report is a collection of various documents to be used in the assessment process by my examination committee. It consists of a my Master of Science Thesis paper supported by several appendices and a direct copy of my Preliminary Thesis.

A lengthy road has been followed to come to this final version of the report. When starting this project back in November 2018, I could not have imagined the way the subject grabbed my attention and has essentially been the reason that I will be starting with ATCo training in April this year.

There are several people I would like to thank explicitly. Clark, thank you first and foremost for the willingness to hand me this assignment and the effort you have taken to convince LVNL to step onboard. I have learned a lot from your continuous drive to put theory into a broader perspective and the numerous (often way too long) brainstorms we have had. In this light, I would also like to apologize to Hans for having to endure all these conversations.

Max, I have a lot of respect for the time you make for your students and the sincerity with which you treat each of them, both during and outside office hours. Thank you for all professional, but also personal advice you have given me throughout this project.

Ferdinand, based on the countless conversations and discussions we have had, I cannot stop thinking the LVNL could not operate without you. Your intensely deep and broad knowledge on aviation in general, coupled with your immense drive to improve the entire aviation sector, is inspiring. Thank you for everything during my graduation and in advance for all future conversations as a colleague.

Furthermore, I would like to thank you Rolf, for helping me in deciphering some of the code from the beautiful piece of software you have written. Throughout the programming phase of my thesis, I have learned a lot from the level of professionalism of your code.

Another big thank you goes to fellow students in Sim 0.08. I am grateful for all the feedback you have given me, but mostly for all the fun we have had during my graduation time. I cannot imagine having had to sit in a room alone during my research.

Last but definitely not least, I would like to thank you, Anniek, for your unconditional support during the last 16 months. Your calm and relaxed attitude towards all my issues has helped me to put things into perspective more than often. I can safely say that I could not have achieved the same result without you.

Matthijs

Delft, February 26, 2020

Acronyms

1D	One-Dimensional
2D	Two-Dimensional
3D	Three-Dimensional
4D	Four-Dimensional
AC	Aircraft
ACC	Area Control
ADS-B	Automatic Dependent Surveillance - Broadcast
AH	Abstraction Hierarchy
ALT	Altitude
AMM	Aircraft Motion Model
AOC	Airspace User Operations Centre
APM	Aircraft Performance Model
APP	Approach Control
ATC	Air Traffic Control
ATCo	Air Traffic Controller
ATFCM	Air Traffic Flow and Capacity Management
ATM	Air Traffic Management
BADA	Base of Aircraft Data
BoC	Bottom of Climb
BoD	Bottom of Descent
CAS	Calibrated Airspeed
CD&R	Conflict Detection & Resolution
CDM	Collaborative Decision Making
CONOPS	Concept of Operations
COP	Change-Over Point
CPA	Closest Point of Approach
CPDLC	Controller-Pilot Data Link Communication

CTA	Control Task Analysis
CWA	Cognitive Work Analysis
DAC	Dynamic Airspace Configuration
DCB	Demand & Capacity Balancing
DCT	Direct To Command
DL	Decision Ladder
DST	Decision Support Tool
DTG	Distance To Go
DUT	Delft University of Technology
EID	Ecological Interface Design
ETA	Estimated Time of Arrival
FAA	Federal Aviation Administration
FAF	Final Approach Fix
FCA	Flight Centric ATC
FIR	Flight Information Region
FL	Flight Level
FMS	Flight Management System
FUA	Flexible Use of Airspace
GPU	Graphics Processing Unit
GRIB	GRIdded Binary
GS	Ground Speed
HDG	Heading
HIPS	Hyper Interactive Problem Solver
HIRLAM	High Resolution Limited Area Model
HMI	Human-Machine Interface
IAF	Initial Approach Fix
IAS	Indicated Airspeed
IOP	Interoperability
ISA	International Standard Atmosphere
KBB	Knowledge Based Behavior
KNMI	Royal Netherlands Meteorological Institute
LNAV	Lateral Navigation
LoS	Loss of Separation
LVNL	Air Traffic Control the Netherlands
M	Mach number
MUAC	Maastricht Upper Area Control
NextGen	Next Generation Air Transportation System
NM	Nautical Mile
PCE	Polynomial Chaos Expansions
PHARE	Programme for Harmonised ATM Research
PVD	Plan View Display
PZ	Protected Zone

RBB	Rule Based Behavior
RMS	Root Mean Square
RoC	Rate of Climb
RoC	Rate of Descent
RoCD	Rate of Climb/Descent
RTA	Required Time of Arrival
SA	Situational Awareness
SBB	Skill Based Behavior
SESAR	Single European Sky ATM Research
SPD	Speed
SRK	Skill, Rule and Knowledge
STCA	Short-Term Conflict Alert
STD	Standard Deviation
SWIM	System Wide Information Management
TAS	True Airspeed
TBO	Trajectory Based Operations
TCAS	Traffic Alert and Collision Avoidance System
ToA	Time of Arrival
ToC	Top of Climb
ToD	Top of Descent
TP	Trajectory Prediction
TSD	Time Space Display
TSR	Travel Space Representation
TTC	Time To Conflict
TTG	Time To Go
TWR	Tower Control
VHF	Very High Frequency
VNAV	Vertical Navigation
VSD	Vertical Situation Display
WDA	Work Domain Analysis
WPT	Waypoint

List of Symbols

Greek Symbols

δ	Wind correction angle
ϵ	Relative wind angle
θ	Rotation angle
λ	Longitude
λ_0	Central longitude
$\vec{\mu}$	Combined mean
$\bar{\sigma}_c$	Saturated cross-track error standard deviation
$\sigma_{v,climb}$	Vertical error standard deviation in climbing segments
$\sigma_{v,desc}$	Vertical error standard deviation in descending segments
σ_a^2	Along-track error variance
σ_c^2	Cross-track error variance
$\bar{\sigma}_c^2$	Saturated cross-track error variance
$\sigma_{v,climb}^2$	Vertical error variance in climbing segments
$\sigma_{v,desc}^2$	Vertical error variance in descending segments
ϕ	Latitude
ϕ_1	Central latitude

Roman Symbols

A	Fixed pressure
B	Fixed fraction of surface pressure

C	Measure of criticality
$\vec{d}$	Relative predicted position
g	Gravitational acceleration
k	Projection scale factor
n	Pressure layer level
P	Pressure
PC	Instantaneous probability of conflict
P_s	Surface pressure
$\vec{p}$	Nominal position
Q	Combined covariance matrix
R	Universal gas constant
R_{rot}	Rotation matrix
R_e	Earth radius
r_a	Along-track error growth rate
r_c	Cross-track error growth rate
$r_{v,climb}$	Vertical error growth rate for climbing segments
$r_{v,desc}$	Vertical error growth rate for descending segments
s	Distance
T	Temperature
T_{tot}	Time horizon
t	Time
V	Covariance matrix
$\bar{V}$	Covariance matrix in body coordinate frame
V_{GS}	Ground speed
V_{TAS}	True airspeed
V_{Wind}	Wind speed
x	Sector x coordinate
$\vec{x}$	Predicted position
y	Sector y coordinate
z	Height above surface

List of Figures

List of Tables

Contents

Part I

Master of Science Thesis Paper

Adapting the Solution Space Concept for Air Traffic Control: Effects of Wind and Trajectory Uncertainty

M. M. Ottenhoff (MSc Student)
Supervisors: prof. dr. ir. M. Mulder, dr. ir. C. Borst, dhr. F. Dijkstra
Section Control & Simulation, Department Control and Operations, Faculty of Aerospace Engineering,
Delft University of Technology, Delft, The Netherlands

***Abstract*—As a result of the current evolution in the ATM system, a fundamental shift in the ATC work domain is foreseen from *ad-hoc* tactical to more strategic, 4D (i.e., space and time) trajectory management. Both the SESAR programme in Europe and the NextGen programme in the US envision a central role for the human operator, to be aided by high-level automated decision support tools. In an attempt to prototype such support tools, a 4D trajectory management interface was previously designed and experimentally validated. To improve on the maturity of this concept, effects of wind and trajectory uncertainty were integrated into the interface in this present work. Using six professional controllers, the redesigned interface was evaluated in a realistic 4D inbound traffic peak scenario within the Dutch airspace, where small control spaces require a mixed tactical-strategic form of ATC. Results indicated that operators were able to successfully combine conflict and arrival time management in a highly complex traffic scenario despite the added display complexity, although further research will be needed to confirm these findings in a statistically relevant context.**

***Index Terms*—Air Traffic Management, 4D Trajectory Management, Air Traffic Control, Trajectory Uncertainty, Wind, Interface Design, Ecological Interface Design, Decision Support Tool.**

I. INTRODUCTION

WITH global air traffic volumes increasing, the Air Traffic Management (ATM) system is expected to evolve into one with high-accuracy pre-planned Four-Dimensional (4D) aircraft trajectories (i.e., in space and time) [1, 2]. In this new form of Air Traffic Control (ATC), a fundamental shift in the work of the Air Traffic Controller (ATCo) is foreseen from tactical to more strategic tasks, to be supported by advanced automated Decision Support Tools (DSTs) [3].

While considerable research has been devoted to 4D flight planning optimization prior to and during operation, a definite breakdown of the distribution of roles between the ATCo and automation has not yet been well defined. In a system in which the human continues to fulfill a central role, controller acceptance of automated tooling will be of utmost importance with previous efforts not being embraced well by the ATC community [4, 5].

One of the tasks in which the human is expected to remain involved is that of *perturbation management*. Upon flight plan execution, unforeseen airspace perturbations, such as weather, sequencing and changing airspace constraints, will inevitably require aircraft trajectory changes to be made by the ATCo. This mixed tactical-strategic control task will consist of ensuring a safe airspace, while adhering to the strict time constraints imposed by the 4D flight plan, requiring control *predictability* and *flexibility* at the same time. This will increase the complexity of the ATCo work domain, as these constraints (and relations between them) will have to be more strictly adhered to than in the current situation.

A concept 4D Trajectory Management interface, aiming to support control *flexibility*, was designed using the principles of Ecological Interface Design (EID) and initially validated in the Single European Sky ATM Research (SESAR)-funded C-SHARE project [6, 7]. Using the known Required Time of Arrival (RTA) as a fixed constraint, rerouting possibilities are presented to the ATCo, yielding the so-called '*solution space concept*'. The idea behind this approach is to leave the ATCo in direct control of the actions to take, while supporting him or her in the decision-making process.

Control *predictability*, however, is yet to be integrated into this concept. Various essential air traffic and environmental elements, the most noticeable ones being wind and trajectory uncertainty, were not taken into account in previous experiments. Their absence does not only make the current interface less realistic, but also less complex than it would be in real-world operation. Since added interface complexity might result in a loss of overview [8], this forms a drawback to the solution space concept in its current form[1].

In this study, a redesign of the solution space concept is presented, taking into account effects of wind and aircraft trajectory uncertainty. The redesign is evaluated within a realistic inbound traffic peak scenario in the Dutch Flight Information Region (FIR), where a mixed tactical-strategic form of control is necessary due to the small control spaces. Here, the RTA constraints imposed by the 4D flight plans are considered to be crucial for efficient airport planning.

Behind this research lies the question to what extent the seemingly irreconcilable concepts of simultaneous control flexibility and predictability can successfully be combined in an EID-inspired interface, where work-domain constraints are ideally mapped one-to-one onto the resulting display.

Fundamental concepts for the interface redesign are introduced in Section II, the redesign itself is presented in Sections III and IV. The chosen case study to evaluate the redesigned display and the obtained results are presented in Sections V and VI, respectively. This is followed by a discussion in Section VII and conclusions in Section VIII.

[1]As also follows from conversations with Air Traffic Control the Netherlands (LVNL).

II. Theoretical Background

This section presents both theory from previous work as well as necessary assumptions, that together will form the basis for the interface redesign. The inclusion of wind and trajectory uncertainty in the existing interface will increase its complexity, requiring a review of the Concept of Operations (CONOPS) in which the interface will operate. Furthermore, relevant theory on wind and trajectory uncertainty will be reviewed. Lastly, the implications of including the two elements for the human-machine interaction will be discussed.

A. Concept of Operations

To operate a high-accuracy 4D ATM system, shared information management is considered to be crucial. To increase both the reliability and accuracy of the planning process, technology enablers such as System Wide Information Management (SWIM), Collaborative Decision Making (CDM) and improved Flight Management System (FMS) capabilities will minimize uncertainty and allow trajectory updates to be communicated to all relevant stakeholders immediately [9]. To be able to quantify trajectory uncertainty, assumptions will need to be made on the availability of information and the resulting control loop, as discussed in Section II-A1. The gap between these assumptions and the resulting aircraft commands used in the interface's Trajectory Prediction (TP) applications is bridged in Section II-A2.

1) RTA Control Loop: With RTA adherence, some form of closed loop timing control will be needed. Currently, the FMS of most aircraft provide the possibility to fly towards an RTA waypoint. Because wind is a significant factor in determining an aircraft's Estimated Time of Arrival (ETA), FMS RTA functionality accuracy largely depends on the correctness and resolution of wind data available to the FMS. Especially with large unexpected headwinds, RTA deviation can be significant [10].

On the ground, however, detailed wind forecast information is available and is updated continuously. In the Netherlands, the Royal Netherlands Meteorological Institute (KNMI) provides high resolution weather forecasts to the LVNL with a 0.1 latitude/longitude resolution on 40 altitude levels every hour. It should also be mentioned that having data available should be seen separately from being able to effectively use that data. Computational power provided by the FMS will differ per aircraft type and will also likely be less than on the ground. It seems trivial that ETA predictions performed using high-resolution meteorological data will outperform those performed by an FMS, which is limited in terms of both computing power and available information.

Besides the lack of accurate up-to-date wind information onboard, the actual RTA functionality implementation differs per aircraft [11]. The exact implementation of the algorithm is often proprietary information belonging to the avionics manufacturer. From an ATC point of view, it is therefore very difficult to objectively quantify trajectory uncertainty when flying towards a metering fix using the FMS RTA functionality [12].

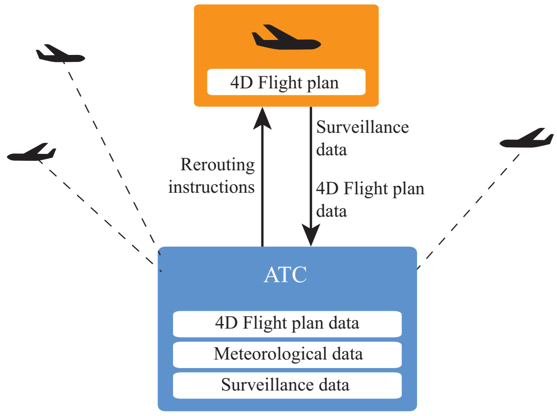

Fig. 1. Proposed information management in the solution space concept CONOPS

With all this in mind, a ground-based control rationale is opted for in this research, as shown in Figure 1. The ground-based control rationale allows for RTA adherence using the most detailed and up-to-date information, while the bypassing of the FMS RTA functionality also turns undesired trajectory *unpredictability* into manageable *uncertainty*. Another advantage of this approach is that the ATCo remains in control of the issued commands. This will likely increase controller acceptance, because he or she remains actively involved in the decision-making process.

2) Aircraft Commands: Following the RTA control loop rationale, a set of autopilot functions and commands to be used as the baseline for all TP applications within the interface can be drafted. An ATCo can instruct an aircraft using commands on Heading (HDG), Speed (SPD) and Altitude (ALT). For each of these, the command types are specified.

a) Lateral Commands: As almost all modern-day aircraft are equipped with Lateral Navigation (LNAV), lateral commands can be given in the form of fixed waypoints. This implies both fly-by and point-reached waypoints, towards and from which a constant track can be flown. The aircraft autopilot is thus assumed to compensate for any incoming lateral path perturbations, such as wind.

b) Velocity Commands: Since the RTA control loop is closed on the ground, SPD commands are issued to all aircraft, instructing pilots to maintain a desired Indicated Airspeed (IAS) / Mach number (M) pair. Aircraft will only alter their velocity when instructed by ATC.

c) Vertical Commands: The three variables that govern altitude changing segments are thrust setting, speed and rate of climb or descent. Controlling an arbitrary two of these variables yields the third variable as output [13].

When climbing, it is common practice to control the throttle setting (set to climb thrust) and keep a constant speed, thereby yielding the Rate of Climb (RoC) as the output variable. This means that, while the Bottom of Climb (BoC) location is known, the Top of Climb (ToC) location can only be predicted. In current ATM practice, this does not form an issue, as altitude constraints in climb typically only limit the upper altitude (in the form of a pass-below constraint).

In descent, airspace constraints often require an aircraft to pass a waypoint below a pre-defined altitude, thereby fixing the Bottom of Descent (BoD) location. Because flying at high altitude is desirable from an efficiency point of view, the required Top of Descent (ToD) to meet the constraints is then calculated. Thrust and Rate of Descent (RoD) are then controlled to ensure that the vertical constraints can be met, yielding the airspeed as output variable. This forms a drawback in 4D ATM, since the ETA at BoD is heavily impacted when applying this method. Because of the high predictability required in 4D ATM, fixing both the RoD and speed is therefore desirable [14]. This yields a *geometric* descent path, which can accurately be flown by any modern-day FMS.

B. Wind

Wind forms an important factor in airborne navigation as it affects an aircraft's performance envelope and directly influences the aircraft's movement with respect to the ground. The models presented in this section are integrated into the existing interface.

1) Wind Field Characteristics: For TP purposes, a dynamic wind field can be seen as a 4D grid (i.e., varying in space and time), where each node has a Two-Dimensional (2D) wind vector containing the horizontal u and v components. Vertical wind is less dominant on a large scale, but can form obstructions for an aircraft. Turbulence effects are not taken into account, as they do not affect an aircraft's ground-based performance envelope much.

2) Aircraft Performance: While the aircraft's local performance envelope is defined relative to its local reference frame, the aircraft's movement relative to the earth is of predominant interest for ATM purposes. To distinguish between movement relative to the local reference frame and ground-based movement, a different speed terminology is used.

True Airspeed (TAS) is defined as the aircraft's speed relative to the surrounding atmospheric parameters, thus including wind. Ground Speed (GS), on the other hand, is defined as the movement relative to the ground. As a result of encountered wind fields, an aircraft's heading and track are not necessarily the same. While an aircraft's heading can be described as the direction the aircraft is facing, the direction of movement is indicated using its track. Especially in strong crosswinds, the two values will differ because of the sideways drift caused by the wind field. Equations (1) and (2) show the impact of lateral wind on an aircraft's GS and the resulting wind correction angle required to maintain an intended track [15], supported by Figure 2.

$$\mathbf{V_{GS}} = \mathbf{V_{TAS}} + \mathbf{V_{wind}} \tag{1}$$

$$\delta = \arcsin\left(V_{wind}\frac{\sin(\epsilon)}{V_{TAS}}\right) \tag{2}$$

As can be seen, an aircraft's ground velocity vector $\mathbf{V_{GS}}$ is the vector sum of the TAS velocity vector $\mathbf{V_{TAS}}$ and present wind vector $\mathbf{V_{wind}}$. Following the geometry presented in Figure 2, the wind correction angle δ required to maintain

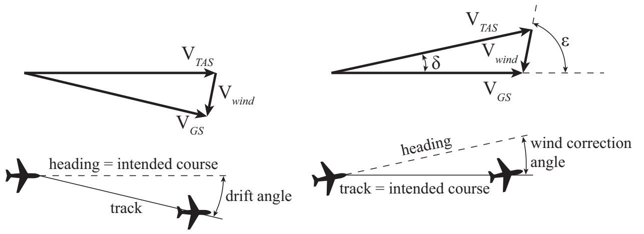

Fig. 2. The effect of wind on aircraft track (reproduced from Ruijgrok [15])

a prescribed track can be calculated using the relative wind angle ϵ, the wind velocity magnitude V_{wind} and the TAS magnitude V_{TAS}.

As an arbitrary wind field continuously affects an aircraft's instantaneous ground-based performance envelope, the complexity of the 4D TP process increases. Linearity of atmospheric parameters between consecutive waypoints can no longer be assumed, resulting in the need to use iterative algorithms to determine the required speed schedule to reach a prescribed metering fix. This has to be taken into account when implementing dynamic wind effects into the interface.

A common algorithm used in TP applications is the well-known binary search or half-interval search method. This algorithm aims to find a target value within a sorted array by testing the middle of an interval, eliminating the half of the search space in which the target value cannot lie. When bounding the search space by an aircraft's minimum and maximum airspeed, the desired IAS to reach a metering fix can efficiently be found using this algorithm.

C. Trajectory Uncertainty

Trajectory uncertainty can be defined as the difference between an aircraft's predicted position and the range of possible actual positions. This typically differs with the prediction horizon, as shown in Figure 3.

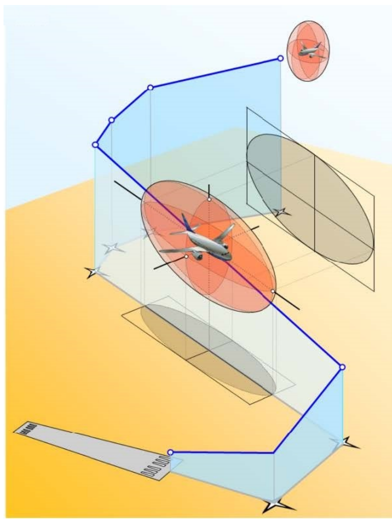

Fig. 3. Representation of spatial TP accuracy (adapted from Casado Magaña [16])

Since the beginning of commercial ATM, trajectory uncertainty has had a large influence on airspace capacity. Estimating an aircraft's future 4D position is required not only for planning purposes, but also to quantify the probability of conflict with other aircraft. As both elements are essential in the solution space concept, a review of trajectory uncertainty metrics, sources of trajectory uncertainty and the chosen implementation for the interface concept is discussed in this section.

1) Metrics: The error between an aircraft's predicted position and actual position has been a frequent topic of research, for which common metrics have been developed and used.

a) Spatial Error: The spatial error can be described using the vector from an aircraft's actual versus its predicted position at a certain point in time. It can be decomposed into a horizontal and vertical error.

The horizontal error measures the horizontal distance between the predicted and actual aircraft position at a certain point in time. This error can be decomposed into an along-track and cross-track component, as shown in Figure 4.

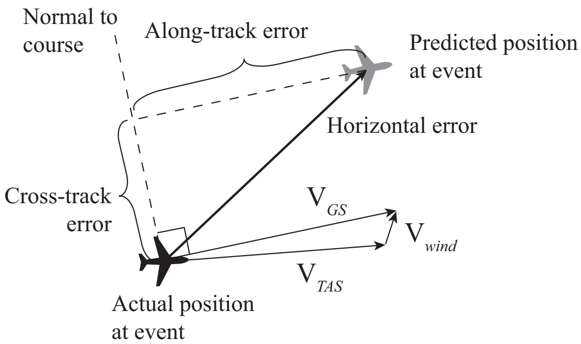

Fig. 4. The relationship between horizontal, cross-track and along-track error (adapted from Mondoloni et al. [17])

The vertical error is defined as the altitude difference between the predicted and actual flight path. Since a modern FMS can maintain a set altitude with an accuracy of $\pm 50ft$, vertical errors are only significant during the climb or descent phases of flight. Vertical errors originate from a variety of parameters, the most important ones being aircraft weight, FMS settings and wind prediction errors [12].

Typically, altitude errors caused by uncertainty in aircraft weight are larger in climb than in descent [18]. This is illustrated in Figure 5, in which the blue line represents a reference flight path and the light blue area represents the vertical uncertainty when varying the aircraft weight. The light red area shows the projection of the uncertainty profile onto the reference level, illustrating the vertical error as a result of aircraft weight deviation.

Vertical errors are complex to model, as more factors are of influence when compared to horizontal errors. In general, however, the vertical error can be modeled as an increasing error from the start of climb or descent. This error will reach a peak value and return to nearly zero after the climb of descent, because FMS altitude hold capabilities are very accurate.

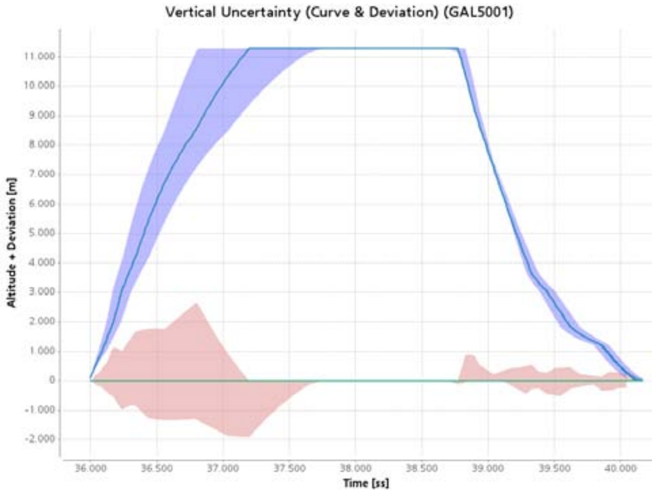

Fig. 5. Vertical error during climb and descent phases of flight with varying aircraft weight (taken from Weitz [18])

b) Temporal Error: Temporal error is defined as the time difference between the predicted and closest on-track flight position at a particular event. The closest on-track flight position is in this case defined to be the closest on-track point from the actual aircraft position, measured using the great circle distance formula [18].

Using the temporal error, a flight can be classified as being early, on time or delayed. Note that when a flight is on time (i.e., a zero temporal error), this does not mean that the spatial error is equal to zero, as cross-track deviations are still possible. This is illustrated in Figure 6.

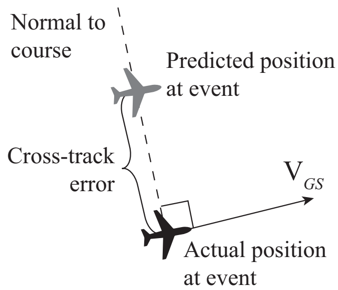

Fig. 6. Zero temporal error in the presence of cross-track error

2) Sources: Uncertainty in the execution of a pre-planned flight trajectory can have multiple sources, each of which contributes to a combination of the discussed error metrics. In recent years, significant research has been devoted to the identification and characterization of these sources [18–22].

a) Initial Conditions: When estimating a flight path in both space and time, initial conditions have to be set. Some initial conditions are of stochastic nature. Two important factors are aircraft weight and departure time.

b) Modeling Errors: When estimating a flight trajectory, a combination of models is used. Each of these models has its own assumptions and known imperfections, which consequently contribute to inaccuracy in the TP process.

c) Aircraft Intent: Seeing the aircraft as the combination of the flight crew and actual aircraft, this category can be divided into pilot intent and aircraft behavior as a result of FMS settings.

d) Flight Technical Errors: These errors are defined as inaccuracies in flight control due to FMS performance. These errors are considered the FMS tolerance limits.

e) Weather Forecast: Wind forecast errors form a very large, if not the largest, source of trajectory uncertainty [23], especially for along-track errors. In a working paper [24], ICAO already mentions 'buffers' to be introduced when determining the possible ETA range as a result of meteorological errors. It is known that wind direction deviation induces larger errors than wind speed deviation [18].

Besides wind, deviations in predicted local temperature and pressure also impact TP accuracy, because the calculation of different speeds (such as Calibrated Airspeed (CAS) and M) from TAS depends on these parameters [19].

3) Modeling Approach: Although in principle any number of uncertainty sources can be taken into account when modeling trajectory uncertainty, the focus in this paper is put on wind prediction error.

Multiple methods to model the spatial trajectory uncertainty exist, each differing in fidelity and computational load. For the on-line application purpose required in an interactive interface, parametric estimations are chosen. The model will need to predict with acceptable accuracy roughly within the time horizon of an airspace sector. To this end, parametric mid-range conflict prediction models with a time horizon in the order of tens of minutes are deemed most suitable in a design concept phase.

Well-known research examples are provided by Yang and Kuchar [25] and Prandini et al. [26], all investigating the 2D TP case from an initial known position (e.g., the present radar state). In these parametric estimations, the cross-track and along-track errors are modeled as zero-mean components with an increasing variance in time, creating uncertainty contours around an aircraft's nominal predicted position. This is illustrated for a series of waypoints P_{j-1} to P_{j+1} in Figure 7.

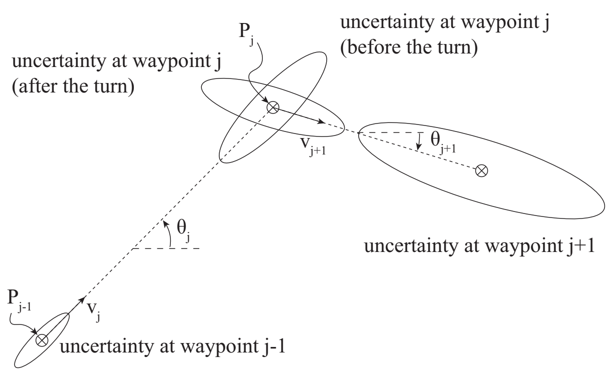

Fig. 7. Mid-range prediction for aircraft motion (adapted from Prandini [26])

$$\sigma_a^2(t) \sim r_a^2 t^2 \tag{3}$$

$$\sigma_c^2(t) \sim \min\{r_c^2 s^2(t), \bar{\sigma}_c^2\} \tag{4}$$

Equations (3) and (4) [26] mathematically describe this model. The variance of the along-track error component $\sigma_a^2(t)$ grows quadratically with look-ahead time t and the along-track error growth rate r_a. The variance of the cross-track error component $\sigma_c^2(t)$ grows quadratically with traveled distance s and cross-track error growth rate r_c until a saturation point $\bar{\sigma}_c^2$ is reached. Together, both error components form the radii of an equiprobable position contour surrounding an aircraft.

These uncertainty distributions can in turn be used to predict conflict probability. When assuming uncorrelated covariance matrices of different aircraft, they can be added together to calculate the conflict probability [26].

The assumption of uncorrelated covariance matrices is rather unrealistic, since the along-track error is largely caused by the wind error, which is correlated in both space and time. It has been shown that the assumption of uncorrelated wind errors can be seen as being conservative, since conflict probability is consistently overestimated using this assumption [27, 28].

Because the ETA management control task is executed by the ATCo as a result of the proposed CONOPS, σ_a^2 can be assumed to keep growing, as pilots will not compensate for a changing ETA as a result of wind prediction error without being instructed by the ATCo. Equation (3) is therefore considered a reasonable model. Similarly, Equation (4) is considered reasonable in the proposed CONOPS, as the FMS is expected to correct for the incoming wind vector and the cross-track error will therefore have a saturation point.

Because 4D flight plans are available at all times, the nominal trajectory $\vec{p}(t)$ is readily available for computational use. Using the parameterized tracking error variances, the resulting aircraft's position $\vec{x}(t)$ can be described using Equations (5) to (8) [26].

$$\vec{x}(t) \sim \mathcal{N}(\vec{p}(t), V(t)) \tag{5}$$

$$V(t) = R_{rot}(\theta)\bar{V}(t)R_{rot}(\theta)^T \tag{6}$$

$$\bar{V}(t) = \text{diag}(\sigma_a^2(t), \sigma_c^2(t)) \tag{7}$$

$$R_{rot}(\theta) = \begin{pmatrix} \cos(\theta) & -\sin(\theta) \\ \sin(\theta) & \cos(\theta) \end{pmatrix} \tag{8}$$

The aircraft's position at an arbitrary point in time is described using a Gaussian distribution centered around the mean $\vec{p}(t)$ with a multi-dimensional covariance matrix $V(t)$.

The initial covariance matrix $\bar{V}(t)$ is made up of the computed along-track error variance $\sigma_a^2(t)$ and cross-track error variance $\sigma_c^2(t)$, after which it is rotated to align it correctly with the aircraft's direction of movement. This is done using the rotation matrix $R_{rot}(\theta)$ associated with angle θ, defined as the present track of the aircraft.

Using this description for an aircraft's multivariate stochastic position at any moment in the time interval between the present time and 20 minutes ahead, allows the calculation of conflict probability $PC(t)$ between two aircraft in a sector. The predicted distance between the two aircraft at any point in time $\vec{d}(t)$ is defined as the distance between the predicted position of aircraft A $\vec{x}^A(t)$ and aircraft B $\vec{x}^B(t)$. This distance can stochastically be described with the combined mean $\vec{\mu}(t)$ and combined covariance $Q(t)$ of two aircraft. Integrating the resulting probability density function $\vec{p}_{\vec{d}_t}(y)$ over the circular Protected Zone (PZ) with a diameter of five nautical miles yields the probability of conflict, as shown in Equations (9) to (13) for a conflict between aircraft A and B [26].

$$PC(t) = \int_{y \in PZ} \vec{p}_{\vec{d}_t}(y)dy \tag{9}$$

$$\vec{d}(t) = \vec{x}^A(t) - \vec{x}^B(t) \tag{10}$$

$$\vec{d}(t) \sim \mathcal{N}(\vec{\mu}(t), Q(t)) \tag{11}$$

$$\vec{\mu}(t) = \vec{p}^A(t) - \vec{p}^B(t) \tag{12}$$

$$Q(t) = V^A(t) + V^B(t) \tag{13}$$

The maximum value of the instantaneous conflict probabilities within the chosen time interval T_{tot} is then taken to be the *measure of criticality* C, or resulting conflict probability as illustrated in Equation (14) [26].

$$C = \max_{t \in [0, T_{tot}]} PC(t) \tag{14}$$

As all nominal trajectories are already pre-computed in 4D, the nominal Closest Point of Approach (CPA) can be determined in both position and time directly. The maximum $PC(t)$ will then be at this specific point in time and can be computed directly, greatly reducing computational load.

When extending this modeling approach to the 3D case, the vertical tracking error will need to be modeled as well. When climbing or descending, the assumption is made that vertical tracking errors build up until the set altitude is reached, after which they return to zero again. The vertical error standard deviation in both climb ($\sigma_{v,climb}$) and descent ($\sigma_{v,desc}$) can therefore be characterized using Equations (15) and (16) for climbing and descending segments, respectively.

$$\sigma_{v,climb} \begin{cases} = 0 & 0 < t < t_{BoC} \\ \sim r_{v,climb}t & t_{BoC} < t < t_{ToC} \\ \sim -r_{v,climb}t & t_{ToC} < t \end{cases} \tag{15}$$

$$\sigma_{v,desc} \begin{cases} = 0 & 0 < t < t_{ToD} \\ \sim r_{v,desc}t & t_{ToD} < t < t_{BoD} \\ \sim -r_{v,desc}t & t_{BoD} < t \end{cases} \tag{16}$$

The vertical tracking error starts to build up from the beginning of the climbing or descending segment, corresponding to t_{BoC} or t_{ToD}. It grows linearly with time and with the estimated error growth rate $r_{v,climb}$ or $r_{v,desc}$ until the nominal trajectory has reached the target altitude. After reaching t_{ToC} or t_{BoD}, the vertical tracking error starts to decrease until it reaches zero again.

The relationship between the different types of spatial errors is qualitatively summarized in Figure 8. As can be seen, the along-track error grows linearly with look-ahead time until corrective action is taken by ATC. The cross-track error grows linearly until it reaches a saturation point, as there is in general a maximum deviation from the desired aircraft track that results from the FMS track adherence capability. Vertical errors will start to increase initially and reduce after the nominal desired altitude has been reached.

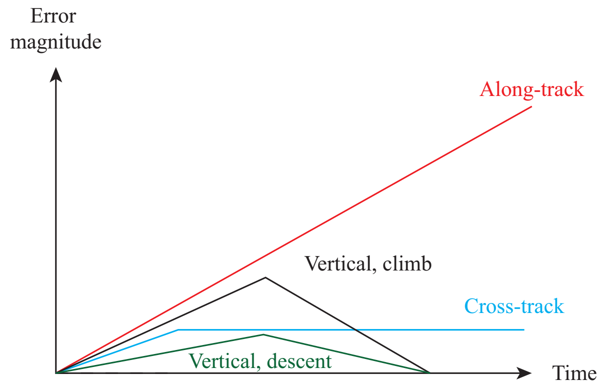

Fig. 8. Qualitative description of spatial error components magnitude versus look-ahead time

D. Implications for Human-Machine Interaction

The baseline for the display redesign will be formed by the solution space concept, as discussed by Klomp et al. [29]. It tries to overcome the challenges of automation by visualizing the possible solution spaces in each dimension, without making suggestions on what control action to take. This design philosophy is inspired by EID, where work domain constraints are ideally mapped one-to-one onto the interface, showing the user what limits their control actions.

When applying the Ecological Design Rationale, a Cognitive Work Analysis (CWA) is often performed to guide the design process. For the baseline interface without wind and trajectory uncertainty, a CWA has been performed in great detail by Riegman [30].

Following CONOPS rationale described in Section II-A, ATC will be in charge of RTA adherence, thereby introducing a new control task to the ATCo. This extra control task has to be integrated and made visible to the operator in the interface. When interacting with the interface, the user will therefore need to perform two separate tasks (i.e., Conflict Detection & Resolution (CD&R) and ETA management).

In addition to this, the impact of the wind effects and trajectory uncertainty on the work domain will have to be shown on the interface. To increase controller acceptance and better support the creation of a good mental model of the work domain, means-ends links should be made visible to the user [31]. This forms a design challenge, as the resulting display complexity increases with the risk of introducing screen clutter.

III. Interface Redesign

The implementation of wind and trajectory uncertainty implies not merely *adding* these features, but rather *integrating* them into the baseline display. Therefore, a comprehensive redesign process was carried out, of which the results are presented here. Special care has been taken to ensure consistent use of colors and symbols across each display to achieve maximum intuitiveness and situation awareness as described by Endsley [32] and Wickens [33].

The starting point of this display is explained in great detail by Klomp et al. [29]. For the sake of completeness, every display is revisited and explained in this section. This is done in a step-by-step manner, firstly introducing the core solution space concepts and 4D contract manipulation options, to be followed by an explanation of constraint mapping with added wind and uncertainty effects.

A. Control Space

When the RTA is used as a fixed constraint, the available control space in each dimension is bounded by a combination of airspace regulations, flight dynamics and an aircraft's performance envelope, which is in turn affected by the encountered wind field.

1) Lateral Solution Space: An aircraft's lateral flight plan is made up of a series of waypoints which are to be flown in sequence. The lateral solution space presents the user with rerouting possibilities by breaking up one straight segment into two segments using an intermediate waypoint.

As already stated by Klomp et al. [34], any lateral deviation from the originally planned straight trajectory between two route points will require the aircraft to fly faster to compensate for the added track miles. The maximum operating speed V_{max} determines the outer bounds of this control space. This principle is illustrated in Figure 9a, where the solution space with rerouting possibilities is shown.

In this example, rerouting the aircraft using WP_A will imply a 10 kts velocity increase. The larger the path deviation, the larger the velocity increase will need to be. Close to the bounds of the performance envelope, a different color is used. This indicates possible undesired areas of the control space, as the aircraft will have to fly close to the boundaries of its performance envelope.

Similarly, the minimum operating speed V_{min} dictates the boundaries of the solution space when track miles have to be added to meet the metering fix (i.e., a dog leg), as shown in Figure 9b. Rerouting the aircraft using WP_A will in this case cause the aircraft to arrive at the next waypoint too early. When WP_B is used, the aircraft will be able to meet its assigned RTA.

To minimize pilot workload, the two resulting segments are assumed to be flown at constant IAS. With the introduction of a dynamic wind field, however, the resulting GS for both segments does not necessarily have to be equal. To find a single IAS with which the metering fix can be achieved, a binary search algorithm is used.

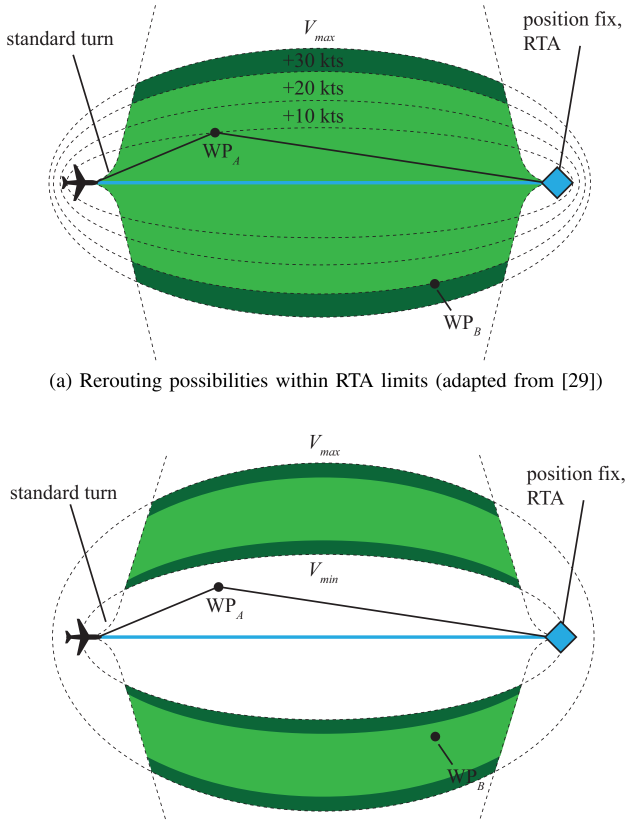

(a) Rerouting possibilities within RTA limits (adapted from [29])

(b) Rerouting required for RTA adherence

Fig. 9. Lateral solution space

2) Time-based Solution Space: When viewing an aircraft's flight plan in the time domain, one can make a Time Space Display (TSD). This illustrates the current distance to go on the horizontal axis and the time on the vertical axis. The latter is flipped vertically relative to the previous design, because a speed increase now implies dragging the label upwards instead of downwards, which is deemed to better fit the user's mental model according to the principle of pictorial realism [33].

Similar to the lateral solution space, the time-based solution space breaks up one segment by placing an intermediate constraint. Without altering the original lateral or vertical aircraft flight plan, an aircraft can accelerate or decelerate, thus changing the timing at intermediate route points. As the aircraft has to reach its RTA, any speed instruction given is accompanied by an opposite instruction. That is, any speed increase for a segment is paired with a speed decrease for the other segment to reach the RTA and vice versa.

This principle is shown in Figure 10. In this example, rerouting the aircraft using WP_A would imply a velocity *decrease* when flying towards this waypoint, to be followed by a velocity *increase* after passing this waypoint in order to meet the RTA at sector exit. While rerouting the aircraft using intermediate waypoint WP_B would also be possible, this would cause the aircraft to arrive too early at the sector exit, because it cannot slow down sufficiently after having passed WP_B.

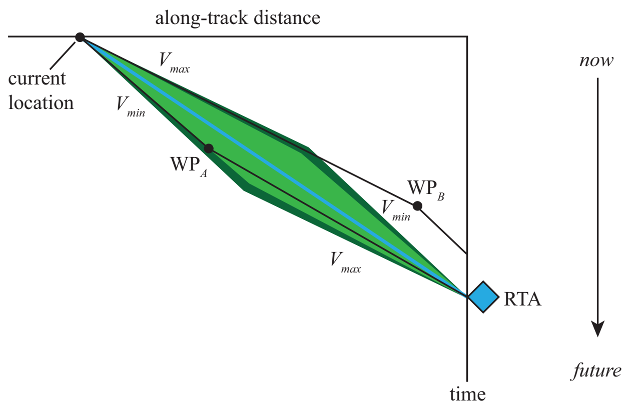

Fig. 10. Time-based solution space

3) Vertical Solution Space: The vertical solution space can be visualized using a Vertical Situation Display (VSD), on which the distance to go is displayed on the horizontal axis, and the Flight Level (FL) on the vertical axis. The vertical solution space breaks up one level flight segment into multiple new segments with a new level altitude. Because the aircraft has to respect its 4D contract, any altitude change will need to be reverted before reaching the sector exit. The vertical solution space is bounded by airspace regulations and the aircraft's performance envelope. Upper and lower altitude limits are dictated by the airspace regulations and the aircraft's operational ceiling. This principle is illustrated in Figure 11a.

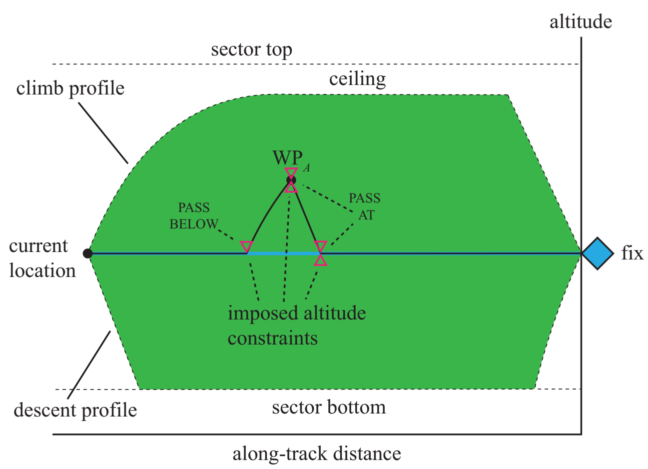

(a) Level segments

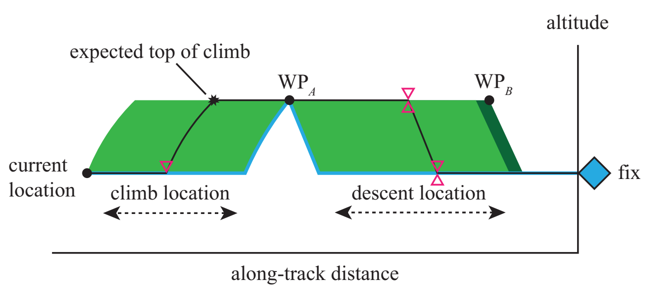

(b) Non-level segments

Fig. 11. Vertical solution space

When selecting an intermediate waypoint WP_A, the user effectively selects an intermediate flight level segment passing through this waypoint. After selecting a location for the new level segment, the limit case where the aircraft will climb and immediately descend again will be shown to the user together with the specified altitude constraints. The aircraft's vertical profile is guided by a pass-below altitude constraint, after which the climbing phase is initiated, followed by to pass-at constraints two command the geometric descent path.

After selecting a location for the new level segment, the location of the climb or descent profile can be altered, presenting the user with a second solution space, as shown in Figure 11b. This presents the user with feasible points to climb and descend. Moving the segments effectively moves the location of the altitude constraints. In this case, the climb segment has been brought forward, while the descent has been shifted to a later point. Because the ToC location is uncertain and cannot be controlled, it is shown with a separate symbol. To meet the RTA, the required IAS is adjusted, compensating for altitude-dependent velocity changes, as already described extensively by Riegman [30]. In this case, the aircraft has to start its descent before reaching WP_B, as any later point will cause the aircraft to arrive too early at the sector exit.

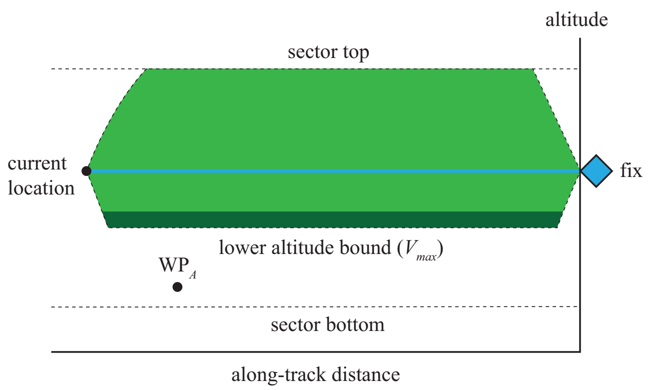

Fig. 12. Vertical solution space for level segments bounded by aircraft velocity limits

In some cases, the vertical solution space for level segments can also be bounded by the aircraft's velocity envelope. This is shown in Figure 12, where the aircraft has to fly close to its maximum operating speed to meet the RTA. In this situation, selecting an intermediate level segment at WP_A will render the 4D contract unreachable even the limit case of a descent segment and immediate subsequent climb segment, as the aircraft will arrive at the sector exit too late.

Depending on the current altitude of the aircraft, upper and lower velocity limits may dictate either the higher or lower altitudes. This is the result of the difference in flying above or below cross-over altitude, at which the transition between flying at constant M and IAS is made, affecting the way velocity is altitude-dependent. This effect is described in detail by the EUROCONTROL Experimental Centre [13].

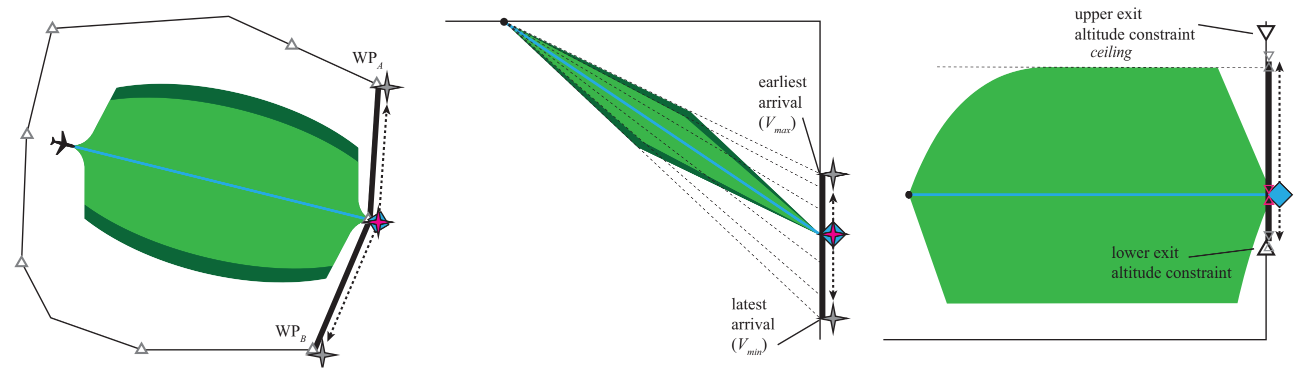

(a) Lateral contract manipulation (b) Time-based contract manipulation (c) Vertical contract manipulation

Fig. 13. 4D contract manipulation options mapped onto the interface

B. 4D Contract Manipulation Space

Other than visualizing only the available control space within which the 4D contract can be adhered to, the options for the ATCo to break the 4D contract in each dimension are supported as well. For each display, the available contract manipulations for the governing dimension *while keeping the other contract components fixed* are displayed. Contract manipulation possibilities can be restricted by aircraft performance, as well as airspace constraints.

1) Lateral Contract Manipulation: A lateral contract modification corresponds to a change in exit waypoint. Possibilities are presented to the user through a thick border at the sector boundary, as shown in Figure 13a. As the exit altitude and timing are kept constant, the range of available exit points is partly dictated by the aircraft's performance envelope. Exit waypoints located close to the aircraft's radar position cannot be reached on time, because the aircraft will have to fly below its minimum speed to comply with the RTA requirement.

Furthermore, airspace regulations can impact the available lateral contract manipulation possibilities. In this case, airspace regulations only allow a change of exit waypoint between WP_A and WP_B. The total lateral contract manipulation space can be seen as the intersection between the performance-based and regulation-based possibilities.

2) Time-based Contract Manipulation: When fixing the lateral and vertical path, a contract manipulation consists of a changed sector exit time. The range of possibilities for exit time manipulation are presented to the user with a thick strip located at the vertical timing axis, as shown in Figure 13b. The bounds of this range are determined by the aircraft's ground speed envelope, as the maximum operating speed yields the earliest possible arrival time and vice versa.

Because – following the CONOPS presented in Section II-A – the operator is responsible for managing an aircraft's ETA, the aircraft's ETA will start to diverge from its RTA when there is a prediction error. This will cause the magenta exit waypoint to diverge from the blue diamond. The user can then choose to align the two again, thereby calculating a new speed command with which the RTA should be reached.

3) Vertical Contract Manipulation: Vertical contract manipulation corresponds to a change in sector exit altitude, while keeping the lateral profile and sector exit timing fixed. Similar to the time-based contract manipulation, the range of possibilities is presented to the user by means of a thick strip at the vertical axis, as shown in Figure 13c. Upper and lower altitude limits at sector exit are dictated by airspace regulations and the aircraft's performance envelope, which is affected by both wind and altitude.

C. Constraints

Within the control space in every dimension, traffic intent constraints can be mapped to inform the ATCo. Within every solution space, the maximum probability of a future Loss of Separation (LoS) can be computed using the model described in Section II-C. These conflict probabilities can be mapped onto a contour plot, where contours represent arbitrary pre-defined thresholds on what is in reality a 3D surface. This is illustrated in Figure 14.

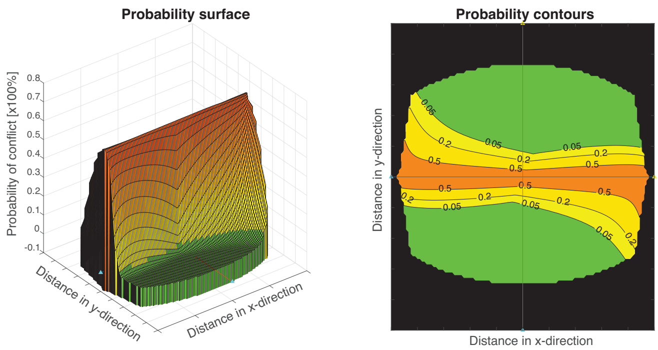

Fig. 14. Representation of 3D surface on 2D screen using contours

1) Lateral Constraints: Using different colors, pre-defined probability thresholds are mapped onto the already existing lateral solution space, as shown in Figure 15a.

Three thresholds are used, yielding a total of four colors. The lower and upper thresholds indicate the probability of a safe situation (green color) or certain conflict (red color), respectively. A third threshold set between these two can indicate the 'tipping point' for possible user interaction. Yellow and orange colors are used to indicate this. The color coding

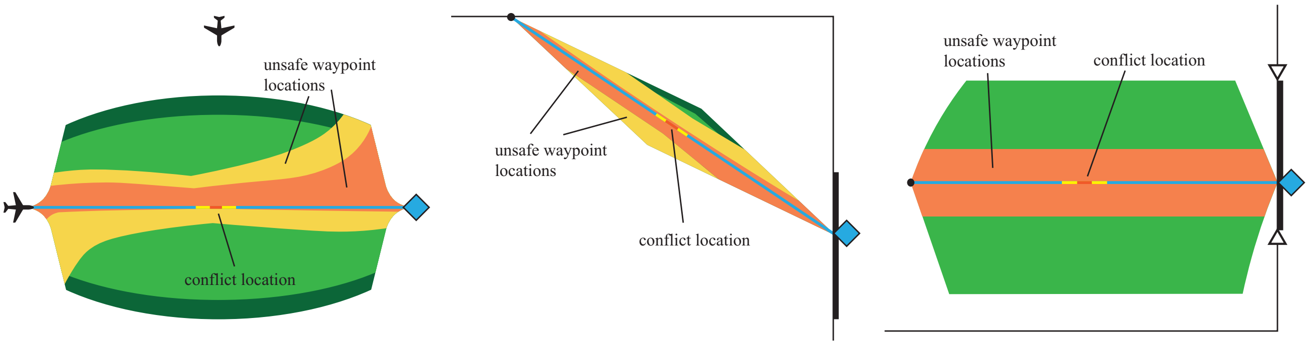

(a) Lateral constraints (b) Time-based constraints (c) Vertical constraints

Fig. 15. Constraints mapped onto the solution spaces with large look-ahead time

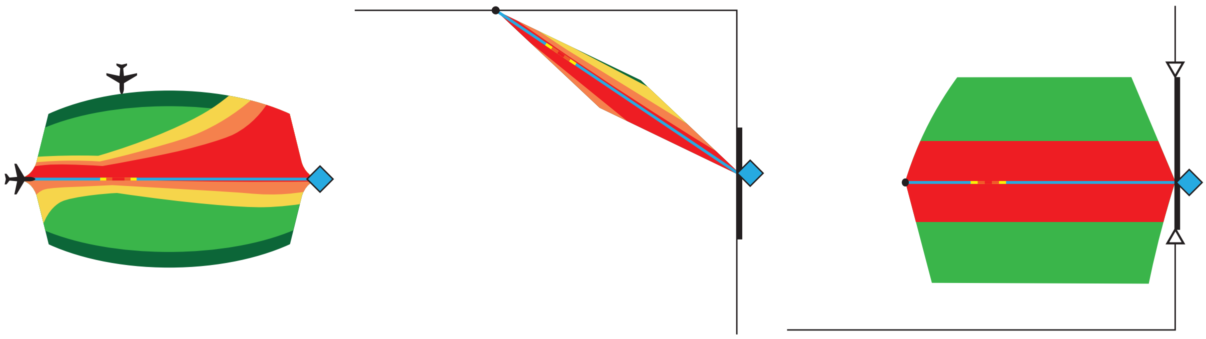

(a) Lateral constraints (b) Time-based constraints (c) Vertical constraints

Fig. 16. Constraints mapped onto the solution spaces with small look-ahead time

can be used by the operator to judge the predicted conflict situation and aid in the process to already take action to resolve the emerging conflict or not.

Placing a waypoint somewhere in the yellow region will lead to a conflict probability between 5% and 50%, whereas placing a waypoint somewhere in the orange region will lead to a conflict probability between 50% and 90%. The location of the conflict itself can be obtained by inspecting the colors on the trajectory path line from the aircraft towards its exit waypoint, for which the same coloring scheme is applied.

Because prediction accuracy decreases with look-ahead time and distance, the location of the predicted CPA influences the according conflict probability. Because of the large Time To Conflict (TTC) in Figure 15a, the maximum conflict probability is less than 90%. When inspecting the same traffic scenario with a smaller TTC in Figure 16a, a red zone emerges. This zone indicates a $>$90% conflict probability.

2) Time-based Constraints: When fixing the aircraft's lateral and vertical paths, the maximum probability of conflict with any other aircraft in the time-based solution space can also be computed. Similar to the lateral solution space, the new nominal trajectory for every point within the control space can be calculated and compared with all other traffic. The results are illustrated in Figures 15b and 16b.

The same color coding is used, showing the user conflict probabilities at all possible waypoint locations. The location of the conflict can be obtained by inspecting the colors along the time-space trajectory line moving from the current aircraft location towards the RTA location on the vertical time axis. Note that, similar to the lateral solution space, the maximum conflict probability increases when the nominal TTC decreases.

3) Vertical Constraints: When mapping constraints onto the vertical solution space, all possible nominal trajectories for every point in the control space (as illustrated in Figure 11b) are checked for their maximum conflict probability with all other traffic, making the vertical solution space computationally exhaustive when compared to the lateral and time-based solution spaces.

The result for a crossing conflict with a large look-ahead time is shown in Figure 15c. All altitudes separated less than the required vertical separation distance of 1,000 ft from the crossing aircraft are blocked, because adding a new level segment at those altitudes will never resolve the conflict using vertical separation only.

Similar to the lateral and time-based solution spaces, the location of the predicted LoS can be observed when inspecting the color of the vertical trajectory line, drawn from the aircraft's current location towards its altitude fix at sector exit. Maximum conflict probability again increases with decreasing TTC, as shown in Figure 16c.

After selecting a waypoint on the initial vertical solution

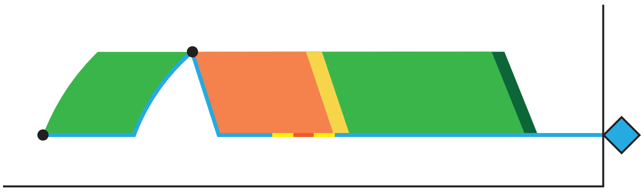

(a) Large TTC

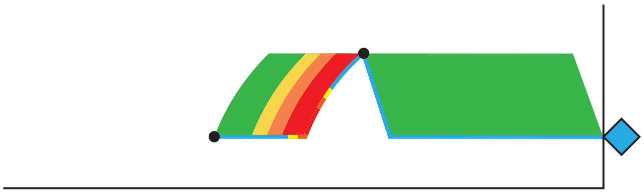

(b) Small TTC

Fig. 17. Constraints mapped onto the non-level vertical solution space

space, the locations of the climb and descent segments can be modified. The constraints are also shown on the non-level vertical solution spaces for these actions. Shown in Figure 17 for a large and a small TTC, maximum conflict probability with varying climbing and descending segment locations are presented to the user.

Figure 18 illustrates more possible shapes for traffic intent constraints on the level segment vertical solution space, showing the intents of two crossing aircraft. While the nature of both predicted conflicts and hence the nominal conflict locations (i.e., PZ_A and PZ_B) is similar, the resulting constraint shapes for both look differently.

To illustrate, the case where a level segment waypoint is to be placed somewhere along the desired flight level is considered. Because the aircraft can only start climbing safely after PZ_A has been cleared, a large part of the area above PZ_A is red. For PZ_B, on the other hand, the location of the climbing segment can be chosen, such that the desired flight level is reached safely before PZ_B is reached, explaining why all waypoint locations above PZ_B are shown in green.

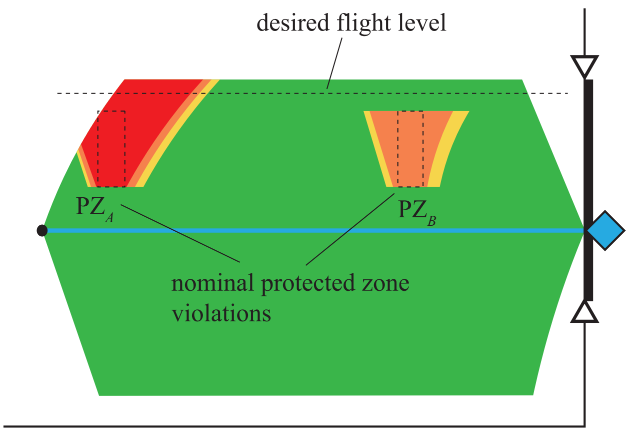

Fig. 18. Alternative crossing aircraft constraints mapped onto the level vertical solution space

D. *Wind Influence & Visualization*

The presence of an arbitrary wind field affects the shape of each of the discussed control spaces, because the aircraft ground performance envelope changes with added wind. Because of the binary search algorithm used in the TP software to generate the control spaces, the wind information is effectively already 'included' in the control spaces. Upon the user's preference, the wind information can also be displayed separately on each display to make the desired means-ends coupling.

It should be noted that all wind field visuals in this paper are presented by means of *static* arrows, where arrow length and direction indicate the wind vector. In the interface, wind vectors are represented using *dynamic* moving particles. In both the paper and the actual interface, the wind speed is also illustrated using different colors.

1) Lateral Solution Space: The effect of wind on the lateral solution space is shown in Figure 19, illustrated with a (rather unrealistic) synthetic wind field changing direction. Encountered wind around the aircraft's lateral path is displayed by means of moving wind vectors. As can be seen, the control space is no longer symmetrical due to the encountered wind.

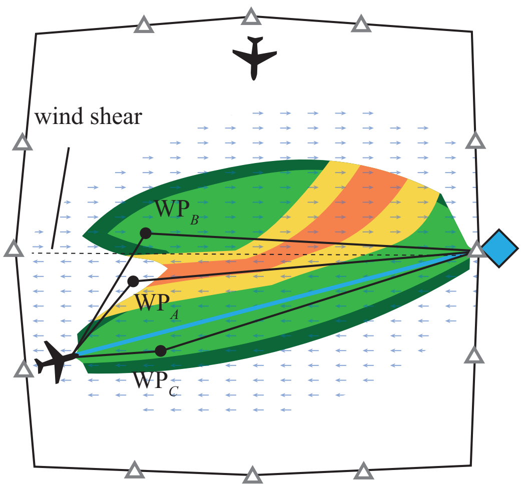

Fig. 19. Effects of wind on the lateral solution space

To illustrate the effect of the encountered wind field, two intermediate waypoints WP_A and WP_B are shown. Without rerouting the aircraft, an almost direct head-wind is encountered along path. As a result, rerouting possibilities are limited around the nominal trajectory. Placing an intermediate waypoint WP_A will result in the aircraft arriving too late at sector exit. Because of the sudden change in wind direction north of the nominal trajectory, however, extra maneuvering room is created. Placing an intermediate WP_B will, although located further from the nominal trajectory than WP_A, enable the aircraft to arrive at sector exit on time.

In this scenario, the wind field visualization can serve not only as a means-ends coupling for the shape of the solution space, but can also inform the user of possible undesired areas of the control space. While rerouting the aircraft using WP_B will allow the aircraft to meet its RTA, turbulence is likely to be encountered as the aircraft will be flying close to an area with significant wind shear. To that end, modifying the aircraft's trajectory using WP_C, where the wind shear is not crossed and the RTA can still be reached, could be preferable.

2) Time-based Solution Space: The effect of an arbitrary wind field on the available time-based solution space is shown in Figure 20. The along-track projection of the wind vector is directly made visible to the user. On the vertical axis, information on the path-dependent wind over time can be obtained. Thus, the horizontal line of wind vectors at the top of the figure represents the encountered wind at the current moment, while the horizontal line of wind vectors at the bottom of the figure represents the encountered wind on the aircraft path after the aircraft has already left the sector.

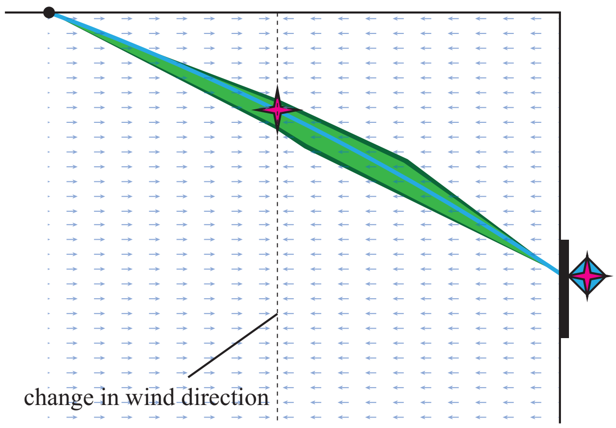

Fig. 20. Effects of wind on the time-based solution space

In this example scenario, the aircraft makes a turn halfway through the sector, causing the along-track encountered wind vector tangent to change sign. This impacts the available ground speed envelope for both segments and, in turn, affects the visible solution space. As can be seen, the control space and nominal trajectory both become 'steeper' after the turn, resulting from the change in wind direction.

3) Vertical Solution Space: Wind velocity magnitude can change rapidly with altitude, as can be seen in Figure 21. Similar to the time-based solution space, the along-track projection of the wind vector is made visible to the user.

In the presented example, the aircraft encounters a light tail-wind along its current nominal path at the current altitude. At higher altitudes, the wind speed increases, impacting the maximum length of the level segment at high altitude. The aircraft will therefore have to commence its descent before reaching WP_A to meet its RTA at sector exit.

IV. Working with the Interface

All solution spaces together operate within the integrated display concept. This section presents an overview of this concept, along with the workflow and possible modes of user interaction.

A. Integrated Display Concept

Figure 22 shows the Plan View Display (PVD), which functions as the primary monitoring screen when no aircraft

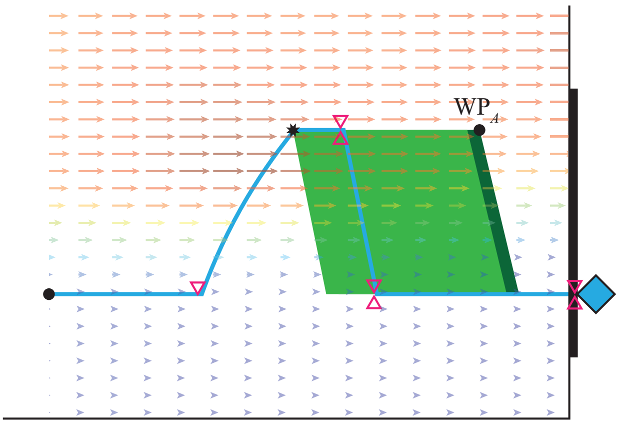

Fig. 21. Effects of wind on the vertical solution space

is selected. To alert the user for any required action, the aircraft conflict indication and current RTA deviation are directly perceivable on the PVD. The color of the aircraft's protected zone (i.e., the small circle surrounding an aircraft blip) indicates the aircraft's maximum probability of conflict with *any* of the other aircraft in the current sector, based on the intent of all aircraft. Rounded to the nearest five seconds, the current RTA deviation is located top right next to the aircraft label, where the magnitude of the deviation determines the text color. Deviations of less than 15 seconds are shown in black, whereas deviations between 15 and 30 seconds are shown in yellow. RTA deviations of 30 seconds or more are shown to the user in red, indicating the need for possible user action.

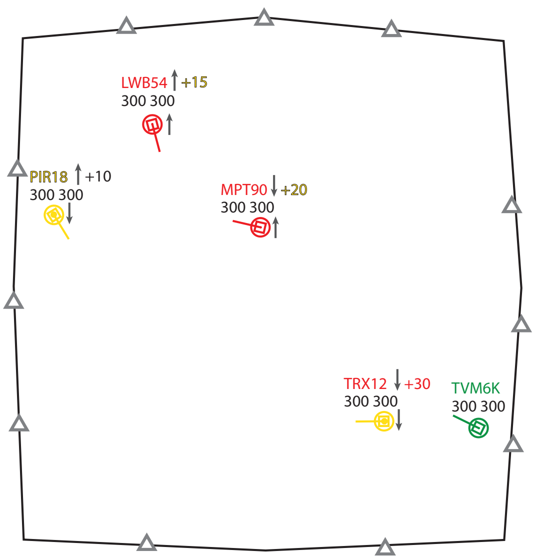

Fig. 22. PVD with no aircraft selected

To expose to the operator the *dynamic* nature of the work domain, arrows next to the RTA deviation indication and conflict probability indication show the first-order time derivative of these values. These can keep the operator more actively involved in the control loop and provide more information on whether or not to take action at this moment in time.

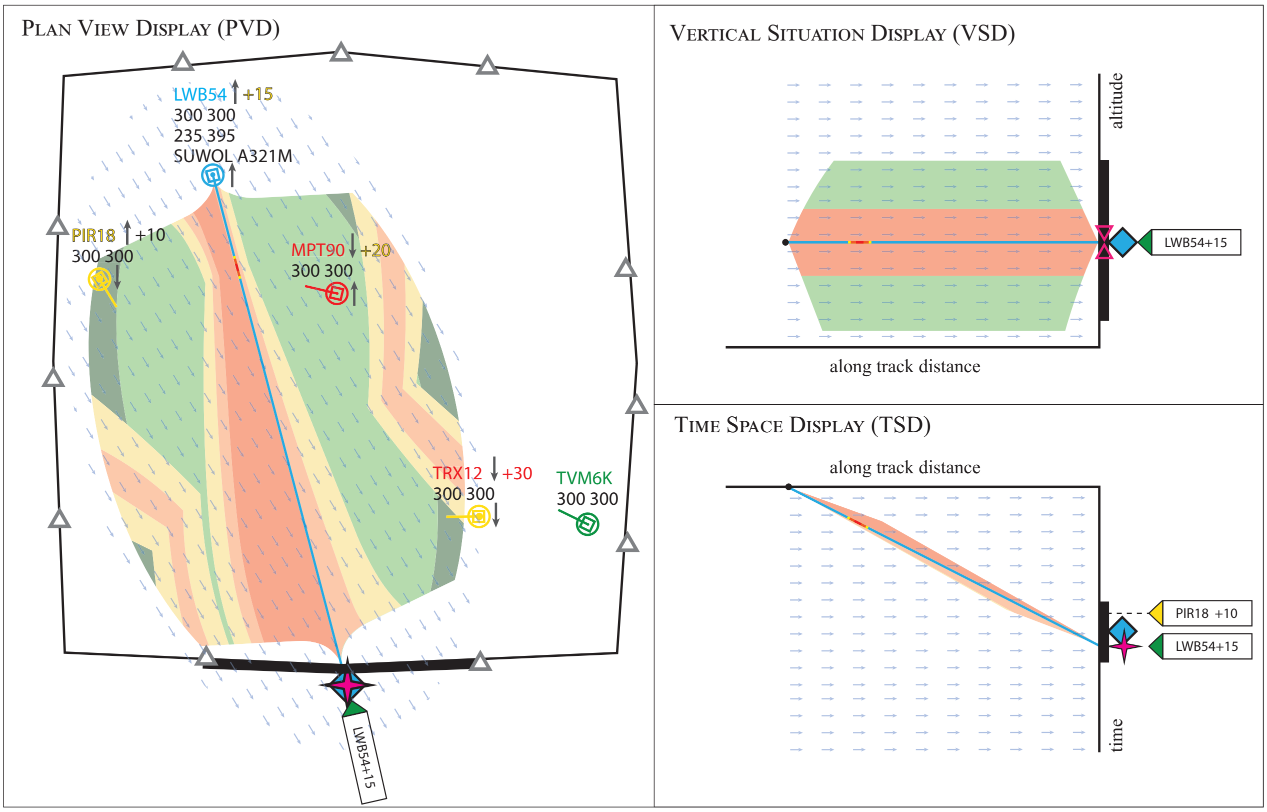

Fig. 23. Integrated solution space interface elements

To illustrate, LWB54 is compared to TRX12. LWB54 will currently be arriving 15 seconds too late at sector exit with the derivative arrow pointing upwards, indicating an *increase* in this RTA deviation. The controller might want to take corrective action at this point. TRX12 will be arriving 30 seconds too late, but the time derivate arrow is pointing downwards, hinting at a *decrease* in RTA deviation. As this problem could therefore potentially resolve itself, the controller might decide not to take corrective action for this aircraft at this moment in time.

Figure 23 shows the lay-out of the redesigned integrated solution space concept. The left-hand side of the display is reserved for the PVD, while the top and bottom right parts are used for the VSD and TSD, respectively. With respect to the original design, the TSD and VSD have swapped places and the vertical axis of the TSD has been flipped, as stated before. The former has been done to better fit the user's mental model according to the design principle of pictorial realism [33], as *altitude* is now controlled on the *upper* part of the screen.

When an aircraft is selected, the TSD and VSD become active and all rerouting possibilities for this specific aircraft are presented to the user by means of solution spaces and 4D contract manipulation options for every dimension. For the currently selected aircraft LWB54 (blue), the solution spaces in every dimension are presented to the user.

This aircraft has a predicted conflict with MPT90, as can be noted when inspecting the conflict location on the PVD, shown to the user on the trajectory path line. The red color indicates that action is strongly recommend, as the predicted conflict probability is more than 90%. To obtain information on how to best resolve this predicted conflict, the user can inspect the various solution spaces shown across the different displays. The TSD informs the user that this conflict cannot be resolved with solely a velocity change, as no green area is shown. Accordingly, this conflict can be resolved either by applying vertical separation or by making a change in the aircraft's lateral flight plan. Should the user decide to opt for the latter, it can be seen that a smaller path deviation is required when rerouting LWB54 aircraft *behind* MPT90 when compared to a reroute *in front of* MPT90.

Furthermore, MPT90 will currently arrive too late at the sector exit. To correct for this, the TSD can be used to align the aircraft label with the blue diamond again. Because the wind RTA deviation is *increasing* with respect to its current value, as can be seen when inspecting the arrow next to the RTA deviation value, the user might decide to 'over-correct' the ETA for this aircraft, thereby anticipating on the assumed wind prediction error.

To ensure maximum visual momentum across the various displays as described by Woods [35], all displays are strongly coupled. A trajectory modification made in one of the displays will simultaneously show in the other two as well. To illustrate, a lateral flight plan modification for LWB54 to resolve to predicted conflict with MPT90 will immediately be shown in the TSD. Any subsequent ETA modifications using the TSD immediately take this lateral path deviation into account.

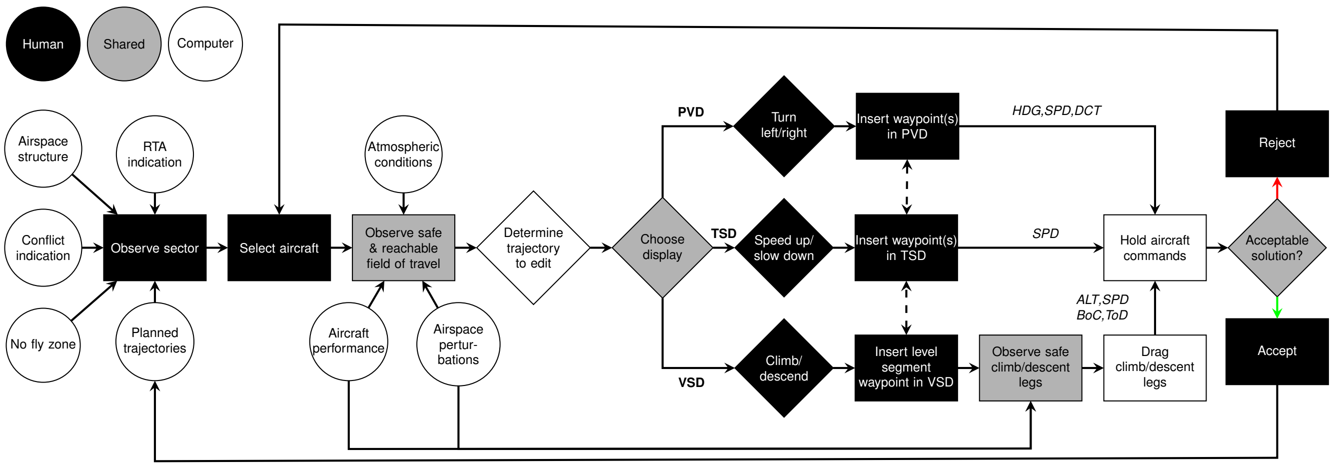

Fig. 24. Workflow of the redesigned integrated solution space concept

B. Workflow

The typical workflow when interacting with the display is shown in Figure 24. When no aircraft is selected, the PVD functions as the traditional radar screen, showing all aircraft currently present in the sector. Based on all information presented, the user may decide to modify one of the trajectories. When selecting an aircraft, all safe and reachable fields of travel are presented. Upon request, the atmospheric conditions can be shown to increase understanding of the presented solution spaces. When enough information has been gathered by the user, he or she can determine the trajectory to edit. Any (combination of) display(s) can then be used to modify a given 4D trajectory. The predicted effects of the desired commands are then visualized, after which the user can decide to either accept or reject the made trajectory modification.

In the solution space concept, human and machine work together to perform the required control tasks (i.e., CD&R and RTA management). Data relevant to the control task (e.g., aircraft performance, atmospheric conditions, flight plans, airspace structure) are stored and processed by the computer, while the decision-making is left to the human. Through the solution spaces, the computer supports the human in the decision-making process, creating a shared task division for some workflow elements.

C. Trajectory Manipulations

To explain the workflow of the trajectory manipulations, a crossing conflict will be discussed. For each display, a step-by-step explanation of possible user interaction will be given.

1) Lateral Manipulations: Figure 25a shows the initial solution space on the PVD for a selected aircraft currently in crossing conflict. At this point, the user can decide to reroute the aircraft while respecting the 4D exit waypoint, or to break the 4D contract by altering the exit waypoint.

When respecting the 4D contract, the user can inspect the solution space to see that the aircraft can either be routed behind or in front of the other aircraft. When an intermediate waypoint location has been chosen, the operator can directly insert this, as shown in Figure 25b. The resulting situation is shown in Figure 25d, where the original route segment has been split into two new segments. The conflict with the other aircraft has now been resolved, while the RTA at sector exit is respected. The control space itself does not limit the user in waypoint placement. Placing a waypoint outside the control space is possible, but will cause the aircraft to be delayed.

If the user wishes to alter the exit waypoint, inspection of the gray area at the sector boundary shows the possible new exit waypoints. When clicking and dragging the aircraft label towards a different waypoint, as shown in Figure 25c, the 4D flight plan is modified. As can be seen in Figure 25e, the aircraft will now fly towards the new exit waypoint, which it will reach at the time it was planned to be at its original exit waypoint. As can be seen, the conflict with the other aircraft has been resolved.

2) Time-based Manipulations: Figure 26a shows the initial solution space on the TSD for a selected aircraft currently in crossing conflict. At this point the user can decide to reroute the aircraft while respecting the 4D exit waypoint, or to break the 4D contract by altering the exit time.

When respecting the 4D contract, the user can place an intermediate waypoint inside the drawn control space. As can be seen, there is relatively little control space available to resolve this conflict using only velocity. There is a small green area above the current trajectory, indicating possibilities for an initial speed increase to be followed by a speed decrease. Placing an intermediate waypoint here, as shown in Figure 26b, will resolve this conflict while adhering to the RTA at sector exit. The resulting display is shown in Figure 26d. Contrary to the PVD, waypoint placement outside the control area is limited, since the aircraft's performance envelope dictates the reachability of intermediate waypoints.

The user can also alter the timing at the sector exit, thus temporally breaking the 4D contract. The range of available sector exit times, as governed by the aircraft's performance envelope, can be obtained by inspecting the gray area on the vertical axis. To alter the exit time, the user can click and drag the aircraft label and move this towards the new desired location, as shown in Figure 26c. The resulting situation after modification is shown in Figure 26e.

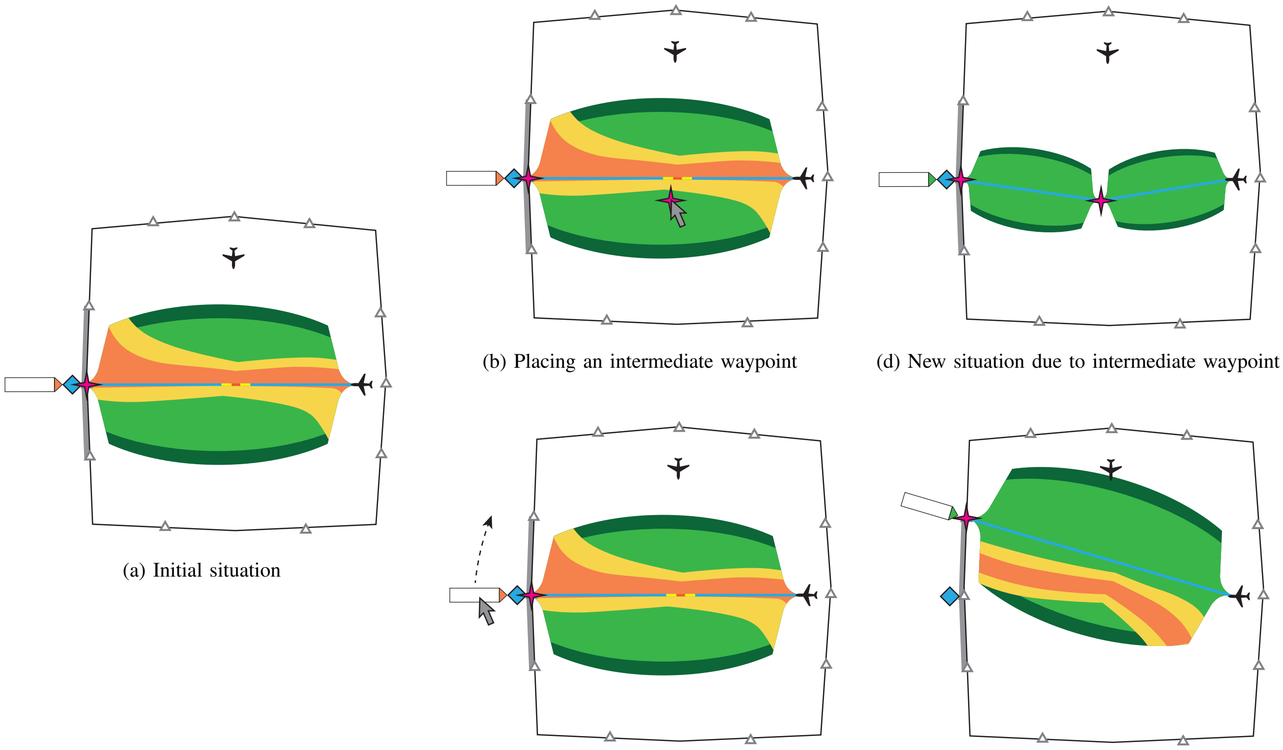

(a) Initial situation

(b) Placing an intermediate waypoint

(c) Moving the exit waypoint

(d) New situation due to intermediate waypoint

(e) New situation due to changed exit waypoint

Fig. 25. User interaction with the PVD

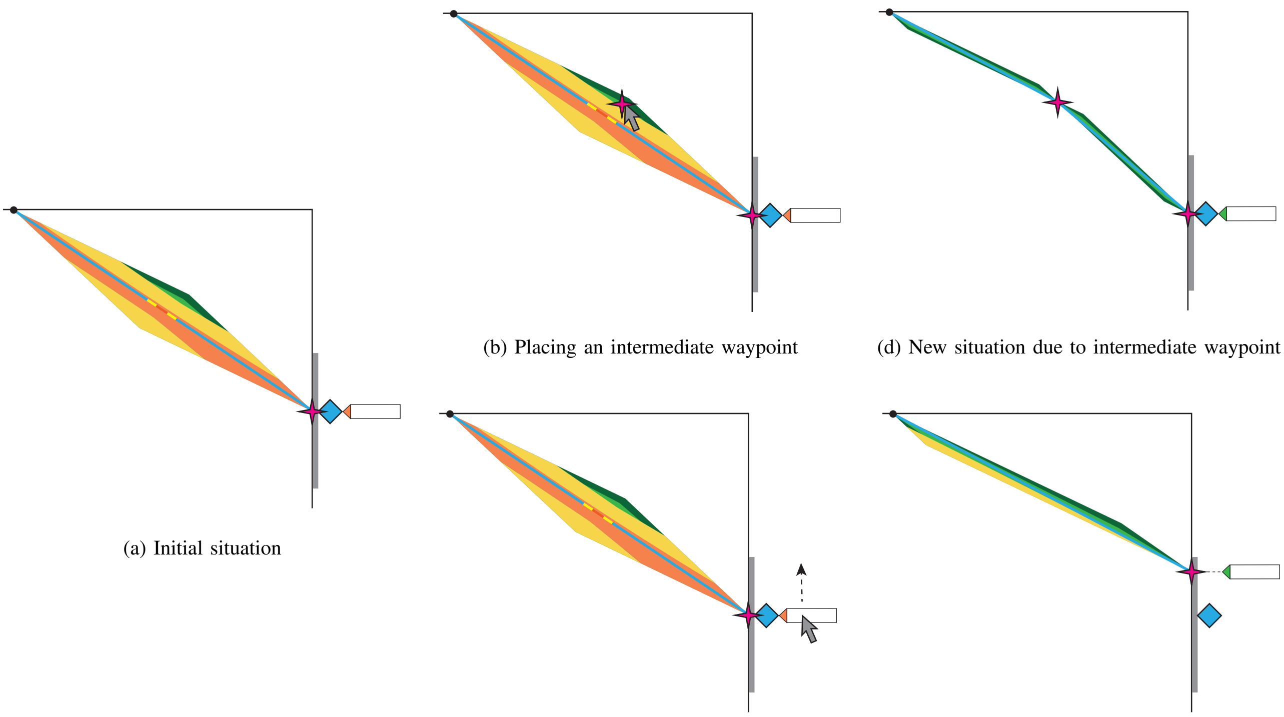

(a) Initial situation

(b) Placing an intermediate waypoint

(c) Changing the exit time

(d) New situation due to intermediate waypoint

(e) New situation due to changed exit time

Fig. 26. User interaction with the TSD

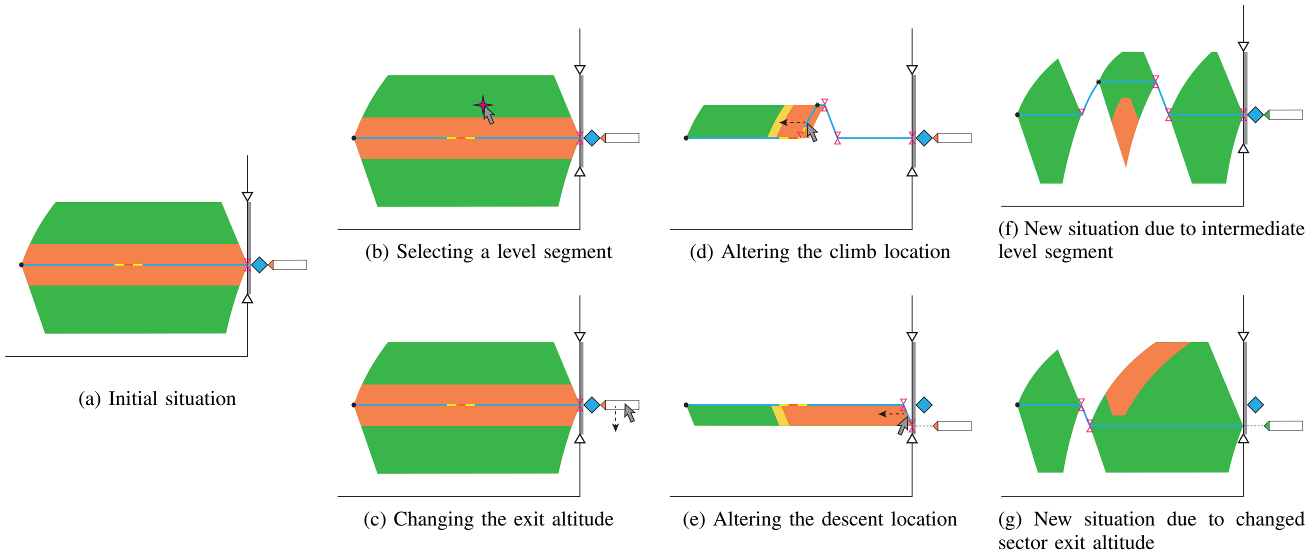

Fig. 27. User interaction with the VSD

3) Vertical Manipulations: Figure 27a shows the initial solution space on the VSD for a selected aircraft currently in crossing conflict. At this point the user can decide to reroute the aircraft while respecting the 4D exit waypoint, or to break the 4D contract by altering the exit altitude.

When respecting the 4D contract, the user can place an intermediate waypoint in the control space. In this case, all altitudes within the 1,000 ft vertical separation margin are unsuitable for an intermediate flight level. Placing an intermediate waypoint above the crossing aircraft, as shown in Figure 27b, imposes a set of altitude constraints to the aircraft for the limit case where the aircraft will climb and immediately descend again. The climb location can then be altered to resolve the conflict. Upon clicking and dragging the climbing segment, the range of options is presented to the user, as shown in Figure 27d. After dragging the climbing segment into the green area, the conflict is resolved. This new situation is shown in Figure 27f.

Options for altering the sector exit altitude while maintaining the RTA, are presented to the user using the gray area located at the vertical axis. If the user wishes to break the 4D contract by changing the sector exit altitude, he or she can do this by clicking and dragging the aircraft label next to the vertical axis, as shown in Figure 27c. In this particular case, the sector exit altitude is decreased. After doing this, the descent phase has to be brought forward to resolve the conflict. This can be done by clicking and dragging the descent segment into the green area, as shown in Figure 27e. The resulting situation is shown in Figure 27g.

V. Case Study

The original Travel Space Representation (TSR) interface was validated in a series of experiments by Klomp et al. [30, 36]. Because much complexity has been added to the interface and the corresponding simulation environment when compared to these experiments, the redesigned interface needed to be re-evaluated in a realistic setting to see how real operators interact with it and manage the assigned control task.

To do this, the prototyped interface and back-end TP environment have been implemented in an inhouse-developed ATC simulator. It has been validated that all presented solution spaces can be rendered in real-time without performance issues. The implementation of the solution spaces is carried out using the Graphical Processing Unit (GPU), meaning that all the required calculations can be performed 'per pixel' in an efficient parallel process.

LVNL currently already sets an Expected Approach Time (EAT) for all inbound Schiphol traffic at the Initial Approach Fix (IAF), allowing for it to be handled as 4D traffic using the redesigned interface. A case study was therefore conducted using inbound Schiphol traffic with an already existing 4D flight plan to be controlled by professional ATCos.

During and after the case study, participant control strategies and feedback were asked. Upon completion, the ATCo feedback on various interface components was combined with the gathered data to evaluate the concept (i.e., interface + operational environment).

A. Goal

The primary goal of this case study was to evaluate the redesigned display in a realistic, complex setting using qualitative expert feedback supported by gathered simulation data.

Because one of the main areas of interest was how the interface performs in complex, realistic ATC scenarios, the chosen case for this study could be motivated. The chosen traffic scenario required the participants to merge air traffic in a mixed tactical-strategic setting, something that is very difficult in real life with added wind and wind prediction error influence. To illustrate this, LVNL currently sets a 300-second time window (thus allowing for a 150-second deviation) for every flight to reach its EAT over the IAF.

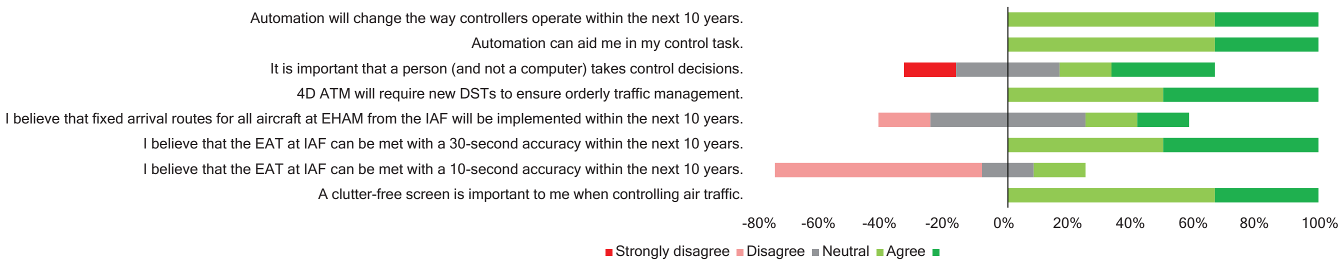

Fig. 28. Participant pre-questionnaire results

To evaluate the use of the display, three primary areas of interest were identified. Firstly, controller acceptance of the display was judged based on the qualitative feedback. Secondly, the controller's ability to fulfill the assigned control task when using the interface within the assumed CONOPS was assessed. The last area of interest was to see if the controllers could execute their preferred control strategy within the assumed CONOPS when using the interface.

B. Participants

Six professional Area Control Center (ACC) ATCos working at LVNL participated in this case study. Because all participants were familiar with both the control task and the presented traffic scenarios, they could focus solely on evaluating the interface.

During the evaluation, software issues caused the simulation to crash with two of the six participants, possibly corrupting the recorded data during these runs. These participants' simulation data are therefore not presented in the results section. Because these two participants did successfully complete the training phase and the majority of scenarios, allowing them to obtain a good impression of the interface, their qualitative feedback is presented in the results section.

To mitigate training effects and allow for fair quantitative support of the obtained feedback, the order of scenarios was different for the four participants that successfully completed all scenarios. The latin square matrix used is presented in Table I.

TABLE I
LATIN SQUARE SCENARIO SET-UP

	Run 1	Run 2	Run 3	Run 4
Participant 1	S1	S2	S3	S4
Participant 2	S2	S3	S4	S1
Participant 3	S3	S4	S1	S2
Participant 4	S4	S1	S2	S3

Prior to the case study, participants were asked to fill out a form questioning their current thoughts on automation and future ATC, of which the results are shown in Figure 28. In this figure (and all questionnaire result figures in the remainder of this work), the percentage of operators in agreement or disagreement with respect to the neutral line is presented to the left and right of this line, respectively.

There was a general consensus amongst participants that automation can aid them in their control task and will change the way controllers operate in the future, especially with 4D ATM being operative.

Whether or not a human should take the control decisions was not answered unambiguously. While opinions differ on who is to take the control decision (human or computer), however, participants agreed that as long as a human is *responsible* for handling air traffic, he or she should at least have a large influence on the control decisions.

With regards to the EAT at IAF, a 30-second accuracy was thought to be very realistic within the next 10 years (some indicated that this is already possible now if the involved actors show the willingness to do so). A 10-second accuracy was deemed less likely, mostly because of *unexpected* and last-minute changes in air traffic that cannot be accounted for.

Lastly, controllers indicated that a clutter-free screen is important when controlling air traffic.

C. Scenarios

A total of four scenarios was presented to every participant, each based on real-life traffic and atmospheric data. An overview of the traffic flow in all scenarios used in this case study is shown in Figure 29.

1) Airspace: The controlled airspace was the Dutch FIR, simplified for the type of traffic in this case study. Traffic entered the airspace at one of three entry Change-Over Points (COPs), EEL, RKN or NORKU, from which they followed a certain route towards ARTIP. Typically, this traffic arrives on the radar at cruise altitude somewhere north or east of the Dutch FIR and has to descend to reach the altitude constraints at ARTIP. To simulate an operative 4D environment, the initial speed schedule of all aircraft was pre-optimized with respect to the EAT at ARTIP using the predicted wind information. The used routes, including any present altitude constraints, are summarized in Table II.

TABLE II
INBOUND ROUTES USED IN CASE STUDY

Route	Waypoint	Altitude Constraint	Value
EELDE1A	EEL	PASS BETWEEN	FL200-260
	ARTIP	PASS BETWEEN	FL70-100
NORKU2A	NORKU	PASS BETWEEN	FL240-FL280
	ARTIP	PASS BETWEEN	FL70-100
REKKEN2A	RKN	PASS BETWEEN	FL200-FL280
	OSKUR	-	-
	ARTIP	PASS BETWEEN	FL70-100

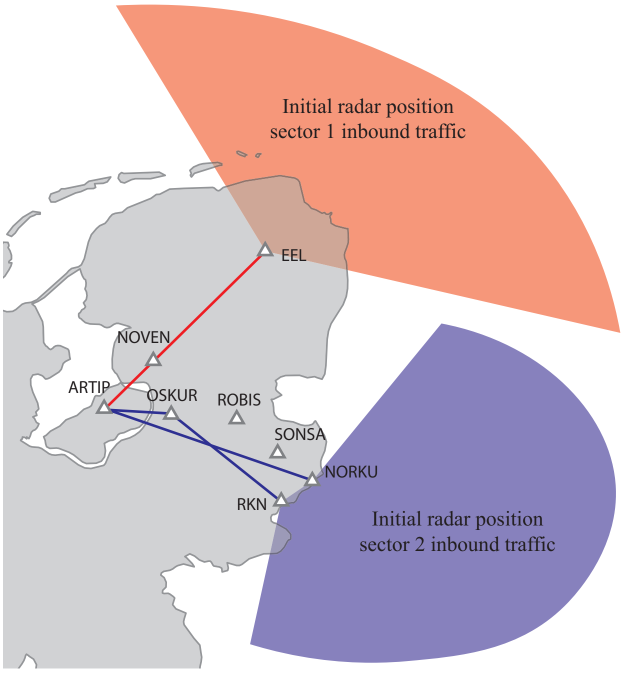

Fig. 29. Scenario used in case study

2) Traffic Mix: The traffic mix was determined from actual initial flight position radar data as recorded by LVNL. To simulate the aircraft, the Base of Aircraft Data (BADA) performance models (v3) were used [13]. Inbound traffic peak samples from between 17:00 and 18:00 UTC were taken to increase the difficulty of the scenarios, as the traffic density is relatively high at this time of day (around 30 inbound aircraft).

3) Wind: The wind information from the specific day and time was taken from the hourly high-resolution weather forecast made by the KNMI. The zero-hour forecast, or *nowcast*, was used as the actual wind field in the simulation. To simulate wind prediction error, a three-hour forecast error was used for all ground-based support tools.

4) Scenario differences: The scenarios were chosen based on their difference in wind prediction error. To illustrate the wind prediction error, the median of all aircraft's 'unedited' RTA deviation per scenario (i.e., had the participants not done anything) is used as a metric. Furthermore, as real-life inbound traffic was chosen, the number of aircraft varied slightly per scenario. An overview of both is presented in Table III.

TABLE III
DIFFERENCES BETWEEN CASE STUDY SCENARIOS

Scenario	Day	Aircraft count [-]	RTA deviation [s]
1	2018-02-04	28	4.92
2	2018-11-02	37	16.15
3	2018-11-11	33	10.45
4	2019-04-26	28	9.12

D. Procedure

After filling out the pre-evaluation questionnaire, participants were provided with a step-by-step interactive training script, guiding them through different training scenarios to get familiarized with the interface and scenarios. During training, participants were allowed to ask questions to increase their understanding of the interface. In the actual measurement runs, participants were continuously observed, but no interaction between the observer and the participant took place. After each run, the observed control strategy was discussed with the participant to confirm the observer's findings.

During the simulation runs, participants were asked to rate their subjective workload at 2-minute scenario time intervals using the Instantaneous Self Assessment (ISA) method, through a 0-100 scale bar on the left side of the interface. Scenario playback speed was set to 4x the actual speed to lower the required time to complete all scenarios, meaning that one scenario took around 20 minutes to complete for every participant.

E. Control Task

Participants were asked to perform the following objectives:

- Guide all incoming traffic towards ARTIP between FL70 and FL100.
- Deliver aircraft as close as possible to their EAT.
- Avoid any LoS between aircraft.

To increase realism of the control space, participants were only allowed to add any lateral waypoints inside the Dutch FIR. Vertical and time-based manipulations were always possible along with the option to remove the entry COP, thus effectively giving an aircraft a Direct To Command (DCT) towards ARTIP. When the entry COP was removed, the altitude constraint was projected abeam onto the new, direct route of the aircraft.

F. Interface

Due to the nature of the traffic scenario, the complexity of the interface and limited training time available, several interface features were disabled or not implemented into the simulation:

- (Disabled) Lateral 4D contract modification (as shown in Figures 25c and 25e) was not allowed, meaning that deviation from ARTIP as the exit waypoint was not possible.
- (Disabled) The geometric descent paths could not be modified, meaning that the only effective altitude control available to the participants was the hand-over altitude at ARTIP and the location of the initial descent segment before the entry COP.
- (Unimplemented) Direct waypoint placement in the VSD (as illustrated in Figure 27b) was not possible. Because of this, the vertical solution space for level segments (see Figure 11a) was also not shown to the participants.

Except for the features described above, participants had full interface availability. As an extra feature, conflict prediction could be done with either the uncertainty model as described in Section II-C or using the nominal CPA only. Participants were free to use whatever mode they preferred at any time.

In the modeling of trajectory uncertainty, an along-track error growth rate of 7 m/s and cross-track error growth rate

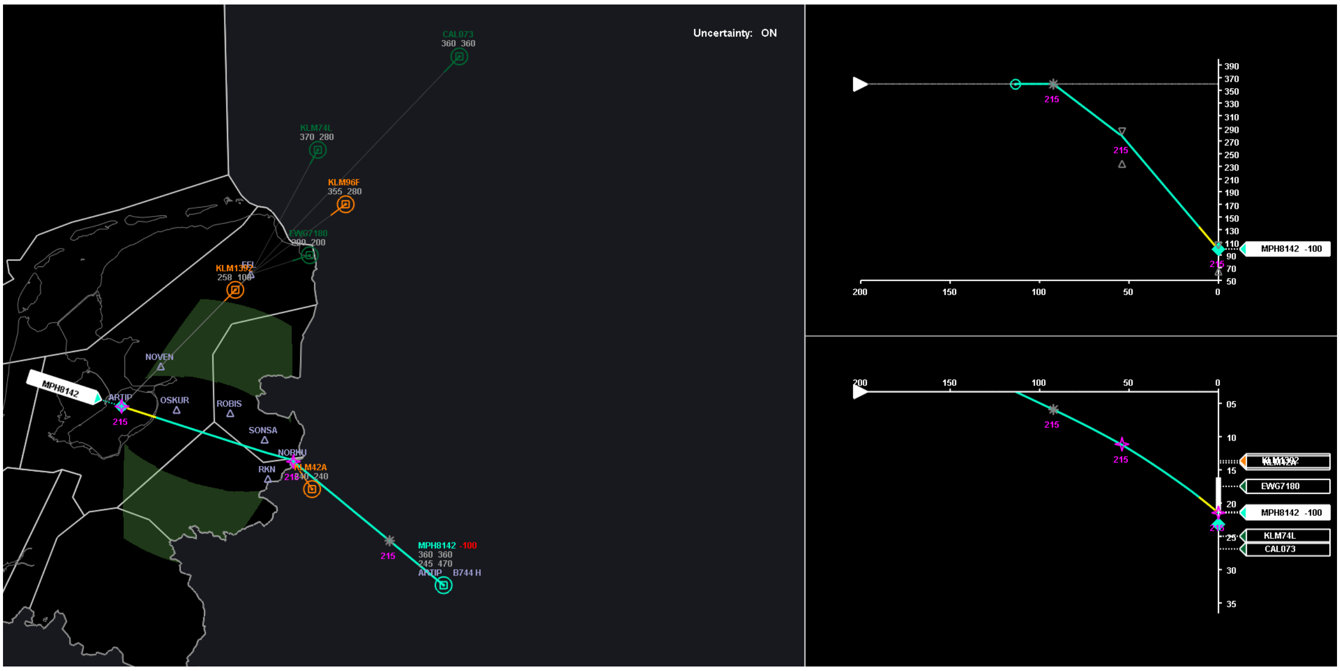

Fig. 30. Screenshot of the interface used during the case study

of 1/150 $[-]$ coupled with a maximum cross-track error of 0.5 nmi was used in all scenarios. Vertical uncertainty was not used, as the geometric descent paths were assumed to be flown error-free.

A screenshot of the interface during one of the case study runs is shown in Figure 30. In all runs, a 24" LCD display with a screen resolution of 1920x1080 was used.

VI. Results

This section is divided into three parts. Firstly, general feedback regarding the interface is presented. Subsequently, the control task adherence results are presented. Lastly, control strategies are discussed. Where possible, participant feedback is compared to gathered simulation data.

A. General Feedback

Figure 31 shows general participant feedback regarding the simulation. Most participants agreed that the air traffic control simulation resembled reality. The behavior of aircraft and traffic mix was found to be realistic. Points of criticism were that no outbound or crossing traffic was present, all aircraft responded directly to any given commands (as no Radio Communications were required) and that the descent profiles were rather unrealistic, as aircraft were immediately cleared to FL100 and no intermediate FLs could be given. One participant indicated he had little situation awareness due to the amount of applied automation, and therefore found it very difficult to tell if the simulation was realistic.

Opinions on the added situation awareness of the new display elements versus the added screen clutter caused by these elements differed. Some participants argued that the added display elements somewhat cluttered the screen while

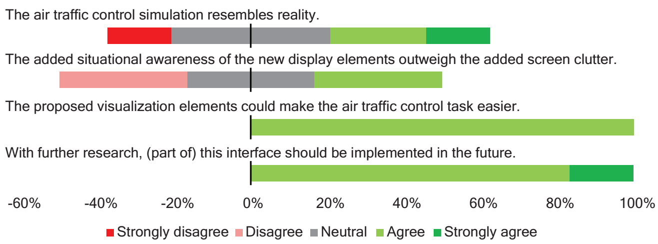

Fig. 31. General participant interface feedback

adding little situation awareness, especially for the solution spaces (always shown with an aircraft selected) and presented wind visualizations (shown only upon the user's preference). The fact that some elements could be turned 'on' or 'off' was found to be positive. Furthermore, participants mentioned that especially around ARTIP, information was sometimes poorly readable due to screen resolution limits and the fact that zooming in on the display was not possible during the scenarios.

All participants were positive on the proposed visualization elements and way of working, mentioning that these types of tools will *'inevitably be required to increase accuracy and predictability'*. Especially the integration of high-resolution wind data into the TP software was found to be very useful.

Participants overall agreed that parts of the interface should be implemented in the future, but that *'balancing of information would be very important and appropriate training would be required'*, hinting at possible unnecessary screen clutter.

B. Control Task

1) RTA Management: Figure 32 shows the participant feedback on the RTA management control task. Participants found it relatively easy to deliver all aircraft at their required EAT. Especially the inclusion of high-resolution wind information into the TP process was found to be very helpful. Negative feedback included the difficulty to read (partly) overlapping aircraft labels in the TSD due to the low screen resolution, and the means of control (through mouse dragging). This sometimes led to frustration, as participants they knew what they wanted to do but could not get the interface to cooperate.

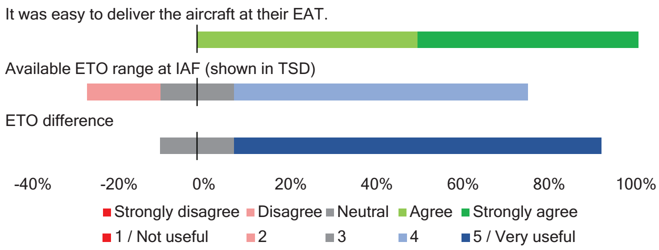

Fig. 32. Participant feedback on EAT adherence

Overall, the available Estimated Time-Over Difference (ETO) range (i.e., the vertical strip shown on the TSD) at the IAF was rated as useful. Participants liked that they could see the reachable timing limits imposed by the aircraft's performance bounds and found the presentation of this information clear.

The ETO difference indication (i.e., the delta shown in the PVD next to the aircraft symbol) was deemed to be very useful. Participants could quickly scan all aircraft for actions needed and used this to fine-tune the aircraft's arrival times. Furthermore, the ETO difference was found to be necessary in order to fulfill this specific control task.

The RTA deviation is shown per scenario for each participant in Figure 33. The 'unedited' RTA deviation (had the participants not done anything) is also shown as a measure of the wind prediction error per scenario. In scenarios with a low wind prediction error, the unedited RTA deviation is low because the initial speed schedule for each aircraft was already computed with the high-resolution wind data taken into account. It should be noted that, as the RTA deviation was rounded to the nearest 5 seconds, participants could only actively manage the RTA deviation at this resolution.

For all scenarios, all participants were able to decrease RTA deviation with respect to the unedited situation with final values ranging between around 0 and 15 seconds, well under the desired long-term LVNL aim of 30 seconds. Two exceptions to this were two aircraft in Scenario 2, which had the largest wind prediction error and aircraft count, with an RTA deviation of more than 30 seconds. Manual inspection of the data and observations showed that the RTA deviations of these aircraft had gone unnoticed for too long (for P2) or was a deliberate choice in tactical conflict management (for P4).

2) Maintaining Separation: Figure 34 shows the obtained participant feedback on maintaining separation between all aircraft. Overall, the estimated conflict probabilities drawn in the solution spaces were found to be helpful in estimating the consequence of one's control actions. This was confirmed by observations throughout the runs, where participants were seen to seek confirmation in proposed waypoint locations by

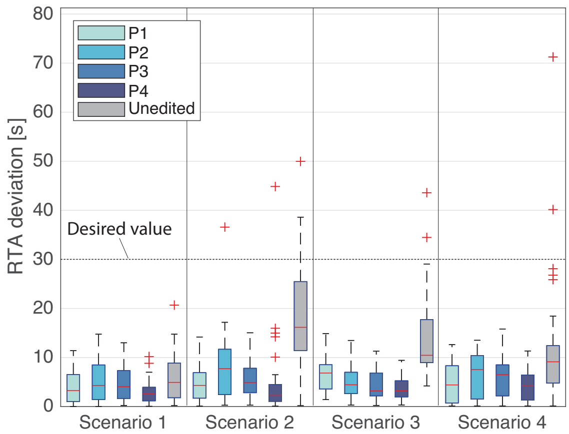

Fig. 33. RTA deviation per aircraft

inspecting the solution spaces. Controllers indicated that their situation awareness increased throughout the runs, and that more training would likely improve the added value of the conflict-based solution spaces.

The aircraft conflict indication when no aircraft was selected was found to be helpful. The route-dependent conflict detection algorithm was seen as an added value. One participant rating the conflict indication algorithm poorly indicated that this was because his trust in the system greatly decreased when a short-term tactical conflict close to ARTIP was missed by the detection algorithm. This likely to be the result of the assumption of uncorrelated position covariance matrices, which is known to be violated when aircraft are in close proximity, and numerical integration limits on the GPU, necessary to manage the computational load.

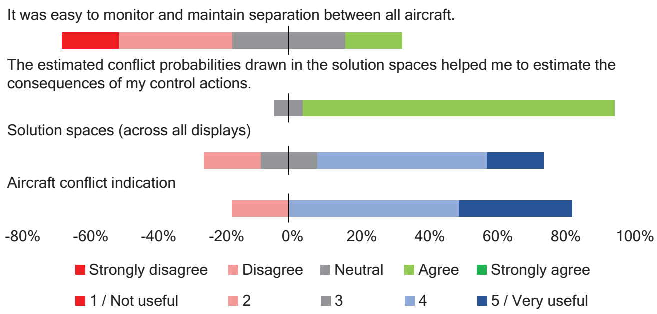

Fig. 34. Participant feedback on maintaining separation

Despite the overall positive feedback on the conflict indication and solution spaces, participants found it difficult to actively monitor and maintain separation between all aircraft. According to the controllers, situation awareness was reduced, especially with regards to vertical separation, as one would have to fully trust the system in conflict management. As mentioned above, this trust greatly decreased when the algorithm turned out to misjudge an emerging conflict.

Furthermore, some participants indicated that the PVD control spaces were sometimes too restrictive, as it was always drawn between consecutive waypoints. Therefore, waypoints in the PVD sometimes had to be removed to yield the 'full' range of available lateral solutions (i.e., the solution space drawn between only the aircraft's radar position and ARTIP) to resolve a conflict.

When inspecting the simulation data, a total of 4 losses of separation were recorded in two of the 16 runs. The locations of these losses of separation are shown geographically in Figure 35. All were found to have occurred closely around ARTIP, where controllers indicted they were required to operate in a more tactical manner to maintain separation. Participants indicated that the relatively low screen resolution and the inability to zoom in on the PVD caused difficulties in managing conflicts close to ARTIP.

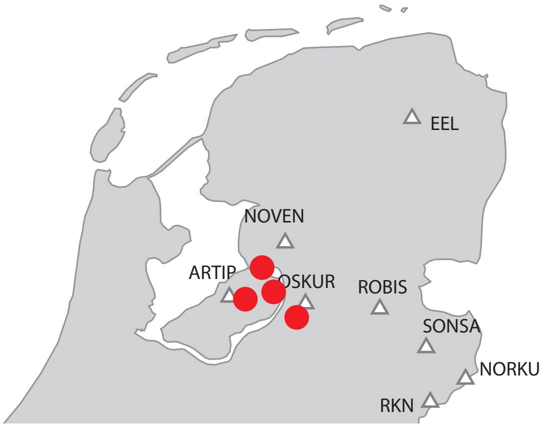

Fig. 35. Geographic location overview of occurred losses of separation

With some participants, remarkable conflict resolutions were observed for two merging aircraft. Participants would try to make one aircraft fly a dog-leg in an attempt to build a sequence. In the strict 4D CONOPS, however, adding track miles to an aircraft's flight plan goes hand-in-hand with a velocity increase to meet the RTA. This caused some confusion for participants in their early runs, although these 'thinking errors' were not observed in later runs. Participants also indicated they understood why they were confused. These events illustrate the necessity for adequate training when moving towards an operational 4D concept, as common practices will have to be adapted.

C. Control Strategies

After each run, participants were asked to briefly summarize their applied control strategy. Furthermore, observations were made during the runs to try and identify the applied control strategies and were discussed with the participants afterwards.

Figure 36 shows participant feedback with regards to the applied strategies. Within the constraints set for the case study (i.e., fixed descent paths), participants indicated that they were able to derive and execute their preferred strategy. Also, although their applied strategy differed greatly from their current working practice, this difference could be attributed to the strict 4D ATC control task as well as the flown geometric descent paths, rather than to being limited by the interface. For some participants, this caused difficulties in answering this question, because they were adopting new strategies while progressing through the runs.

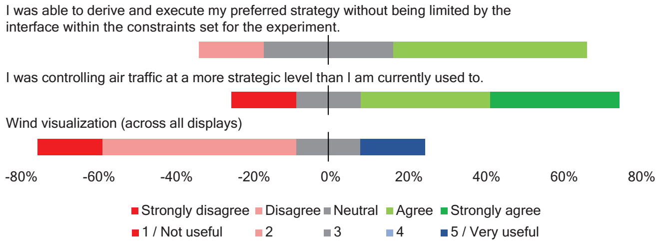

Fig. 36. Participant feedback on applied control strategies

Participants indicated that they were controlling the air traffic at a more strategic level than they are currently used to. The only participant with a negative response here indicated that situation awareness was very low and therefore he did not feel as if he was 'controlling' anything.

The wind visualization was rated as not very useful by the participants, with the main motivation being that the visual information was not needed as wind data were already used in all TP calculations. Participants did indicate that visualization was very helpful, to see the wind field characteristics at the beginning of a run.

When inspecting the gathered data and observations, similar strategies between participants could be identified. Initial structuring of the air traffic streams was done mostly on the PVD, where the entry COP was often removed. This allowed aircraft to fly a direct route to ARTIP, meaning a more efficient trajectory. Besides increased efficiency, participants indicated that this gave them more maneuvering space later on, as more 'excess' speed could be utilized in tactical conflict management, while still respecting the RTA.

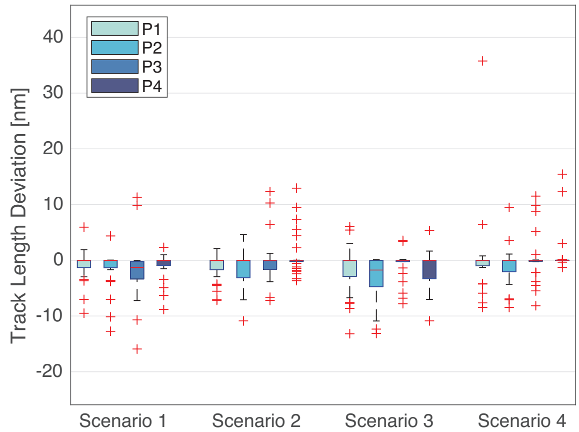

Fig. 37. Track mile deviation with respect to originally planned route per aircraft

Figure 37 shows the deviation of track miles with respect to the originally planned route. The median for all participants in all scenarios was at or below zero, corroborating the frequent removal of the entry COP. Manual inspection of one outlier for P1 in Scenario 4 showed that a large dog-leg, paired with the necessary velocity increase, was added for this aircraft, to eliminate any conflict probability. The other participants applied a similar, but smaller, dog-leg without any resulting LoS, indicating the conservatism of P1's resolution.

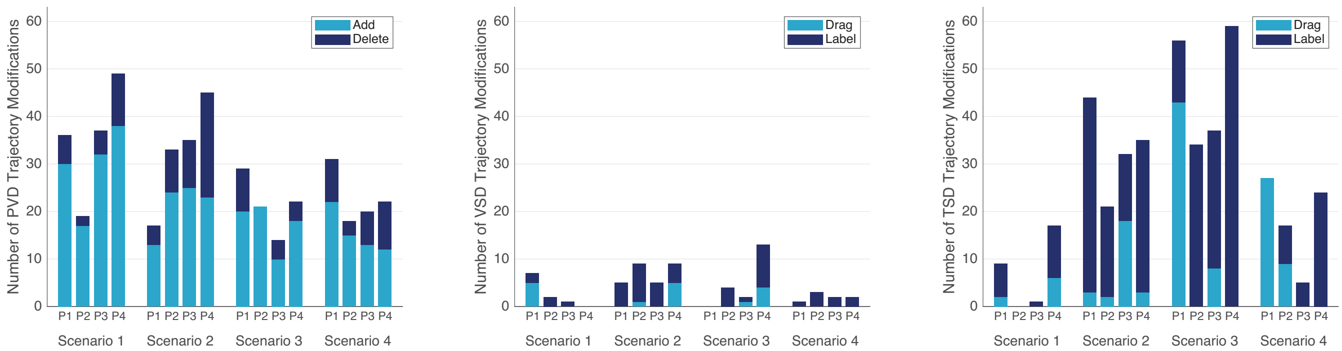

Fig. 38. Overview of given commands per display by all participants

After initial air traffic structuring, arrival times and possible conflicts were actively monitored. When time allowed (i.e., no conflicts requiring immediate action), participants would manage the arrival times using the TSD. If a conflict could not be resolved laterally (e.g., when two aircraft had similar EATs over ARTIP), participants would apply vertical separation using the VSD.

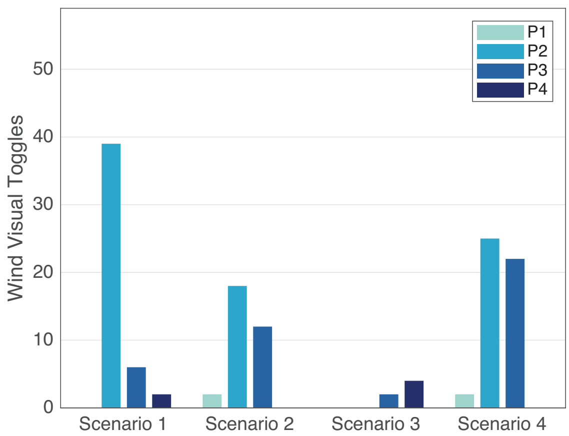

Fig. 39. Participant wind visualization toggle usage

Figure 38 shows the number of trajectory modifications for every screen per participant, including modifications that were made but not executed. The largest number of modifications were made in the PVD and TSD, with the VSD being used considerably less. The number of TSD modifications increased considerably with the increasing wind prediction error (in Scenarios 2 and 3), indicating that the TSD was being used mostly for aircraft ETA adjustments. Within the TSD, some participants modified the trajectory mostly by using the aircraft label, whereas others dragged waypoints itself. This is likely the result of the label being poorly selectable with multiple overlapping labels, in which case dragging the last waypoint would yield the same result. No direct waypoints were added inside the TSD.

In Figure 39, the number of times the wind visualization toggle was used is shown. P2 and P3 frequently used the wind visual toggle, whereas others did not. This does not correspond with the observations and feedback that this toggle was not used much. Manual inspection of the data revealed that these toggles were likely to be unintended, as the SHIFT key needed to do so was located next to the CTRL key needed to enter trajectory manipulation mode. Holding and pressing the SHIFT key would repeatedly trigger the toggle in very rapid fashion, explaining the large number of toggles.

Figure 40 shows the number of times the conflict prediction mode toggle was triggered. Large differences between participants are noted. This corresponds to the observed usage, as P2 and P3 frequently switched between conflict prediction modes, to obtain more information on the nature of impeding conflicts, whereas others chose to work with one mode active throughout most of the simulation.

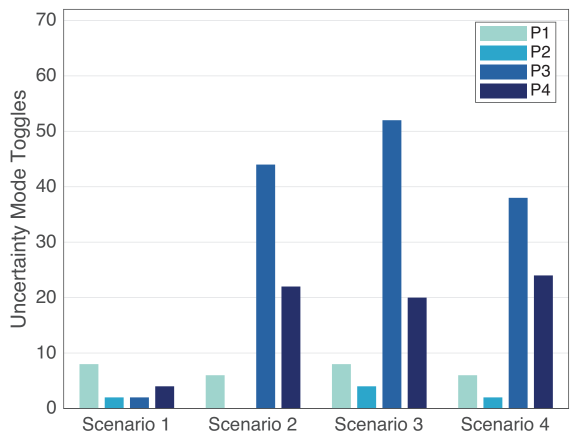

Fig. 40. Participant uncertainty mode toggle usage

P1 and P4 elected to work mostly with uncertainty on, as they felt that this gave a more realistic estimate. In observations, it was noted that some participants chose not to immediately resolve conflicts with a low conflict probability (as they wanted to see how the situation would unfold), whereas others would immediately try to resolve conflicts as soon as conflict probability rose beyond 5% (and the aircraft thus turned yellow).

Figure 41 shows the number of commands given per aircraft per participant for each scenario. The median value for all scenarios does not exceed two commands per aircraft, with several outliers of four or more commands issued. This is the result of multiple SPD commands being issued to the aircraft. Scenarios 2 and 3 contained the largest amount of commands

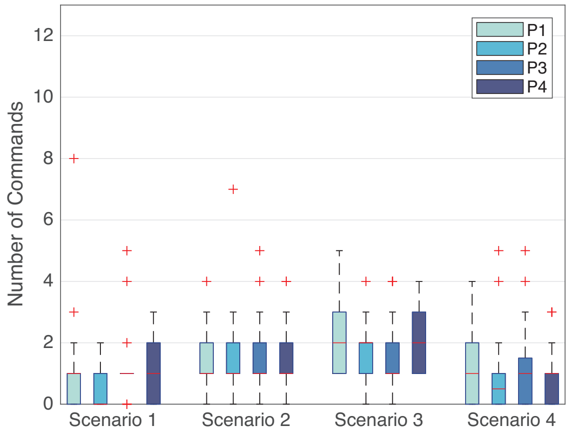

Fig. 41. Number of commands given per aircraft

per aircraft. While this could be caused by the relatively large aircraft count in these scenarios, the large wind prediction error deemed a more likely cause, as the ETA of all aircraft had to be adjusted in these scenarios to ensure RTA adherence.

D. Workload

During the simulation runs, participants were asked to rate their subjective workload. Figure 42 shows the mean of the normalized workload ratings for all participants per scenario.

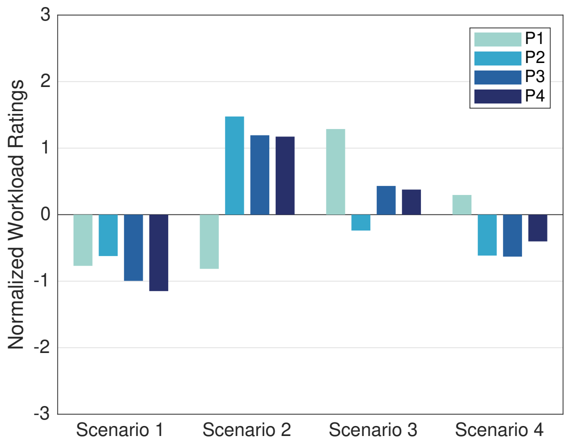

Fig. 42. Normalized workload ratings (Z-scores)

The perceived workload in Scenarios 2 and 3 was higher than in Scenarios 1 and 4, with Scenario 2 having the highest relative workload. Although no statistically significant conclusions are drawn due to the low number of participants, the wind prediction error and the perceived workload appeared to be related. An exception to this is the workload of P1, which was considerably lower in Scenario 2. This can be explained by the fact that this participant was very early in noticing the geographic characteristics of the wind prediction error and pre-adjusted arrival times with this error in mind, likely lowering the workload.

To illustrate the impact of the wind prediction error in terms of user activity, Figures 43 and 44 show the mouse movements of one participant in Scenarios 1 and 2, respectively. Considerably more mouse activity was observed in both the PVD and the TSD in Scenario 2 when compared to Scenario 1. While the increase in the PVD could also be caused by the slightly higher aircraft count in Scenario 2, the additional movements on the vertical TSD axis indicate frequent ETA adjustment. This is likely the result of the larger wind prediction error, leading to an increase in perceived workload.

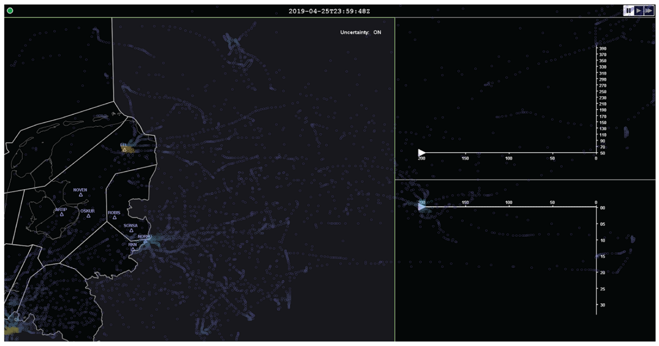

Fig. 43. Heatmap of mouse activity of P2 in Scenario 1

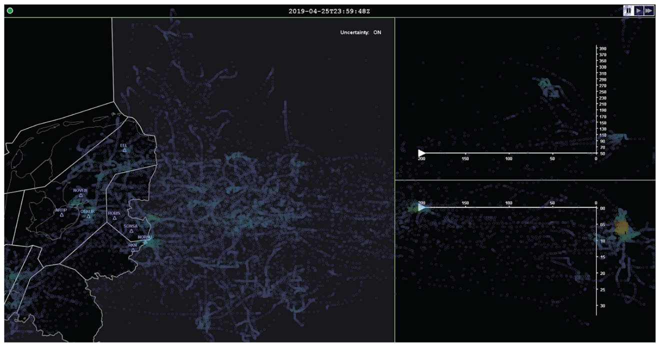

Fig. 44. Heatmap of mouse activity of P2 in Scenario 2

VII. Discussion

The discussion is aimed at summarizing the main research areas: the CONOPS, the interface and the evaluation.

A. Concept of Operations

In the assumed CONOPS, the RTA control loop is closed on the ground. While this is deemed beneficial for predictability from an ATC point of view, the situation where an aircraft FMS takes responsibility for adhering to the RTA should also be considered. With FMS RTA functionality enabled, the uncertainty model as implemented would have to be revised, as a continuous along-track error build-up could no longer be assumed. The error propagation rates would become dependent on the implementation of the RTA functionality within the FMS. Further research would be required to assess this for different wind conditions and FMS settings per FMS manufacturer. It is reiterated that the strength of the proposed CONOPS, where the RTA control loop is closed on the ground, lies in the fact that this research is not needed, and therefore predictability for all aircraft is high, since the FMS implementation is eliminated as a source of uncertainty.

To compute the shape of the solution spaces, the RTA is used as a fixed constraint. While this is a reasonable assumption in inbound traffic, all having to be sequenced to a fixed end point, more freedom exists for other types of traffic. In outbound and en-route scenarios, the RTA could also be loosened for strategic ATC purposes, with multi-sector planning procedures updating 4D flight plans along the route. In this case, upper and lower ETA limits could also be taken into account for the interface and solution spaces could be designed accordingly.

Currently, the solution spaces are based on 4D waypoints, as the metering fix at each waypoint is used to compute these. In reality, however, 4D flight plans and COPs often have a velocity constraint defined in addition to this. In the real-life case study scenario, for example, aircraft have to be handed over to Approach Control (APP) over ARTIP with an IAS of 250 kts. Implementing velocity constraints as part of the 4D contract would increase the computational complexity of the solution space, but would not necessarily affect the interface presentation itself. While the control space would change, especially for shorter trajectories, this is not foreseen to form a problem for the user. Further research would become needed to confirm this, however.

To accurately predict climb and descent performance, assumptions on the chosen climb and descent profiles are necessary. In the assumed CONOPS, climbing and descending is always done by means of a Flight Level Change (FLCH) or geometric path, respectively. The geometric descent path is chosen because of the high spatial predictability, yielding temporal uncertainty as the only unknown. Especially in descent, situation-dependent settings are used in practice. The implementation of these more complex Vertical Navigation (VNAV)-based descent paths would affect the TP process, as more spatial uncertainty in descent would be present. This would impact the uncertainty model.

B. Interface

Currently, all solution spaces are drawn between consecutive waypoints. This can cause possible conflict resolutions to be missed by the interface, as the drawn control space is currently more restrictive than it needs to be. The implementation of floating waypoints or the option to draw solution spaces between more than one waypoint could address this issue. This is something already experimented with in a previous display adopting the solution space concept for a cockpit display [37], as illustrated in Figure 45. In this design, the solution space is drawn between an initial point and a lateral position fix. Velocity-based and altitude constraints are shown on the display, but the lateral solution space is not drawn between these consecutive points, as they are not fixed laterally.

Within solution spaces, trajectory uncertainty is currently taken into account in conflict prediction, but the control space

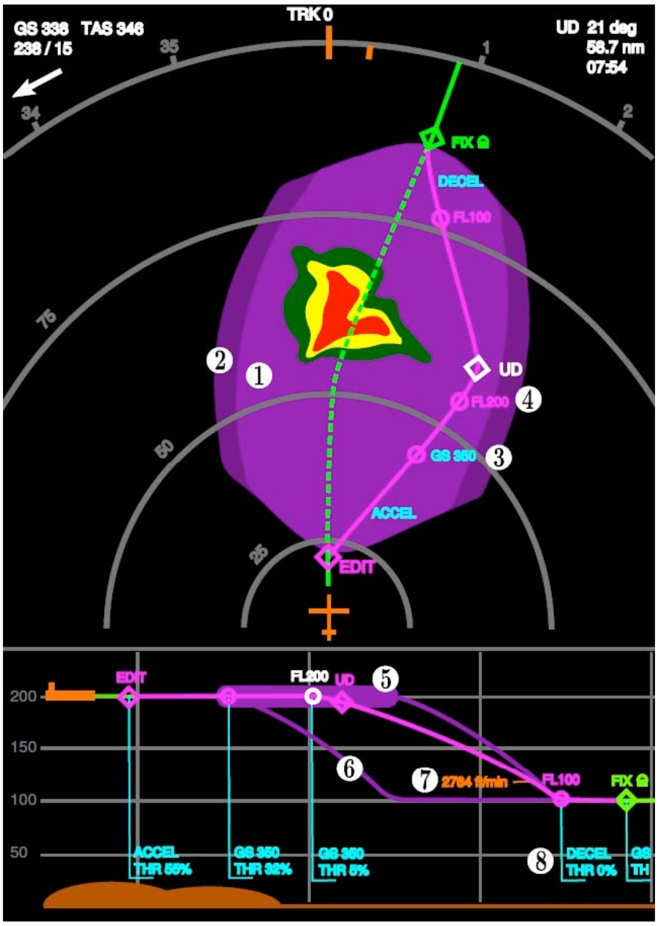

Fig. 45. Display design of a cockpit-based 4D trajectory revision interface (taken from [37])

(i.e., the green area) is based solely on the nominal trajectory. This is not fully correct, as the outer boundaries of the control space are often bounded by the aircraft performance envelope. The wind prediction error could therefore cause the aircraft to fail to reach its RTA at the next waypoint, although a waypoint within the green control space had been selected. The impact of this shortcoming is relatively small, as controllers tend to minimize path deviation to increase efficiency. Therefore, the absolute limits of the performance envelope are not often reached.

The types of trajectory uncertainty currently implemented in the interface are limited, as the uncertainty now only comes from the wind prediction error. In reality, more sources of trajectory uncertainty exist, the most noticeable ones being aircraft weight and pilot intent [12]. The absence of these sources makes the control task easier, because aircraft behave in a more predictable way. Because the focus of this research was to try to visualize trajectory uncertainty *in some form* in the existing interface, the presence of solely the wind prediction error as trajectory uncertainty source sufficed. This greatly simplified the calculation process and allowed for the uncertainty model of Prandini et al. [26] to be used. Mapping all stochastic causes onto the resulting output position distribution at any future point is a complex and time-consuming process. To further increase the realism of the interface and corresponding simulation environment, however, including more sources of trajectory uncertainty remains an important element.

When solving a conflict, controllers often issue commands to two aircraft simultaneously to form a cooperative solution. This concept is currently not supported very well by the interface, where solution spaces are based on resolving conflicts from the point of view of the selected aircraft only. Although this approach works from an ATC point of view, it could be undesirable to make a large trajectory modification for one aircraft only, while two smaller adjustments for two aircraft would also suffice. This could be implemented by including a probing function with multiple aircraft, as is also discussed in previous work by Nagaraj et al. [38], instead of only probing a single trajectory. Doing so would likely increase the number of cooperative solutions formed.

In the proposed CONOPS, the RTA control loop is closed on the ground, but the task division of ETA management between human and machine is not specified. In the current interface, this control task lies solely with the operator, as action is required to correct RTA deviation and adjust an aircraft's speed schedule. In the case study results, signs of increased workload and lowered task performance could be noticed with increasing wind prediction error. Shifting (part of) this control task towards the computer could have a beneficial effect on task performance and perceived workload. It could, however, also result in a loss of overview and a loss of acceptance, as the computer would autonomously take decisions, taking away some form of direct control from the ATCo. Further research would be required to investigate the effects of this new task division.

One might argue that the solution spaces could also be used as inputs for fully autonomous decision-making algorithms. While this could be possible, this new breakdown of roles between the human operator and automation would not be desirable. Supervision of the algorithm would be required, placing the human at a more distant role when compared to direct hands-on control. This could lead to a reduced understanding of the work domain and ultimately to skill degradation and reduced task performance [39].

C. Case Study

Several useful results were obtained from the case study. First and foremost, it should be mentioned that the case study was intended to serve as a 'proof of concept' of the interface in a complex, realistic scenario with mixed tactical-strategic characteristics. To that end, control task adherence and controller acceptance are considered the most important result areas.

Perhaps the most important result is that the two-fold control task (conflict and ETA management) can be executed successfully without any major problems. To illustrate the significance of the achieved RTA accuracy, the actual RTA deviation for each of the flights is presented in Figure 46. A large part of this difference can be attributed to the inclusion of high-resolution wind data directly into the computation of an aircraft's speed schedule in the case study, something that is not done in current working practice. Although the actual flights have been impacted by many more factors than were present in the case study (e.g., more types of uncertainty, other traffic) and a direct quantitative comparison is there difficult to justify, the achieved RTA accuracy in the case study is considered to be extremely good.

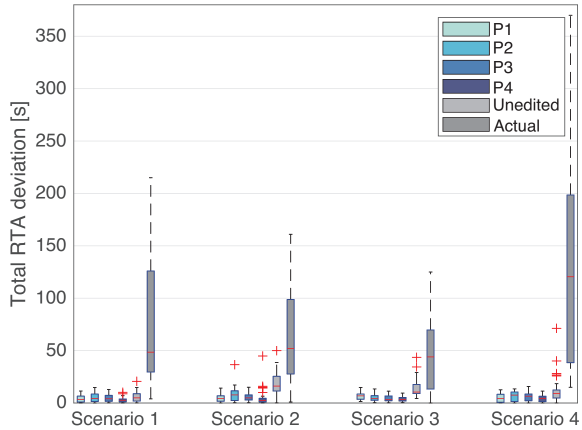

Fig. 46. RTA deviation per aircraft of actual and case study data

The interaction between both decision processes worked as expected, with participants continuously switching between the two control tasks depending on the necessary action. The LoSs that arose, were all in the tactical work domain and multiple factors that contributed to their creation can be pointed out. Besides scenario playback speed and screen size (both discussed later in this section), the type of conflict prediction model used plays a role. The implemented model used is for Medium-Term Conflict Detection (MTCD) purposes, whereas in situations with a small TTC, Short-Term Conflict Alert (STCA) algorithms would ideally be implemented. With some controllers, the conflict prediction model misjudged several situations with a low TTC, immediately causing controller distrust in the system. With a better conflict prediction algorithm implementing STCA methods, this issue would likely be resolved.

The conflict indication thresholds for the case study were set at 5%, 50% and 90% for green, yellow, orange and red colors, respectively. While immediate action was therefore not required when an aircraft's conflict indication turned yellow, some controllers saw any color other than green as an immediate trigger for action. While not forming safety-related issues, this has potentially increased the number of commands given to each aircraft and therefore reduced the overall efficiency. Altering conflict indication thresholds would largely impact controller behavior. Further research would become required to assess the effect of the threshold values. In addition to this, the number of thresholds (and therefore the number of different colors used) would also likely affect controller behavior.

Interestingly, wind visualization was not deemed very useful by the participants and was also not purposely used much during the simulation runs. This is likely caused by the relatively small scale of the controlled sector, causing the solution spaces to look similar in all situations. Therefore, the means-ends coupling as intended was not needed in the scenarios. Because users had the freedom to turn the visualization on or off, this had little impact on the results. In larger-scale en-route scenarios, in which more variation in along-track wind is present, wind visualization could potentially be used more by participants, as solution spaces might take on less intuitive shapes. This would have to be confirmed in a controlled experimental setting.

In the chosen traffic scenarios, only inbound traffic was present. This was done deliberately to reduce the complexity of the scenarios, given the limited training time all participants had. It does, however, affect the realism of each scenario as crossing and outbound traffic is present in the actual traffic scenarios during inbound peaks. In real-life, the lateral manipulation space would therefore likely be smaller, making the scenario more complex and therefore increasing perceived workload.

For time-management purposes, scenario speed for all traffic scenarios was set to 4x the actual speed. This makes the control task harder, as decisions have to be made faster than in the real-life situation, allowing the participants less time to get a good overview and mental picture of all traffic currently in the controlled airspace. This has likely resulted in several conflict resolutions that would have been handled differently, had there been more time available to carefully inspect all available options.

Furthermore, the increased scenario speed has likely altered the participants' perception of the number of commands given per aircraft. During the runs, participants mentioned that they felt as if they were giving more instructions than usual. Figure 47 compares the number of commands given by participants to the number of commands given during the actual flights. Although a quantitative comparison of the two should again be made with caution, this figure illustrates that the number of issued commands in the case study is, actually, relatively low.

Something that was mentioned much by participants was the relatively small screen size. For computational reasons, the case study was run on a screen with a 1920x1080 resolution. This meant that information was sometimes poorly readable on the screen, especially when aircraft were located close together. This 'handicap' for the participants resulted in frustration, but also in some difficulties when operating in the tactical work domain (often close to ARTIP). It is likely that the LoSs were caused partly by this small screen resolution. Improving computational power would solve this and should not be a problem, since the simulation was run on a standard consumer laptop during the case study.

In the case study, the geometric angle used in the geometric descent was set to be non-editable, resulting in fixed vertical trajectories after the entry COP. This meant that controllers had little freedom in altering vertical paths, which possibly also caused the limited number of trajectory modifications made using the VSD. Some controllers mentioned that they felt limited by the fact that they could not select an intermediate flight level during the descent. Having this option available would imply a change in descent angle, which itself is limited at a maximum, depending on the aircraft type and atmospheric conditions. The descent angle limits would have to be made visible to the user to allow for this type of trajectory modifications.

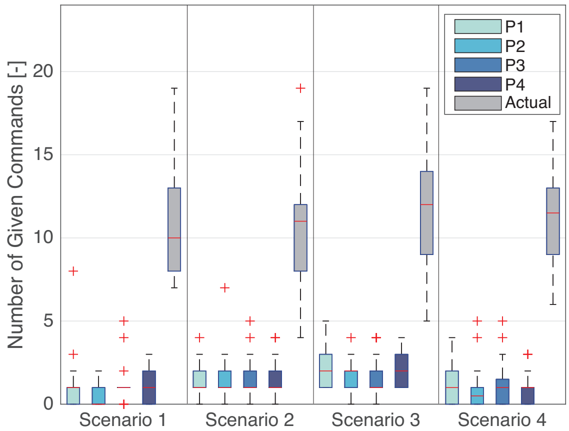

Fig. 47. Number of given commands per aircraft in actual and case study data

To support the participant feedback on the interface, gathered simulation data were used. While six participants in total worked with the interface extensively enough to give their feedback, the data of only four were used to support this feedback. Some opinions presented in the feedback results are therefore not reflected in the data. Although this means that a one-to-one coupling of the feedback and the simulation data is not possible, the data still directly supports two-thirds of the presented operator feedback. This is deemed enough to be able to draw conclusions on the correlation between both, also because operators were united in most of their feedback.

To conclude this discussion, it is mentioned that the decision for the chosen inbound traffic scenarios was motivated by the high familiarity of these scenarios to the expert operators. The aim of this approach was to obtain high-quality feedback on solely the interface and to shorten the required training time, as the operators were already familiar with the airspace and traffic mix. While the results show positive signs in terms of controller acceptance and control task adherence, the case study in fact validates only part of the interface redesign, as several interface elements were disabled as a result of the chosen scenarios (see Section V-F). To validate the complete interface and assumed CONOPS, an experiment with a more complex traffic scenario, including en-route and outbound traffic, would become necessary. This would, however, require extensive participant training, as the complete interface takes time to work with efficiently due to its increased complexity.

VIII. Conclusions

To increase the maturity of the existing solution space concept for 4D trajectory management, effects of wind and trajectory uncertainty have been implemented into the interface.

The focus of this redesign has been on managing the increase in interface complexity, while aiming to retain controller acceptance and ultimately the viability of the concept.

The inclusion of trajectory uncertainty has implied a change in user interaction, as active arrival time management has become an extra control task. As wind affects an aircraft's performance envelope, the resulting solution spaces in every dimension have been impacted. Adding both effects has led to an almost complete interface redesign, where special care has been taken to ensure that information is presented consistently across the various displays present in the interface.

To evaluate the redesigned interface, a case study was performed using six professional air traffic controllers in a realistic 4D inbound peak traffic scenario within the Dutch FIR, where a mixed tactical-strategic form of air traffic control is required. Results have indicated that controllers are able to combine the two-fold conflict and arrival management control task using their own preferred strategy. Overall, the interface gained controllers' acceptance, although maintaining situation awareness and general trust in the system will continue to form an important aspect for future research.

The aim of this work was to unite control flexibility and predictability in 4D trajectory management in an operating environment centered around the human controller. The concept and results show that, despite the increased complexity in both computational load and display elements, this is possible, even in a highly complex, realistic operational setting. The next step in developing the interface would be to test the full interface in a controlled en-route scenario, where all newly developed display elements would be fully active, although the current work has also shown that extensive training would be required to efficiently interact with the full interface.

Acknowledgment

The author would like to thank LVNL and Ferway for providing the required air traffic and meteorological data needed to perform the case study. Without this, the level of realism and complexity strived for in the case study setup would not have been possible. Furthermore, the author would like to explicitly thank all participants.

References

[1] Federal Aviation Administration, "NextGen Implementation Plan," 2016. [Online]. Available: https://www.faa.gov/nextgen/media/NextGen_Implementation_Plan-2016.pdf

[2] EUROCONTROL, "Trajectory Based Operations (TBO): Central to the Latest ATM Concepts," 2017. [Online]. Available: https://www.eurocontrol.int/news/trajectory-based-operations-tbo-central-latest-atm-concepts

[3] T. Prevot, J. R. Homola, L. H. Martin, J. S. Mercer, and C. D. Cabrall, "Toward Automated Air Traffic Control - Investigating a Fundamental Paradigm Shift in Human/Systems Interaction," *International Journal of Human-Computer Interaction*, vol. 28, no. 2, pp. 77–98, 2012.

[4] M. Bekier, B. R. Molesworth, and A. Williamson, "Tipping Point: The Narrow Path Between Automation Acceptance and Rejection in Air Traffic Management," *Safety Science*, vol. 50, no. 2, pp. 259–265, 2012.

[5] C. Westin, C. Borst, and B. Hilburn, "Strategic Conformance: Overcoming Acceptance Issues of Decision Aiding Automation?" *IEEE Transactions on Human-Machine Systems*, vol. 46, no. 1, pp. 41–52, 2016.

[6] M. M. van Paassen, C. Borst, M. Mulder, R. E. Klomp, P. van Leeuwen, and M. Mooij, "Designing for Shared Cognition in Air Traffic Management," *Journal of Aerospace Operations*, vol. 2, no. 1-2, pp. 39–51, 2013.

[7] R. E. Klomp, C. Borst, M. M. van Paassen, and M. Mulder, "Expertise Level, Control Strategies, and Robustness in Future Air Traffic Control Decision Aiding," *IEEE Transactions on Human-Machine Systems*, vol. 46, no. 2, pp. 255–266, 2016.

[8] C. Borst, J. M. Flach, and J. Ellerbroek, "Beyond Ecological Interface Design: Lessons From Concerns and Misconceptions," *IEEE Transactions on Human-Machine Systems*, vol. 45, no. 2, pp. 164–175, 2015.

[9] SESAR Consortium, "The ATM Target Concept," SESAR Consortium, Toulouse, France, SESAR Definition Phase D3: DLM-0612-001-02-00, 2007.

[10] D. De Smedt and G. Berz, "Study of the Required Time of Arrival Function of Current FMS in an ATM Context," *26th Digital Avionics Systems Conference, Dallas, TX*, pp. 1.D.5–1–1.D.5–10, 2007.

[11] M. D. McPartland, M. J. Sandberg, C. Edwards, T. L. Teller, S. W. Troxel, and T. G. Reynolds, "Wind Information Requirements for NextGen Applications Phase 3 Final Report," Massachusetts Institute of Technology, Lexington, MA, Project Report ATC-422, 2014.

[12] S. Torres, "Trajectory Accuracy Sensitivity to Modeling Factors," *15th AIAA Aviation Technology, Integration, and Operations Conference, Dallas, TX*, no. AIAA 2015–2599, 2015.

[13] EUROCONTROL Experimental Centre, "User Manual for the Base of Aircraft Data," EUROCONTROL, Brussels, Belgium, Technical Report No. 2010/003, Rev. 3.8, 2010.

[14] K. Tong, E. G. Schoemig, D. A. Boyle, J. Scharl, and A. Haraldsdottir, "Descent Profile Options for Continuous Descent Arrival Procedures within 3d Path Concept," *26th Digital Avionics Systems Conference, Dallas, TX*, pp. 3.A.3–1–3.A.3–11, 2007. [Online]. Available: http://ieeexplore.ieee.org/document/4391872/

[15] G. J. J. Ruijgrok, *Elements of Airplane Performance*, 2nd ed. Delft, The Netherlands: VSSD, 2009.

[16] E. J. Casado Magaña, "Trajectory Prediction Uncertainty Modelling for Air Traffic Management," Ph.D. dissertation, University of Glasgow, Glasgow, Scotland, 2016. [Online]. Available: http://theses.gla.ac.uk/7700/

[17] S. Mondoloni, S. Swierstra, and M. Paglione, "Assessing Trajectory Prediction Performance - Metrics Definition," *24th Digital Avionics Systems Conference, Washington, D.C.*, pp. 3.C.1–1–3.C.1–13, 2005.

[18] P. Weitz, "Determination and Visualization of Uncertainties in 4D-Trajectory Prediction," *2013 Integrated Communications, Navigation and Surveillance Conference (ICNS), Herndon, VI*, 2013.

[19] E. J. Casado Magaña, C. Goodchild, and M. A. Vilaplana, "Identification and Initial Characterization of Sources of Uncertainty Affecting the Performance of Future Trajectory Management Automation Systems," *Proceedings of the 2nd International Conference on Application and Theory of Automation in Command and Control Systems, London, United Kingdom*, pp. 170–175, 2012. [Online]. Available: https://dl.acm.org/citation.cfm?id=2325699

[20] S. Torres, "Determination and Ranking of Trajectory Accuracy Factors," *29th Digital Avionics Systems Conference, Salt Lake City, UT*, pp. 1.C.1–1–1.C.1–12, 2010.

[21] S. Mondoloni and I. Bayraktutar, "Impact of Factors, Conditions and Metrics on Trajectory Prediction Accuracy," *6th USA/Europe ATM R&D Seminar, Baltimore, MD*, 2005. [Online]. Available: http://atm-seminar-97.eurocontrol.fr/past-seminars/6th-seminar-baltimore-md-usa-june-2005/papers/paper_062

[22] A. Warren, "Trajectory Prediction Concepts for Next Generation Air Traffic Management," *3rd USA/Europe Air Traffic Management R&D Seminar, Napoli, Italy*, 2000. [Online]. Available: http://citeseerx.ist.psu.edu/viewdoc/download;jsessionid=CF17AA2DBB4F1A919401AB48AB6547CE?doi=10.1.1.473.9089\&rep=rep1\&type=pdf

[23] ICAO, "Managing Unpredictable Evolution in Trajectory Based Operations," International Civil Aviation Organisation, Toulouse, France, ATMRPP-WG/WHL/4-WP/601, 2014.

[24] ICAO, "Time Adherence in TBO," International Civil Aviation Organisation, Montreal, Canada, ATMRPP-WG/27-WP/636, 2014. [Online]. Available: http://www.sesarju.eu/sites/default/files/documents/reports/WP636_Trajectory_adherence_in_TBO.pdf?issuusl=ignore

[25] L. C. Yang and J. K. Kuchar, "Using Intent Information in Probabilistic Conflict Analysis," *Guidance, Navigation, and Control Conference and Exhibit, Boston, MA*, no. A98–37082, 1998.

[26] M. Prandini, J. Hu, J. Lygeros, and S. Sastry, "A Probabilistic Approach to Aircraft Conflict Detection," *IEEE Transactions on Intelligent Transportation Systems*, vol. 1, no. 4, pp. 199–220, 2000.

[27] J. Hu, M. Prandini, and S. Sastry, "Aircraft Conflict Detection in Presence of Spatially Correlated Wind Perturbations," *AIAA Guidance, Navigation, and Control Conference and Exhibit, Austin, TX*, no. AIAA 2003–5339, 2003.

[28] G. Chaloulos and J. Lygeros, "Effect of Wind Correlation on Aircraft Conflict Probability," *Journal of Guidance, Control, and Dynamics*, vol. 30, no. 6, pp. 1742–1752, 2007.

[29] R. E. Klomp, E. J. P. Riegman, C. Borst, M. Mulder, and M. M. van Paassen, "Solution Space Concept: Human-Machine Interface for 4D Trajectory Management," *Thirteenth USA/Europe Air Traffic Management Research and Development Seminar (ATM2019), Vienna, Austria*, 2019.

[30] E. J. P. Riegman, "Effects of Vertical Situation Diagram in 4D Trajectory Management Interface," Master's thesis, Delft University of Technology, Delft, The Netherlands, 2018, unpublished. [Online]. Available: http://resolver.tudelft.nl/uuid:89e072c6-e179-4a17-98ac-3e06909692ff

[31] J. Rasmussen, "Skills, Rules, and Knowledge; Signals, Signs, and Symbols, and Other Distinctions in Human Performance Models," *IEEE Transactions on Systems, Man, and Cybernetics*, vol. SMC-13, no. 3, pp. 257–266, 1983.

[32] M. R. Endsley, "Toward a Theory of Situation Awareness in Dynamic Systems," *Human Factors: The Journal of the Human Factors and Ergonomics Society*, vol. 37, no. 1, pp. 32–64, 1995.

[33] C. D. Wickens, J. Lee, Y. Liu, and S. G. Baker, *An Introduction to Human Factors Engineering*, 2nd ed. Upper Saddle River, New Jersey: Pearson, 2004.

[34] R. E. Klomp, C. Borst, M. Mulder, and G. Praetorius, "Ecological Interface Design: Control Space Robustness in Future Trajectory-Based Air Traffic Control Decision Support," *2014 IEEE International Conference on Systems, Man, and Cybernetics (SMC), San Diego, CA*, pp. 329–334, 2014.

[35] D. D. Woods, "Visual Mmomentum: A Concept to Improve the Cognitive Coupling of Person and Computer," *International Journal of Man-Machine Studies*, vol. 21, no. 3, pp. 229–244, 1984.

[36] R. E. Klomp, "Solution Space Concept for Trajectory-Based Air Traffic Control: An Ecological Approach," Ph.D. dissertation, Delft University of Technology, Delft, The Netherlands, 2020, to be published.

[37] B. J. A. van Marwijk, C. Borst, M. Mulder, M. Mulder, and M. M. van Paassen, "Supporting 4D Trajectory Revisions on the Flight Deck: Design of a Human–Machine Interface," *The International Journal of Aviation Psychology*, vol. 21, no. 1, pp. 35–61, 2011.

[38] R. Nagaraj, R. E. Klomp, C. Borst, M. M. v. Paassen, and M. Mulder, "Exploring the Potential Benefits of Multi-Aircraft Trajectory Manipulation in Future Air Traffic Control," *2019 IEEE International Conference on Systems, Man and Cybernetics (SMC)*, pp. 3699–3704, 2019.

[39] L. Bainbridge, "Ironies of Automation," *Automatica*, vol. 19, no. 6, pp. 775–779, 1983.

Part II

Preliminary Thesis Report [1]

[1] The content in this part has been graded as part of the preliminary thesis report under AE4020.

Introduction

Research Background & Problem Statement

In the coming years, global air traffic numbers are projected to rise (STATFOR Team, 2018). To facilitate this increase in air traffic, the Air Traffic Management (ATM) system will need to change. Currently, both the Single European Sky ATM Research (SESAR) program (carried out by EUROCONTROL) and the Next Generation Air Transportation System (NextGen) program (led by the Federal Aviation Administration (FAA)) envision an ATM system governed by Four-Dimensional (4D) aircraft trajectory management (i.e., in time and space) (European Commission & EUROCONTROL, 2015; Federal Aviation Administration, 2016). In 4D flight, both the aircraft's position and time are pre-computed, allowing for an airspace in which air traffic flows are optimized and can be de-conflicted before operation.

When these pre-planned trajectories are subsequently executed, unforeseen airspace perturbations, such as weather, sequencing and changing airspace constraints, will inevitably require small changes in the trajectories to be made by the Air Traffic Controller (ATCo). This *perturbation management* control task will consist of ensuring a safe airspace *while adhering to the strict time constraints imposed by the 4D flight plan.* This will increase the complexity of the ATCo work domain, as these constraints (and relations between them) will have to be more strictly adhered to than in the current situation. Both the SESAR and NextGen program therefore foresee a fundamental change in the Air Traffic Control (ATC) environment, where the ATCo is aided by high-level automated Decision Support Tools (DSTs).

Automation for the ATCo will, however, have to be implemented with caution. Previous efforts to design computer-based automation tools have not been well accepted by the ATC community (Westin, Borst, & Hilburn, 2015). Furthermore, it is known that wrongly applied automation may result in a reduced understanding of the system (Bainbridge, 1983), and ultimately worse task performance in safety critical situations. Therefore, DSTs with joint human-automation cognition are currently being researched with the aim to aid, rather than replace, the human.

A concept Human-Machine Interface (HMI) for 4D trajectory management has been designed using the principles of Ecological Interface Design (EID) and initially validated at Delft University of Technology (DUT). Using the known Required Time of Arrival (RTA) from the 4D flight plan as a fixed constraint, rerouting possibilities are presented to the ATCo, creating the so-called Travel Space Representation (TSR). The idea behind this approach is to leave the ATCo in direct control of the actions to take, while supporting him or her in the decision-making process.

Previous experiments carried out with the TSR interface show positive results in terms of controller workload and task performance (Klomp, n.d.). Various essential air traffic and environmental elements, however, the most noticeable ones being wind and trajectory uncertainty, are still to be integrated into both the interface and corresponding simulation environment. Their absence does not only make the current interface less realistic, but also less complex than it would be in real-world operation. Since added interface complexity might result in a loss of overview, this forms a drawback for the TSR interface in its current form, as also follows from conversations with Air Traffic Control the Netherlands (LVNL).

Additional research is therefore needed to investigate the impact of integrating both wind and trajectory uncertainty information into the interface. Behind this lies the question to what extent complexity can be added to an EID-inspired interface, where work-domain constraints are ideally mapped one-to-one onto the resulting display, without it becoming too cluttered and eventually unworkable for the operator.

Aims & Objectives

Research Objectives

Following the research background and problem statement, the primary research objective is set to be:

To contribute to the development of a 4D ATC decision support interface by investigating the integration of wind and trajectory uncertainty information into such an interface.

This objective can be divided into three secondary objectives. The first will be to gain a comprehensive understanding of the influence of both wind and trajectory uncertainty on 4D trajectory management by simulating their effects on the current interface using known models. The second will be to thoroughly evaluate the rationale behind the current TSR interface and changes to be made to include wind and trajectory uncertainty by performing a Cognitive Work Analysis (CWA). The third and last secondary objective will be to quantify the effects of the added components on measured control strategies, workload and task performance by conducting a human-in-the-loop validation experiment using the final interface.

Scope

In order to accomplish the mentioned objectives, a scope has been defined to frame the research to be conducted during this thesis. While no specific type of ATC field is yet determined for the TSR, the focus for this research will be set on Area Control (ACC). This restricts the types of traffic to be handled when using the interface. Furthermore, the current TSR interface developed at DUT will serve as a starting point for this research, as the interface has already successfully been used in-house. It therefore forms a logical baseline for further development.

Research Questions

Based on the problem statement, objectives and scope, a main research question and a set of sub-questions is drafted. These research questions aim to fulfill the research objectives within the scope stated. The aim of this preliminary thesis is to set a framework for the final research goal by answering the first three sub-questions.

Research Question

What are the effects on measured control strategies, workload and task performance of implementing wind and trajectory uncertainty information in an existing strategic 4D ATC ACC decision support interface?

Sub-questions

1. How does wind affect 4D trajectory management and how can these effects be modeled?
2. How does trajectory uncertainty affect 4D trajectory management and how can these effects be modeled?
3. How can wind and trajectory uncertainty information best be visualized in a 4D ATC decision support interface?
4. How do control strategies, workload and task performance change when wind and uncertainty information is integrated into an existing 4D ATC decision support interface?

Methodology

To answer the posed research questions, an extensive literature study on all relevant areas of research will be conducted. After this, a variety of methods will be used, each of which will be briefly introduced.

Preliminary MATLAB Research

Since the effects of wind and trajectory uncertainty on the TSR are still unknown, the first research step will be to gain a preliminary understanding of how the solution space changes in each dimension with the addition of wind and trajectory uncertainty information.

To do this, a MATLAB package will be developed to generate TSR display images for pre-programmed traffic situations. Using the already existing Java simulation package used during previous experiments at DUT, the developed MATLAB package can be verified. MATLAB is preferred over Java in this case because it allows for easier debugging, especially since part of the Java package is handled within GPU shaders (which can be 'debugged' only by setting color outputs on a screen). Models for wind fields and trajectory uncertainty will be implemented in this MATLAB package.

Cognitive Work Analysis

Using the principles of EID, a study will be performed on how the user should interact with the final experiment interface. This study will form the basis for how both the wind and trajectory uncertainty information should be displayed. Since there is no 'optimal' solution in interface design, several display concepts - all adhering to the EID design principles - will be generated. These concepts will be judged by real ATCos at LVNL, resulting in the selection of a preferred interface to be used in the validation experiment.

Validation Experiment

The MATLAB models will be dialed into the existing Java simulation platform to prepare the validation experiment. This simulation environment will allow for the simulation to be run with an actual wind scenario with a stochastic input process. The ATC DST interface will show the wind prediction (as is known in real-life) and trajectory uncertainty using the chosen and calibrated models. It should be noted that any stochastic elements added to the simulation will be pseudo-random. This will allow for the experiment to be executed with a small number of participants, as is usually the case with human-in-the-loop experiments.

Thesis Outline

This preliminary thesis has been divided into three parts. In **??**, literature on topics relevant to the field of research is presented. This starts with Chapter 1, where the current and future states of ATM are discussed. Display design guidelines are presented in Chapter 2. A selection of previous relevant work on DSTs is outlined in Chapter 3 as well as a detailed summary of the current TSR interface. Subsequently, wind fields are discussed in Chapter 4. The concept of trajectory uncertainty, its modeling, quantification and possible visualization are summarized in Chapter 5.

The second part summarizes preliminary research already conducted to answer the research questions. This starts with an outline of the envisioned Concept of Operations (CONOPS) needed for the interface in Chapter 6. The effects of wind and trajectory uncertainty on 4D trajectory management and the TSR interface are discussed in Chapters 7 and 8, respectively. Following this, a CWA is performed in Chapter 9 to analyze the interface requirements. Lastly, concepts of the interface to be designed and the subsequent final interface to be used in the remainder of this thesis are outlined in Chapter 10.

Part III sets out the work to be done in the remainder of this thesis. This starts with a description of the planned experiment to validate the interface in Chapter 11, followed by a summary, outlook and recommendations in Chapter 12.

Chapter 1

Air Traffic Management

Since the TSR interface is designed to provide decision support in 4D ATM, a thorough literature research has been conducted on the current and future states of ATM and the envisioned role of the ATCo. In Section 1-1, the current state of ATM will be discussed, along with currently applied ATM control strategies. The future state of ATM, with a special focus on the ATCo role in 4D ATM, will be summarized in Section 1-2. Challenges for automation acceptance in ATM are discussed in Section 1-3. Lastly, the relation of future ATM concepts to interface design is reviewed in Section 1-4.

1-1 Current State of ATM

ATM is defined as *'dynamic, integrated management of air traffic and airspace — safely, economically and efficiently — through the provision of facilities and seamless services in collaboration with all parties'* by ICAO (2005). As part of ATM, ATC is a service provided to ensure that both air traffic flow and safe separation between air traffic is maintained.

1-1-1 Airspace Structure

To ensure a safe and manageable operation, the airspace is divided into different sectors, each of which is controlled by an ATC instance. In the Netherlands, LVNL is the authority responsible for all ATC through civil airspace.

ATC is split up into three disciplines, each of which is displayed in Figure 1-1. Firstly, Tower Control (TWR) handles aircraft on active runways and airborne aircraft that are within sight of the runway within the airspace around the airport. Approach Control (APP) handles arriving traffic from Initial Approach Fix (IAF) to Final Approach Fix (FAF) as well as departing traffic. Lastly, ACC takes care of the upper airspace, handling both traffic to and from APP and overflights. Between sector borders and adjacent ATC disciplines, air traffic is handed over between controllers.

To ensure an orderly and manageable air traffic flow, flight plans are used. Each aircraft is required to have an approved flight before take-off, containing its route destination intentions and other relevant information, such as take-off weight.

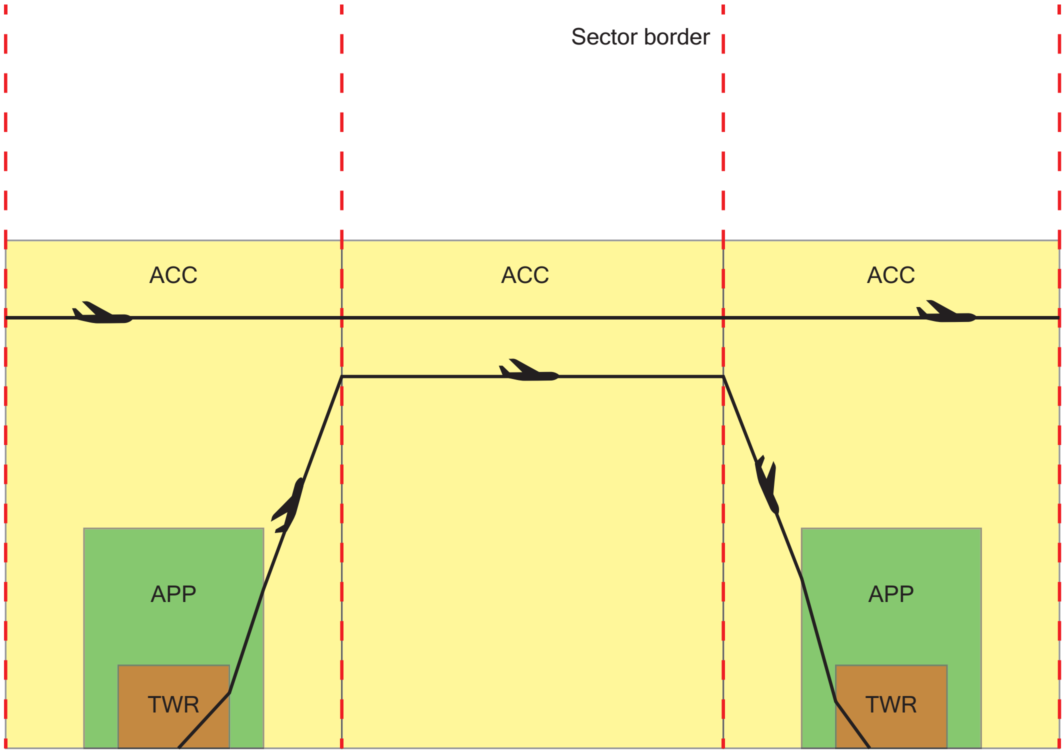

Figure 1-1: Overview of ATC disciplines

1-1-2 Role of the ATCo

The role of the ATCo is to guide an aircraft through a traffic sector. In this process, the ATCo decides *ad hoc* where the aircraft is and is not allowed to go. The primary goal of the ATCo is to ensure an efficient and productive airspace, while maintaining safe separation between all aircraft at all times. Currently, little automation is used in achieving this goal. An example of a current interface used by an ATCo is shown in Figure 1-2.

In ATC, a distinction is made between the executive controller and the planning controller (SESAR Consortium, 2019). The executive controller has direct responsibility for traffic management and for different tactical tasks. In tactical tasks the executive controller is aided by the planning controller, who is also responsible for planning and coordination of aircraft entering, leaving or currently inside the sector.

As a result of the low level of automation, a variety of control strategies are currently applied by ATCos depending on personal preference (Rantanen & Nunes, 2005). In a given conflict, multiple resolution options are often available and therefore the applied resolutions by different humans tend to differ (Prevot, Homola, Martin, Mercer, & Cabrall, 2012).

It can be stated that although different control strategies exist, standard practices can be identified amongst controllers. Fothergill and Neal (2013) stated that controllers scan sectors

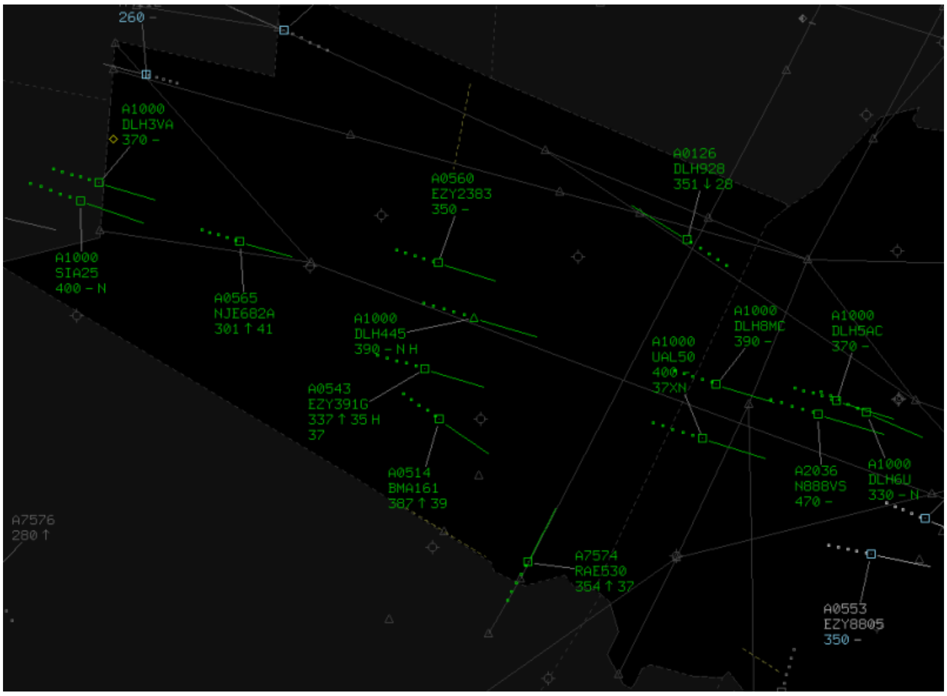

Figure 1-2: Screenshot of part of the Maastricht Upper Area Control (MUAC) radar screen (EUROCONTROL, 2012)

using clockwise and top-bottom patterns and group aircraft having similar characteristics. Furthermore, D'Arcy and Della Rocco (2001) stated that controllers adapt their strategy to the perceived air traffic complexity.

Emerging separation conflicts can be resolved by ATCos using any combination of heading, altitude and velocity commands. For crossing traffic streams, an altitude change is often applied (Fothergill & Neal, 2013).

Considerable research effort has been put into the automation of Conflict Detection & Resolution (CD&R) specifically in the 1990s, as is summarized by Kuchar and Yang (2000). As a result, low-level CD&R automation has made its way into the operation in the last two decades. Controller acceptance of such automation has, however, been relatively low (Westin et al., 2015). Requirements for Short-Term Conflict Alert (STCA), providing ATCos conflict indication warnings within the two minute time horizon, have been summarized by EUROCONTROL (2009).

1-2 Future State of ATM

It is predicted that global air traffic numbers will increase in the coming years (STATFOR Team, 2018). Future ATM plans from aviation authorities in the US and Europe can be found in Federal Aviation Administration (2016) and European Commission and EUROCONTROL (2015), respectively. Preliminary findings, summarizing similarities and differences between SESAR and NextGen have been documented by Enea and Porretta (2012).

1-2-1 4D ATM & TBO

Both the FAA and EUROCONTROL share the vision that more accurate planning forms an important aspect of future ATM. Eventually, it is expected that 4D trajectory management will make its way into operation, where all aircraft trajectories are computed beforehand in position as well as time.

4D trajectory management relies heavily on Trajectory Based Operations (TBO), a concept defined as *'the exchange, maintenance and use of consistent aircraft trajectory and flight information for collaborative decision-making on the flight'* by EUROCONTROL (2017). TBO forms the framework for the trajectory planning process. Preliminary trajectory planning starts years in advance, and is continuously updated, after which a final 4D flight plan is issued minutes before take-off. The different trajectory planning stages according to SESAR's terminology are displayed in Figure 1-3. As can be seen, planning resolution shifts from air traffic flows to individual aircraft as time progresses.

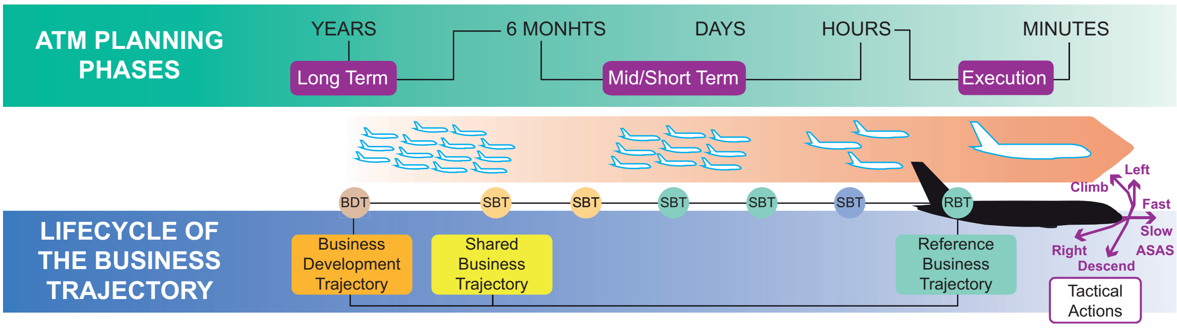

Figure 1-3: Business trajectory life cycle (SESAR Consortium, 2007)

The final part of the Trajectory Prediction (TP) process requires an increasing level of accuracy. The required accuracy level for decreasing time horizon, along with the different involved ATM disciplines are displayed in Figure 1-4. Air traffic flows are determined first using a relatively low resolution TP, after which they are de-conflicted. The ATC disciplines of executive planning and executive control require shorter look ahead times, while safety nets such as STCA (for the ATCo) and Traffic Alert and Collision Avoidance System (TCAS) (for the pilot) require the shortest, but most accurate TP.

While often referred to as being the same, 4D trajectory management and TBO are two different concepts and should be treated as such. TBO relies heavily on System Wide Information Management (SWIM) and Collaborative Decision Making (CDM); all together, TBO can be seen as a technology enabler for 4D trajectory management. The implementation of TBO is a relatively slow process, as many different stakeholders are involved.

For a trajectory to be defined as 4D, however, the only factual difference with respect to current trajectories is the inclusion of time as a parameter. 4D trajectory management is something that is already being implemented in parts of flight. LVNL currently sets an IAF target time for ACC, thus effectively making this a 4D waypoint.

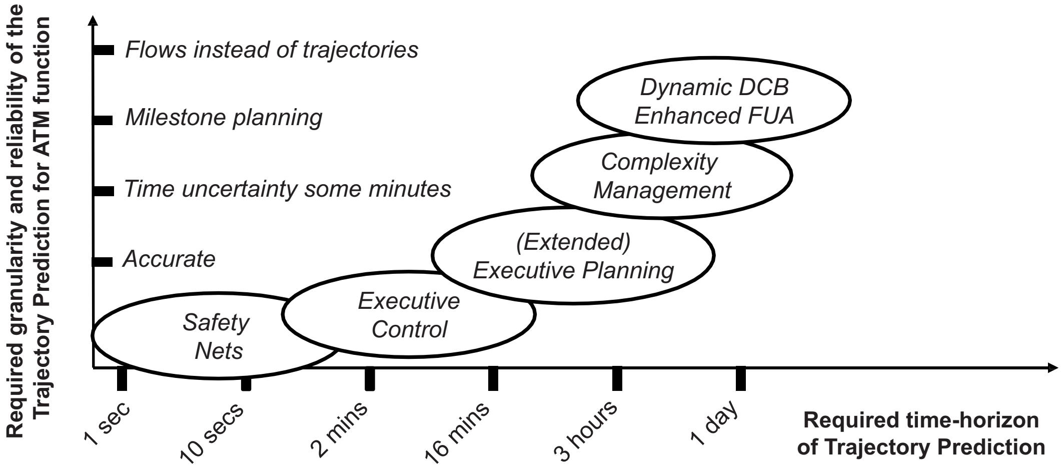

Figure 1-4: Required TP accuracy at different time horizons with ATM functions involved (ICAO, 2014a)

1-2-2 Airspace Structure

Based on 4D trajectories, different airspace structures compared to the 'traditional' fixed airspace sectors used today are envisioned. Two well-adopted structures are those of Dynamic Airspace Configuration (DAC) and Flight Centric ATC (FCA).

In DAC, sectors are not fixed in size anymore, but will be dynamically assigned. This allocation can be done to evenly distribute ATC workload, balancing out air traffic instead of surface area (Kopardekar, Bilimoria, & Sridhar, 2007). FCA, also known as 'sector-less ATM', abandons the use of airspace sectors all together. The FCA concept has already been researched since the beginning of the century (Duong, Gawinowski, Nicolaon, & Smith, 2001) and more recently by Korn et al. (2009).

1-2-3 Role of the ATCo

Regardless of the type of airspace structure, it is expected that more automation will make its way into the ATCo work domain. This is likely to drastically change the controller's role (Prevot et al., 2012). Both the NextGen and the SESAR program foresee a prominent role for advanced DSTs to aid the ATCo in controlling traffic.

Although 4D flight trajectories are computed and de-conflicted before operation, unforeseen events will still require the ATCo to make small changes in pre-planned trajectories, also referred to as *perturbation management*. The ATCo will therefore operate at a more strategic level than in current ATM practice (Klomp, Borst, Mulder, & Praetorius, 2014).

1-3 Automation Acceptance in ATC

While it is widely accepted that automation is going to play a large role in future ATC, automation is currently not well accepted amongst ATCos. Previous efforts for separation management DSTs are frequently left unused (Bekier, Molesworth, & Williamson, 2012; Whiteley & Wilson, 1999).

Low automation acceptance can be attributed to numerous reasons. Recent research argues that ATC automation acceptance will be low if controllers have to conform to automated advisories (Westin, Borst, & Hilburn, 2016). In an experiment designed to measure trust in automation, Hilburn, Westin, and Borst (2014) showed that controllers sometimes even reject their own solution if they think it has been created by an automated tool.

Automation tools should be reliable. It has been shown by Metzger and Parasuraman (2005) and Rovira and Parasuraman (2010) that unreliable automation can cause problems to be missed that would have otherwise been caught by the human. It seems trivial that unreliable automation will lower controller acceptance.

To increase controller acceptance, automation should also be designed with the user in mind. Billings (1996) already published guidelines on how human-centered automation can be applied in aviation. The user should remain actively involved in the decision making process, allowing him or her to remain aware of the situation on a tactical level (Metzger & Parasuraman, 2001).

When keeping ATCos involved in the decision making process, they can maintain applying their own personal control strategies and use the automation to validate their choices (Merritt & Ilgen, 2008). Using automation as a supportive instead of a replacement tool will likely increase controller acceptance.

1-4 Interface Design for Future ATM Concepts

Because a variety of future ATM concepts is currently being researched, interfaces should be designed with flexibility in mind. Whether it be DAC, FCA or any other kind of ATM concept, the interface available to the ATCo should be able to effectively show the work domain and applicable constraints when managing air traffic. For example, future interfaces should not be designed to handle traffic in airspace sectors specifically, as one might move away from airspace sectors all together.

The current TSR interface (discussed in detail in Section 3-3) is very powerful, because it approaches ATC tasks using a single aircraft. This allows it to be applied in virtually any ATM concept.

Regardless of the ATM concepts involved, more automation will need to be implemented as the ATCo work domain inevitably becomes more complex. As explained in Section 1-3, this automation will have to be implemented with caution. Again, the TSR interface proves a very promising platform, because it allows the ATCo to apply their own conflict resolution strategies and aids the ATCo in decision-making instead of making automated decisions.

Chapter 2

Interface Design

When designing an interface, it is important to know what elements should be present and how they should be presented. While not an exact science, frameworks exist to aid in HMI design. This chapter can be seen as a guide in HMI design. In Section 2-1, human behavior when dealing with complex interfaces is discussed. The Ecological Design Rationale is subsequently outlined in Section 2-2, after which several previously conducted display design guideline studies are mentioned in Section 2-3.

2-1 Human Behavior

Automation should be implemented with caution. Bainbridge (1983) already mentioned that wrongly applied automation might result in a reduced understanding of the system, and ultimately worse task performance in critical situations. Hilburn, Parasuraman, Jha, and McGarry (2006) confirmed these findings in ATC specific context. In order to properly design an HMI with significant automation levels, a thorough understanding of human behavior is therefore required.

In a study that formed the basis for HMI design studies since its publishing, Rasmussen (1983) argues that human beings cannot be viewed as simple input-output devices. Instead, they are driven towards a certain goal and display *teological* behavior (i.e., behavior that is modified during its course by signals from the goal) by nature. In his paper, Rasmussen described several frameworks to illustrate human behavior.

2-1-1 Skills, Rules and Knowledge

Rasmussen makes a distinction between three types of human behavior in terms of performance: Skill, Rule and Knowledge (SRK)-based behavior. These types require an increasing amount of cognitive processing from bottom to top. At the bottom, Skill Based Behavior (SBB) can be identified, where sensory input is directly mapped to output. This happens almost instantaneously and without conscious control. When trained, riding a bicycle can be seen as an example of SBB.

On level above SBB stands Rule Based Behavior (RBB). In RBB, a recognized set of procedures is followed by the human being to achieve the goal. Input-output mapping is slower than in SBB, as the human being has to think before performing the prescribed actions. Following a recipe to make a cake is a good example of RBB.

Activities with significant cognitive processing require Knowledge Based Behavior (KBB). Used in unfamiliar situations, this type of behavior is the slowest and most error-prone of the three. It requires the interpreting of input signals and reasoning which actions are needed to achieve the goal.

The same control task can be executed using different types of behavior depending on user experience. Tying your shoe laces for example can be considered a rule-based task for a child, while an older person (with years of experience) performs this task skill-based (and does not even think anymore while doing so).

Signals, Signs and Symbols

Closely related to SRK behavior is the segmentation of information into signals, signs and symbols. When applying SBB, information is perceived as a time-based signal, which is acted upon by the perceiver. At rule-based level, information is typically perceived as a sign to activate a set of prescribed rules. Lastly, information in symbols is perceived using its true meaning. It can serve as a starting point for knowledge-based reasoning.

Depending on the perceiver, information can be perceived as either of these three. This is illustrated using Figure 2-1, where the same physical indication on a control panel is used to interpret a signal, sign or symbol depending on the control task.

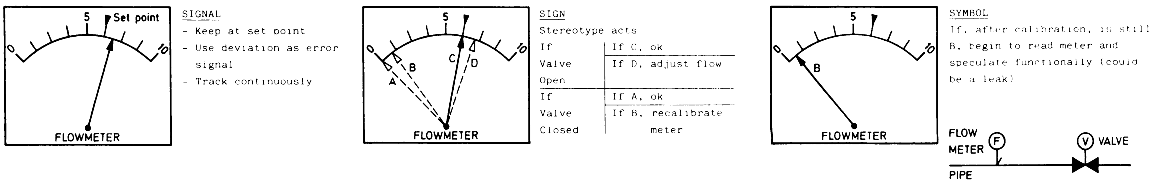

Figure 2-1: Same physical instrument to serve information as signal, sign or symbol (Rasmussen, 1983)

2-1-2 Abstraction Hierarchy

In the same paper, Rasmussen proposes a framework to map complex work domains using different abstraction levels. Each level fully describes the system, yet on a different level of abstraction (Rasmussen, 1983). On the lower layers, the physical form of the system is described, while its functional purpose sits at the top of the Abstraction Hierarchy (AH).

In later papers, the AH concept has been slightly modified and expanded. Rasmussen (1986) included *means-end* links between the different abstraction layers, illustrating the coupling between different levels of abstraction. These links can be seen as a '*why-what-how*' description of system components and are illustrated together with the different abstraction levels in Figure 2-2.

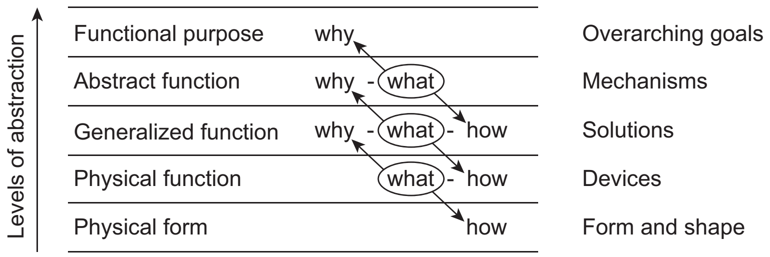

Figure 2-2: Different AH levels and '*why-what-how*' relationship representation (Borst, 2019; Rasmussen, 1986)

The AH can also be extended with the part-whole decomposition of system components (Rasmussen, 1986). Incorporating this into the AH strictly separates *aggregation* from *abstraction*, which are often confused. The resulting abstraction-decomposition hierarchy principle is displayed in Figure 2-3.

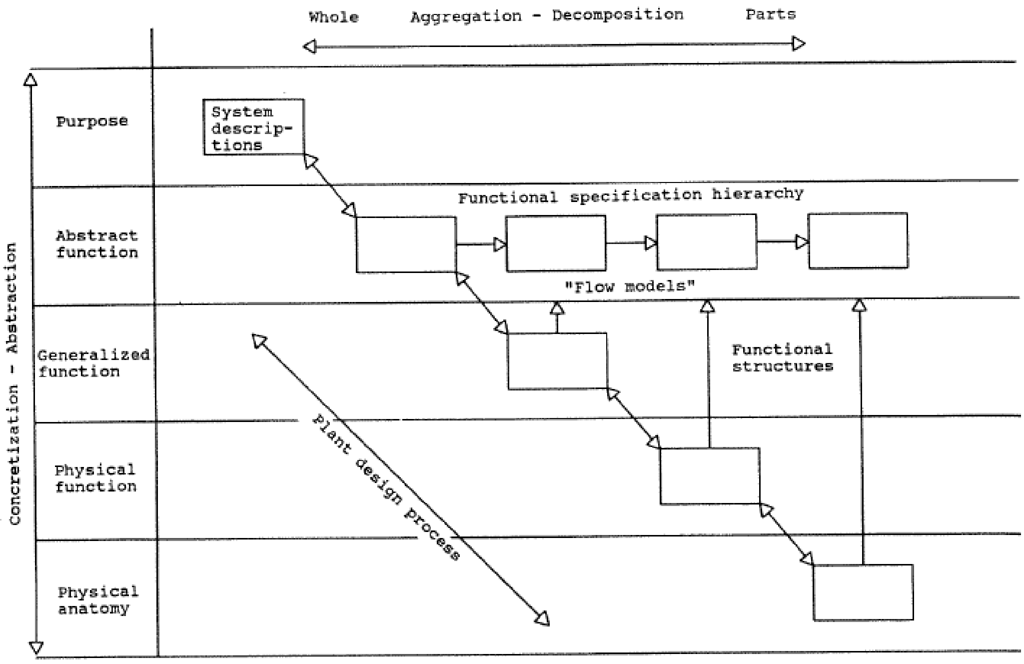

Figure 2-3: Generalized abstraction-decomposition diagram (Rasmussen, 1986)

2-1-3 Decision Ladder

First proposed by Rasmussen (1976), the Decision Ladder (DL) aims to visualize the human decision-making process when interacting with process control interfaces. The DL concept is shown in Figure 2-4. Here, clear links with SRK behavior are also pointed out.

When making a decision, a user starts at the bottom left when a need for action is detected. After this, a set of observations is made which in turn are used to identify the current system state. Depending on the goal, a certain task will be defined, after which a set of procedures can be formulated and subsequently executed.

Depending on the level of user experience and the task to be performed, shortcuts can be made in the DL. The power of the DL for a certain control task lies in identifying the shortcuts that are already there, and possible shortcuts that can be made by the interface to facilitate the decision-making process.

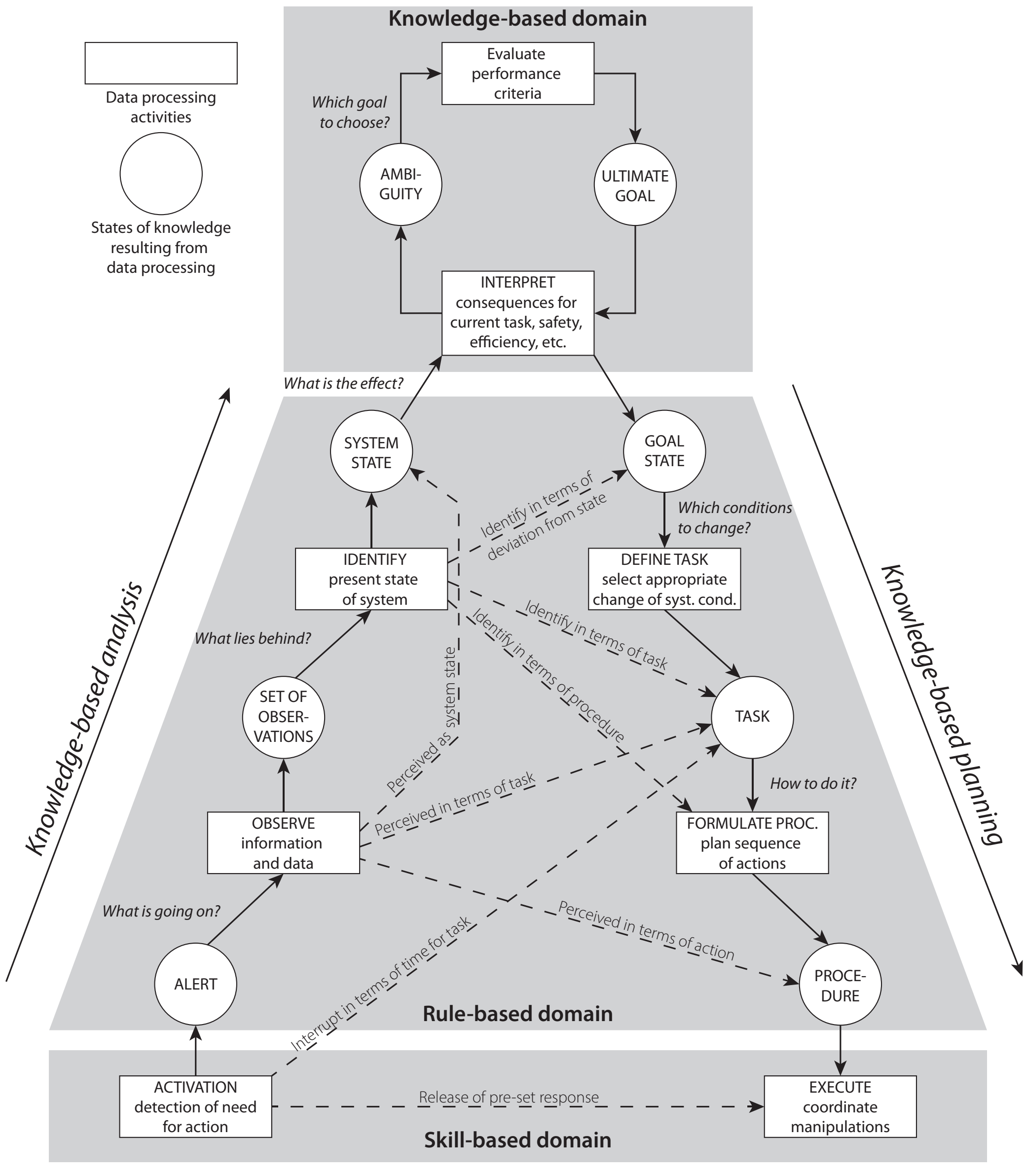

Figure 2-4: Generalized Decision Ladder (adapted from Rasmussen (1976))

2-2 Ecological Interface Design

2-2-1 Ecological Design Rationale

The ecological approach to interface design was proposed by Flach, Tanabe, Monta, Vicente, and Rasmussen (1998), with the aim to let human and machine cooperate in an effective manner. When applied correctly, the EID framework *'transforms a cognitive task into a perceptual task by providing meaningful information about the work domain that humans can directly perceive and act on accordingly'* (Borst, Mulder, & Van Paassen, 2010).

As opposed to user- or technology-centered design approaches, the focus of EID is placed on the work domain, a *use-centered* approach. Irrespective of whom (i.e., man or machine) is doing what, the activities that need to be executed are analysed. Subsequently, a task division can be made between man and machine by designing an interface that supports SRK behavior. This is illustrated in Figure 2-5.

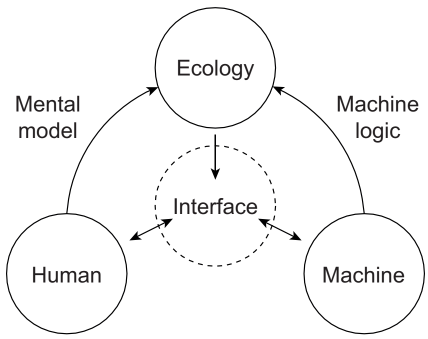

Figure 2-5: Schematic representation of EID framework (Borst et al., 2015)

Although commonly explained as such, a display designed using EID principles does not necessarily have to be simple, intuitive and therefore require minimal training (Borst et al., 2015). When introducing the EID concept, Vicente and Rasmussen (1992) were aiming at displays developed for domain experts. Displays designed according to EID are therefore often also complex and require significant user experience before being used to their full potential.

2-2-2 Cognitive Work Analysis

When applying the Ecological Design Rationale, a CWA is performed on basis of which the interface is designed. In a CWA, five steps are followed as defined by Vicente (1999):

1. Work Domain Analysis (WDA): *What are we working with?* The work domain is analysed to define the constraints and their relations. This is done using the AH or Abstraction Decomposition as described in Section 2-1-2. When designing the interface, important means-end links should be made visible to the user.

2. Control Task Analysis (CTA): *What must be done?* Following the WDA, the control tasks are analysed. To map the control task(s) to be performed (irrespective by whom)

onto a visual framework, the DL as described in Section 2-1-3 is used. The interface can be designed to support rule-based shortcuts, thereby transforming KBB into RBB.

3. Strategies Analysis: *How is the control task executed?* Typically, the control task can be performed using a variety of strategies. These strategies can be mapped onto information flow maps.

4. Social Organization Analysis: *Who performs each task?* Here, activities to be performed when executing the control task are divided between man and machine. The level of automation should be decided in a way to support the strengths of both man and machine, while mitigating their weaknesses.

5. Worker Competencies Analysis: *How can humans be supported in their task?* The worker is analysed to identify the cognitive load required to perform the different parts of the control task(s). Again, the DL can be used as a framework.

2-3 Display Design Guidelines

The *form* in which content is displayed on the display forms a large part of interface design. Various studies have been published with the aim of providing a framework for display design. In this section, an overview of selected frameworks is given.

2-3-1 Visual Momentum

A well-known display design framework was proposed by Woods (1984), who introduced the concept of visual momentum. Specifically aimed at multi-display interfaces, visual momentum is defined as *'a measure of the user's ability to extract and integrate information across displays'* (Woods, 1984). Simply put, this is a measure of how attention is distributed.

When switching between screens, the user needs a certain time to perform a 'mental reset' before new information can be perceived. When visual momentum is supported well by the interface, this reset time is minimized. Similarly, bad visual momentum will cause the user to need more time to perceive the information on the new display. Several actions can be taken when designing a display to ensure good visual momentum, as depicted in Figure 2-6.

A so-called 'long shot' provides the user with a zoomed-out overview of the display structure as well as a summary of the current system status. Perceptual landmarks can be used between displays to aid the user in quickly moving from one display to the other. Another tool is the application of overlap between the different displays to effectively form one big display instead of multiple small ones.

The eventual goal of the display designer is to provide spatial cognition, a concept that has a lot of similarities with the EID approach discussed in Section 2-2. Because the TSR interface consists of multiple displays, the concept of visual momentum is considered relevant in its (re)design.

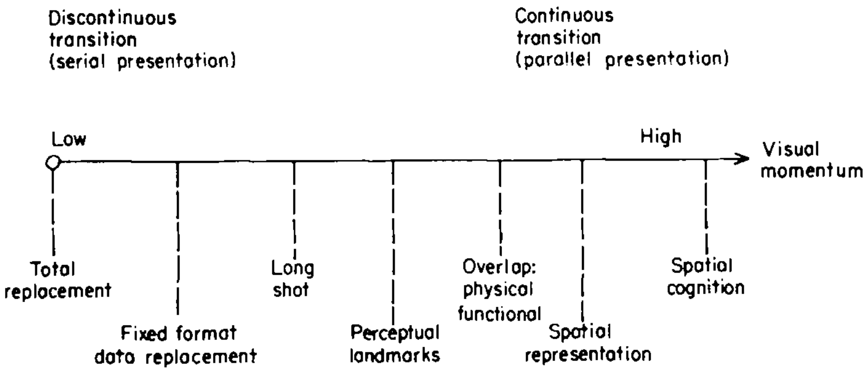

Figure 2-6: The dimension of visual momentum (taken from Woods (1984))

2-3-2 13 Principles of Display Design

Wickens, Lee, Liu, and Baker (2004) summarized 13 rules that can be used as a guideline when designing displays. These rules have been divided into four categories: perceptual, mental model, attention-based and memory principles.

The perceptual principles deal with the way information is initially perceived by the user. Information should be presented in a clear and unambiguous manner to avoid any possible confusion.

People often interpret a display based on their own experiences, with which they have formed a mental model of how the system works. Mental model principles are there to ensure that the information presented on the display match with that mental model, as this will facilitate information processing.

Complex displays require different types of user attention (Parasuraman & Davies, 1984). Attention-based principles are there to make sure that the types of user attention are used to their strengths, while mitigating their potential weaknesses.

Lastly, memory-based principles are there to help decide what information needs to be remembered and what should be continuously shown on the display.

2-3-3 Situation Awareness

Defined by Endsley in 1995, the framework of Situational Awareness (SA) is proposed to provide a theoretical model for human decision-making in dynamic systems. In ATC specifically, SA is considered very important (Endsley, 1995). The SA framework can be used to aid in display design.

SA is defined on three levels, showing similarities with the DL shown in Figure 2-4. When all levels of SA are present, the user fully understands the system he or she is interacting with.

- Level 1: Perception of the elements in the environment

- Level 2: Comprehension of the current situation
- Level 3: Projection of future status

To stimulate the presence of sufficient SA through display design, several generalized concepts are hypothesized. According to Endsley, attention and working memory are limited. The interface should therefore show information related to SA Levels 2 and 3. Information should be presented in terms of the operator's major goals instead of in its raw form. Top-down and bottom-up processing is also mentioned to support SA. It should, however, only be applied for critical events, as attention is easily captured for such systems. Lastly, the importance of attention division between multiple displays is mentioned, which can be related to the work of Woods (1984).

Chapter 3

Previous Work

In previous studies, numerous conflict detection and resolution DSTs have been researched and prototyped. This chapter provides an overview of these studies. Firstly, the Programme for Harmonised ATM Research (PHARE) Hyper Interactive Problem Solver (HIPS), one of the more elaborate research projects, is discussed in Section 3-1. Other relevant studies are briefly reviewed in Section 3-2. Lastly, the DUT TSR is thoroughly discussed, as this will be the baseline interface for this thesis.

3-1 PHARE Hyper Interactive Problem Solver

The PHARE project was a collaborative research program set up and managed by EUROCONTROL in the 1990s with the aim to investigate a future ATM concept. It can more or less be seen as SESAR's predecessor. As a part of the research program, conflict solving tools were developed. This yielded the HIPS, a highly automated DST for solving airborne separation conflicts.

3-1-1 System Overview

Although the initial aim of the HIPS was to provide ATCos with highly automated conflict resolution tools, this approach was discontinued at a relatively early stage of development due to controller opposition (Whiteley & Wilson, 1999). The subsequent redesign aimed at recognizing potential future conflicts by comparing the computed 4D trajectories of all aircraft in a sector and checking if the minimum separation standards are met. An extra separation buffer is implemented to account for TP uncertainty. If a conflict is recognized, the controller is notified, after which one of the two conflicting aircraft can be selected as the *subject aircraft*.

When selected, all possible future trajectories for the aircraft are calculated from the current location. For each trajectory, potential conflicts with other trajectories are computed. This leads to the computation of *no-go zones*, showing the controller areas of conflict if the subject aircraft were to be rerouted through them.

To visualize the rerouting possibilities in all dimensions (by making a turn, changing the altitude or changing the velocity), the 4D trajectory is mapped onto three displays. On each display, no-go zones are displayed in red. The first display shows the horizontal rerouting possibilities on a radar-like display, by having the aircraft initiate a turn to solve a conflict. A screenshot of this display is shown in Figure 3-1a.

The other two displays show rerouting possibilities using altitude or velocity changes. An example of these displays is shown in Figure 3-1b. Both displays show the on-track distance ahead on the horizontal axis. The altitude manipulation display shows reachable altitudes on the vertical axis, using aircraft climb/descent performance together with computed no-go zones. The speed manipulation display shows the time difference relative to the nominal trajectory on the vertical axis together with computed no-go zones.

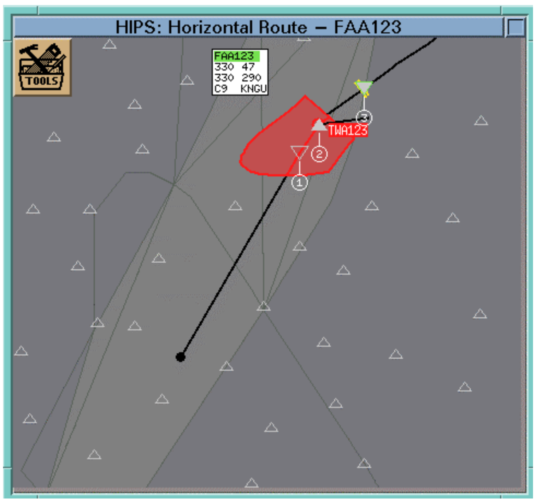

(a) Lateral route manipulation

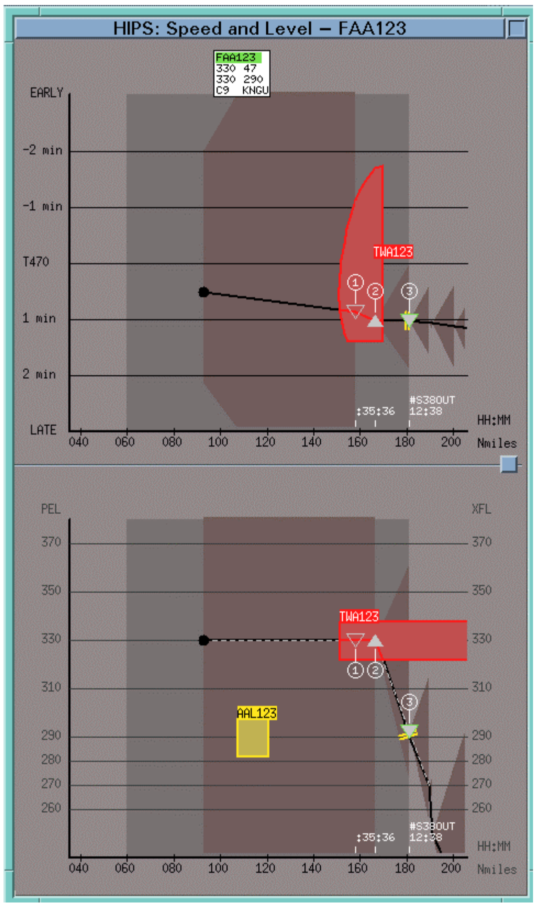

(b) Altitude and velocity manipulation

Figure 3-1: Screenshots of the HIPS interface (taken from Whiteley and Wilson (1999))

3-1-2 Experiment Results

Since HIPS was a prototype interface, problems inevitably arose when experimenting with it. One of the main drawbacks was the relatively large computing power required to generate real-time no-go zones during traffic scenarios. Because computing power was still limited in the 1990s, simplified conflict detection algorithms had to be used in the interface. This sometimes caused ambiguous information between the HIPS and the conflict-detection algorithms already present, leading to controller distrust and therefore lowered acceptance of the interface.

During different demonstrations where the HIPS was used, controller feedback was obtained. What came forward was that the interface intuitiveness was not optimal in some situations (Gingell & Fox, 1997). Especially the velocity manipulation window was considered difficult to interpret, because speed was not displayed directly within the window.

Furthermore, the 'safe' zones as indicated by the interface were sometimes not considered conservative enough by controllers. While this is the result of HIPS conflict zones arising from simple geometric calculations (and are not necessarily wrong), it led to controller distrust in the presented no-go zones (Whitaker & Marsh, 1997).

Lastly, it was found that the constant re-computation of no-go zones led to confusion amongst controllers using the interface. While mathematically correct, controllers felt out of control and found the no-go zones to be non-intuitive at times.

Despite the mentioned drawbacks, the overall consensus between controllers was that the HIPS concept was very promising, and should be developed further (Whitaker & Marsh, 1997).

3-1-3 Research Conclusions

Generally speaking, the HIPS was received quite well by the ATC community. Despite initial promising results, it was predominantly a lack in interface intuitiveness that eventually caused insufficient controller acceptance. The main lesson learnt from the HIPS prototyping process is that controller acceptance and interface intuitiveness play a crucial role in any future ATC DST. This is important to take into account in the further development of the TSR interface.

3-2 Other Work

Besides the HIPS discussed in Section 3-1, numerous other CD&R DSTs have been developed and tested. Several concepts of interest are shown in this section. Firstly, the interface by Prevot, Lee, Smith, and Palmer (2005) is discussed, because it already successfully combined numerous complex elements (including CD&R and Estimated Time of Arrival (ETA) management) into one display. Following this, the probabilistic CD&R display designed by H. Lee and Milgram (2008) is discussed, as the visualization of uncertainty patterns is of key interest for this thesis. Lastly, the 4D trajectory revision interface from Van Marwijk, Borst, Mulder, Mulder, and Van Paassen (2011) is discussed because it is effectively the predecessor of the TSR interface and therefore shows many similarities.

3-2-1 Prevot, Lee, Smith, and Palmer (2005)

In a thorough study performed in 2005, Prevot et al. researched ATC technologies for both Controller Managed as well as Autonomous Flight Operations. Task allocation and coordination between different actors involved in Flight Operations are of particular interest. It is noted that in trajectory-based ATC, automation support should be available to the ATCo for Separation Assurance and Traffic Flow Management (i.e., managing aircraft ETA versus RTA). Controller-Pilot Data Link Communication (CPDLC) is assumed to be operative, allowing for easy editing and uplinking of edited flight plans between ATC and the flight crew. Concept DSTs for both Separation Assurance and Traffic Flow Management are presented in an integrated display concept, of which a screenshot is provided in Figure 3-2.

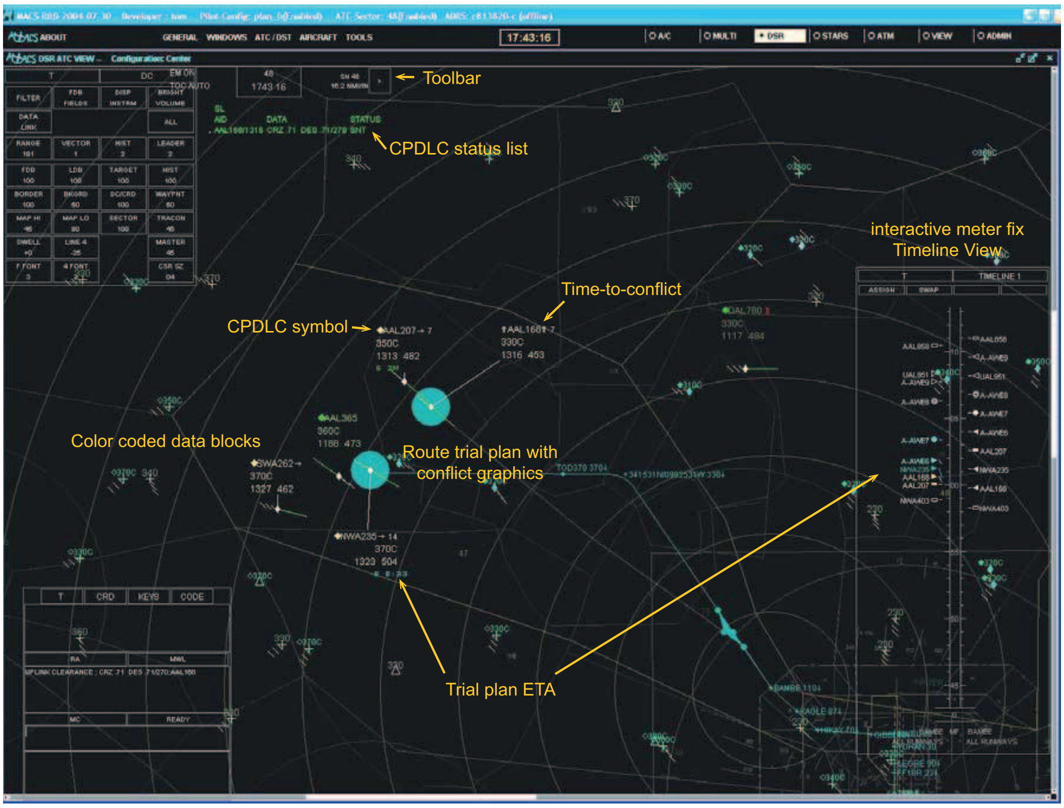

Figure 3-2: Example 4D trajectory management interface by Prevot et al. (2005)

In the interface, Separation Assurance is partly automated. Potential conflict indication is given using Time To Conflict (TTC) in the aircraft data tag and a separate conflict list. Clicking on either of the conflicting aircraft triggers conflict graphics, depicting the conflicting aircraft and the likely location of conflict. When adjusting the flight plan, the controller can directly see 'safe' (no Loss of Separation (LoS)) and 'unsafe' (likely LoS) future trajectories.

To support decision making in Traffic Flow Management, RTA values are constantly being held against ETA values to check if speed or altitude modifications are required to adhere to the RTA. When velocity changes are not sufficient anymore, the interface indicates the amount of time the aircraft will be too early or too late at its metering fix. Controllers can interactively 'swap' RTAs of different aircraft when deemed necessary.

Various experiments were executed, in which four controllers each operated an airspace sector using the interface, and three retired controllers operated adjacent sectors. Overall, controller feedback was found to be very positive. Using the automation tools, ATCos found it relatively easy to monitor and maintain separation with moderate traffic load and very easy to deliver aircraft at their RTA. Particularly the conflict display and seamless integration of Traffic Flow Management support tools received positive feedback. Overall controller acceptance was measured to be around 4.5 on a scale of 5.0.

3-2-2 Lee and Milgram (2008)

In their display concept, Lee and Milgram introduce a CD&R display for ATC with a focus on uncertainty visualization. Conflict probability here is generated by a combination of TTC, spatial probability and temporal probability patterns.

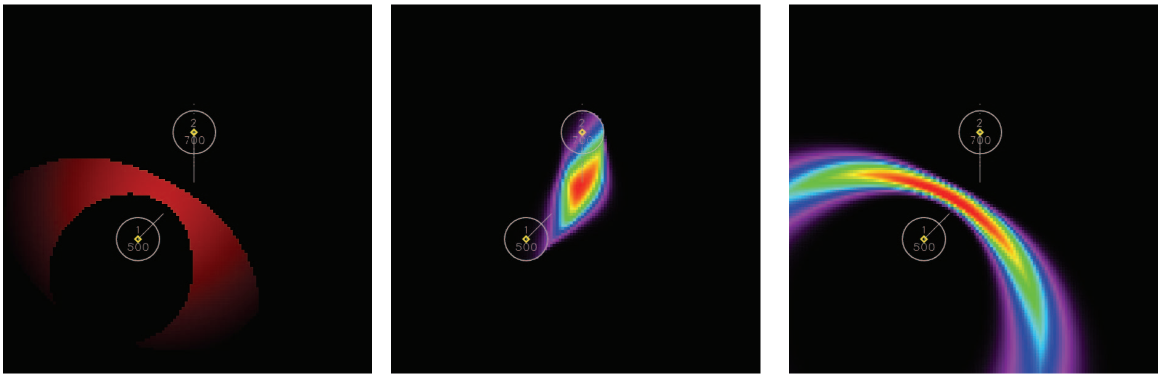

(a) TTC information **(b)** Spatial intersection probability **(c)** Temporal intersection probability

Figure 3-3: Interface screenshots for probabilistic CD&R display (taken from H. Lee and Milgram (2008))

TTC information is defined as an estimate of the potential arrival time of any pair of aircraft at a given point in space. It is purely based on velocity; from a known position, an aircraft is assumed to be anywhere on the constant radius surrounding it after a time multiplied by its current velocity. This is illustrated in Figure 3-3a.

Spatial probability information is calculated assuming a normally distributed value around a nominal heading. When assuming constant velocity, conflict probabilities can be computed as is shown in Figure 3-3b.

Temporal probability information is obtained using assumed stochastic velocity values. An example is depicted in Figure 3-3c.

An example of the combined patterns, creating the final interface concept, is shown in Figure 3-4.

The rationale behind the interface is that future air traffic flows will be complex and therefore not maintain constant headings or velocities. The interface aims at capturing and displaying these uncertainties, so that ATCos can act accordingly when needed. This rationale has already been applied and experimentally tested in naval conflict management by Telner, Milgram, and Williamson (2003). Results indicated a task performance increase with the

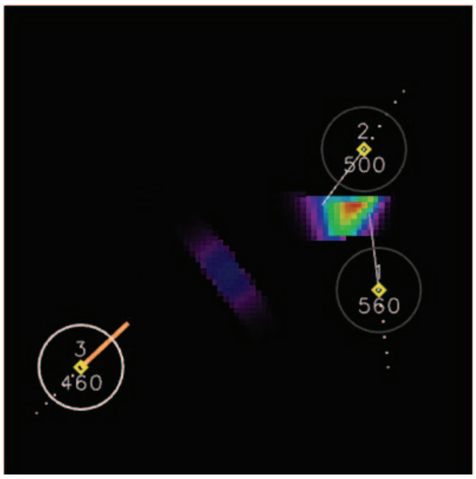

Figure 3-4: Conflict probability created by TTC, temporal, and probabilistic information (taken from H. Lee and Milgram (2008))

interface available. While not directly designed for 4D trajectory management, this display is of interest because of the approach to uncertainty visualization.

3-2-3 Van Marwijk, Borst, Mulder, Mulder, and Van Paassen (2011)

In 2011, a study was published about an HMI for supporting 4D trajectory management on the flight deck. The interface has been designed using the principles of EID (see Section 2-2), resulting in the display depicted in Figure 3-5.

Two displays are shown on the interface; a radar-like display, containing lateral rerouting possibilities and a vertical view, containing altitude rerouting possibilities. Lateral tolerance zones are implemented into the display to account for trajectory uncertainty. In the vertical view, the descent profile and allowed Top of Descent (ToD) range is displayed. Separation conflicts caused by other aircraft were beyond the scope of this research project; the focus is on rerouting the aircraft around an en-route constraint (e.g., a weather cell) while adhering to the RTA.

When rerouting an aircraft using lateral commands (i.e., making a turn), the pilot can immediately observe the valid waypoints to choose from. In the vertical display, the climb profile can be adjusted to comply with the RTA (exploiting the difference in Indicated Airspeed (IAS) vs. True Airspeed (TAS) at different altitudes). This display concept has many similarities with the DUT TSR, explained in the next section.

3-3 DUT Travel Space Representation

Developed at DUT, the TSR aims at providing decision support for the ATCo when managing 4D flight trajectories. As it will form the baseline interface for this thesis, a thorough review is presented.

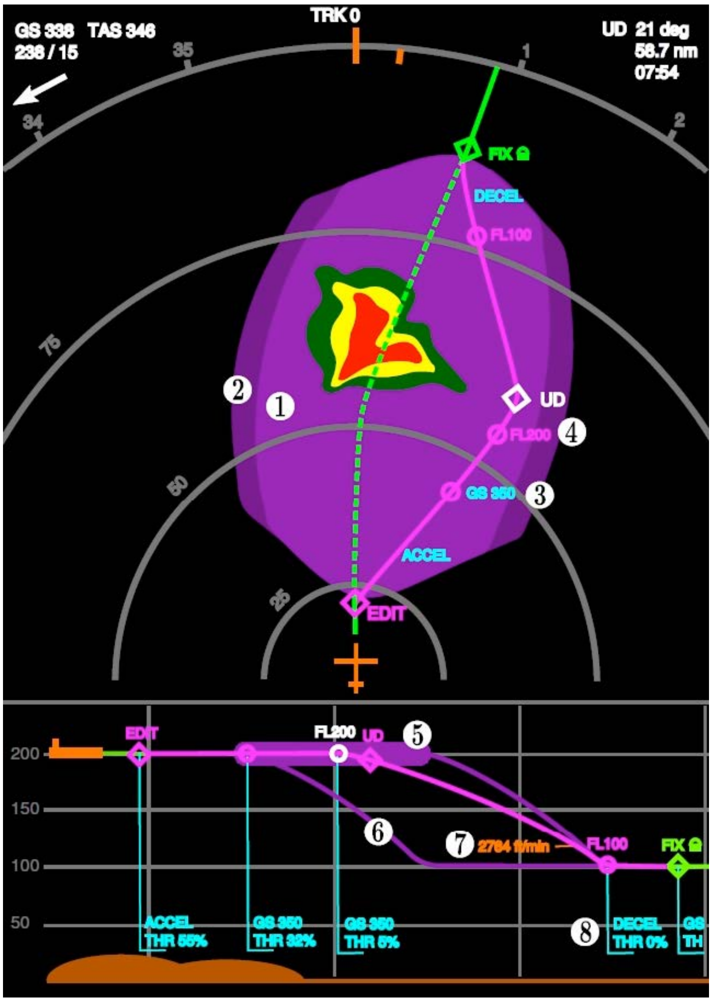

Figure 3-5: Display design of 4D trajectory revision interface (taken from Van Marwijk et al. (2011))

3-3-1 Scope

Assumed are the availability of pre-planned 4D flight trajectories, from which alterations can be made (Klomp, Van Paassen, Borst, & Mulder, 2012; Van Paassen et al., 2013). Currently, experiments have been performed focussing on en-route traffic scenarios, meaning that the original 4D trajectories must be adhered to as much as possible to prevent potential planning hazards in adjacent traffic sectors.

3-3-2 Design Rationale

The TSR interface has been designed using the principles of EID, with the aim of shared cognition between man and machine. The interface is designed to exploit the strengths of both, while minimizing the effects of their weaknesses. With the TSR, so-called *solution spaces* are computed to visualize the range of possibilities to the user. These solution spaces are formed using the RTA at the sector exit waypoint as a fixed constraint in combination with the aircraft performance envelope. This leaves the decision-making process in the hands of the ATCo, thereby supporting individual-sensitive automation. This should increase controller acceptance (Hilburn et al., 2014).

3-3-3 Interface Layout

The TSR consists of three displays each showing different control dimensions, together forming the complete interface. Upon aircraft selection, each display shows the solution space in the relevant dimensions.

Solution Space Rationale

The primary screen is the Plan View Display (PVD) depicted in Figure 3-6a. It shows the lateral solution space, governed by both the aircraft speed and turn envelope and the RTA at sector exit.

The Time Space Display (TSD), shown in Figure 3-6b, combines time and space into a single diagram, with the along-track distance and time to exit waypoint on the horizontal and vertical axes, respectively. The aircraft speed envelope forms the basis for the solution space. A steeper curve indicates a slower speed (more time is needed to cover a certain distance) and vice versa.

Added by Riegman (2018), the Vertical Situation Display (VSD) forms the latest addition to the interface. The vertical solution space, as shown in Figure 3-6c, is bounded by the climb and descent profiles together with performance reachability of the level segment velocity required to adhere to the RTA.

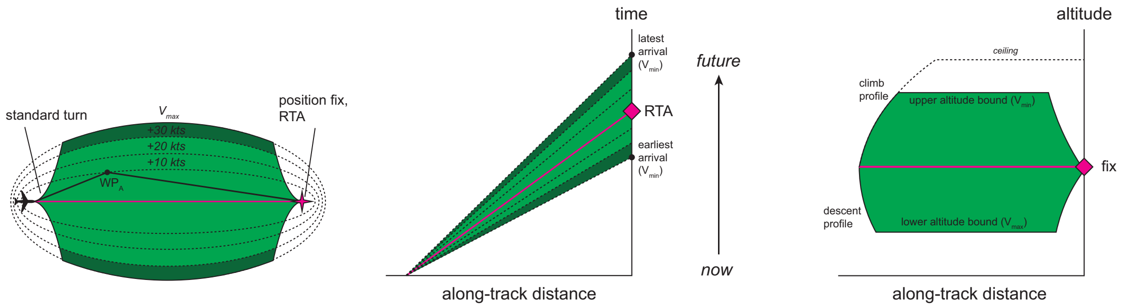

(a) Lateral solution space **(b)** Time-based solution space **(c)** Vertical solution space

Figure 3-6: Solution space interface concepts (adapted from Klomp et al. (2019))

Constraint Mapping

When other aircraft are present, conflicting waypoints in the solution space are shown. Conflicting waypoints are in this case waypoints where LoS would occur if selected. In most ATC sectors, a separation of five nautical miles (lateral) and 1,000 feet (vertical) must be maintained to guarantee a 'safe' traffic structure. For an example crossing conflict, the constraint mapping onto the solution space is shown in Figure 3-7. The integrated TSR display concept is displayed in Figure 3-8.

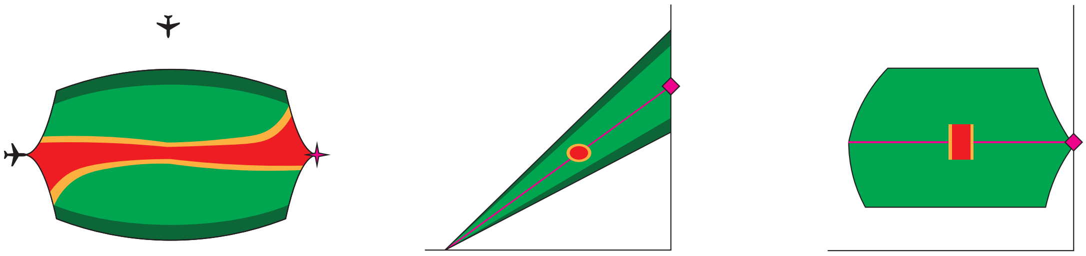

(a) Lateral constraints **(b)** Time-based constraints **(c)** Vertical constraints

Figure 3-7: Constraints mapped onto the TSR (adapted from Klomp et al. (2019))

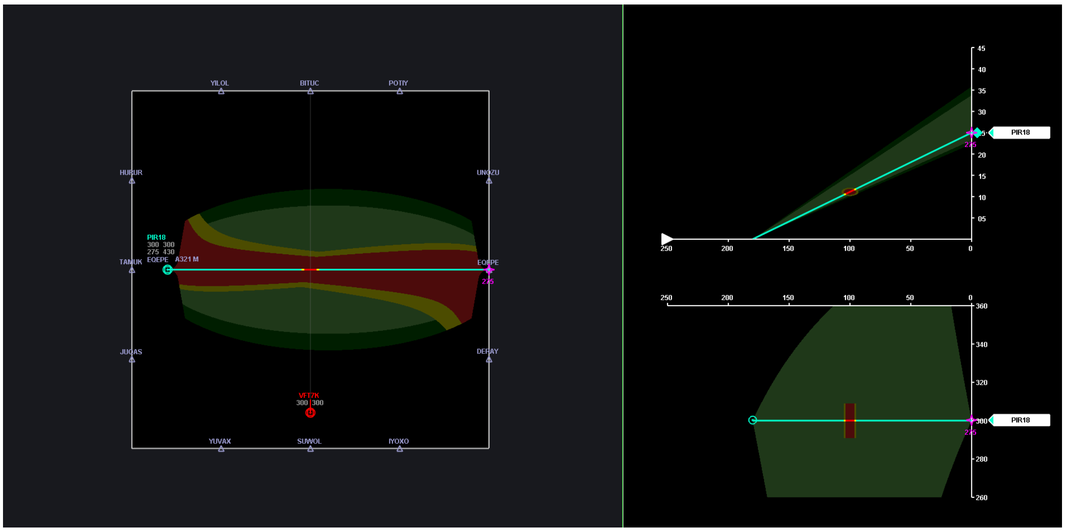

Figure 3-8: Screenshot of the TSR interface

3-3-4 Concept of Operations

With the TSR, the current ATM CONOPS remains largely intact. The ATCo provides instructions to flight crews to ensure that all aircraft adhere to their 4D contract while maintaining separation. Therefore, the availability of a 4D flight plan for every aircraft present in the sector is required. The only difference with respect to the current ATM CONOPS is the inclusion of time as a strict flight plan parameter.

While designed with full data-link availability between all its users, only air-to-ground and ground-to-air communication is required for the TSR to function properly.

The fact that the TSR shows the solution spaces in which all other conflicting aircraft have already been taken into account, makes it very convenient. When an aircraft is rerouted, other aircraft do not have to edit their trajectory, making the TSR very convenient to use, regardless of the ATM concept in operation. Whether it be DAC, FCA or any other ATM concept, the TSR interface is a very powerful concept as it focuses on displaying constraints and solution spaces for a single aircraft.

3-3-5 Current Recommendations

Following previous research, recommendations have been made on improvements to be made to the interface. Furthermore, important elements required for a realistic simulation environment are currently still missing from the interface.

Missing Elements

The most noticeable missing elements from the current display are those of wind and trajectory uncertainty. As a result the ATCo Air Traffic Flow control task mentioned by Prevot et al. (2005) is currently not required to be executed as all trajectories are fully deterministic, lowering the realism and real-life applicability of the interface.

Realistic climb profiles are currently also missing from the interface. A constant IAS climb/descent is now always assumed when computing the climb and descend legs. Especially at high altitude (above around Flight Level (FL)260), this becomes a constant Mach number (M) climb in reality. The effects of this assumption are considered too large to be ignored and should be addressed.

Interface Improvements

Following his experiment, Riegman (2018) made a number of recommendations that could improve the interface:

- The TSD was found to be difficult to interpret by the participants. This might have contributed to the interface being used less frequently than the other two. Suggestions are made to swap the TSD and VSD screens, thereby also swapping the TSD vertical axis. This would mean that dragging up the label in the TSD increases speed and vice versa, forming more similarity with the user's mental model.
- The VSD currently allows little flexibility in the manipulation of vertical flight paths. Only the start of climb or descent can be chosen, after which the level segment altitude can be altered for the last segment only. In more complex traffic scenarios with climbing and/or descending traffic, especially those with adjacent APP control, more flexibility will be required in the modification of altitude.

Chapter 4

Wind

Known to have a significant impact on ATM, wind is one of the most dominant missing elements from the current TSR interface. As wind effects will be implemented in the interface, a review on wind in ATM context is presented in this chapter. This starts with a general description of wind fields in Section 4-1, followed by a study on wind prediction in Section 4-2. Lastly, the influence of wind on aircraft performance with a focus on 4D ATM is discussed in Section 4-3.

4-1 Wind Field

4-1-1 Wind Field Properties

Simply put, a wind field can be seen as a 3D time-varying vector field. This vector field has certain properties, which will be discussed here.

- **Average wind**: An important property of a wind field is its average direction and magnitude (Reynolds, Glina, & Mcpartland, 2012). It changes with time and space. When looking at wind fields from a frequency perspective, average wind is its low-frequency component.
- **Atmospheric turbulence**: Turbulence can be seen as *'continuous random pulsation superimposed on average wind'*(Cui & Lei, 2015). Again making the frequency perspective analogy, turbulence can be seen as the high-frequency component. While aircraft are designed to handle the structural loads imposed by turbulence, it can form no-go zones for commercial aviation as passenger safety is at risk when encountered (Golding, 2002).
- **Wind shear**: Occurs when the average wind vector changes significantly in one of the spatial dimensions or a combination of those. This produces a boundary layer between the two average vector fields. ATCos find these types of wind fields to be very difficult, because of the changing conditions (Reynolds et al., 2012).

- **Microburst**: This is a special case of wind shear, where an intense small-scale downdraft is produced by a rain shower or thunderstorm (Cui & Lei, 2015). Microbursts are known to be dangerous in aviation, because a sudden loss of lift is encountered, causing the aircraft to drop in altitude.

- **Gust**: A wind gust can be seen as a local, small-scale form of wind shear. Wind gusts are present in the wake of wind turbines for example, where the average wind direction is typically locally different than in the atmospheric average surrounding it.

4-1-2 Wind Field Visualization

Wind influence will have to be incorporated into the DUT TSR. It is therefore likely that the wind vector fields will somehow need to be displayed dynamically on a display. When discussing wind fields in conference papers or journal articles, static contour plots of the u and v components are usually shown, as illustrated for example by A. Lee, Weygandt, Schwartz, and Murphy (2009). Purely for visualization purposes, however, more sophisticated tools have been developed. Some examples of these tools are shown in Figure 4-1.

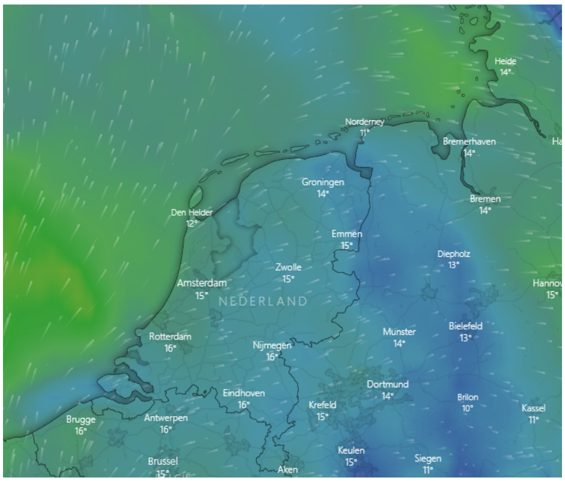

(a) Windy (taken from `windy.com`)

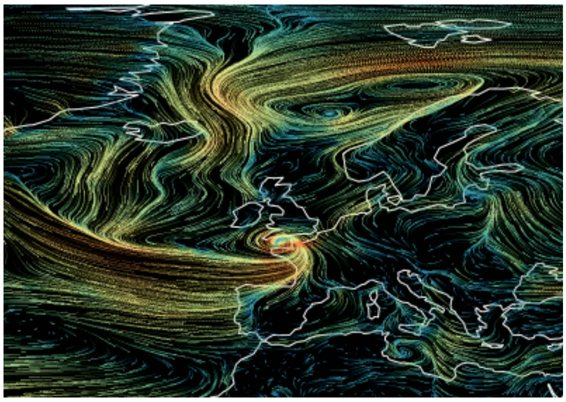

(b) Mapbox (taken from `mapbox.github.io/webgl-wind/demo/`)

Figure 4-1: Examples of dynamic wind field visualization applications

4-2 Wind Prediction

Because of its influence on ATM and in other industries where wind information is important, wind fields need to be predicted using a forecast model. Because of uncertainties in this process, there will always be an error between the true and predicted wind field. The aim of forecast models is to minimize this forecast error, usually expressed in terms of the Root Mean Square (RMS) vector error or Standard Deviation (STD).

4-2-1 Forecast Error

Forecast models differ in terms of the horizontal resolution. In their study on wind information requirements for 4D operations, Reynolds et al. (2012) provide an excellent overview of different available forecast models and their properties. This summary is shown in Table 4-1.

Table 4-1: Wind model forecast summary (adapted from Reynolds et al. (2012))

Forecast Model	Horizontal Resolution	RMS Vector Error	Comments
Rapid Update Cycle (RUC)	60 km	12 kts	Prior operational model.
	40 km	9-11 kts	Prior operational model. Errors aggregated over all (0-6 hr) forecast times.
	13 km	8-10 kts (<25 kft) 10-11 kts (25-50 kft)	Recent prior operational model. Errors for 3-hr forecast.
Rapid Refresh	13 km	7-10 kts (<25 kft) 10-11 kts (25-50 kft)	Errors for 3-hr forecast.
North Atlantic European Model (NAE)	12 km	7-8 kts	Current operational European model. Will be replaced by upgraded Global Model in 2012. Estimated from component error graphs.
Integrated Terminal Weather System (ITWS) TWINDS	10 km	7-9 kts	This was a pre-operational research configuration. No Doppler winds included. Current ITWS TWINDS has 2- and 10-km internal grid resolutions.
WAFTAGE	5 km	6 kts	Estimated from component error graphs.
High Resolution Rapid Refresh (HRRR)	3 km	8-10 kts below 25 kft 10-12 kts @ 25-45 kft	Experimental, widely used. Errors are for 6-hr forecast.

Several remarks can be made following Table 4-1. First of all, the RMS vector error of the wind forecast increases with models with larger horizontal resolution. Furthermore, the RMS forecast error is typically larger at higher altitudes, as shown in Figure 4-2a, because less validation measurements can be done. Recent developments have shown, however, that Automatic Dependent Surveillance - Broadcast (ADS-B) technology can be used to increase the model accuracy at higher altitudes (Haan, Haij, & Sondij, 2013).

In a study performed to compare operational wind forecasts with actual flight data, Robert and De Smedt (2013) showed that the 95% confidence interval of the forecast RMS vector error and wind direction were found to be 19.0 kts and 47.0 degrees, respectively. This is also illustrated in Figure 4-2c.

The forecast error magnitude also varies with predicted time ahead. Predicting further ahead introduces more uncertainty and therefore a larger RMS forecast error (A. Lee et al., 2009). Lastly, the error is known to vary slightly with time of the year, as is also shown in Figure 4-2b.

4-2-2 Synthetic Wind Field Generation

For experiment purposes, synthetic wind fields will likely have to be generated. More specifically, a 'true' and 'predicted' wind field will have to be generated. This can be done by assuming a fixed wind field and superimposing a generated wind prediction error field to generate the two required data sets.

When looking at wind field prediction error properties, it can be noted that these errors are not randomly distributed. Instead, the errors are found to be correlated in both spatial

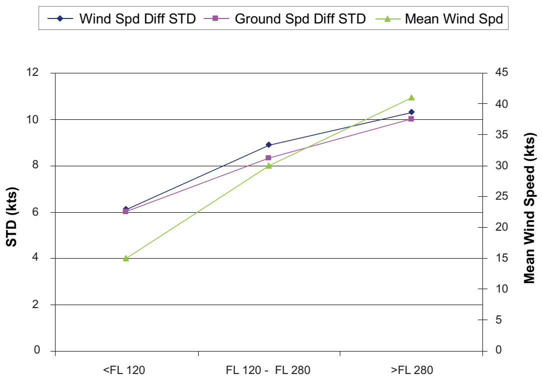

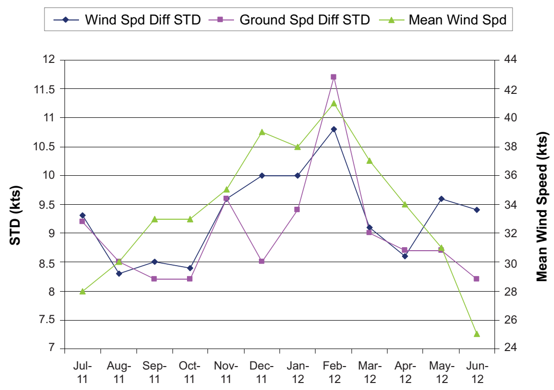

(a) Altitude variation of wind & ground speed error STD and mean wind speed

(b) Seasonal variation of wind & ground speed error STD and mean wind speed

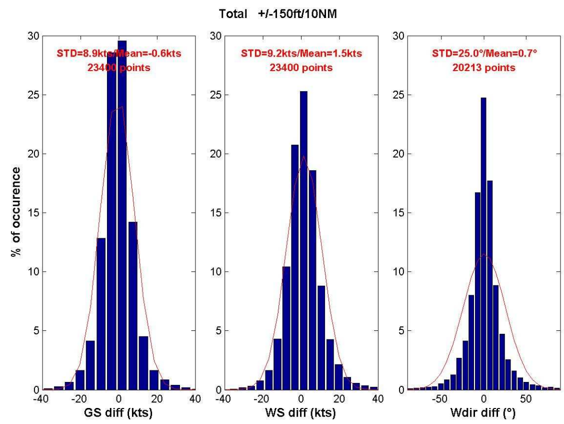

(c) Ground speed (left), wind speed (centre), wind direction (right) difference distribution for the total number of comparison points

Figure 4-2: Comparison of operational wind forecast data with recorded flight data (taken from Robert and De Smedt (2013))

and temporal dimensions (Vaddi, Tandale, & Lin, 2013). To generate these error fields, a technique originally used by Forkel, Schinnenburg, and Ang (2004) in mobile radio network simulation can be applied (Glina, Reynolds, Troxel, & Mcpartland, 2013). This principle, in which random uncorrelated error fields are convolved with a Gaussian filter kernel to create correlated error fields, is illustrated in Figure 4-3.

4-2-3 Operational Wind Forecasts in the Netherlands

GRIdded Binary (GRIB) is a common data structure used in meteorology to store historical and forecast weather data. Every hour, the Royal Netherlands Meteorological Institute (KNMI) publishes a high resolution weather forecast made using the High Resolution Limited Area Model (HIRLAM) (see `http://hirlam.org/`) in GRIB format. Here, atmospheric predictions are provided on a total of 40 pressure layers containing 2D grids with a 0.1 degrees

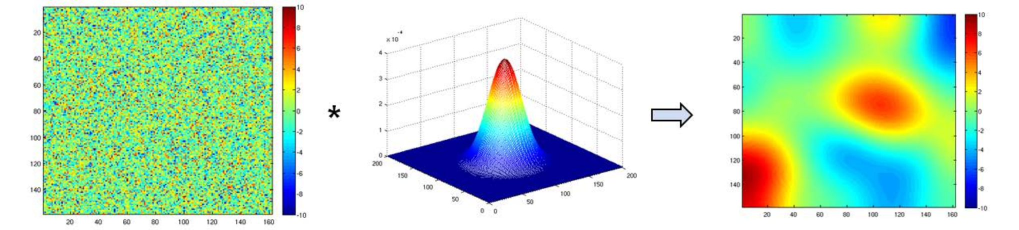

Figure 4-3: Generation of random correlated vector error fields (Glina et al., 2013)

resolution for latitude and longitude. These layers use a so-called 'hybrid level definition': close to the surface the pressure layers follow the terrain contours, while higher up this transforms to pressure levels. This is described in Equation (B-1), where $A(n)$ and $B(n)$ are constant values indicating the fixed pressure for level n and fixed fraction of surface pressure for level n, respectively. The values for $A(n)$ and $B(n)$ on each pressure level are given in Table A-1.

$$P(n) = A(n) + B(n)P_s \tag{4-1}$$

To calculate the resulting altitude from these pressure levels, Equation (B-2) and Equation (B-3) are used. Here, level 40 is the level closest to the surface and level 1 is the top level.

$$z(40) = \frac{[(P_s - P(40))]RT(40)}{0.5(P_s + P(40))g} \tag{4-2}$$

$$z(n) = z(n+1) + \frac{(P(n+1) - P(n))R(T(n+1) + T(n))}{(P(n+1) + P(n))g} \tag{4-3}$$

An example of real-life atmospheric weather forecast data is shown in Figure B-1. As can be seen, the lowest layer resembles an altitude profile close to the ground. Upon inspection, the altitude profile in Figure B-1 matches that of the corresponding real-world location, showing altitude peaks in the south-west resembling the Belgian Ardennes.

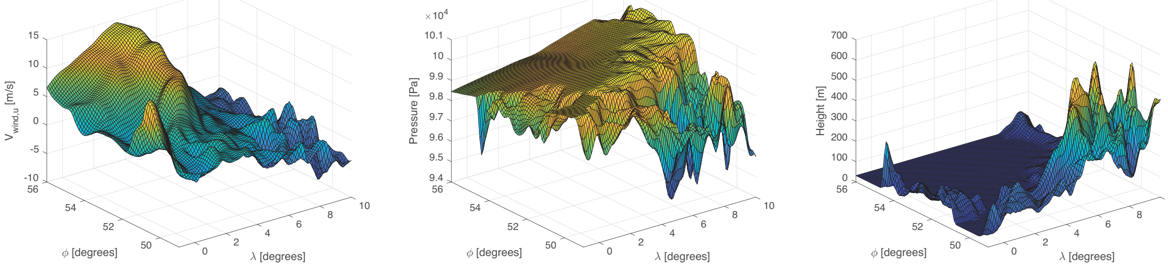

Figure 4-4: Visualization of layer 40 (closest to the ground) of a KNMI GRIB weather file of November 29th, 2018

4-3 Wind Impact on 4D ATM

4-3-1 Wind Influence on Airborne Navigation

While an aircraft's performance is defined relative to its local aerodynamic reference frame, the aircraft's movement relative to the earth is of predominant interest for ATM purpose. To distinguish between movement relative to the local reference frame and ground-based movement, different speed terminology is used.

TAS is defined as the aircraft's speed relative to the surrounding atmospheric parameters, thus including wind. Ground Speed (GS) on the other hand, is defined as the movement relative to the ground.

As a result of encountered wind fields, an aircraft's heading and track are not necessarily the same. While an aircraft's heading can be described as the direction it is facing, the direction of movement is indicated using its heading. Especially in strong crosswinds, the two values will differ because of the sideways drift caused by the wind field.

For navigational purposes, pilots like to maintain a constant track, implying that a correction will need to be to made the aircraft's heading depending on the wind field. This correction is defined as the wind correction angle δ, as is illustrated in Figure 4-5. The relation between the different speed vector angles is given by Ruijgrok (2009):

$$V_{GS} = V_{TAS} \cos \delta - V_{Wind} \cos \epsilon \tag{4-4}$$

$$V_{GS} = V_{TAS} \sqrt{1 - \frac{V_{Wind}}{V_{TAS}} \sin^2 \epsilon} - V_{Wind} \cos \epsilon \tag{4-5}$$

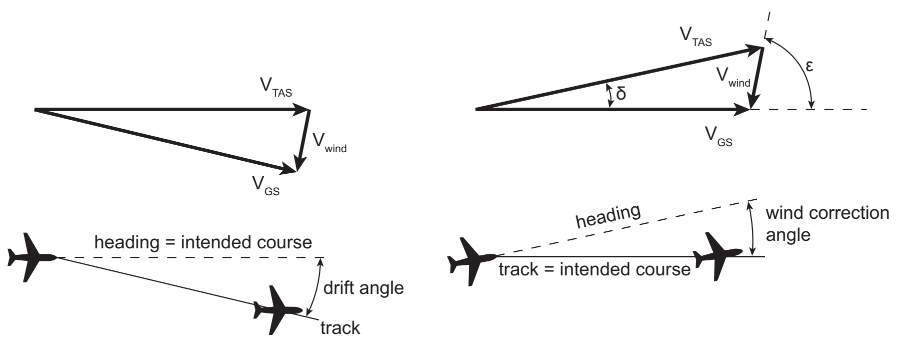

Figure 4-5: The effect of wind on aircraft track (reproduced from Ruijgrok (2009))

From Figure 4-5, the required wind correction angle to adhere to a prescribed track with a known wind field can also be derived:

$$\delta = \arcsin \left(V_{Wind} \frac{\sin \epsilon}{V_{TAS}} \right) \tag{4-6}$$

4-3-2 Wind in 4D Operations

Wind affects an aircraft's minimum and maximum reachable GS and therefore impacts its performance envelope. This has consequences for 4D flight TP, where predicted wind conditions are already taken into account.

The accuracy of these wind predictions have significant impact on the feasibility of a 4D flight plan. As can be imagined, it will be difficult for an aircraft to reach RTA waypoints from a 4D flight plan that was designed with a large tailwind in mind, when a headwind will be encountered during actual flight.

Considerable research has therefore been devoted to defining the wind information requirements to support 4D trajectory planning. This dates back to the PHARE project, where a maximum RMS error of 5 kts is stated as a requirement (Forrester & Davis, 1994). Cole, Green, Jardin, Schwartz, and Benjamin (2000) assessed wind prediction accuracy for the application in ATM DSTs, concluding that improvements needed to be made in the prediction accuracy. Especially errors that persist along flight paths were found to be detrimental to DST performance.

Glina et al. (2013) conducted experiments where a series of Monte Carlo simulations were conducted to assess RTA adherence feasibility at different levels of wind prediction information. Results indicate that the required wind prediction accuracy depends on the applied strategy to meet the RTA. When speeds are continuously adjusted to match the ETA with the RTA, combined forecast/Flight Management System (FMS) RMS errors of no more than 5 kts are allowed.

Chapter 5

Trajectory Uncertainty

Since the beginning of commercial ATM, trajectory uncertainty has had a large influence on airspace capacity. Estimating its magnitude has been important not only in planning, but also in quantifying conflict probability. This chapter aims to provide an overview of the subject, starting with the definition of trajectory uncertainty metrics in Section 5-1. Following is a summary of the sources of trajectory uncertainty in Section 5-2. Following in Section 5-3 is a description of different modeling techniques for estimating trajectory uncertainty. Lastly, uncertainty visualization is discussed in Section 5-4.

5-1 Trajectory Uncertainty Metrics

As trajectory uncertainty is being frequently researched, common metrics are used in discussing the subject. These metrics all refer to the flight path deviation in different dimensions.

5-1-1 Spatial Error

The spatial error can be described by the vector from an aircraft's actual versus its predicted position at a certain point in time. It can be decomposed into different sub-categories, as described in this section.

Horizontal Error

The horizontal error measures the horizontal distance between the predicted and actual aircraft position at a certain point in time. This error can be decomposed into an along-track and cross-track component, as shown in Figure 5-1.

In most modern FMS, track adherence properties are sufficient to maintain a maximum cross-track error of less than 0.5 Nautical Mile (NM). The along-track error is not bounded

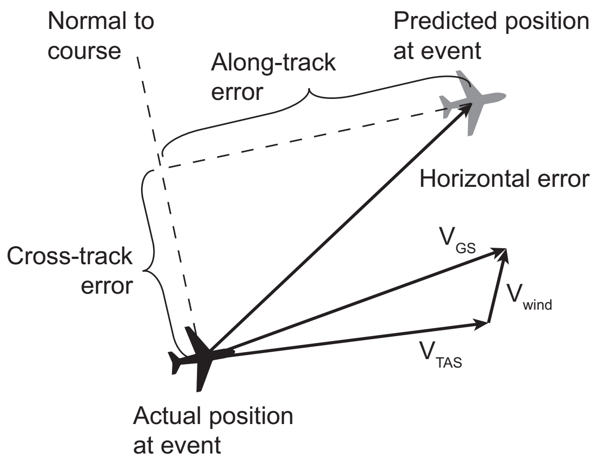

Figure 5-1: The relationship between horizontal, cross-track and along-track error (adapted from Mondoloni et al. (2005))

by a maximum value, however, and grows linearly with look-ahead time (Paielli & Erzberger, 1997) unless corrected by either the pilot or the FMS. In modern aircraft with RTA navigation capability, an aircraft will automatically adjust its velocity to meet the assigned RTA, causing the along-track error to return to zero at the RTA Waypoint (WPT).

Vertical Error

The vertical error is defined as the altitude difference between the predicted and actual flight path. Since a modern FMS can maintain a set altitude with an accuracy of $\pm 50ft$, vertical errors are only significant during the climb or descent phases of flight. Vertical errors originate from a variety of parameters, the most important ones being aircraft weight and FMS settings (Torres, 2015).

Typically, altitude errors caused by uncertainty in aircraft weight are larger in climb than in descent (Weitz, 2013). This is illustrated in Figure 5-2, where the blue line represents a reference flight path and the light blue surface represents the vertical uncertainty when varying the aircraft weight. The light red surface shows the projection of the uncertainty profile to the reference level, illustrating the vertical error as a result of aircraft weight deviation.

Vertical errors are complex to model, as more factors are of influence when compared to horizontal errors. In general, however, the vertical error can be modeled as an increasing error from the start of climb or descent. This error will reach a peak value and return to zero after the climb, because FMS altitude hold capabilities are very accurate.

5-1-2 Temporal Error

Temporal error is defined as the time difference between the predicted and closest on-track flight position at a particular event. The closest on-track flight position is in this case defined

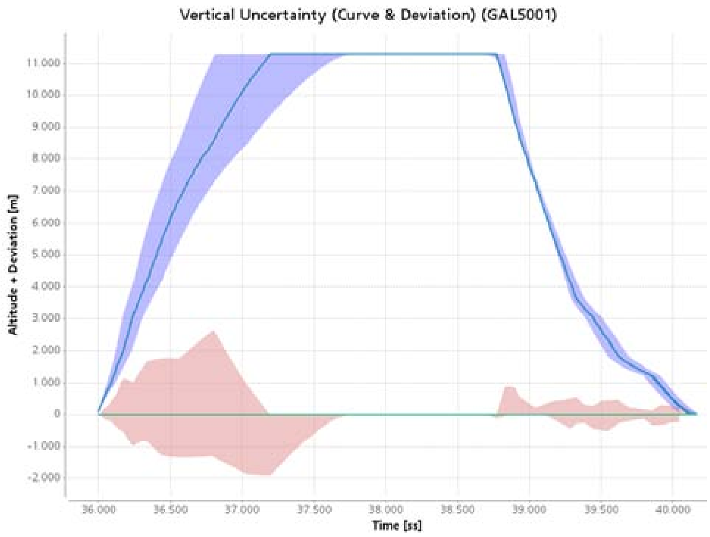

Figure 5-2: Vertical error during climb and descent phases of flight with varying aircraft weight (Weitz, 2013)

to be the closest on-track point from the actual aircraft position, measured using the great circle distance formula (Weitz, 2013).

Using the temporal error, a flight can be classified as being early, on time or delayed. Note that when a flight is on time (i.e., a zero temporal error) this does not mean that the spatial error is equal to zero, as cross-track deviations are still possible. This is illustrated in Figure 5-3.

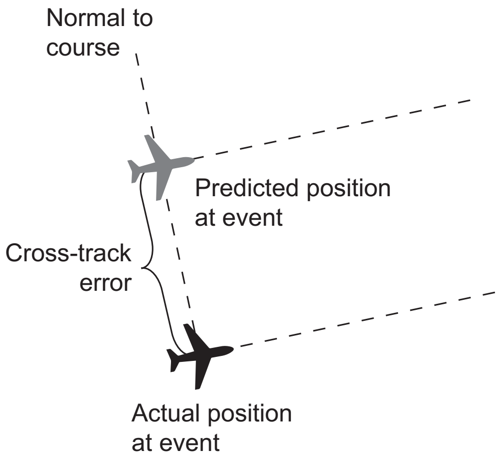

Figure 5-3: Zero temporal error in the presence of cross-track error

5-2 Sources of Trajectory Uncertainty

Uncertainty in the execution of a pre-planned flight trajectory can have multiple sources. In recent years, significant research has been devoted to the identification and characterization of these sources (Casado Magaña, Goodchild, & Vilaplana, 2012; Mondoloni & Bayraktutar, 2005; Torres, 2010; Warren, 2000; Weitz, 2013). The sources resulting from these studies are summarized in this section.

5-2-1 Initial Conditions

When estimating a flight path in both space and time, initial conditions have to be set. Some initial conditions are of stochastic nature. Two important factors are aircraft weight and departure time.

Aircraft Weight

As already shown by Weitz (2013), aircraft weight is largely responsible for climb rate uncertainty. Deviations in estimated aircraft weight are mainly caused by payload weight uncertainty.

Departure Time

In pre-departure phase, an aircraft's departure time is subject to large uncertainties (Torres, 2010), making 4D TP difficult. The industry is constantly trying to decrease departure time uncertainty by means of SWIM.

5-2-2 Modeling Errors

When estimating a flight trajectory, a combination of models is used. Each of these models has its own assumptions and known imperfections, which consequently contribute to inaccuracy in the TP process.

Aircraft Performance Model

The Aircraft Performance Model (APM) contains aircraft parameters needed to perform calculations on thrust, drag and fuel flow for example (e.g., Base of Aircraft Data (BADA) maintained by EUROCONTROL). Being largely parameterized models describing aircraft behavior in different phases of flight, errors in TP result from the APM. They are considered second order and not significant from an ATM point of view.

Aircraft Motion Model

The Aircraft Motion Model (AMM) is used to perform the kinematic calculations needed to predict aircraft motion. Simplifications in the equations of motion (e.g., small-angle approximations) and numerical methods contribute to the TP error (Torres, 2015). They are considered second order not significant from an ATM point of view.

Earth Model

When calculating distances and gravitational acceleration, a model of the earth's surface has to be used. Errors in TP arise form simplifications and other known inaccuracies in this model. As already indicated by Torres (2015), these errors are second order and not significant from an ATC point of view.

5-2-3 Aircraft Intent

Seeing the aircraft as the combination of the flight crew and actual aircraft, this category can be divided into pilot intent and aircraft behavior as a result of FMS settings.

Pilot Intent

When ATC instructs an aircraft to change its route, this will introduce some form of stochastic behavior, as the reaction time and and exact procedure followed by the pilot will not be constant.

FMS Settings

The modern day FMS utilizes different settings to determine the aircraft behavior. These settings include the cost index, turn parameters, thrust de-rating, engaged navigation mode (Lateral Navigation (LNAV),Vertical Navigation (VNAV)) and settings on for example RTA navigation. Even when known beforehand to ATC, the resulting aircraft behavior is difficult to predict, as the exact implementation of an FMS is largely proprietary.

5-2-4 Weather Forecast

Already discussed in Chapter 4, inaccuracies in wind forecast form a very large, if not the largest source of trajectory uncertainty (ICAO, 2014a), especially for along-track error. In a related working paper, ICAO (2014b) already mentions 'buffers' to be introduced when determining the possible ETA range as a result of meteorological errors. It is known that wind direction deviation induces larger errors than wind speed deviation (Weitz, 2013).

Besides wind, deviations in predicted local temperature and pressure also impact TP accuracy, because calculation of different speeds (such as Calibrated Airspeed (CAS) and M) from TAS depends on these parameters (Casado Magaña et al., 2012).

5-2-5 Flight Technical Errors

These errors are defined as inaccuracies in flight control due to FMS performance. These errors are considered the FMS tolerance limits and should be taken into account when modeling aircraft behavior in conflict prediction.

5-3 Quantifying Trajectory Uncertainty

The quantification of trajectory uncertainty consists of estimating the probability distributions of the spatial error parameters as deviations from a nominal flight path. Added together, these form a Three-Dimensional (3D) covariance ellipsoid that changes over time, as shown in Figure 5-4. When these distributions and thus the covariance ellipsoid are known, probable future aircraft positions can be estimated. Conflict probabilities can then also be estimated by looking at joint probability distributions (Matsuno & Tsuchiya, 2014; Prandini, Hu, Lygeros, & Sastry, 2000). Multiple techniques can be used to estimate the magnitude of the covariance ellipse at each point in flight.

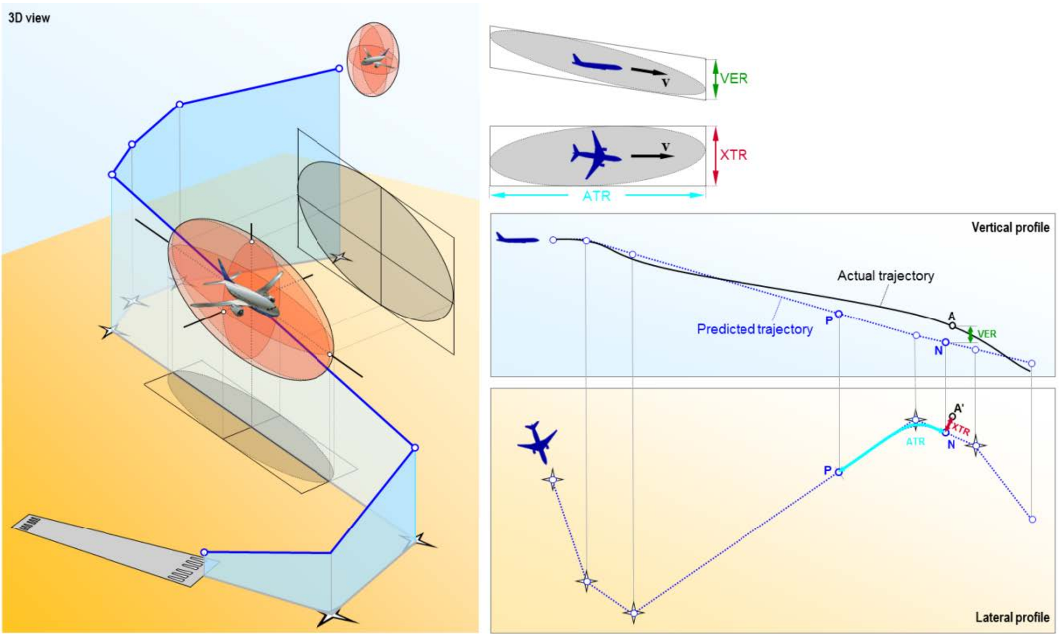

Figure 5-4: Representation of spatial TP accuracy (taken from Casado Magaña (2016))

5-3-1 Parametric Estimations

In the research field of mid-range conflict probability estimation (i.e., within a time horizon in the order of tens of minutes), the aircraft's covariance matrix is often estimated using relatively simple parametric estimations. Well-known research examples are provided by Yang and Kuchar (1998) and Prandini et al. (2000) and all look at the Two-Dimensional (2D) case of trajectory prediction from a certain known position.

In these parametric estimations, the cross-track and along-track error components are modeled as zero-mean components with an increasing variance in time, creating uncertainty contours around an aircraft's nominal predicted position. This is illustrated in Figure 5-5.

These uncertainty distributions can in turn be used to predict conflict probability. When assuming uncorrelated covariance matrices of different aircraft, they can be added together to calculate the conflict probability (Prandini et al., 2000).

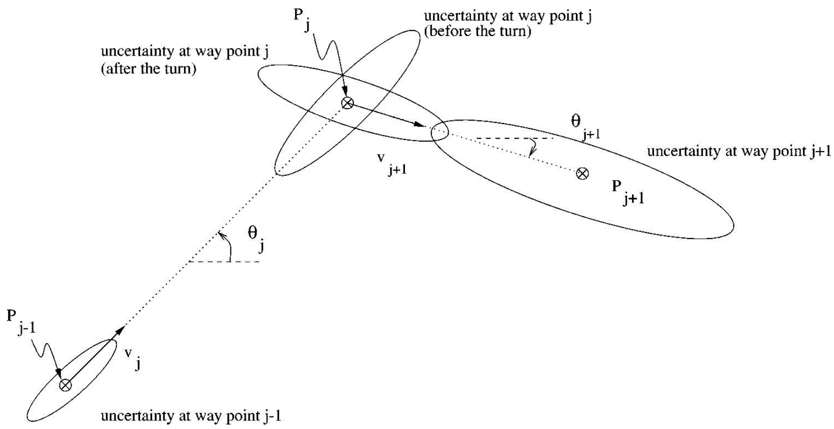

Figure 5-5: Mid-range prediction for aircraft motion (Prandini et al., 2000)

The assumption of uncorrelated covariance matrices is rather unrealistic, since the along-track error is largely caused by the wind error, which is correlated in both space and time (see also Section 4-2). Chaloulos and Lygeros (2007); Hu, Prandini, and Sastry (2003) have shown that the assumption of uncorrelated wind errors can be seen as being conservative, since conflict probability is consistently overestimated using this assumption.

5-3-2 Monte Carlo Simulations

When multiple stochastic inputs need to be 'mapped' onto their resulting stochastic output, Monte Carlo simulations are often used. Monte Carlo simulations have been applied in the validation of mid-range conflict prediction methods, but are also used to estimate the flight path sensitivity to TP uncertainty sources, as for example by Torres (2015). Monte Carlo simulations are rarely applied in on-line applications, since many runs (5000+) are typically required to achieve a statistically relevant result.

5-3-3 Polynomial Chaos Expansions

Being relatively new in the field of TP uncertainty, Polynomial Chaos Expansions (PCE) is a method with which similar results as the Monte Carlo method can be obtained, but at a considerably lower computing cost (Casado Magaña, Civita, Vilaplana, & McGookin, 2017; Matsuno & Tsuchiya, 2014). Despite this decrease in computational load, time needed for calculations usually still is in the order of seconds for a single aircraft trajectory (Casado Magaña et al., 2017), making PCE unsuitable for the highly flexible on-line calculation required by the TSR interface. Furthermore, as the application of the concept is relatively new, little research on PCE in TP applications is available. Because the aim of this research is to effectively visualize uncertainty and not to model it as accurately as possible, the concept of PCE is considered beyond the scope of this literature study. It is explained in detail by Casado Magaña (2016).

5-4 Visualization of Trajectory Uncertainty

TP uncertainty will have to be visualized on a radar-like HMI in the DUT TSR. Besides the probabilistic CD&R display by H. Lee and Milgram (2008) already discussed in Section 3-2, several other methods to visualize TP uncertainty exist. Knorr and Walter (2011) used the concept of growing ellipsoids to visualize uncertainty to the user, while Weitz (2013) made use of 'uncertainty tubes' to visualize potential flight paths. Both are shown in Figure 5-6.

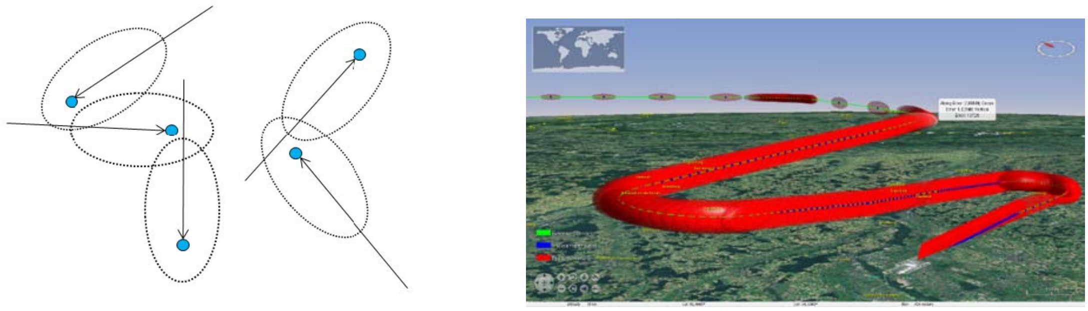

(a) Knorr and Walter (2011) **(b)** Weitz (2013)

Figure 5-6: Examples of trajectory uncertainty visualization

Chapter 6

Concept of Operations

In future ATM visions described by the FAA and EUROCONTROL, 4D trajectory management forms an important aspect to facilitate the projected increase in air traffic in the coming decades. Technologies such as CDM and SWIM will minimize uncertainty and allow altered flight trajectories to be communicated to all relevant stakeholders immediately. The resulting ATM CONOPS is, however, not yet fully defined. For the design of a new conceptual DST, assumptions regarding the CONOPS will therefore have to be made. This chapter presents the envisioned CONOPS that will form the basis for proposed interface additions in the remainder of this thesis. This starts with assumptions on the availability of data, such as flight plans, surveillance data and meteorological forecasts in Section 6-1. The resulting CONOPS rationale for each TSR display is presented in Section 6-2.

6-1 Data Availability

When defining the CONOPS for the DUT TSR with added wind and trajectory uncertainty information, new information has to be integrated into the interface. As the interface itself is merely a DST, this information integration process cannot be seen separately from the ATM CONOPS.

Being mentioned in numerous documents on future ATM visions (European Commission & EUROCONTROL, 2015; Federal Aviation Administration, 2016; SESAR Consortium, 2007), the concept of 'data-link' and 'SWIM' has a broad understanding. In all visions, the idea is that different types of information are stored in a central location, where its stakeholders can read from or publish to. Since all stakeholders have access to all information, trajectory uncertainty will decrease and planning will be more accurate.

In Figure 6-1, a SESAR overview of the envisioned aircraft participation in SWIM is presented. As can be seen, the idea of data-link in Air/Ground SWIM is that different types of data (Surveillance, Flight, Aeronautical, Meteo) are shared between ground stations and aircraft.

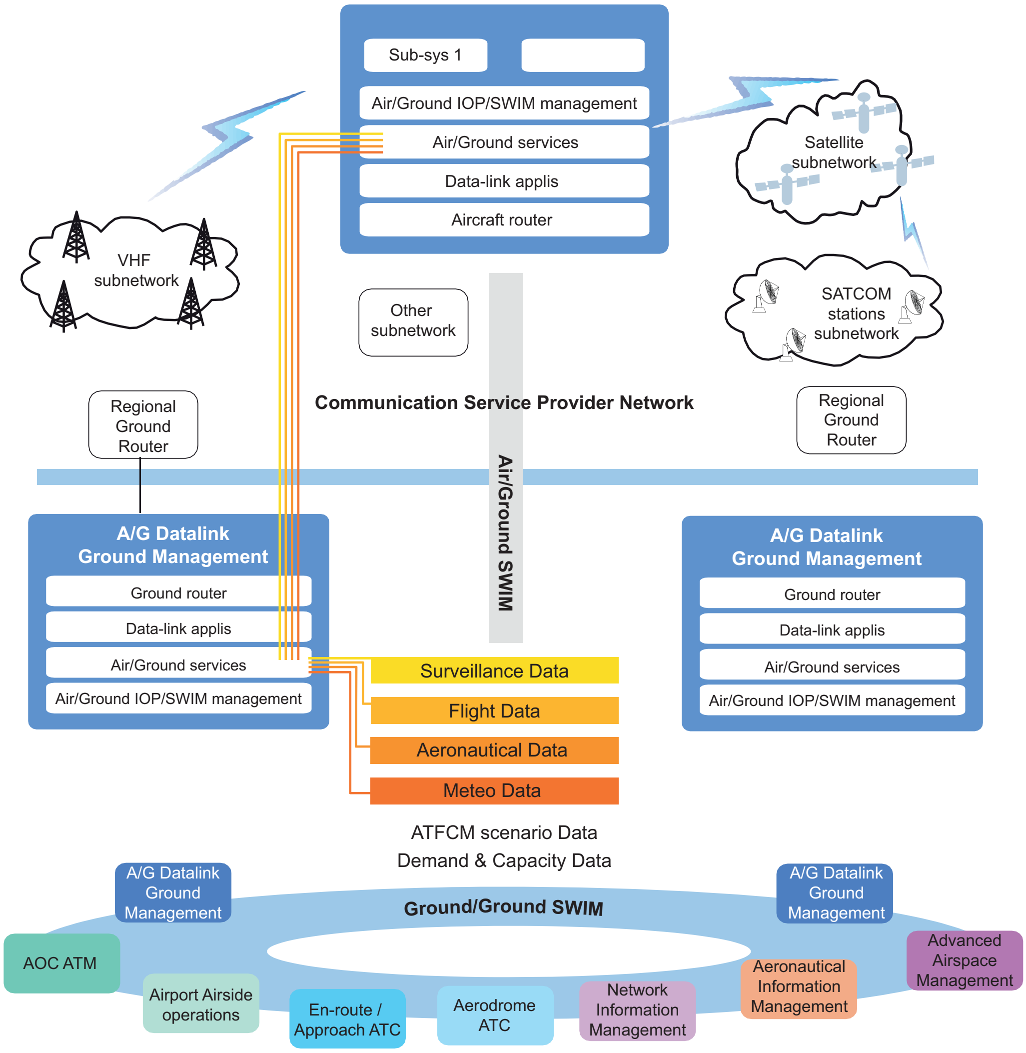

Figure 6-1: Envisioned aircraft participation in SWIM (SESAR Consortium, 2007)

This is to be done by making use of regional ground routers and sub-networks such as Very High Frequency (VHF) and satellite communications.

At the moment, SWIM concepts are still in a preliminary phase. In the traditionally slowly-evolving ATM sector, full data-link availability in SWIM is not expected to be operational before 2030 (European Commission & EUROCONTROL, 2015), with further implementation delay not being unlikely.

It should also be mentioned that *having data available* should be seen separately from *being able to effectively use that data*. Computational power provided by the FMS will differ per aircraft type and will also likely be less than on the ground. In the development of the DUT TSR, full data-link availability should therefore not be taken for granted without further thought.

A modern day FMS has limited capability of storing wind information (Reynolds et al., 2012). Most airlines have wind data at several flight levels available along their flight path at specified points only. Because wind is a significant factor in determining an aircraft's ETA, FMS RTA functionality largely depends on the amount and resolution of wind data available to the FMS. Especially with large unexpected headwinds, RTA deviation can be significant (De Smedt & Berz, 2007).

On the ground, however, detailed wind forecast information is available and is updated continuously (see Table 4-1). In the Netherlands, the KNMI provides high resolution weather forecasts with a 0.1 latitude/longitude resolution on 40 altitude levels every hour. It seems trivial that ETA predictions performed using this kind of data will outperform those performed by an FMS limited in both computing power and available information.

Besides the wind information ability, the actual RTA functionality implementation differs per aircraft (McPartland et al., 2014). The exact implementation of the algorithm is often proprietary information belonging to the aircraft manufacturer. From an ATC point of view, it is therefore very difficult to objectively quantify trajectory uncertainty when flying towards a metering fix using the FMS RTA functionality (Torres, 2015).

Following this reasoning, decisions can be made on where different types of calculations should be performed and what information should be shared between aircraft and ATC. The result is summarized in Figure 6-2.

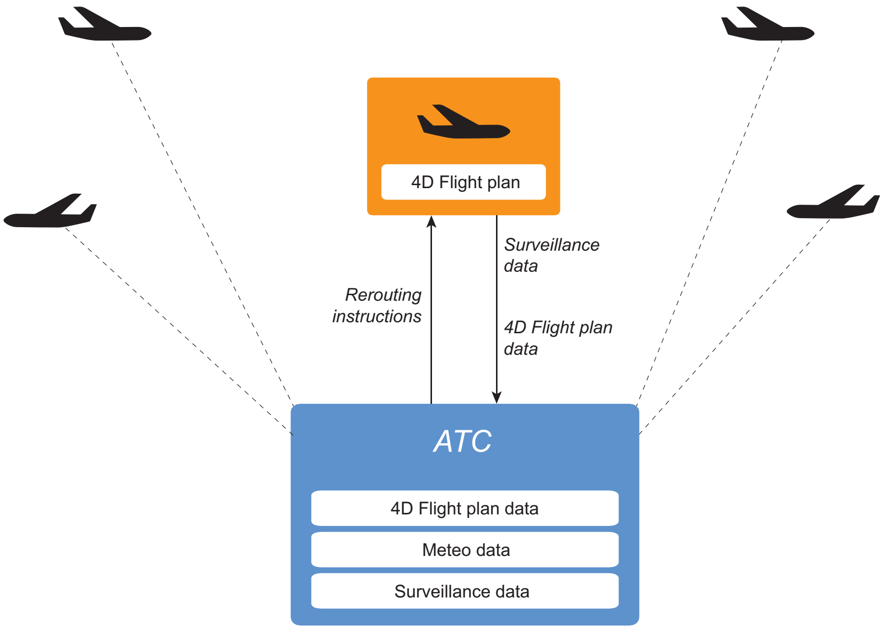

Figure 6-2: Information management in proposed DUT TSR CONOPS

As can be seen, most of the calculations to predict ETA are performed by ATC and not by the FMS. The 'RTA control-loop' is therefore closed on the ground instead of in the air. This increases prediction accuracy, as detailed weather forecasts can be used, and reduces unpredictable en-route aircraft behavior because the 'black-box' FMS RTA functionality can be bypassed.

Another advantage of this approach is that the ATCo remains in control of the commands issued to the aircraft. This will likely increase controller acceptance, because they remain actively involved in the decision-making process.

6-2 Concluding CONOPS Rationale

Based on the envisioned information organization and data-link definitions discussed, the CONOPS rationale for each display can be reasoned. To explain the rationale in the to-be-designed interface, the assumptions behind the current TSR CONOPS (already mentioned briefly in Section 3-3) will be discussed first, followed by a description of the proposed CONOPS rationale.

6-2-1 Current Operational Assumptions

Besides pre-planned 4D flight plans being used, the current TSR CONOPS is based on a number of key operational assumptions that allow the generation of the solution space in each display. These operational assumptions, together with their reasoning, will be summarized in this section per display.

PVD

For the PVD, the solution space is constructed using the assumption that the original route segment will be split into two new segments which are to be flown *at constant IAS*. This implies a single new Speed (SPD) command to be given only once, which is supposed to reduce pilot and ATCo workload. Together with the SPD command, a Heading (HDG) command is given. When turning back to the exit waypoint, a Direct To Command (DCT) is given.

Furthermore, the exit waypoint is fixed, meaning that the ATCo cannot issue a change in flight plan. This choice has been made to keep the pre-planned 4D flight plans operative as much as possible, since modifications might introduce planning problems in adjacent sectors.

TSD

For the TSD, no constraining assumptions are currently made. The aircraft speed envelope is mapped onto the display, giving the ATCo a range of possibilities to adjust an aircraft's velocity, with the option to alter the Time of Arrival (ToA) at exit waypoint. A SPD command is thus given.

VSD

In the VSD, the solution space is currently constructed using the assumption of a constant IAS climb or descent, where the pilot will receive a new SPD command at the start of the level segment to meet the RTA. The exit altitude is fixed, meaning that the aircraft in question will always have to return to the original altitude before leaving the sector. Along with the SPD command at the level segment, an Altitude (ALT) command (to set the level segment altitude) and Bottom of Climb (BoC) or ToD command (to determine the start of the first climbing or descending segment) is given.

As already mentioned in Section 3-3, the constant IAS climb/descent assumption is a rather unrealistic one, since aircraft climb and descend at constant M above *crossover altitude* (EUROCONTROL Experimental Centre, 2010), as is illustrated in Figure 6-3.

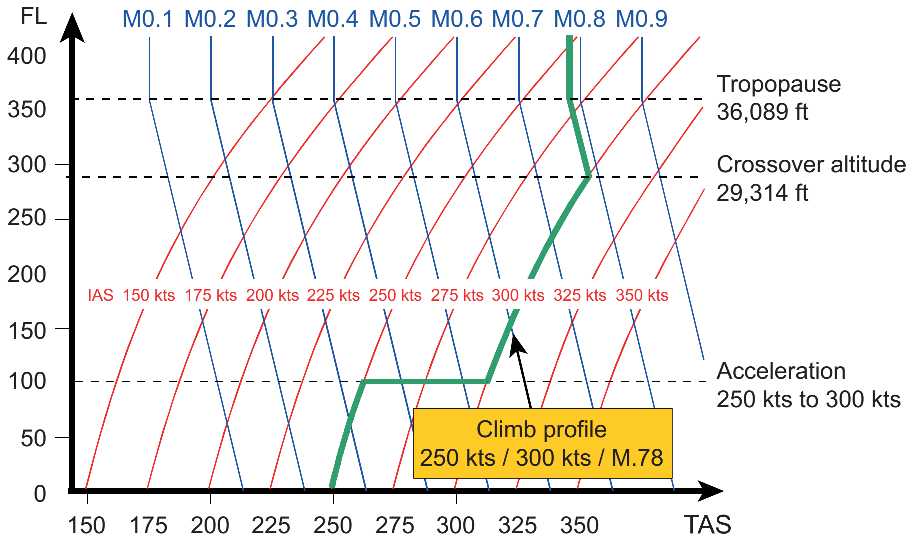

Figure 6-3: A standard climb profile for the Airbus A320 family (Airbus Customer Services, 2002)

In a typical climb profile, aircraft start climbing at a relatively low constant IAS to achieve a high Rate of Climb (RoC) and get into thin air as quickly as possible. Then, an acceleration is made at a level segment (in this case to an IAS of 300 kts at FL100), after which the climb profile is continued at constant IAS. This continues until crossover altitude (in this case at 29,314 ft, where an IAS of 300 kts equals M 0.78) is reached, where the pilot switches from a constant IAS to a constant M climb. Because the cross-over altitude is usually located below cruise level, constant M climb profiles are relevant to include in the interface.

6-2-2 Proposed CONOPS

The operational assumptions resulting from the approach stated in Section 6-1 and additional operational assumption alterations are summarized per display in the remainder of this section.

PVD

Because rerouting instructions are given by ATC in the proposed CONOPS, a constant IAS can still be instructed to the pilot. A different GS per segment will, however, follow from the present wind field. These ground speeds will in turn affect the ETA at sector exit waypoint. This effect will have to be taken into account when constructing the solution space.

TSD

As no operational assumptions needed to be made in the current TSD, this will not change. The conversion from TAS to GS will have to be incorporated into the solution space, because the reachable ToA range at sector exit will be impacted by the presence of wind.

VSD

Apart from the TAS to GS conversion being implemented in the VSD, the climb profile assumption will be altered. Using the BADA models, the crossover altitude from IAS to M can be calculated (EUROCONTROL Experimental Centre, 2010). Furthermore, inclusion of the tropopause (>FL360 when adhering to the International Standard Atmosphere (ISA)) can be included. Using this information gives more realistic climb/descent profiles. The impact of this difference in climbing performance is illustrated in Figure 6-4.

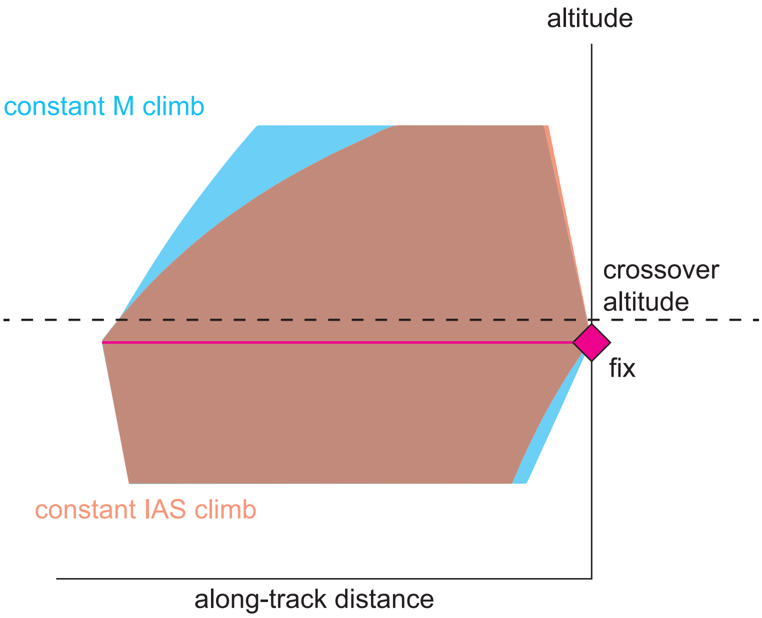

Figure 6-4: Effects of constant IAS climb profile assumption versus IAS to M crossover in VSD

As can be seen, the constant M climb segments are steeper than their constant IAS counterparts. This can be explained by the increasing amount of excess thrust available to the aircraft in a constant M climb (because IAS is decreasing). This excess thrust is used to increase the RoC once the crossover altitude has been reached.

The implementation of constant M climb profiles also impacts the constraints to be checked when constructing the VSD. At increasing altitudes, the same IAS results in a higher TAS, whereas the TAS will drop if the IAS is held constant at decreasing altitudes (Ruijgrok, 2009). In the current algorithm, a FL above current altitude is therefore checked against the aircraft's minimum IAS whereas a FL below current altitude is checked against the aircraft's maximum IAS.

In a constant M climb, the TAS decreases during climb, meaning that an aircraft's *maximum* IAS can also become a limiting factor at a FL *above* the current altitude. To illustrate this, two identical scenarios with different climb strategies are shown in Figure 6-5. As can be noted, the reachable FL range is impacted considerably by the transition from a constant IAS to constant M climb.

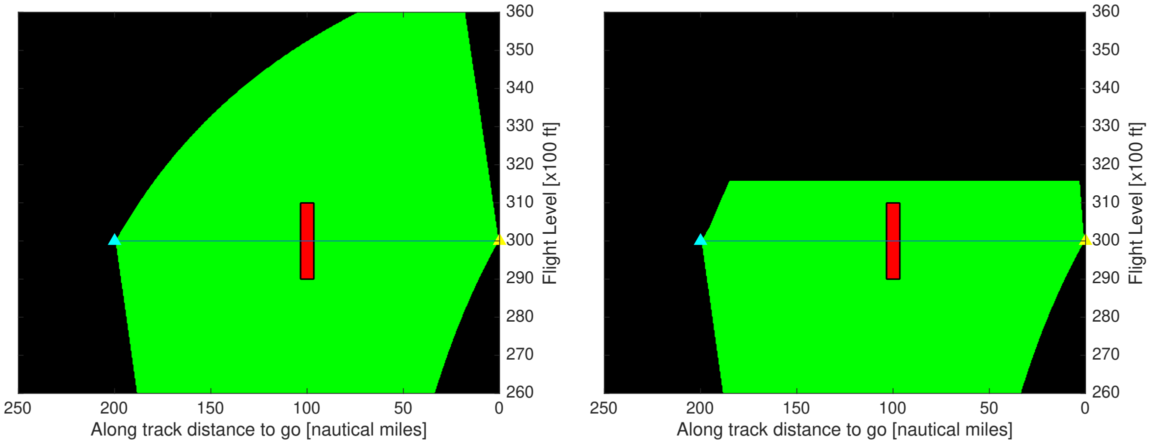

(a) Constant IAS climb only

(b) Transition from constant IAS to constant M climb

Figure 6-5: Effects on solution space of maximum IAS constraint in constant IAS versus constant M climb

Chapter 7

Effects of Wind

Following the envisioned CONOPS as described in Chapter 6, the effects of a wind field on perturbation management in 4D ATM is investigated. This is done in terms of the effect on the solution space in the TSR. The modeling approach to perform this analysis is presented in Section 7-1, with the corresponding simulation results shown in Section 7-2.

7-1 Modeling Approach

When viewing the wind field as a spatial 3D grid on which 2D vectors represent wind velocity, a simulation can be set up to investigate the effects of these wind fields in different traffic scenarios.

A modern FMS can compensate for an encountered wind field, causing the aircraft to adhere to a pre-defined track. Therefore, it is assumed that, with an instructed IAS and track, the FMS will determine the wind correction angle to be applied using Equation (4-6).

As a result of the wind field, an aircraft's GS will change. Since the GS is relevant for calculating emerging separation conflicts and ETA at sector exit, the reachable (from performance point of view) and safe (without LoS) field of travel will be impacted.

7-1-1 Wind Model

Two types of models will be used when investigating wind effects in an integrated MATLAB package. Firstly, an implementation using constant wind fields will be used. After that, a more elaborate model using dynamic weather forecasts is used. Both are discussed in this section.

1D Wind Fields

To have the freedom of wind scenario and model fidelity, synthetic wind fields are investigated first, starting with impact of a static 1D wind field (average wind velocity and direction, not changing over time). Dynamic wind effects and changing wind vectors in both altitude and location are not incorporated. Although this does not resemble a real-life scenario, an average wind direction and velocity is commonly used in low fidelity weather forecasts. As a result, the wind vector will be constant in both time and space and calculations will be linear for each track segment.

3D Wind Fields

When upgrading the model fidelity, a 3D grid is used on which 2D vectors represent lateral wind velocity. Therefore, dynamic wind vector fields can be implemented. The KNMI data structure (see Section 4-2-3) and resolution will be adhered to, as this type of forecast could also potentially be used in operation.

When wind prediction data is needed for TP purposes, the data will be needed on an x, y, z grid. To this end, a stereographic projection has been used to map the decimal coordinates onto x, y coordinates as shown in Equation (B-4) to Equation (B-6) (Snyder, 1983).

$$x = k \cos\phi \sin\lambda - \lambda_0 \tag{7-1}$$

$$y = k \cos\phi_1 \sin(\lambda - \lambda_0) \tag{7-2}$$

$$k = \frac{2R_e}{1 + \sin\phi_1 \sin\phi + \cos\phi_1 \cos\phi \cos(\lambda - \lambda_0)} \tag{7-3}$$

As can be seen in Figure B-2, resolution will decrease when moving further away from the central point. As a result, an irregular grid spacing is obtained in all three dimensions (lateral due to the projection, vertical due to the pressure levels being used). This spacing is mapped onto a regular grid using a trilinear interpolation algorithm, significantly reducing computational load.

7-1-2 Solution Space Calculations

In this section, the impact of the wind model on the generation algorithm of the solution spaces will be discussed. This will be done separately for each display.

PVD

In the current PVD, the resulting TAS is calculated using the simple calculation of Distance To Go (DTG) divided by the Time To Go (TTG), which is then converted to IAS. The assumption is made that the two flight segments resulting from the rerouting procedure are still to be flown at constant IAS. With added wind, however, the GS will differ on both ground segments, since the incoming wind angle per segment will not be the same.

With added wind, the ETA at sector exit can be calculated using the track distance of each segment along with the GS vector along each segment, assuming that the FMS applies

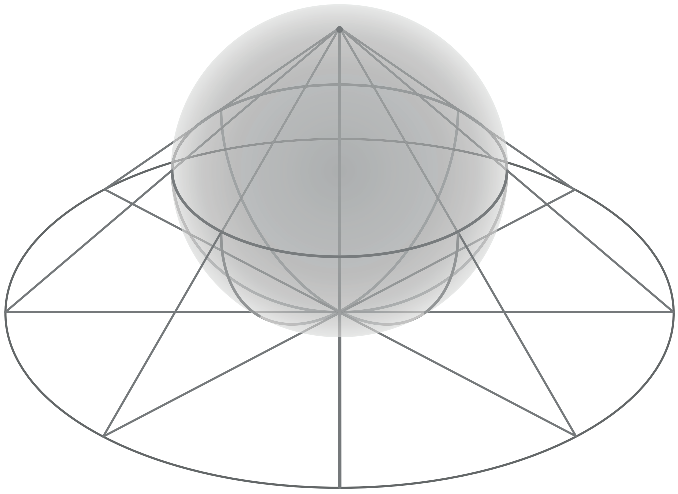

Figure 7-1: 3D representation of a stereographic projection (taken from `wikimedia.org`)

the correct wind correction angle. Because the TAS forms both the input (to calculate the required wind correction angle) and the output (to adhere to the RTA constraint), an iterative solution will be required. This is illustrated in Equation (7-4) to Equation (7-5), which can be applied with a constant wind vector.

$$\delta = \arcsin{(V_{Wind} \frac{\sin \epsilon}{V_{TAS}})} \tag{7-4}$$

$$V_{GS} = V_{TAS} \cos \delta - V_{Wind} \cos \epsilon \tag{7-5}$$

When fully dynamic wind vector fields are to be implemented in the creation of the solution space, the solution to the problem becomes a path integral. Because this drastically increases computational load, this path integral can be split up into several piece-wise linear parts, with each path having its own average wind vector. To calculate the resulting average ground speed per segment, the wind vectors for all paths in the segments are averaged, as shown in Algorithm 1. Separation conflicts are calculated using the Closest Point of Approach (CPA) of two aircraft using the average ground vectors per segment.

This simplification is currently needed to reduce computational load and allow the parallel computing of all pixels and can be justified, because - at high altitude - wind direction and velocity do not rapidly change. Nevertheless, this simplification will introduce an error when rapidly changing wind conditions are present. The implemented algorithm to obtain the required TAS is shown in pseudo-code in Algorithm 2.

TSD

In the TSD, the speed envelope of the aircraft is currently projected onto the vertical axis. With the introduction of wind, the GS envelope will change. This will therefore have to be implemented in the TSD.

```
input  : Wind forecast data, aircraft flight plan
output: Average wind vector per track segment

obtain track segment vectors;
for each segment do
    determine wind vector locations;
    for each location on segment do
        obtain wind vector;
    end
    calculate average wind vector per segment;
end
```

Algorithm 1: Average wind vector for PVD solution space algorithm

```
input  : Average wind vector per track segment, aircraft flight plan
output: Required TAS to adhere to RTA constraint

obtain RTA;
calculate ETA using current TAS as initial estimate;
calculate error;
while absolute error exceeds threshold do
    calculate TAS delta;
    update TAS estimate;
    calculate new ETA;
    calculate new error;
end
```

Algorithm 2: Required TAS estimation for PVD solution space algorithm

Because the TSD is concerned with only one spatial flight path (only the velocity can be adjusted), additional computational load is limited when compared to the PVD and VSD. Therefore, a piece-wise linear resolution equal to the screen resolution can be chosen to calculate the resulting average wind vectors for every point along the flight path, as shown in Algorithm 3.

```
input  : Wind forecast data, aircraft flight plan
output: Average wind vector along flight path

for each calculation point do
    obtain wind speed at point;
    calculate cumulative wind speed from starting location;
    divide cumulative wind speed by number of steps;
end
```

Algorithm 3: Average wind vector for TSD solution space algorithm

VSD

For the VSD, altitudes are currently checked for validity with the aircraft performance envelope. After climbing or descending using the prescribed setting (constant IAS, M or a combination), the length of the level segment and the required time to fly the level segment to reach the RTA result in a prescribed TAS. This TAS is then held against the aircraft flight envelope to check reachability.

In all three segments (two altitude changes and one level segment), wind effects should be taken into account. The altitude changes can be calculated using the fixed climb profiles assumed. Adding wind will affect the distance required to perform the altitude change and therefore also the resulting length of the level segment.

Again, the average wind vector will be computed for all three segments to determine ground speed vectors. This algorithm is illustrated in Algorithm 4.

```
input  : Wind forecast data, aircraft flight plan
output: Average wind vector along flight path
for each calculation point do
    obtain wind speed at point;
    calculate cumulative wind speed from starting location;
    divide cumulative wind speed by number of steps;
end
```

Algorithm 4: Average wind vector for VSD solution space algorithm

7-1-3 Assumptions

As on-line results need to be generated and available computing time is therefore limited, the following assumptions will be made:

- **FMS compensates for wind direction**: As most modern FMS have good track-keeping functionality (within 0.5 NM), it is assumed that the correct wind correction angle to compensate for the incoming wind is automatically applied.
- **No turbulence**: Apart from turbulence being significant enough to become a no-go zone, it is not taken into account in the TP process.
- **No vertical wind component**: Only the lateral wind velocities will be taken into account, as these are the most relevant velocities in TP applications. Vertical wind components will not be modeled (although they might be severe enough to form a no-go zone).
- **No wind gusts and microbursts**: Wind gusts and microbursts will not be taken into account, as these events introduce added computational complexity and are less relevant in TP applications (if not severe enough to form a no-go zone).
- **Smooth wind fields**: The wind vector will be assumed to smoothly change within an airspace sector, allowing for the use of piece-wise linear wind vector segments.
- **ISA**: In the current simulations, the ISA is assumed. In real life, especially temperature fluctuations can cause significant aircraft performance differences when compared to the ISA. As high resolution atmospheric temperature predictions are also made by the KNMI, this will be implemented in the final interface.

7-2 Simulation Results

In this section, simulation results will be presented. Firstly, the effect of wind on each screen will be discussed. Afterwards, a case study will be performed using high resolution modified KNMI weather forecast data. A crossing air traffic scenario in a square sector with a length of 200 NM will be investigated. In all simulations, an Airbus A320 BADA APM (v3.7) will be used. In all wind field visualizations, the PVD shows the lateral wind velocity vector, while the TSD and VSD show the along-track projection of this vector onto the flight path.

7-2-1 PVD

For the PVD, the effects of a uniform wind field are displayed in Figure 7-2. Following is a summary of the most prominent results.

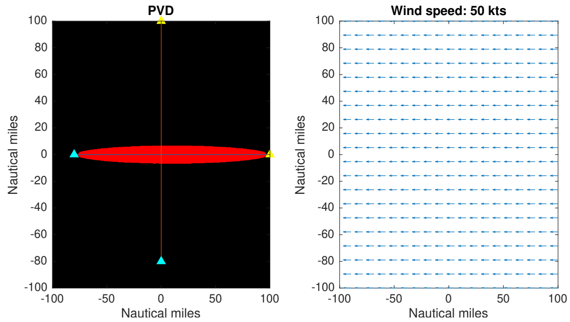

(a) Wind direction 90 degrees

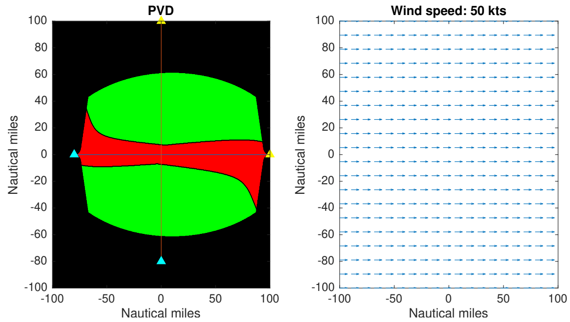

(b) Wind direction 270 degrees

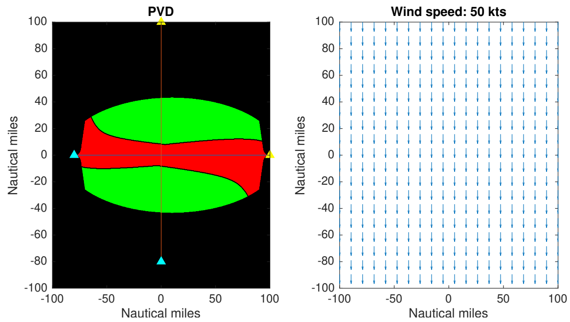

(c) Wind direction 0 degrees

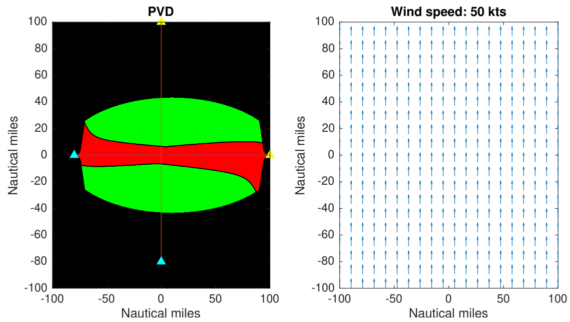

(d) Wind direction 180 degrees

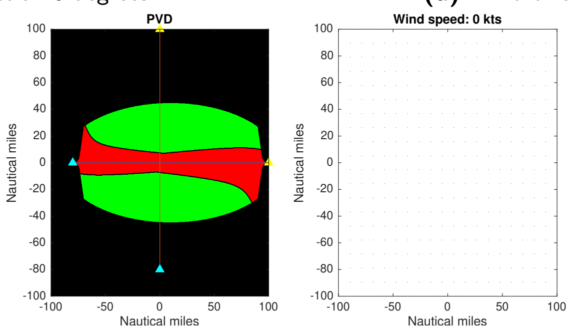

(e) Baseline traffic scenario without wind

Figure 7-2: Effects of uniform wind field on PVD in crossing traffic scenario

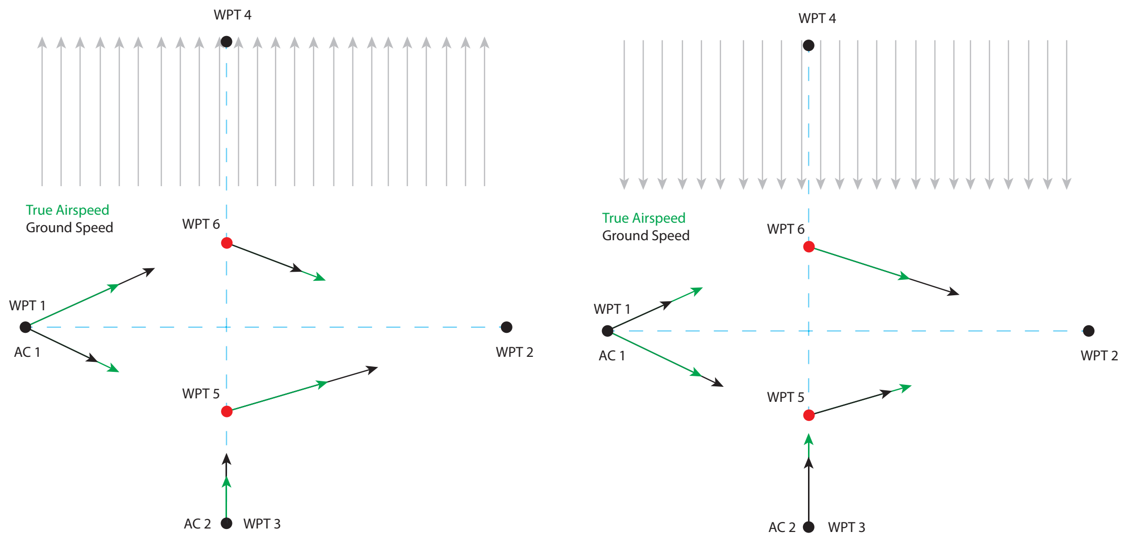

Figure 7-3: Effects of crosswind direction on CPA

- A tailwind increases the performance-based solution space (i.e., the green area) (Figure 7-2b), whereas a headwind (Figure 7-2a) decreases the performance-based solution space. This can be attributed to the fact that the resulting ground speed increases with a tailwind component resulting in more deviation possibilities, while a headwind decreases the ground speed.

- A pure crosswind component, as shown in Figure 7-2c and Figure 7-2d, also decreases the performance-based solution space, as part of the available velocity is needed to compensate for the incoming crosswind. The direction of the crosswind does not matter if its magnitude is equal.

- Crosswind direction significantly impacts the conflict zone (i.e., the red area) (looking at the differences in the red area between Figure 7-2c and Figure 7-2d). This can be explained using Figure 7-3. Resulting from the assumption that both track segments are to be flown at constant IAS, the GS of aircraft 1 will increase from WPT 1 towards WPT 6 and decrease from WPT 1 towards WPT 5 with a southern wind direction. This will decrease the CPA for both trajectories passing through WPT 5 and WPT 6, resulting in a larger area of conflict. This effect is the other way around with a northern wind.

7-2-2 TSD

For the TSD, the effects of a uniform wind field are displayed in Figure 7-4. Following is a summary of the most prominent results.

- A uniform headwind (Figure 7-4a) 'tilts' the beam projection into a steeper shape, because the resulting maximum and minimum ground speeds are decreased, delaying

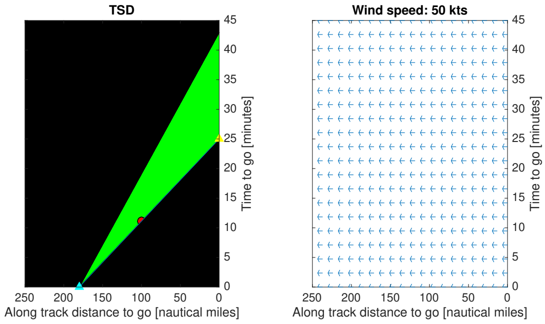

(a) Wind direction 90 degrees

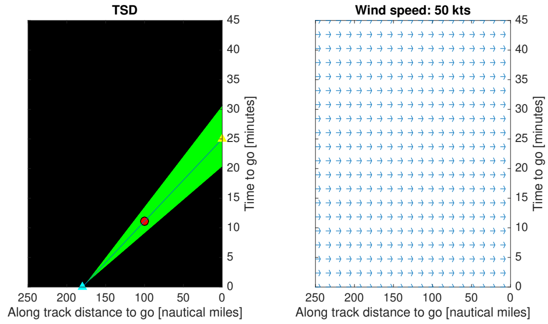

(b) Wind direction 270 degrees

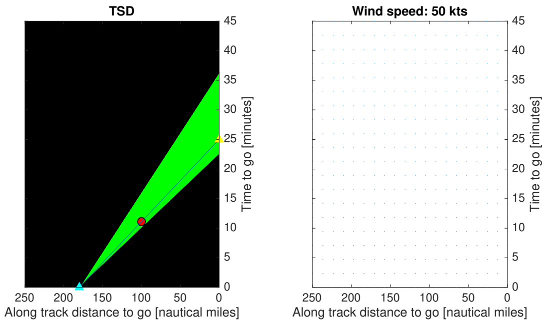

(c) Wind direction 0 degrees

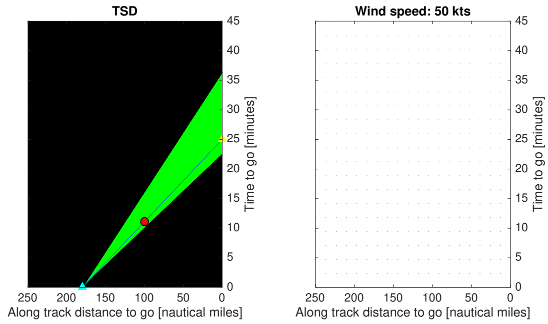

(d) Wind direction 180 degrees

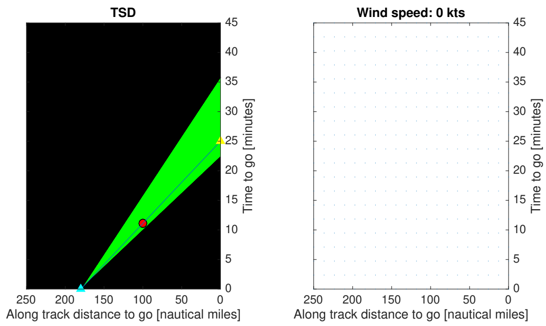

(e) Baseline traffic scenario without wind

Figure 7-4: Effects of uniform wind field on TSD in crossing traffic scenario

the ETA range on the time axis. The opposite is true for a uniform tailwind (Figure 7-4b).

- A crosswind, as shown in Figure 7-4c and Figure 7-4d, slightly decreases the maximum and minimum on-track ground speed when compared to no wind (Figure 7-4e), as part of the 'available GS' has to be used to compensate for the incoming wind.

- The conflict zone in all figures does not change in both along-track distance and TTC. This is to be expected, since the along-track velocity of each aircraft will be equal regardless of the wind scenario (as each aircraft adjusts its velocity to meet its respective RTA).

7-2-3 VSD

For the VSD, the effects of a uniform wind field are displayed in Figure 7-5. Following is a summary of the most prominent results.

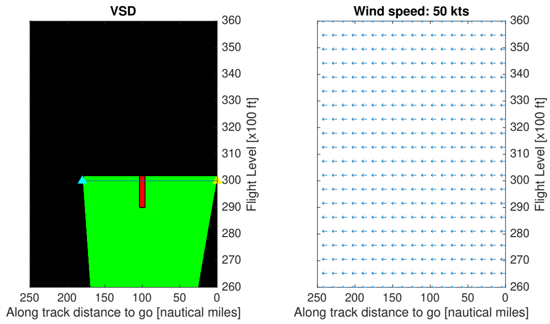

(a) Wind direction 90 degrees

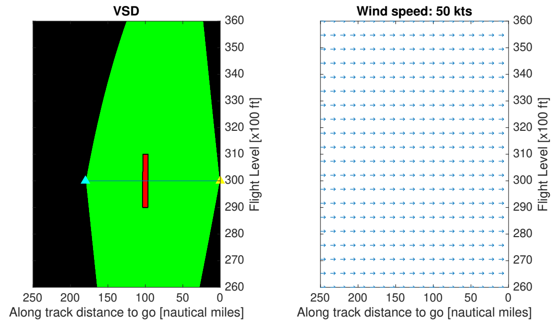

(b) Wind direction 270 degrees

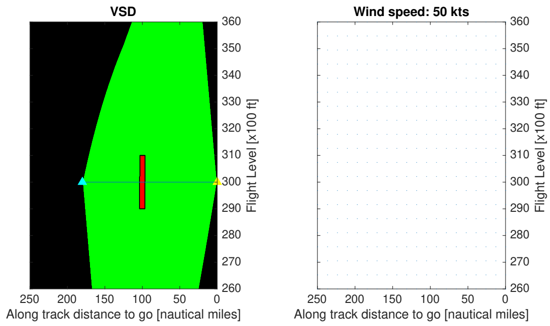

(c) Wind direction 0 degrees

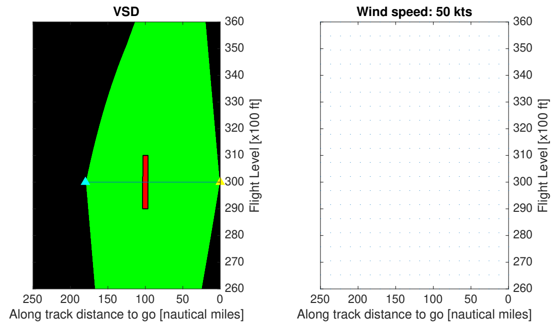

(d) Wind direction 180 degrees

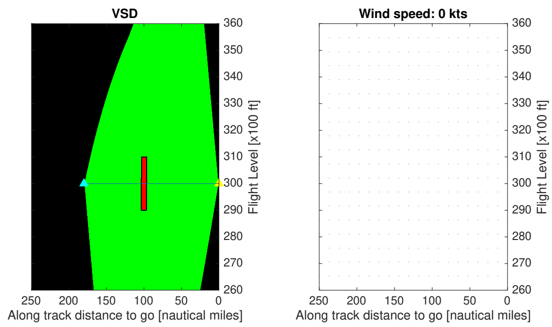

(e) Baseline traffic scenario without wind

Figure 7-5: Effects of uniform wind field on VSD in crossing traffic scenario

- With a strong headwind (Figure 7-5a), higher altitudes are not reachable anymore. In this case, the aircraft's TAS is already close to its maximum to reach the RTA (see also Figure 7-4a). This means that initiating a climb will automatically be at constant M, and will therefore lower the TAS during climb. This will result in the RTA being out of reach at higher altitude. At lower altitudes, the TAS will have to be increased, but as the maximum TAS is also higher at lower altitudes, lower altitudes are reachable.
- Crosswinds (Figure 7-5c and Figure 7-5c) and tailwinds (Figure 7-5b) do not impact the minimum and maximum reachable altitudes in the current traffic scenario.

- A tailwind (Figure 7-5b) implies a larger performance-based solution space when compared to the baseline (Figure 7-5e), as the IAS is lower and therefore the RoC will be higher (more excess thrust can be used to climb).

- The conflict zone does not change in both along-track distance and altitude in all figures.

7-2-4 Case Study

Following the analysis of uniform wind fields on the TSR interface, several cases using the high fidelity model will be discussed in this section. For this, a KNMI GRIB file was manipulated to illustrate the effects of different wind scenarios. The baseline traffic scenario without wind, to which the scenarios with dynamic wind fields will be compared, is shown in Figure 7-6.

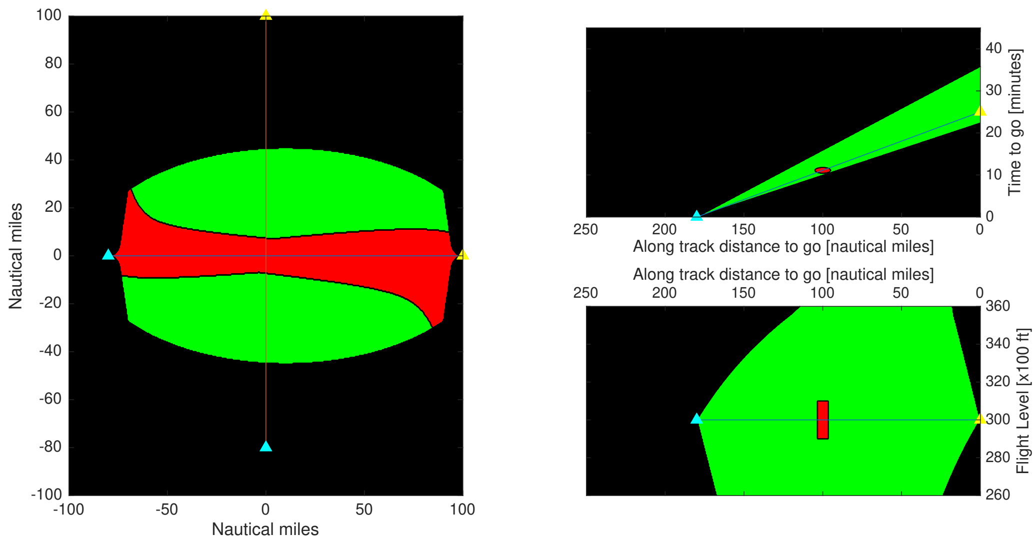

Figure 7-6: Resulting TSR display for baseline traffic scenario without wind

Case I: Lateral Wind Shear

In the first case, a sudden change of wind direction will be discussed, as illustrated in Figure 7-8. This sudden change in wind direction is about five miles north of the nominal aircraft trajectory as can be seen in Figure 7-8.

Because this lateral wind shear is not located on the aircraft's nominal trajectory, the TSD and VSD are not impacted and look 'normal'. The PVD, however, becomes asymmetrical (see Figure 7-7) as the wind components are not constant anymore on the lateral plane. Because there is a relative headwind component north of the nominal trajectory, the resulting solution space is smaller when compared to the south, where there is a relative tailwind.

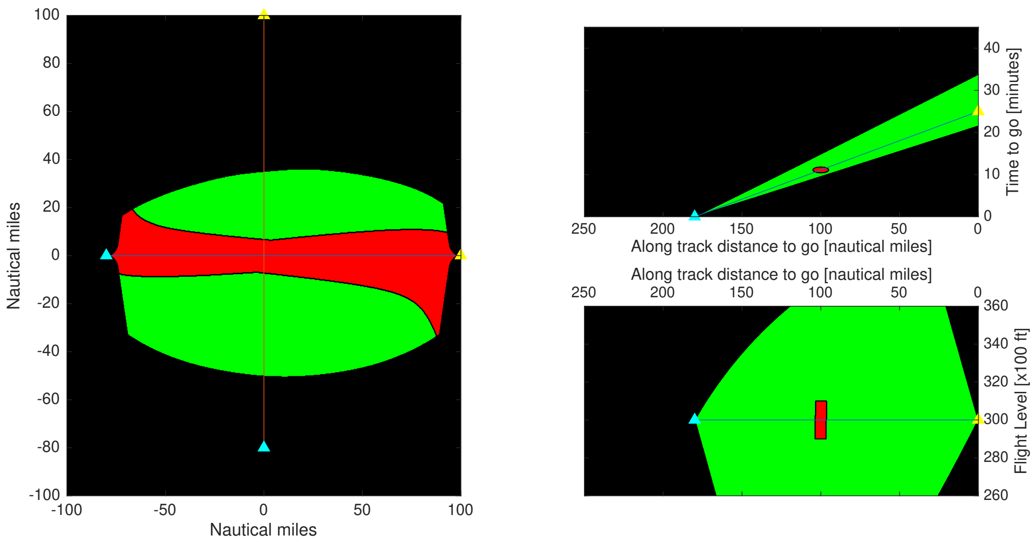

Figure 7-7: Resulting TSR display for lateral wind shear scenario in crossing traffic

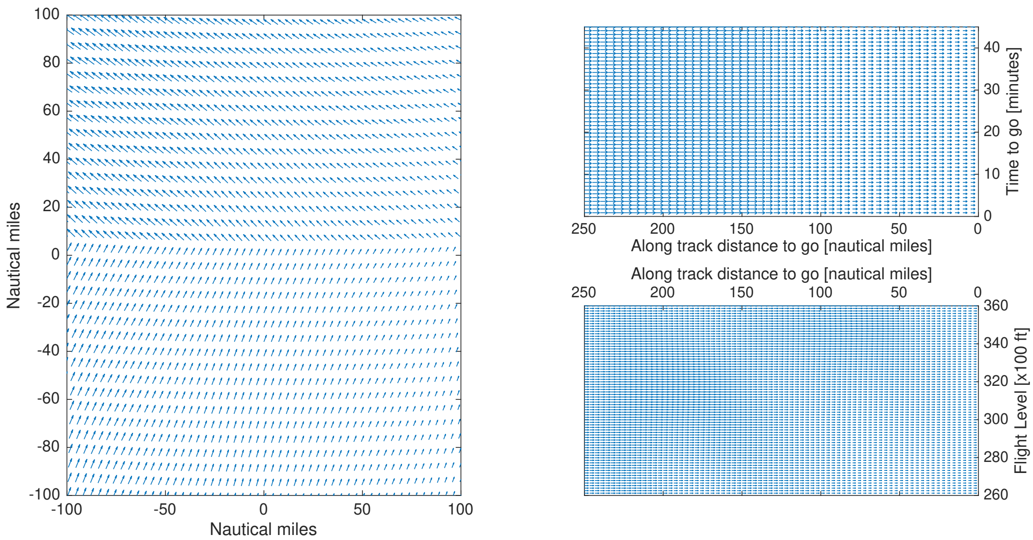

Figure 7-8: Wind field visualization for lateral wind shear scenario

Case II: Increasing Along-Track Wind Velocities

In the second scenario, a tailwind that increases as the aircraft progresses along its track is discussed. This wind scenario, as shown in Figure 7-10, largely impacts both the TSD and PVD.

Because the track segment is to be flown at constant IAS, a traffic situation that would yield a direct conflict without wind, is now conflict-free. This is explained by the fact that the GS of the controlled aircraft is relatively slow in the first half of the sector and increases gradually

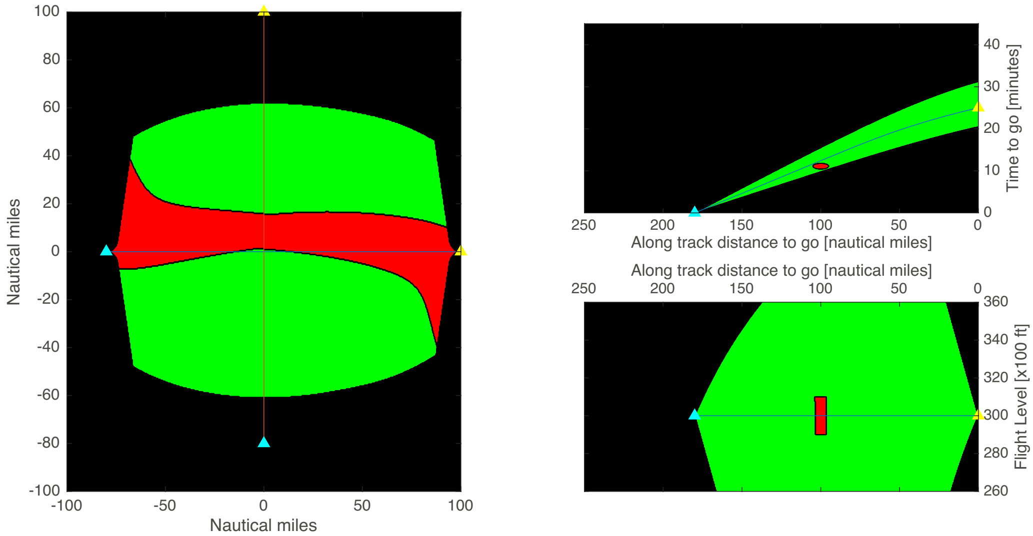

Figure 7-9: Resulting TSR display for increasing along-track wind scenario in crossing traffic

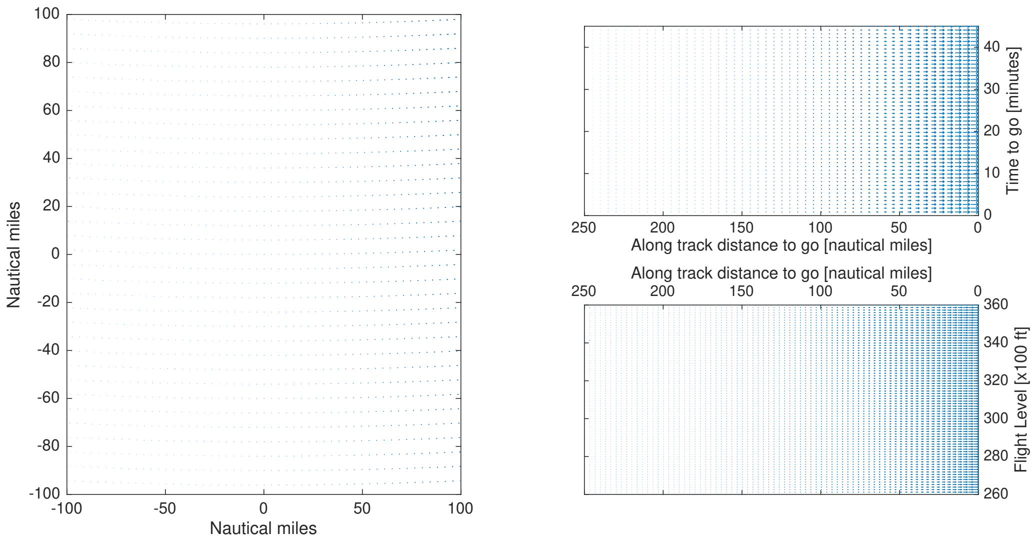

Figure 7-10: Wind field visualization for increasing along-track wind scenario

in the second half of the sector as the wind speed builds up. This allows the observed aircraft to cross the controlled aircraft before a LoS occurs.

In the PVD, this effect can be observed by noticing that the lateral crossing point of the nominal trajectories is now located in the green solution space (see Figure 7-9). In the TSD, the green area is no longer a straight beam, but becomes curved instead. The nominal trajectory follows this curve and thus bypasses the red circle indicating the immediate area of conflict.

When inspecting the VSD, it is observed that the RoC is higher than in the baseline situation.

This can be explained by the fact that the initial IAS is lower because of the tailwind, resulting in more excess thrust usable for the climb and therefore an increased RoC.

Case III: Different Wind Velocities at Different Altitudes

In this case, wind velocities at different altitudes have been manipulated, resulting in a relatively large headwind at approximately FL320 and a relatively large tailwind at approximately FL280. In the lateral plane, the wind scenario has the tendency of a slowly changing southern crosswind across the sector. The visualization is presented in Figure 7-12.

As is expected, this wind scenario introduces noticeable changes in the VSD (see Figure 7-11). The tailwind at high altitude makes the corresponding altitudes fall out of the performance reach, because the aircraft's maximum TAS is not large enough to reach the RTA.

Similarly, the headwind at low altitude makes altitudes around FL270 fall out of the performance reach, because the minimum TAS is still too high and the aircraft will arrive at the sector exit ahead of the RTA.

When inspecting the PVD it is noted that the red conflict area has decreased with respect to the baseline scenario. This is to be expected, since a southern crosswind increases the solution space (see also Figure 7-2d). The green solution space is not severely affected.

Because there is (on average) an along-track tailwind, the TSD beam is tilted downwards slightly with respect to the baseline scenario, indicating a small shift in possible ETA range. Because the wind also increases slightly along-track, the beam is curved. This effect is, however, hardly noticeable.

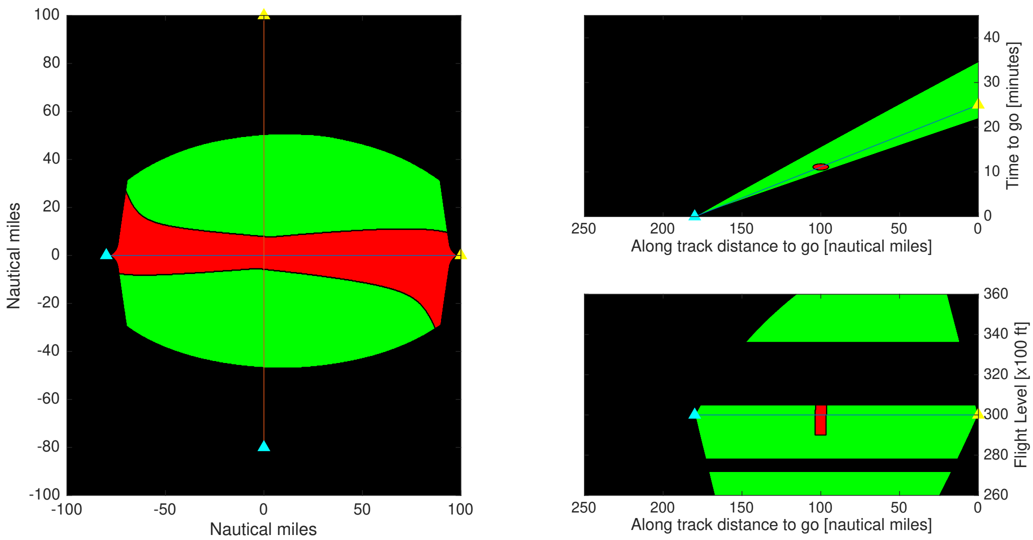

Figure 7-11: Resulting TSR display for changing wind speed at altitude scenario in crossing traffic

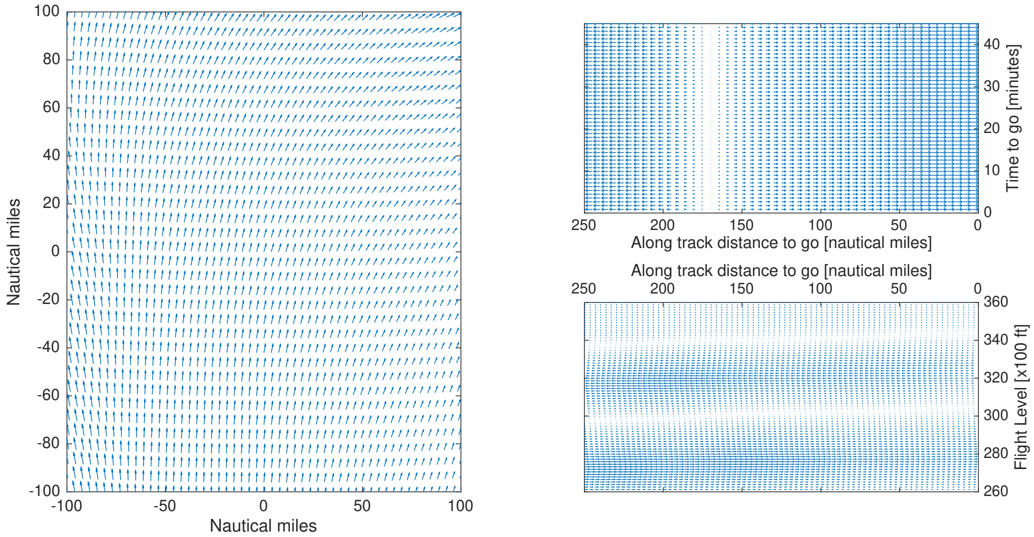

Figure 7-12: Wind field visualization for changing wind speed at altitude scenario

Chapter 8

Effects of Trajectory Uncertainty

In the current TSR interface, all aircraft trajectories are considered fully deterministic and therefore conflict probability is binary. When trajectory uncertainty is taken into account, this conflict probability will not be an integer anymore, but instead a varying value between zero and one. This will impact the TSR interface and the way the solution space in each screen is constructed. In this chapter, the effects of trajectory uncertainty on the solution space is discussed. The modeling approach to trajectory uncertainty is presented in Section 8-1, after which the simulation results are displayed in Section 8-2.

8-1 Modeling Approach

As was already outlined in Section 5-3, numerous methods exist to estimate trajectory uncertainty. Therefore multiple modeling approaches to the posed problem exist. Within the scope of this thesis, however, the focus is not on investigating the effects of all these different models. Instead, a model that fits the purpose needs to be picked and implemented.

8-1-1 Uncertainty Model

When deciding on such a model, several factors are deemed important. First of all, the model should be able to provide on-line results as real-time visualizations will need to be shown without significant delay. This effectively rules out PCE and Monte Carlo methods, as significant computational effort is required to yield the desired results (Casado Magaña, 2016). Parametric estimations provide reasonable accuracy and have a relatively low computational load, making them the preferred type of model.

Secondly, the model will need to predict with acceptable accuracy roughly within the time horizon of an airspace sector. To this end, mid-range conflict prediction models with a time horizon in the order of tens of minutes are most suitable.

Taking both requirements into account, the mid-range conflict detection model proposed by Prandini et al. (2000) is used as a basis for the trajectory uncertainty modeling approach.

Zero-mean Gaussian tracking errors with increasing variance over time are used to model an aircraft's trajectory uncertainty, as shown in Equation (8-1) and Equation (8-2).

$$\sigma_a^2(t) \sim r_a^2 t^2 \tag{8-1}$$

$$\sigma_c^2(t) \sim \min\{r_c^2 s^2(t), \bar{\sigma}_c^2\} \tag{8-2}$$

Because the ETA management control task is executed by the ATCo as a result of the proposed CONOPS, σ_a^2 can be assumed to keep growing, as pilots will not compensate for a changing ETA as a result of wind prediction error without being instructed by the ATCo. Equation (8-1) is therefore considered a reasonable model. Similarly, Equation (8-2) is considered reasonable in the proposed CONOPS, as the FMS is expected to correct for the incoming wind vector and the cross-track error will therefore have a saturation point.

Because 4D flight plans are available at all times, the nominal predicted trajectory $\vec{p}(t)$ is readily available for computational use. Using the parameterized tracking error variances, the resulting aircraft's position $\vec{x}(t)$ can be described using Equation (8-3) to Equation (8-6).

$$\vec{x}(t) \sim \mathcal{N}(\vec{p}(t), V(t)) \tag{8-3}$$

$$V(t) = R_{rot}(\theta)\bar{V}(t)R_{rot}(\theta)^T \tag{8-4}$$

$$\bar{V}(t) = \text{diag}(\sigma_a^2(t), \sigma_c^2(t)) \tag{8-5}$$

$$R_{rot}(\theta) = \begin{pmatrix} \cos\theta & -\sin\theta \\ \sin\theta & \cos\theta \end{pmatrix} \tag{8-6}$$

Using this description for an aircraft's multivariate stochastic position at any time in the time interval between the current time and 20 minutes ahead, enables the possibility to compute conflict probabilities between different aircraft in a sector. This can be done by computing the combined mean and combined covariance matrices of two aircraft and integrating the resulting probability density function over the circular Protected Zone (PZ) with a diameter of five NM, as shown in Equation (8-7) to Equation (8-11) for a conflict between aircraft A and B.

$$PC(t) = \int_{y \in PZ} \vec{p}_{\vec{d}_t}(y)dy \tag{8-7}$$

$$\vec{d}(t) = \vec{x}^A(t) - \vec{x}^B(t) \tag{8-8}$$

$$\vec{d}(t) \sim \mathcal{N}(\vec{\mu}(t), Q(t)) \tag{8-9}$$

$$\vec{\mu}(t) = \vec{p}^A(t) - \vec{p}^B(t) \tag{8-10}$$

$$Q(t) = V^A(t) + V^B(t) \tag{8-11}$$

The maximum value of the instantaneous conflict probabilities at the chosen time interval is then taken to be the *measure of criticality*, or resulting conflict probability as displayed in Equation (8-12).

$$C = \max_{t\in[0,T_{tot}]} PC(t) \tag{8-12}$$

As all nominal trajectories are already pre-computed in 4D, the nominal CPA can be determined in both position and time directly. The maximum $PC(t)$ will then be at this specific point in time and can be computed directly, greatly reducing computational load.

3D Case

When extending this modeling approach to the 3D case, the vertical tracking error will need to be modelled as well. When climbing or descending, the assumption is made that vertical tracking errors build up until the set altitude is reached, after which they return to zero again (as depicted in Figure 8-1). The vertical error standard deviation can therefore be characterized using Equation (8-13) for climbing segments and Equation (8-14) for descending segments.

$$\sigma_{v,climb} \begin{cases} = 0 & 0 < t < t_{BoC} \\ \sim r_{v,climb}t & t_{BoC} < t < t_{ToC} \\ \sim -r_{v,climb}t & t_{ToC} < t \end{cases} \tag{8-13}$$

$$\sigma_{v,desc} \begin{cases} = 0 & 0 < t < t_{ToD} \\ \sim r_{v,desc}t & t_{ToD} < t < t_{BoD} \\ \sim -r_{v,desc}t & t_{BoD} < t \end{cases} \tag{8-14}$$

The resulting covariance matrix and stochastic position becomes a 3D ellipsoid. Subsequent conflict predictions are made using the protected zone, consisting of a cylinder with a height of 1000 ft and a radius of 2.5 NM.

8-1-2 Solution Space Calculations

In this section, the impact of the uncertainty model on the generation algorithm of the solution spaces will be discussed. This will be done separately for each display.

PVD

For the PVD, the CPA is currently computed to calculate conflict possibility. When the CPA violates the 5 NM PZ, a conflict is declared and should be solved by the ATCo. To account for uncertainty, an extra 'artificial' 2.5 NM buffer is used.

With the implementation of the trajectory uncertainty model, real-time conflict probabilities are calculated for each pixel according to Algorithm 5.

```
input  : Controlled aircraft flight plan, observed aircraft flight plan, uncertainty growth rate model
output: Maximum conflict probability
calculate CPA distance & time to CPA;
obtain lateral error covariance matrices at CPA;
calculate combined mean & covariance;
calculate probability of conflict at CPA;
```

Algorithm 5: Maximum conflict probability computation for PVD solution space algorithm

TSD

In the TSD, computations required to calculate the maximum conflict probability in the time-space domain are similar to the PVD. The pseudo-code is presented in Algorithm 6.

```
input  : Controlled aircraft flight plan, observed aircraft flight plan, uncertainty growth rate model
output: Maximum conflict probability
calculate CPA distance & time to CPA;
obtain lateral error covariance matrices at CPA;
calculate combined mean & covariance;
calculate probability of conflict at CPA;
```

Algorithm 6: Maximum conflict probability computation for TSD solution space algorithm

VSD

For the VSD, the computation of the error covariance matrix is somewhat different than for the PVD and TSD. Because the vertical error growth rate is a piece-wise function and depends on the location of the climb segments, the vertical error variance needs to be calculated in two steps, as illustrated in Algorithm 7.

8-1-3 Simulation Parameters

In the model presented in Section 8-1-1, the error growth rates form an important part and are discussed here in more detail. Because error growth rates determine the trajectory uncertainty propagation *for each aircraft individually*, a very flexible simulation environment can be created where growth rates can be set separately for each individual aircraft.

input : Controlled aircraft flight plan, observed aircraft flight plan, uncertainty growth rate model
output: Maximum conflict probability

calculate CPA distance & time to CPA;
obtain lateral covariance matrices at CPA;
obtain vertical error variance at Top of Climb (ToC) or Bottom of Descent (BoD);
obtain vertical error variance at CPA;
calculate combined mean & covariance;
calculate probability of conflict at CPA;

Algorithm 7: Maximum conflict probability computation for VSD solution space algorithm

Along-Track Error

The along-track error can be seen as the sum of various components, of which the most important is the weather forecast error, with wind and temperature as dominant factors. Typical values for the along-track error growth rate, including weather effects and pilot intent, are between 10 kts (low) and 40 kts (high) (Torres, 2015) in cruise flight. In climbing or descending flight, along-track error growth rates usually increase, as the Rate of Climb/Descent (RoCD) adds an uncertainty component to the along-track error growth rate.

Cross-Track Error

The cross-track error consists of an error growth rate and a saturation value. Usually, the saturation value forms the starting point. The time to reach the saturation point then yields the cross-track error growth rate. In aircraft equipped with a modern FMS, the maximum cross-track error is usually kept below 0.5 NM (low) or 2.5 NM (high) and is reached within several minutes from the initial known position.

Vertical Error

The vertical error is the result of multiple parameters. The BoC or ToD is typically considered an important parameter and is largely influenced by the pilot intent. Furthermore, the RoC forms an important factor in climbing segments and is largely influenced by aircraft weight (Weitz, 2013). In his paper, Torres (2015) investigates the resulting RoCD distribution with varying weight, speed, thrust and temperature using a Monte Carlo simulation. This resulting RoCD distribution can subsequently be used as input for the parametric vertical error growth rate.

Relation Between Spatial Error Components

The relationship between the different types of spatial errors is qualitatively summarized in Figure 8-1. As can be seen, the along-track error grows linearly with look-ahead time until corrective action is taken by ATC. The cross-track error grows linearly until it reaches a saturation point, as there is in general a maximum deviation from the desired aircraft track that results from the FMS track adherence capability. Vertical errors will start to increase initially and reduce after the nominal desired altitude has been reached.

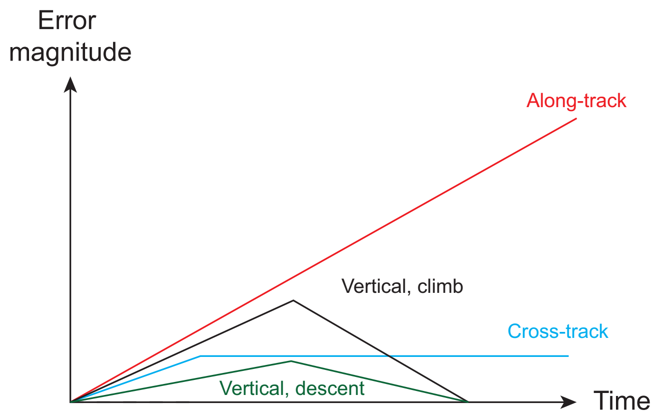

Figure 8-1: Qualitative description of spatial error components magnitude versus look-ahead time

8-1-4 Assumptions

As on-line results need to be generated and available computing time is therefore limited, assumptions will be made. The most important assumptions are listed below:

- **Decoupling of along-track error from vertical error**: It is known that along-track error and vertical error are coupled (Casado Magaña, 2016). This is the reason why climbing and descending segments are usually analyzed using Monte Carlo simulations as in (Torres, 2015). Decoupling the two will result in an underestimation of the along-track error and is therefore an unconservative assumption (and should be addressed in further research).
- **No correlation of wind prediction error**: This greatly simplifies the computations to be performed. Especially aircraft in close proximity of each other will be impacted by this. This assumption is a conservative one, as conflict probabilities will be overestimated when assuming uncorrelated wind prediction errors (Chaloulos & Lygeros, 2007; Hu et al., 2003).
- **Normal distribution for along-track and cross-track error**: Assuming these errors to be normally distributed with a zero mean reduces computational load. The normality of these distributions has been demonstrated by Paielli (1998).
- **Normal distribution for vertical error**: As can be seen in Figure 5-2, the vertical error is not fully normally distributed, but has a skewness after the climbing or descending segment has ended. Assuming a normal distribution therefore introduces a bias after the end of the nominal climbing segment. This bias will be unconservative (and should be addressed in further research), since part of the stochastic position distribution will be in unrealistic altitudes. Therefore, conflict probability will be underestimated for the other positions.
- **Second order errors not taken into account: AMM, APM, Earth Model**: As Torres (2015) already stated in his paper, modeling errors resulting from small angle

approximations, spherical earth and point mass approximations are considered second order and are therefore not taken into account.

8-2 Simulation Results

In this section, simulation results will be presented. Firstly, the effect of trajectory uncertainty on each separate screen will be discussed. Similar to Section 7-2, a crossing air traffic scenario in a square sector with a length of 200 NM will be investigated. In all simulations, an Airbus A320 BADA APM (v3.7) will again be used.

It should be noted that the probabilistic trajectories are only used in the simulations to calculate conflict probabilities. One can imagine that rerouting an aircraft to its absolute performance limits is not very robust. This effect is, however, not taken into account here, as it can be assumed that experienced ATCos will by themselves come up with relatively robust solutions (Klomp et al., 2014).

Because uncertainty grows with look-ahead time, two points in time in the same traffic scenario will be discussed for each display: one with a nominal TTC of 850 seconds and one with a nominal TTC of 170 seconds.

To illustrate the effects, contour plots showing the uncertainty contours will be used. These contours represent pre-defined thresholds on what is in reality a 3D surface. This is illustrated in Figure 8-2.

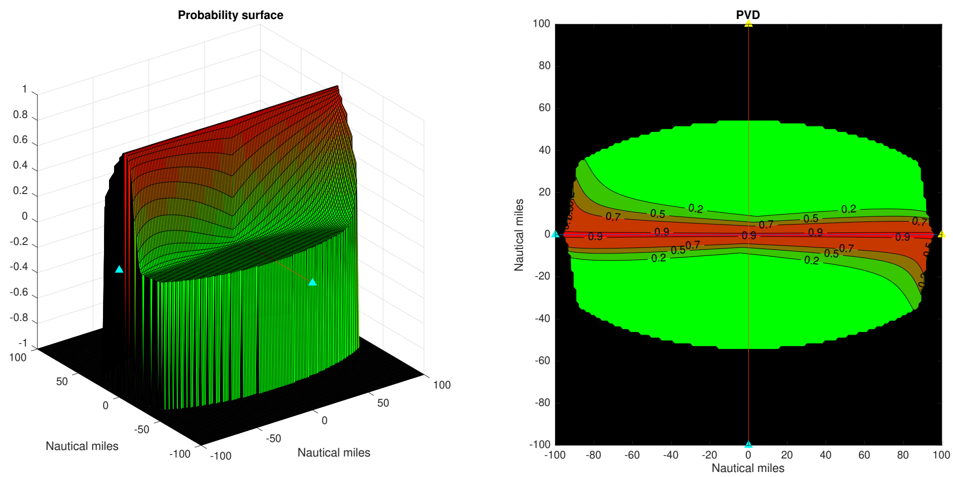

Figure 8-2: Representation of 3D surface on 2D screen using contours

The contours drawn in all figures are the following:

- 0.05 (As this indicates the 95% confidence interval of a solved conflict)
- 0.20
- 0.50

- 0.70
- 0.95 (As this indicates the 95% confidence interval of a persisting conflict)

As input settings, combinations of high and low error bounds for both the along-track and cross-track error will be used to illustrate the decoupled effect of both on the resulting TSR displays. The effect of different vertical error growth rates will be presented separately. A summary of the used parameters can be found in Table 8-1. Along-track and vertical error growth rate settings are based on values used by Torres (2015), whereas cross-track error growth rate settings a based on values used by Prandini et al. (2000).

Table 8-1: Error growth rate settings used in simulations at FL300

	r_a	r_c	$\bar{\sigma}_c$	$r_{v,climb}$	$r_{v,desc}$
Low value	10 kts	1/57	0.5 NM	110 fpm	140 fpm
High value	40 kts	1/150	2.5 NM	325 fpm	350 fpm

8-2-1 PVD

The effects of the uncertainty model on the PVD are shown in Figure 8-3 for a high TTC and Figure 8-4 for a low TTC. Following is a summary of the most prominent results.

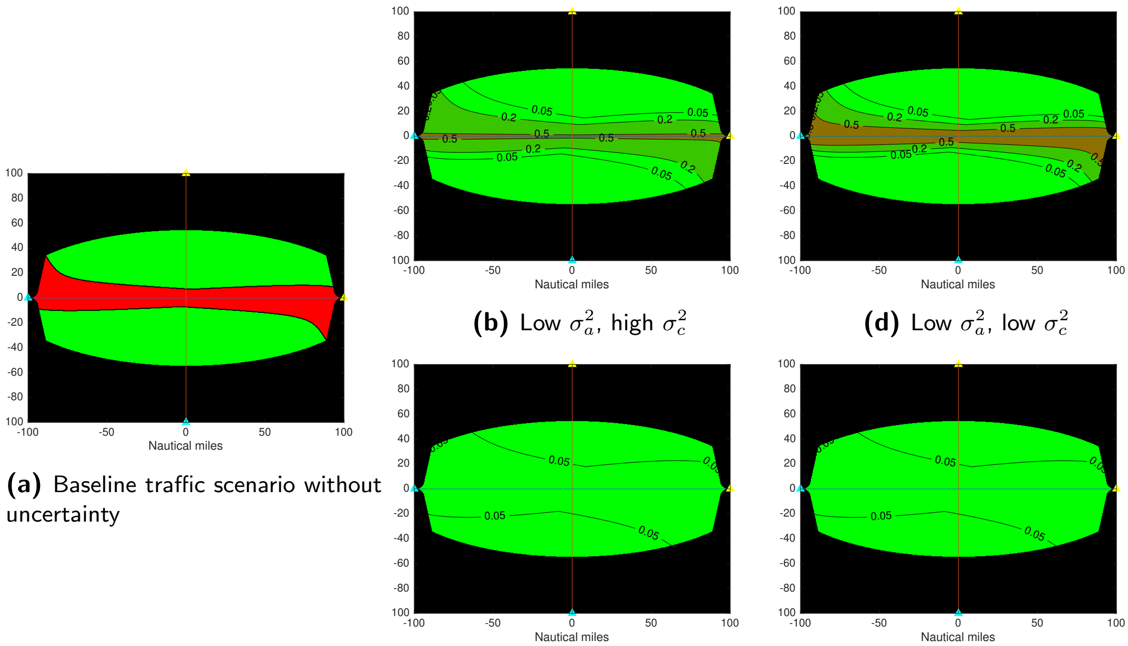

(a) Baseline traffic scenario without uncertainty

(b) Low σ_a^2, high σ_c^2

(d) Low σ_a^2, low σ_c^2

(c) High σ_a^2, low σ_c^2

(e) High σ_a^2, high σ_c^2

Figure 8-3: Effects of trajectory uncertainty on PVD in crossing traffic with a high TTC

- When compared to the baseline, the shape of the conflict zone remains similar. The lower the trajectory uncertainty, the closer the equiprobability contours will be together.

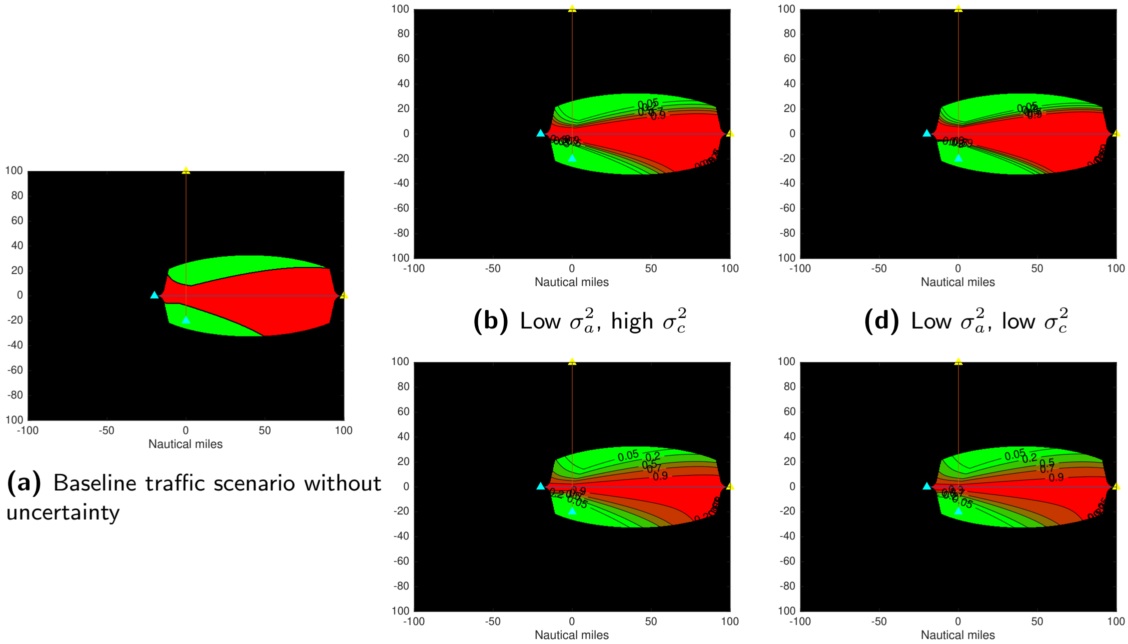

(a) Baseline traffic scenario without uncertainty

(b) Low σ_a^2, high σ_c^2

(c) High σ_a^2, low σ_c^2

(d) Low σ_a^2, low σ_c^2

(e) High σ_a^2, high σ_c^2

Figure 8-4: Effects of trajectory uncertainty on PVD in crossing traffic with a low TTC

As uncertainty approaches zero, the solution space will become almost binary and will yield more or less the same results as the baseline deterministic solution space. As uncertainty increases, contours start spreading to regions beyond the deterministic baseline red area.

- The along-track error growth rate has a larger effect on the conflict probability than the cross-track error growth rate. This applies for both scenarios in time.
- Conflict probabilities are lower with a higher TTC when compared to a lower TTC. This is to be expected, as uncertainty grows with time, making it more difficult to make an accurate prediction when the conflict is still far away. This is also in accordance with current ATCo work practice, where a conflict would in general not be solved when it is still 100 NM away.
- In the scenario with a low TTC, rerouting the aircraft with a WPT south of the nominal trajectory will become the preferred option instead of north. This is true especially for situations with high uncertainty. While this is also true in the baseline scenario, the effect is more dominant when (high) uncertainty is taken into account.

8-2-2 TSD

The effects of the uncertainty model on the TSD are shown in Figure 8-5 for a high TTC and Figure 8-6 for a low TTC. Following is a summary of the most prominent results.

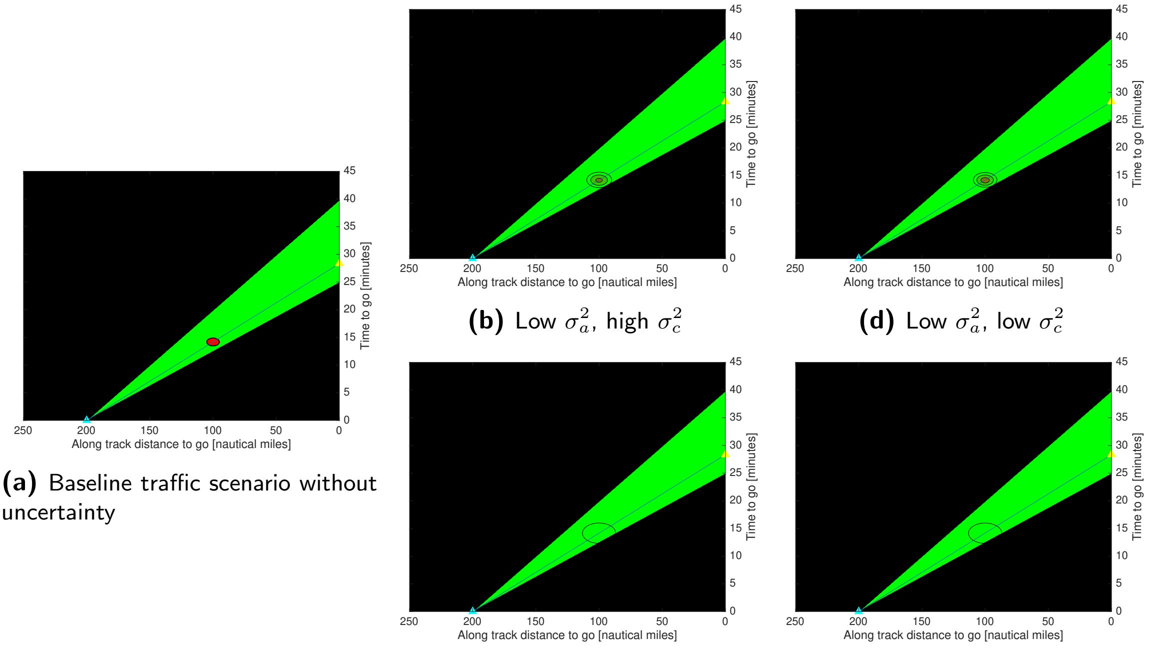

(a) Baseline traffic scenario without uncertainty

(b) Low σ_a^2, high σ_c^2

(c) High σ_a^2, low σ_c^2

(d) Low σ_a^2, low σ_c^2

(e) High σ_a^2, high σ_c^2

Figure 8-5: Effects of trajectory uncertainty on TSD in crossing traffic with a high TTC

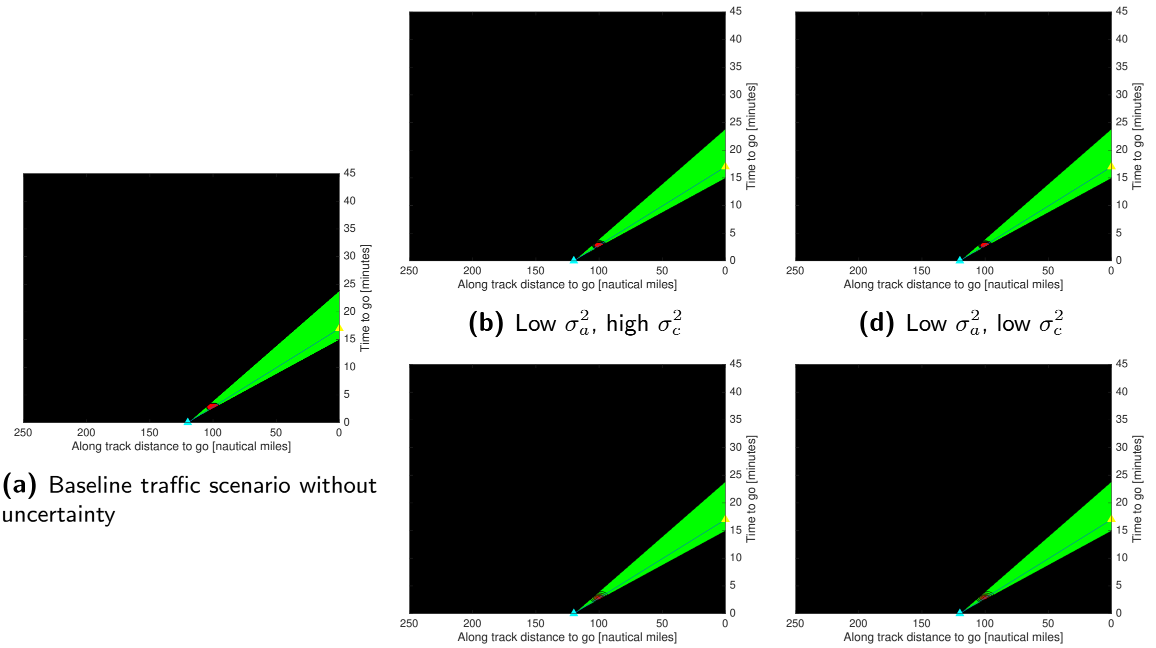

(a) Baseline traffic scenario without uncertainty

(b) Low σ_a^2, high σ_c^2

(c) High σ_a^2, low σ_c^2

(d) Low σ_a^2, low σ_c^2

(e) High σ_a^2, high σ_c^2

Figure 8-6: Effects of trajectory uncertainty on TSD in crossing traffic with a low TTC

- Similar to the PVD, uncertainty contours follow the shape of the deterministic baseline scenario. High uncertainty rates introduce a larger distance between contours, while low uncertainty rates make the shape approach its deterministic equivalent.

- The effect of cross-track error on the solution space shape is minimal with both a high TTC and a low TTC, while the along-track error has a larger influence.

- Because of the implemented uncertainty model, the conflict cannot be safely solved anymore by an initial speed increase followed by a speed decrease. In the deterministic scenario, this was a conflict resolution (rerouting the aircraft 'below' the red conflict area).

8-2-3 VSD

The effects of the uncertainty model on the VSD are shown in Figure 8-7 for a high TTC and Figure 8-8 for a low TTC. Following is a summary of the most prominent results.

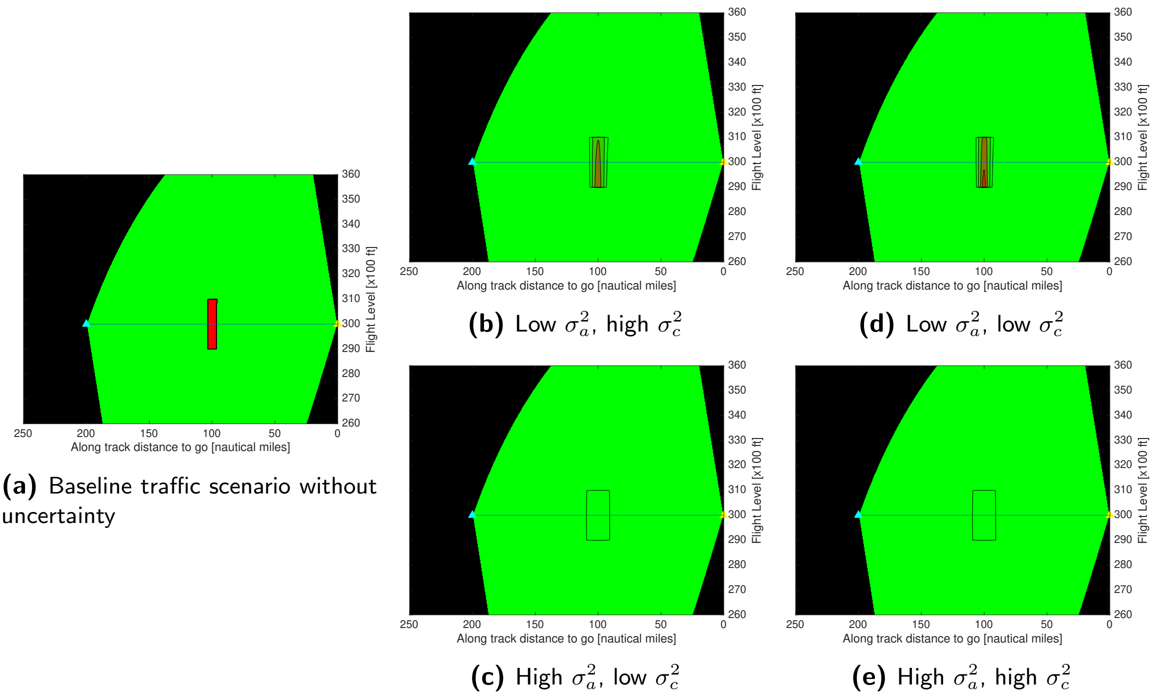

(a) Baseline traffic scenario without uncertainty

(b) Low σ_a^2, high σ_c^2

(d) Low σ_a^2, low σ_c^2

(c) High σ_a^2, low σ_c^2

(e) High σ_a^2, high σ_c^2

Figure 8-7: Effects of lateral trajectory uncertainty on VSD in crossing traffic with a high TTC

- Similar to the PVD and the TSD, uncertainty contours follow the shape of the deterministic baseline scenario. High uncertainty rates introduce a larger distance between contours, while low uncertainty rates make the shape approach its deterministic equivalent.

- Conflict probabilities are lower at higher altitudes than at lower altitudes. This is the result of the inclusion of altitude-dependent growth rates. Because weather predictions are known to be less accurate at higher altitudes, uncertainty is higher and conflicts can therefore be predicted less accurately.

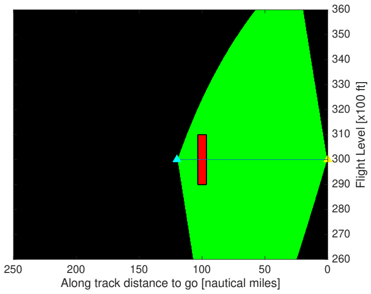

(a) Baseline traffic scenario without uncertainty

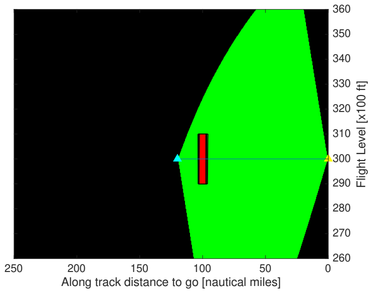

(b) Low σ_a^2, high σ_c^2

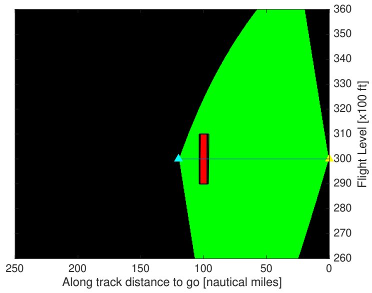

(d) Low σ_a^2, low σ_c^2

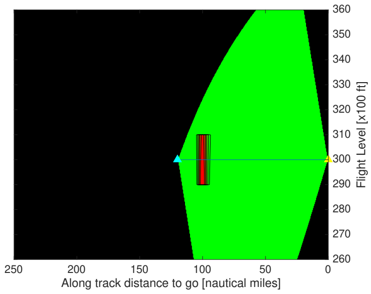

(c) High σ_a^2, low σ_c^2

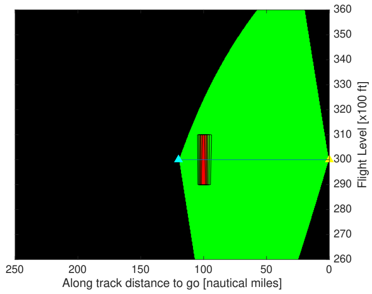

(e) High σ_a^2, high σ_c^2

Figure 8-8: Effects of lateral trajectory uncertainty on VSD in crossing traffic with a low TTC

To illustrate the effects of the vertical error growth rate, a nominal TTC of 127.5 seconds is chosen for the crossing traffic scenario. The vertical error growth rates are then varied as the along-track and cross-track growth rates remain constant. The results are displayed in Figure 8-9.

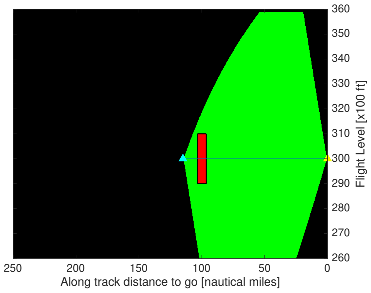

(a) Baseline scenario, no uncertainty

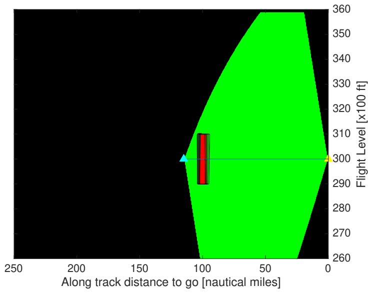

(b) Low $\sigma_{v,climb}^2$, $\sigma_{v,desc}^2$

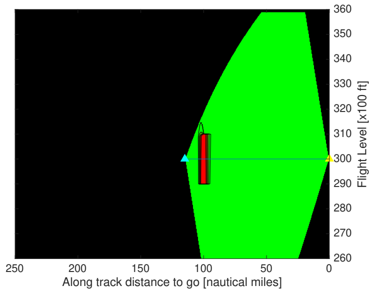

(c) High $\sigma_{v,climb}^2$, $\sigma_{v,desc}^2$

Figure 8-9: Effects of vertical trajectory uncertainty on VSD in crossing traffic scenario

As can be seen, the uncertainty contours start changing as the vertical uncertainty is increased. While this effect is minimal with low uncertainty values, higher values indicate a possible RoC that is too low to solve the emerging conflict. Therefore, it is in this case safer to let the aircraft descend, as Rate of Descent (RoC) uncertainty is lower than RoC uncertainty and the RoC itself is higher.

Chapter 9

Cognitive Work Analysis

Because design decisions will be required when integrating wind and trajectory uncertainty information into the current TSR, a CWA is performed. These decisions will not merely add elements to the current interface. Instead, the new elements will need to be integrated in a logical manner, thereby possibly also influencing existing interface elements. The sections in this chapter cover the five separate parts of a CWA as described in Section 2-2.

9-1 Work Domain Analysis

Starting with the WDA, an AH of the work domain is made. The resulting analysis is shown in Figure 9-1. In the final interface, the important links between relevant work domain elements will have to be made visible to the user.

The top three levels have already been defined for the TSR interface (Klomp et al., 2013) and will not change, as the overall objectives remain unaltered when wind and trajectory uncertainty information is added.

On the lowest level, however, several work domain elements become stochastic. These stochastic elements will in turn affect all connecting elements on all levels. This stochastic nature will have to be made visible to the user.

Furthermore, the inclusion of weather (i.e., wind in this case) will alter the routing possibilities for the ATCo. This effect will also need to be implemented in the interface.

9-2 Control Task Analysis

When looking at the control tasks to be executed by a future ACC ATCo in 4D ATM, several main control tasks can be identified.

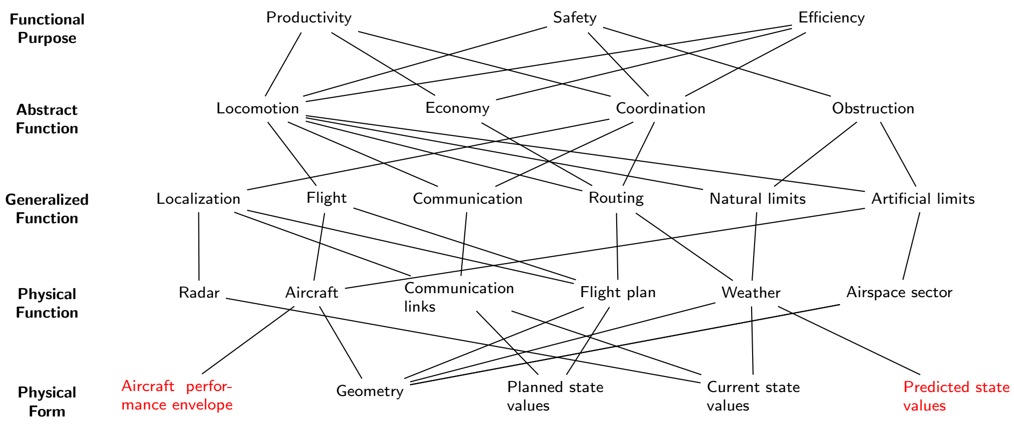

Figure 9-1: AH for future 4D ATC system (Stochastic elements are displayed in red)

- **Welcoming aircraft from adjacent sector**: In current operations, aircraft are welcomed into the sector via voice communication. In future operations, the communication means might change, as more advanced data-link capability will likely exist.
- **Handing over aircraft to adjacent sector**: Similarly, an aircraft has to be handed over to an adjacent sector. Currently, an ATCo provides the aircraft with the new radio frequency to contact the adjacent sector ATC. Similar to the welcoming of aircraft form an adjacent sector, this procedure might be different as communication means might change.
- **Aircraft routing to exit waypoint**: Every aircraft entering the sector has to be routed towards its exit waypoint. This is to be done using lateral, vertical and velocity commands.
- **Aircraft rerouting**:
  - **CD&R**: Emerging separation conflicts should be detected and resolved by the ATCo. Other than in 'conventional' ATC, conflicts should be resolved while adhering to the RTA constraint imposed by the 4D flight plan.
  - **ETA management**: Following the CONOPS rationale presented in Section 6-2, the ATCo will also have to manage all aircraft's ETA and reroute an aircraft when its ETA diverges from its RTA due to unexpected circumstances (e.g., weather cells, wind forecast errors).

As the TSR is designed to support the ATCo in the rerouting sub-tasks, a DL will be shown for both the CD&R (adapted from Riegman (2018)) and ETA management control sub-tasks. The generalized DL as presented in Section 2-2 will be used map out the control sub-tasks, along with the proposed shortcuts to be supported by the interface. While a large variety of shortcuts is in theory possible, the most relevant ones will be highlighted.

It should be noted that both control tasks might trigger one another. For example, when rerouting an aircraft to adjust its ETA, a conflict with another aircraft in the sector might inevitably be introduced. This will then trigger the CD&R procedure for the newly created conflict to be solved.

9-2-1 CD&R

For the CD&R sub-task, the DL is presented in Figure 9-2. As this sub-task is already integrated into the display, the DL aims to represent the way the current interface works.

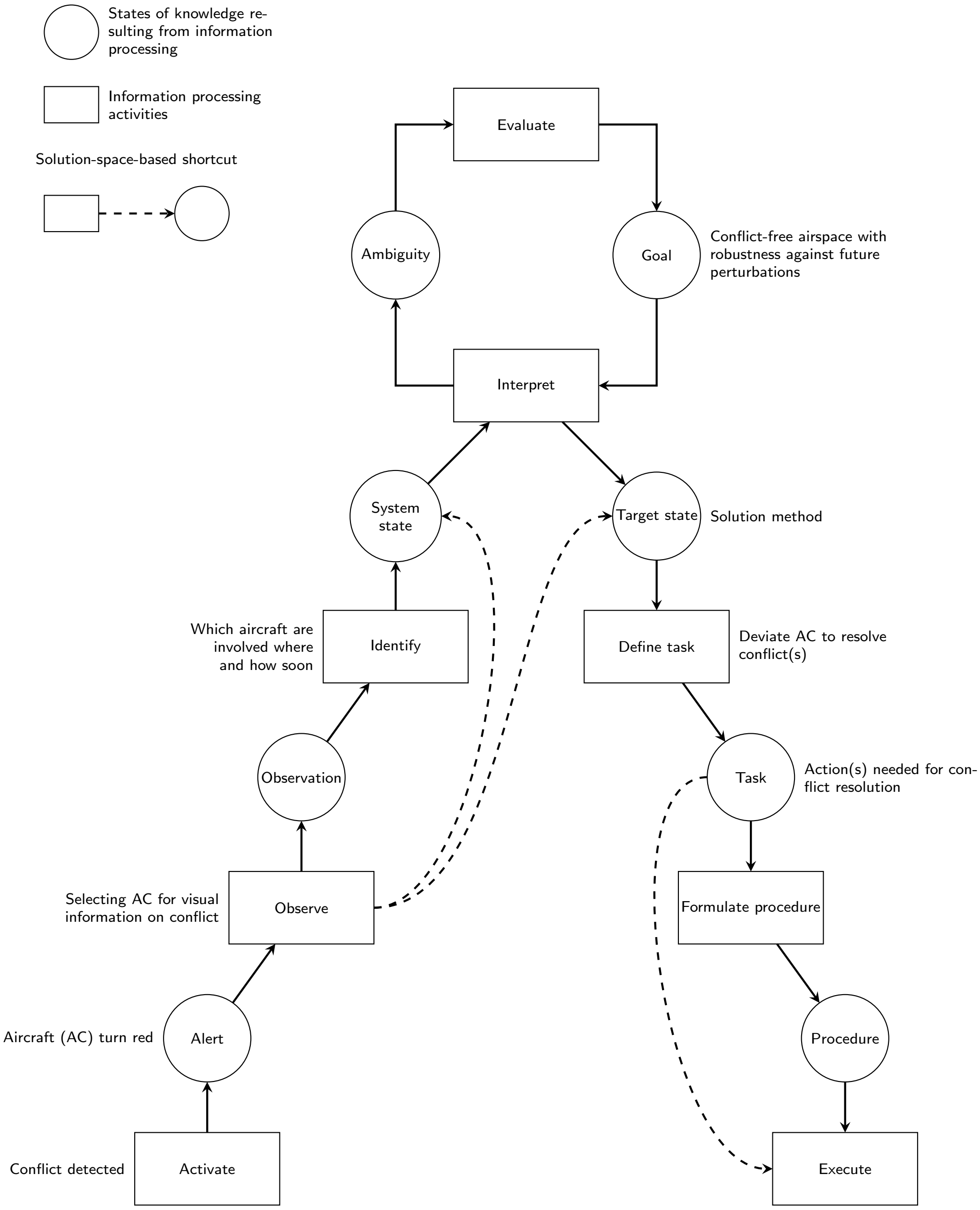

Figure 9-2: DL for CD&R control sub-task with the TSR interface (adapted from Riegman (2018))

Upon conflict detection, the involved aircraft turn red in the PVD, thereby alerting the user (i.e., the ATCo). Subsequently, the aircraft involved can be selected to obtain information on the available solutions for solving the conflict while adhering to the RTA constraint.

When placing a WPT in one of the displays, the effects are immediately shown to the user.

Subsequent commands to be instructed to the aircraft are made visible to the user. These commands have to be communicated with the aircraft when executed.

The most important shortcuts provided by the TSR interface are:

1. **Observe – System State**: The solution space provides clear shortcuts in directly observing the system state by coloring reachable and conflict-free areas. This eliminates the need for the user to identify the system state from the set of observations without the solution space.

2. **Observe – Target State**: While the exact solution method is to be decided by the user, sub-optimal solution methods (with very narrow solution spaces) are less likely to be chosen by the user.

3. **Define task – Procedure**: The interface provides shortcuts in going from task to procedure execution, since commands to be executed directly follow from the manipulation of the aircraft trajectories.

9-2-2 ETA Management

With the introduction of trajectory uncertainty comes the control task of managing ETA at sector exit for all aircraft currently in the sector. As the interface currently assumes fully deterministic trajectories, support for this control task needs to be implemented in the TSR. The DL with envisioned shortcuts for this task is presented in Figure 9-3.

When the ETA – RTA difference exceeds a certain threshold, the user should somehow be alerted. The aircraft involved can subsequently be selected and information on how to adjust the ETA can be obtained. Likely, multiple resolution options will be available to the user, and so one should be chosen. When the resolution strategy has been defined, the trajectory can be modified and commands can be sent to the aircraft.

Envisioned shortcuts to be provided by the interface are:

- **Observe – System State**: Similar to in the CD&R control task DL, the user should be able to directly obtain information on the range of possible solutions to the problem.

- **Observe – Target State**: The target state (i.e., the RTA) should be made clearly visible to the user.

9-3 Strategies Analysis

Each control task can be executed using a variety of control strategies. The interface should allow for many different control strategies, because ATCo strategy is very different depending on personal preference. For both the CD&R and ETA management control tasks, the possible strategies are summarized using information flow maps. Lastly, the current TSR workflow is also mapped on an information flow map, from which modification suggestions arise.

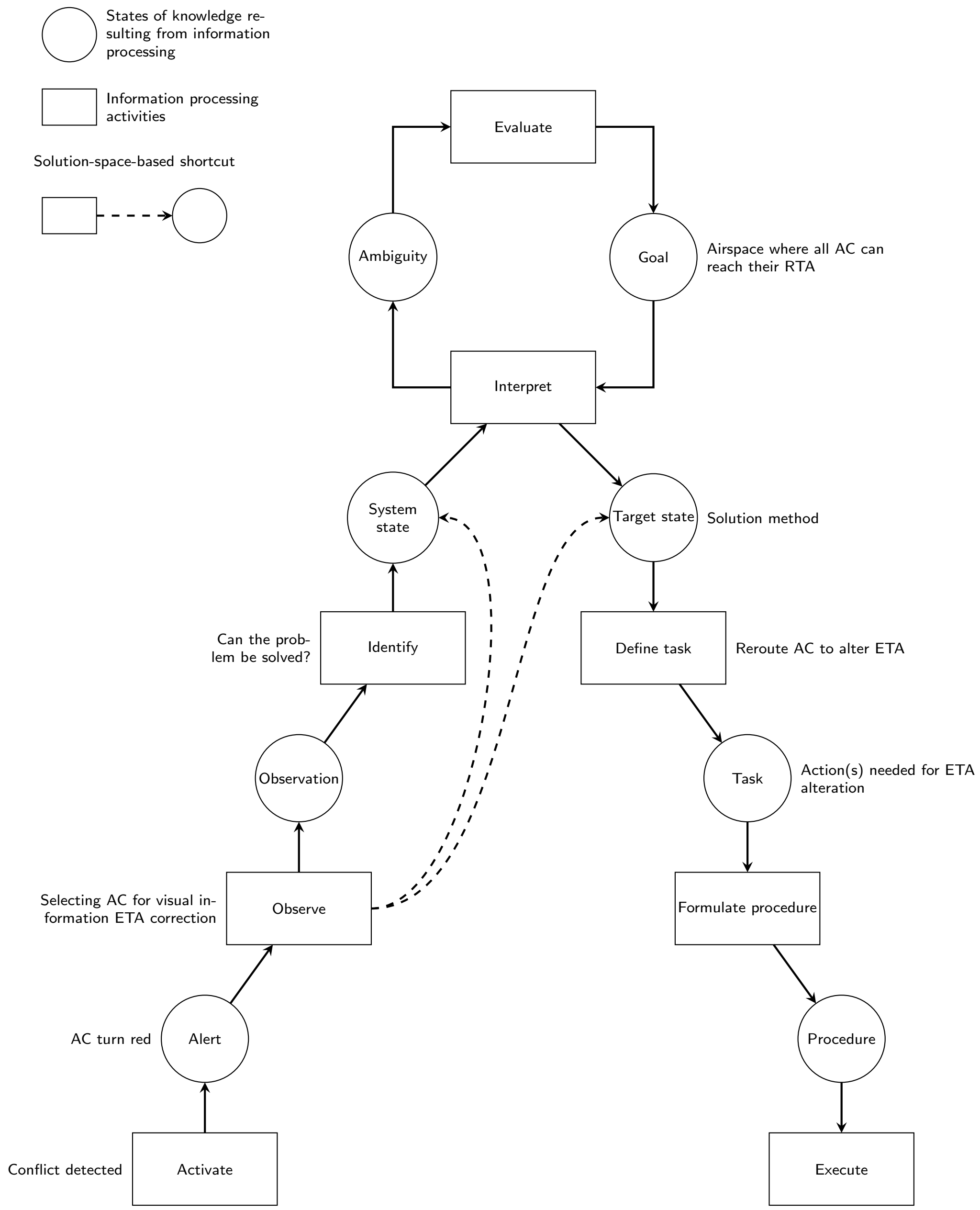

Figure 9-3: DL for ETA management control sub-task with the TSR interface

9-3-1 CD&R

When categorizing CD&R strategies, a distinction is made between two solution types. A separation conflict always involves two aircraft (conflicts with more than two aircraft are seen as multiple separate conflicts). Therefore, the ATCo can decide to solve the conflict by rerouting only one aircraft, or by rerouting both aircraft involved. This is always the case, regardless of the commands applied or the ATM framework in operation.

Rerouting a Single Aircraft

As is illustrated in Figure 9-4, the rerouting process starts with the detection of the conflict. This detection is facilitated by means of planned trajectories, possible conflict indication signs on the display and the airspace structure. Based on the aircraft performance envelopes, atmospheric conditions and airspace perturbations, an aircraft to be rerouted is chosen.

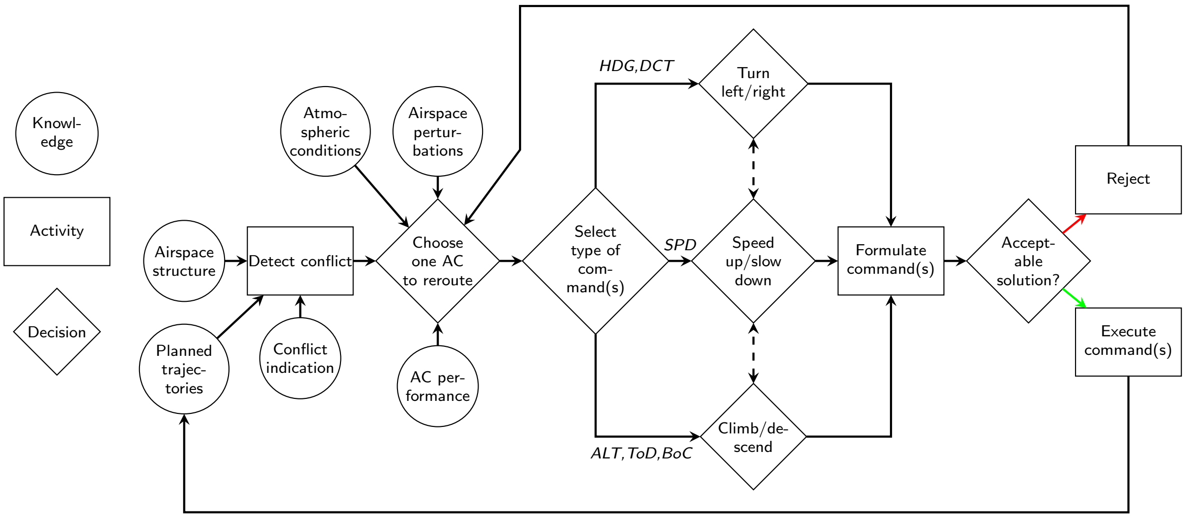

Figure 9-4: Information flow map for CD&R control sub-task with a single AC

A decision then has to be made on how to reroute the aircraft. This can be done by having the aircraft change its lateral/vertical profile or by altering its velocity profile. The available commands to each end are displayed in the figure.

Often, a combination of commands is formulated (e.g., adjust the vertical profile and adjust velocity accordingly). When finished, the formed solution is reviewed. In case of rejection, a different solution is formed. When accepted, the trajectory modification is confirmed.

Rerouting Multiple Aircraft

When solving a conflict by rerouting multiple aircraft, as shown in Figure 9-5, strategies similar to the single aircraft resolution apply. The final solution, however, consists of commands being given to two aircraft, instead of one. Solutions are formed pair-wise (i.e., a command being given to one aircraft together with a command being issued to the other involved aircraft).

From conversations with ATCos at LVNL, it follows that this pair-wise solution making process is an important aspect of this strategy. An interface should therefore allow for this type of strategy to be applied intuitively.

9-3-2 ETA Management

Other than a separation conflict, in which two aircraft are involved, an ETA deviation concerns only one aircraft. It is detected by comparing the planned 4D trajectory with an aircraft's

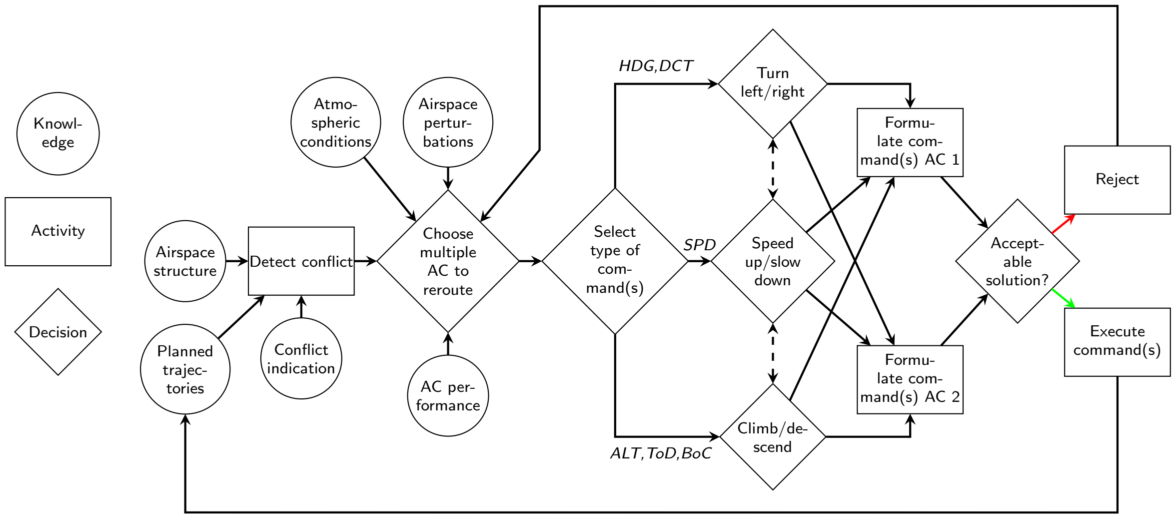

Figure 9-5: Information flow map for CD&R control sub-task with multiple AC

ETA at the pre-defined waypoints. When an ETA deviation is detected, a decision on the type of command to adjust the ETA needs to be made. When a solution is formed, it is reviewed and either accepted or rejected. In case of rejection, a different solution is formed. This process is illustrated in Figure 9-6.

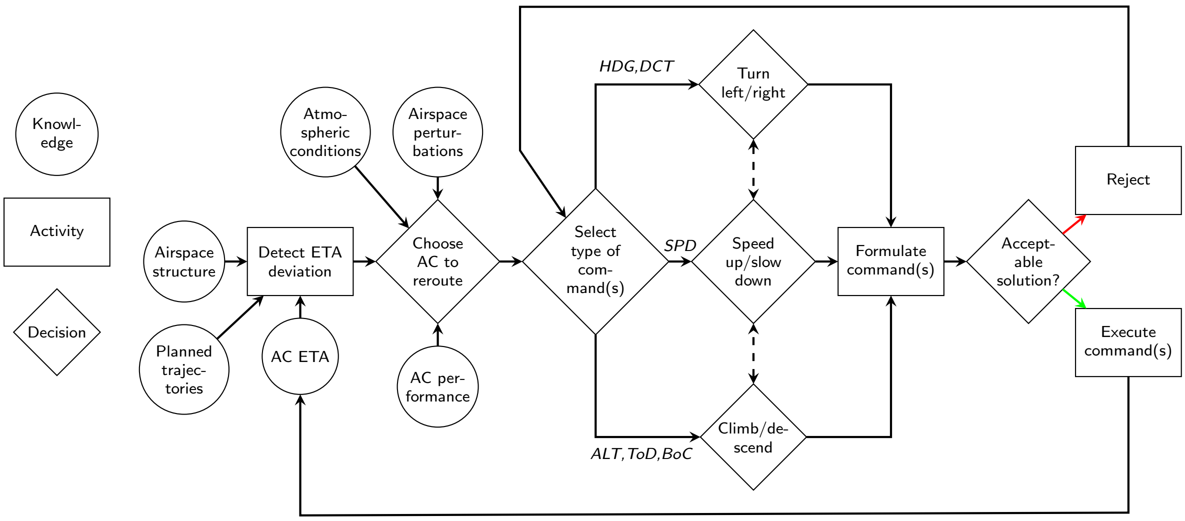

Figure 9-6: Information flow map for ETA management control sub-task

9-3-3 TSR Workflow

The TSR workflow should support all of the mentioned ATCo control strategies. For the CD&R control task, the current workflow has already been summarized by Klomp et al. (2019) and is shown in Figure 9-7.

When comparing the current workflow with the mentioned control strategies, several observations can be made:

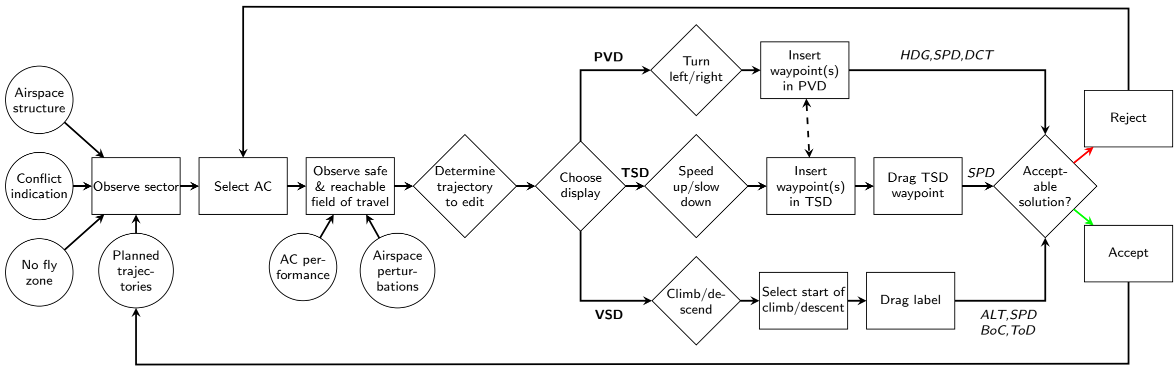

Figure 9-7: Current TSR workflow

- **Missing information**
  - The atmospheric conditions are currently not present in the TSR, whereas rerouting strategies will be using the atmospheric conditions as an input to determine the safe and reachable field of travel.
  - No ETA indication is present, meaning that the operator currently has no way of directly observing whether an aircraft will deviate from its assigned RTA.
- **Missing links**
  - At the moment, commands given on the TSD and VSD cannot be interchanged freely. This leads to confusion amongst controllers, because they cannot always use the display to apply the solution they want.
  - It is currently not possible to 'hold' an applied solution of one aircraft and look at the impact for other aircraft in the sector before executing the commands. When solving a separation conflict by rerouting multiple aircraft, this can be confusing to the controller.

Following these observations, a redesigned workflow can be drawn. This workflow is shown in Figure 9-8.

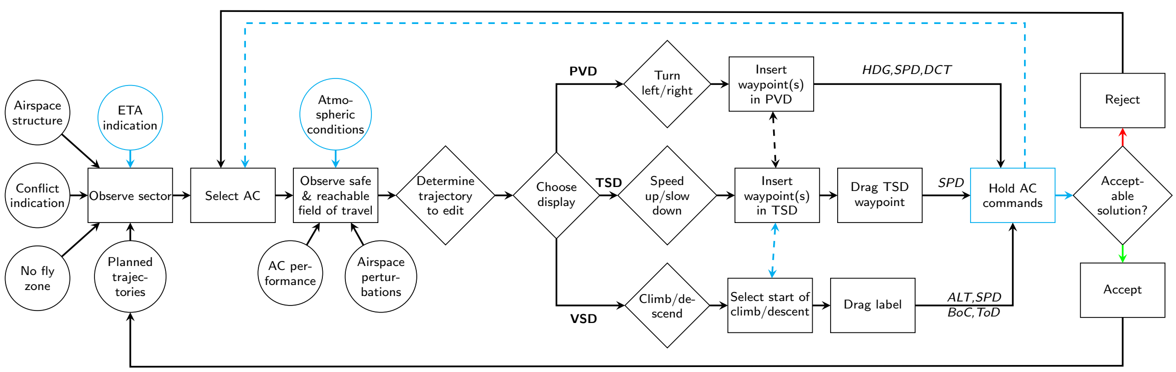

Figure 9-8: Edited TSR workflow (Edited elements w.r.t. Figure 9-7 shown in blue)

9-4 Social Organization

Following the strategies analysis, it should be determined what actor executes which part of each strategy. In this case, the human and the computer are the actors involved and should perform each part of the task either together or alone. This envisioned social organization for each strategy is depicted in Figure 9-9 to Figure 9-11.

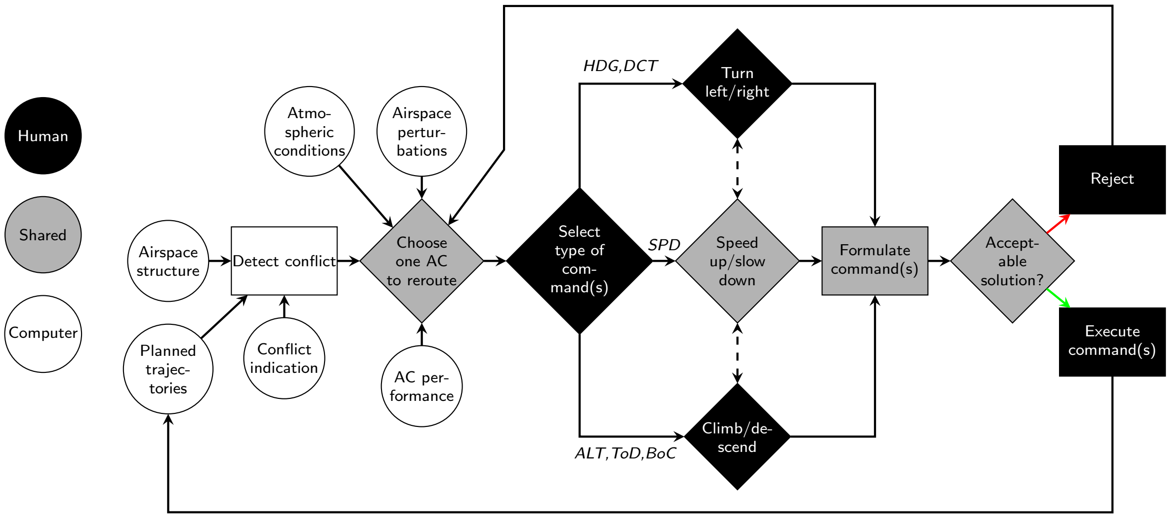

Figure 9-9: Social organization for CD&R control sub-task with a single AC

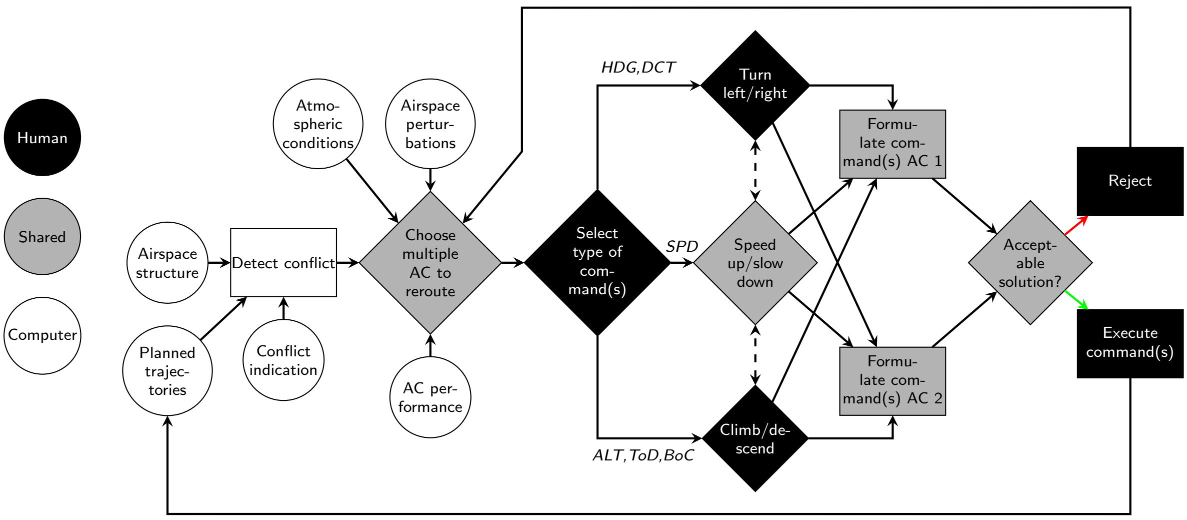

Figure 9-10: Social organization for CD&R control sub-task with multiple AC

When looking at the figures, two general patterns can be noted. Firstly, the knowledge and conflict detection is in hands of the computer in every strategy. The decision blocks are either executed by the human or shared between human and computer. This approach utilizes the strengths of both the human and computer, while mitigating their weaknesses.

Several other observations are:

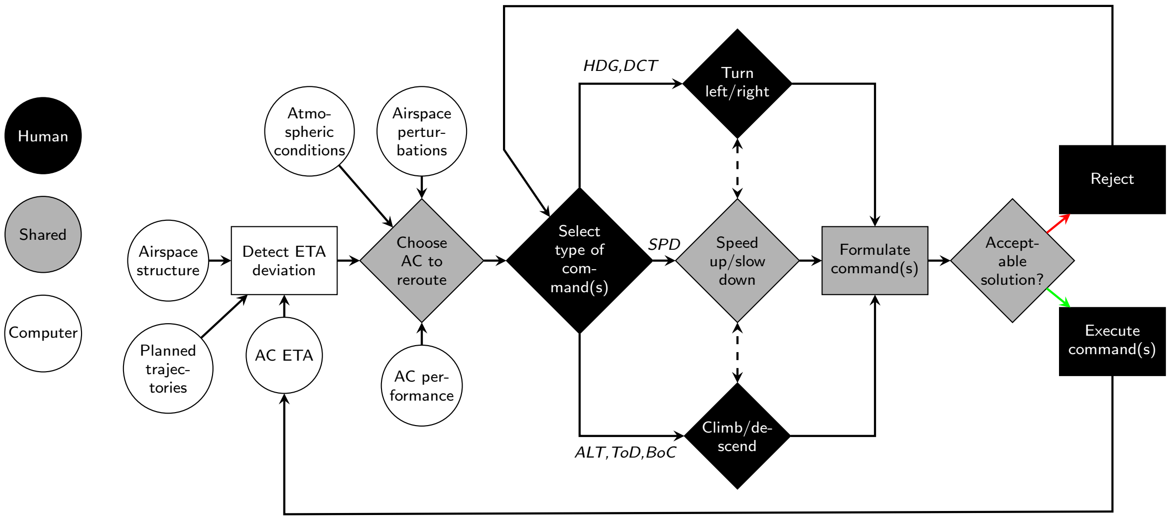

Figure 9-11: Social organization for ETA management control sub-task

- The decision on which aircraft to reroute is made together by the human and the computer. The computer serves the human with all information necessary to make the decision. In the TSR interface, this is done by constructing the solution space.
- The human is fully in charge of the command to be given for lateral or vertical command types. Velocity commands are partly instructed by the computer to adhere to the RTA constraints.
- The human and computer decide together whether the formed solution is acceptable. The computer aids the human by instantly constructing new solution spaces and new potentially emerging conflicts.

9-5 Worker Competencies

The CWA is completed with a worker competencies analysis, where a closer look is taken on how the human can be supported in the control task. This is done by inspecting what types of behavior are supported by the interface in what part of the control task. The results are displayed in Table 9-1 and Table 9-2 for the CD&R and ETA management control sub-tasks, respectively.

Table 9-1: Worker competencies analysis for the CD&R control sub-task with the TSR interface (Riegman, 2018)

Information Processing Step	Resultant Knowledge State	SBB	RBB	KBB
Scan for indicated conflicts	Whether aircraft will be in conflict with each other	Monitoring for signals of conflicts	Identifying conflicts that are present	Reason where conflicts may arise in the future with aircraft not yet in the airspace
Determine conflicts with no-fly zones	Whether one or multiple aircraft will move through a no-fly zone	Monitoring for tracks crossing through red areas	Perceive flights that will breach no-fly zones	Reason which source-sink combinations will have paths crossing no-fly zones
Determine most critical conflict	Which conflict has the largest priority in solving	Perceive which aircraft in conflict are in close proximity on the PVD	Use heuristics to estimate which ACs will first have LoS or breach no-fly zones	Reason, based on visual data, if conflicts with high priority could emerge
Choose method to solve a conflict	Which approach will be most effective in resolving the conflict	Perceive which methods provide many options based on the solution space	Apply doctrine to determine which methods will be tried first	Reason which method is least likely to cause more conflicts in the future while having minimal impact on the trajectory
Determine conflict resolution	The conflict resolution to be executed	Perceive the areas in the solution space that provide conflict resolutions	Apply doctrine/common sense rules to determine a suitable waypoint location in the solution space	Reason whether a waypoint location can cause conflicts in the future and whether it is in line with previous conflict resolutions

Table 9-2: Worker competencies analysis for the ETA management control sub-task with the TSR interface

Information Processing Step	Resultant Knowledge State	SBB	RBB	KBB
Scan for ETA deviations	Whether aircraft will meet their assigned RTA	Monitor ETA deviation signal on radar display	Use rules of thumb to estimate possible ETA deviation (e.g., stronger headwind than expected, so aircraft will be delayed if no action is taken)	Calculate, using airspeed, heading and aircraft locations, the ToA at which each aircraft will reach the sector exit waypoint
Determine most critical ETA deviation	Which trajectory has the largest priority in changing	Perceive the largest ETA time delta value on the radar screen	-	Reason, based on visual data and ETA deviation estimations, which flight plan has the highest priority in adjusting
Choose a method to alter the ETA	Which approach will be most effective in altering the ETA	Directly observe performance envelope and choose a resolution method depending on the available options	Apply common sense to solve the ETA deviation (e.g., aircraft is arriving too late, so increase speed)	Reason how different types of instructions will affect the aircraft's ETA and choose one of them depending on their estimated effect

Chapter 10

Interface Concepts

Following the different analyses performed, interface concepts with included wind and trajectory uncertainty will be presented in this chapter. In order to do this, several changes to the general design of the interface will be proposed in Section 10-1. Afterwards, different concepts for the visualization of wind and trajectory uncertainty will be shown in Section 10-2, after which the final interface concept to be implemented in the remainder of this thesis will be discussed in Section 10-3.

10-1 Design Changes

As a result of the CWA performed in Chapter 9, several design changes to the interface have been proposed. Complementing changes can, however, be determined when looking at the current recommendations (mentioned in Section 3-3) and consistency between displays. These changes are discussed in this section.

10-1-1 Screen Arrangement

One of the recommendations for further research made by Riegman (2018) was to swap the VSD and TSD screen arrangement for two main reasons. Firstly, having the VSD located at the top instead of bottom right makes more sense intuitively, as the altitude screen is located 'higher' on the screen.

Secondly, having the TSD located at the bottom right facilitates the swapping of its vertical axis, meaning that a point in the solution space above the nominal trajectory would imply an initial velocity increase. This forms more similarity with the user's mental model. The adapted screen arrangement is shown in Figure 10-1.

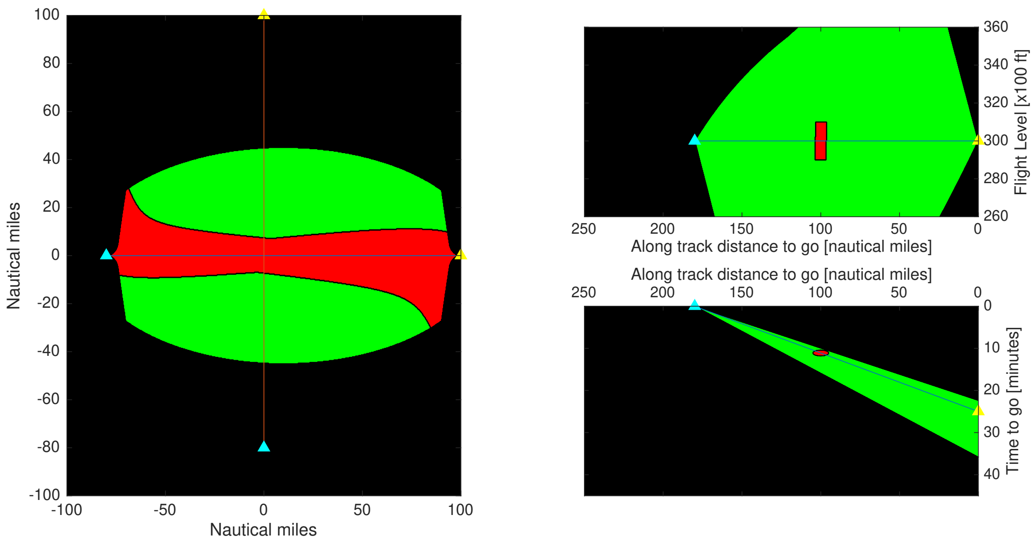

Figure 10-1: Alternative TSR screen arrangement

10-1-2 Display Consistency

In numerous studies on display design (Endsley, 1995; Wickens et al., 2004), consistency is considered an important factor. When looking at the way in which the solution space is constructed in all three screens, however, inconsistencies in both meaning and function are found for different display elements. These inconsistencies are listed in Table 10-1.

Table 10-1: Display element consistency analysis (colored entries relate to solution space colors)

	PVD	**TSD**	**VSD**
Labels on side of display	No label present - -	Label present Label used to edit trajectory while breaking 4D contract (shift ETA) Label can be moved by the computer or by the human	Label present Label used to edit trajectory while adhering to 4D contract Label can only be moved by the human
Solution space color meaning	Waypoints where 4D contract is broken Adhere to 4D contract, separation conflict not solved Adhere to 4D contract, separation conflict solved	Waypoints outside performance envelope Immediate conflict area in along-track distance and time Adhere to aircraft performance envelope, 4D contract can be violated	Waypoints where 4D contract is broken Immediate conflict area in along-track distance and altitude Adhere to 4D contract, separation conflict solved
Solution space function	Entire green area can be clicked	Only point on nominal trajectory can be clicked, after which the line can be dragged	Line can be dragged to new altitude using label, nominal line can be used to set BoC or ToD

One of the strong points of the solution space as constructed in the PVD is the fact that the human is informed on the range of available conflict solutions immediately. When inspecting the TSD and VSD, however, the solution space is found not to be constructed according to the same rationale. Not only is this inconsistent with respect to the PVD, it also reduces effectiveness and intuitiveness of both screens (and therefore also of the entire TSR).

As more functionality will need to be added to the interface (i.e., ETA management information), display consistency is likely to become even more important to prevent confusion when used by its operators. Therefore, several modifications are proposed.

TSD Rationale

When following the PVD solution space rationale, the diverging beam from the aircraft's current location (displaying its velocity performance envelope) will at some point have to converge again to meet the RTA. Constructing this as the green, performance-based solution space makes it consistent with the PVD. The red, conflict-indicating area should also be extended to all points within the performance-based solution space that do not solve the separation conflict. For the TSD, the 'corrected' solution space versus its current counterpart is displayed in Figure 10-2.

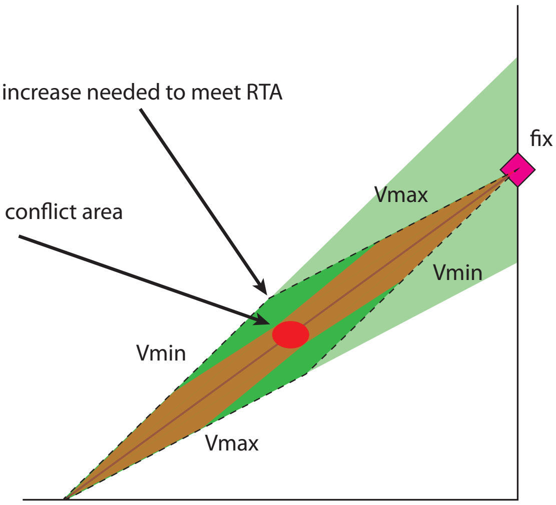

(a) Schematic explanation of alternative TSD rationale

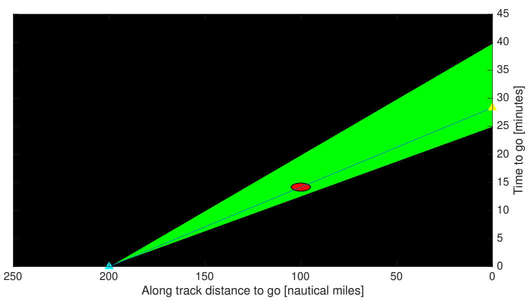

(b) Current display

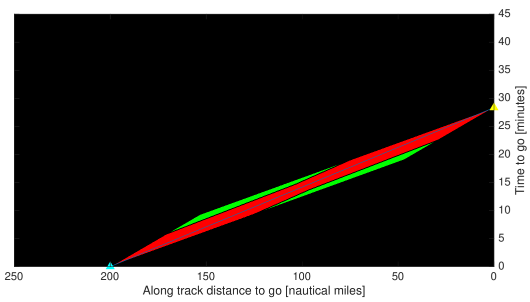

(c) Alternative display

Figure 10-2: Comparison of current and alternative TSD implementation

As can be seen, the original TSD implementation presents the human with an 'optimistic' view on the available 4D solution space in the time-space domain when compared to the 'true' solution space. This corresponds with current ATCo work practice, as conflicts are rarely solved using velocity only.

In the adapted form, direct manipulation of the trajectory is possible. The human is able to directly observe the available options for resolving the conflict and can directly place a waypoint in the solution space, as opposed to placing a waypoint and dragging the nominal trajectory (with the possibility of breaking the 4D contract). The alternative TSD therefore does not only increase its design consistency, but also improves its intuitiveness.

VSD Rationale

When looking at the VSD, creating the 'true' solution space is a more complex process, since three degrees of freedom are involved when altering an aircraft's vertical trajectory (i.e., a climb leg, a descent leg and a level segment). To construct a solution space with a rationale similar to that of the PVD, only two degrees of freedom are allowed (more would lead to ambiguous information).

To solve this, the boundary case with no level segment is considered (i.e., ToC = ToD for initially increasing altitude or BoD = BoC for initially decreasing altitude). A solution space consistent with the PVD rationale can then be constructed, allowing the human to directly select a point inside the solution space. An extra step is then required after this initial 'ToC = ToD or BoD = BoC' waypoint selection, where the climb and descent legs can be adjusted. For this, a second solution space is generated. This new rationale is depicted in Figure 10-3 and partly based on the display concept of Van Marwijk et al. (2011).

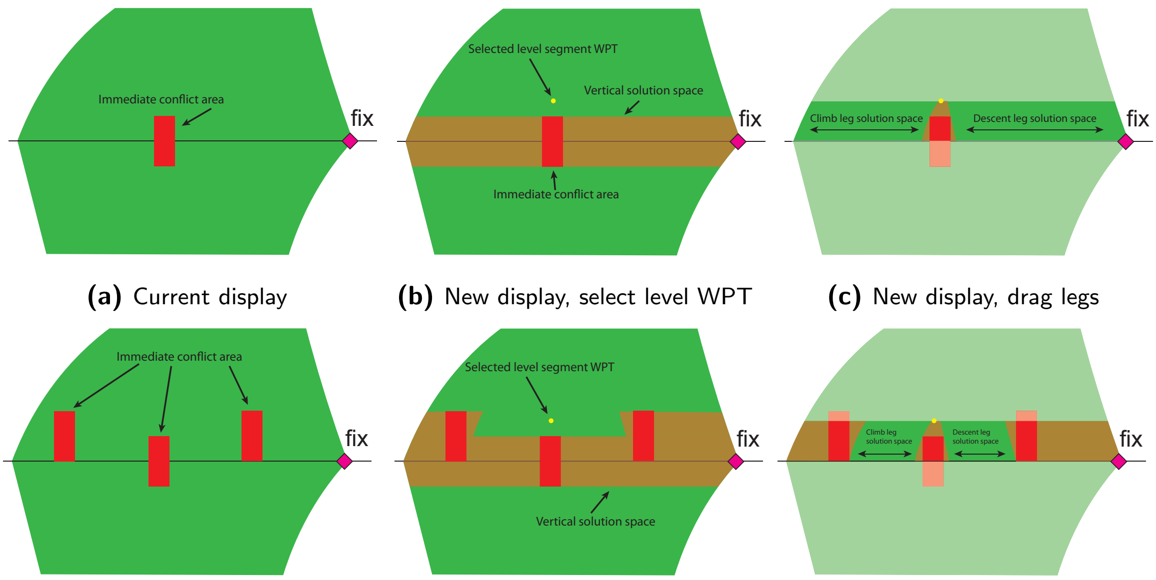

(a) Current display **(b)** New display, select level WPT **(c)** New display, drag legs

(d) Current display **(e)** New display, select level WPT **(f)** New display, drag legs

Figure 10-3: Comparison of current and alternative VSD implementation

This display modification serves multiple extra purposes in addition to the increased design consistency. First of all, the fact that any point inside the solution space can now be selected greatly increases the available flexibility. In its current form, the label on the side of the display needs to be used to drag the altitude, thereby effectively providing only One-Dimensional (1D) altitude control to the operator while showing a 2D solution space.

The latter is also important when wind information is added to the display. Wind fields can cause certain altitudes to be reachable only in parts of a sector as shown in Figure 10-4. While the current VSD would not be able to handle such a scenario (because climb and descent segments cannot be chosen freely), this can be taken into account in the alternative VSD implementation.

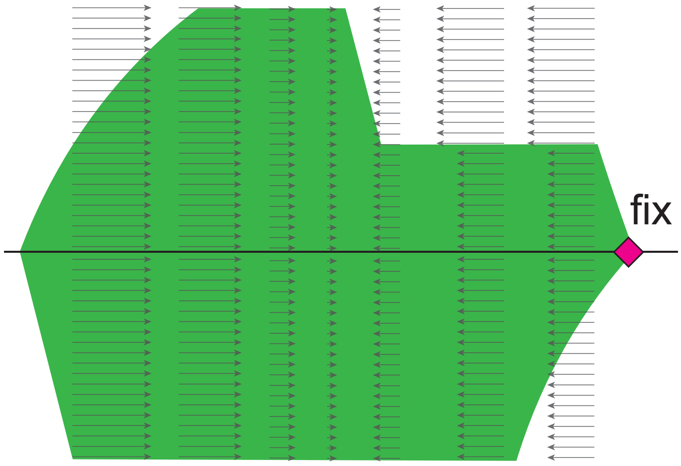

Figure 10-4: Partial altitude reachability as a result of wind conditions

Lastly, the ability to drag climb and descent segment 'legs' makes it intuitive to manipulate the vertical trajectory of aircraft that are already climbing or descending as a part of their flight plan. As this type of traffic will be dominant in ACC sectors, especially at LVNL, this addition will likely benefit ATCo acceptance.

Labels

As can be noted from Table 10-1, the use of labels is not consistent between displays. In the PVD, no label is present, while the labels are used to either break or adhere to the 4D contract in the TSD and VSD, respectively.

To increase consistency between displays in the alternative TSR, the label is chosen to indicate the possibilities for the ATCo to deviate from the 4D contract if desired. For the TSD, this means that the label meaning will be unaltered. The TSD label in particular can be used to adjust an aircraft's ETA at sector exit if the RTA will not be met with the current velocity.

With the alternative solution space implementation in the VSD, the label does not need to be used to manipulate the vertical trajectory anymore. This leaves design space for the display design to be made more consistent. The VSD label can then be used to change altitude at sector exit.

Lastly, a label can be added to the sector exit waypoint in the PVD. This label can then be dragged to change the lateral sector exit location.

To indicate the available options to the operator when moving the label, the reachable part of the axis can be highlighted on each display. For the TSD, this resembles the projection of the performance envelope onto the vertical time axis (thereby also ensuring that this information is not ‘lost’). In the VSD, the set of reachable exit altitudes can be shown, while the PVD can display available waypoints for rerouting purposes.

Integrated Design Changes

The changes mentioned in the previous sections can be integrated to form an alternative display concept as shown in Figure 10-5. Here, the use of rationale behind the solution space and the use of labels is consistent across all displays. In short, the solution spaces can be used to manipulate trajectories while adhering to the 4D contract, while the labels on the sides of the displays can be used to make modifications to the 4D contract. As an addition to the solution space, the immediate conflict area is also displayed in each screen. This allows the operator to quickly observe where the solution space constraints originate from.

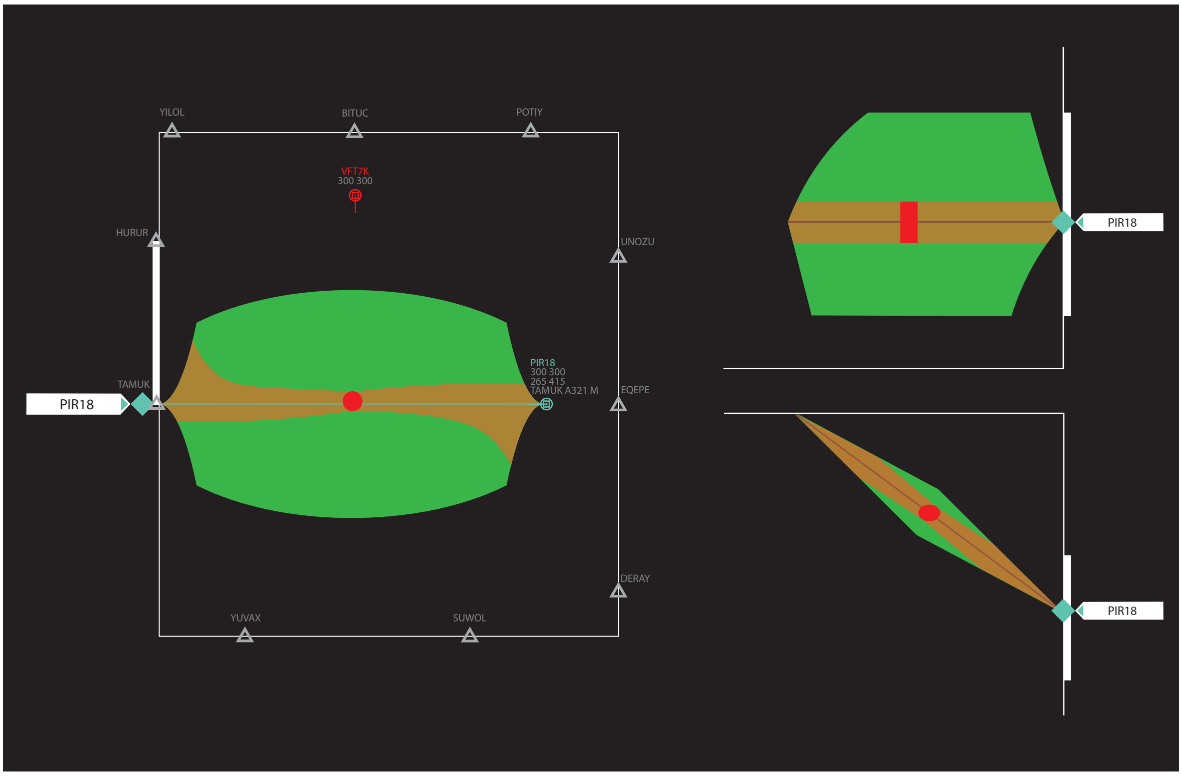

Figure 10-5: Proposed TSR design changes following from display consistency analysis

The limits of label movement are conceptually indicated by thick white spaces on the axis of interest. In the PVD, this area represents the available exit waypoints if an ATCo decides to manipulate the lateral flight plan. On the TSD, the label range represents the speed envelope of the aircraft. This label range is equal to the projection of the old TSD ‘beam’ onto the time axis. For the VSD, the set of reachable sector exit altitudes can be displayed. These reachable altitudes can be constrained by either the aircraft’s performance envelope or airspace regulations. It should be noted that these ranges will also have some stochastic component added in the final interface. This relates, for example, to the minimum and maximum reachable ETA buffer mentioned by ICAO (2014b). This will be researched in the remainder of this thesis.

As a result of the proposed changes, the TSR workflow will change. The final proposed workflow is shown in Figure 10-6.

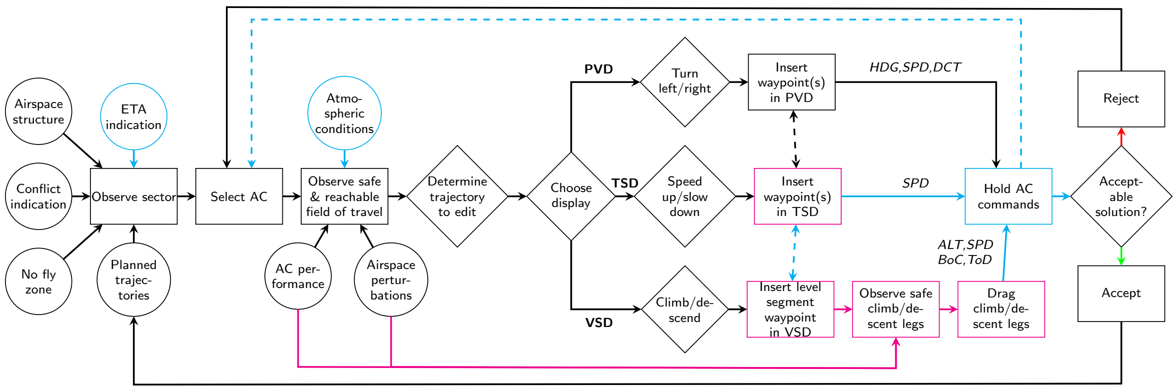

Figure 10-6: Final proposed TSR workflow (Edited elements w.r.t Figure 9-7 following from the CWA shown in blue, edited elements w.r.t Figure 9-7 following from the changed display rationales shown in magenta)

10-2 Interface Concepts

With the adapted baseline display as discussed in Section 10-1, various concepts on the inclusion of wind and trajectory uncertainty information can be presented. This is done separately for both elements in Section 10-2-1 and Section 10-2-2, respectively.

10-2-1 Wind Visualization

As discussed in Chapter 7, wind fields impact the shape of the resulting solution space in each display. While the solution space itself is sufficient to make the required CD&R decisions, the wind field characteristics itself should also be displayed on the display. This shows the means-ends link between wind and resulting solution space directly to the human, thereby increasing system state understanding. A possible (static representation of dynamic) visualization of these wind fields is given in Figure 10-7.

10-2-2 Trajectory Uncertainty Visualization

In Chapter 8, the effects of trajectory uncertainty on the solution space in each display was discussed. Contours displaying equiprobability curves of separation conflicts were drawn on all displays. In the final interface, visualization of trajectory uncertainty comes down to deciding on what contours to display as this can make a large difference in perception. To illustrate this, Figure 10-8 is shown. Here, different visualizations of the same traffic and weather scenario are given, but the contour levels and color coding are different.

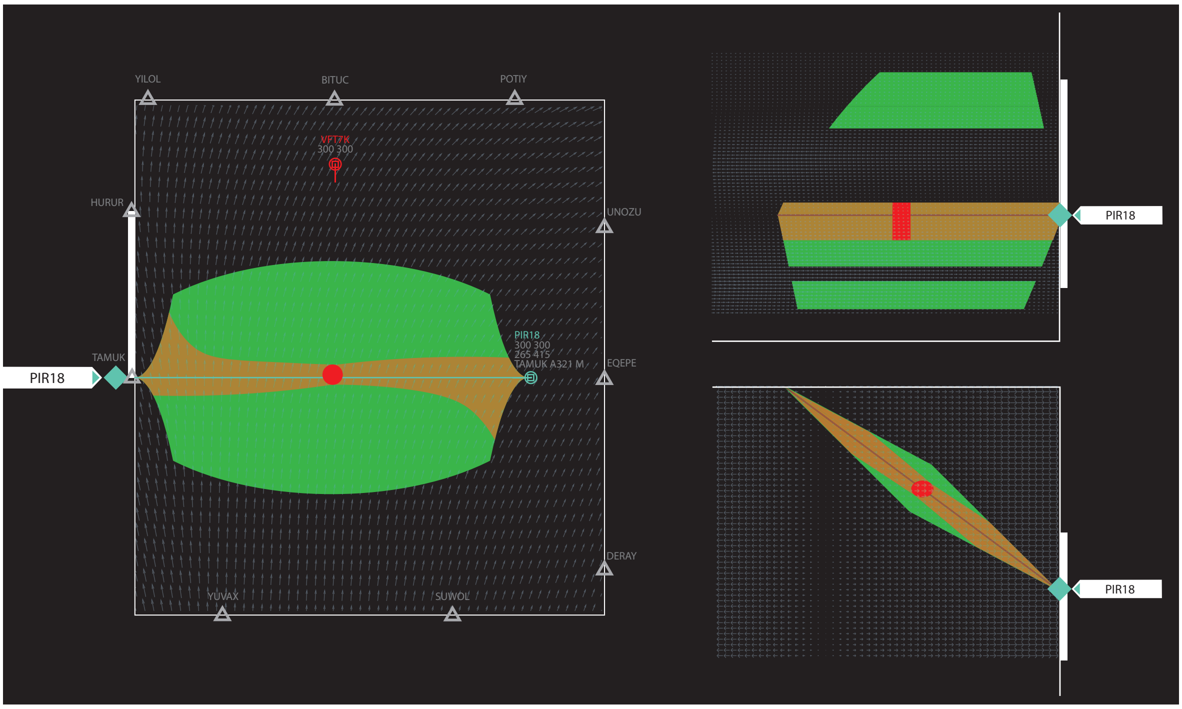

Figure 10-7: Visualization of wind field on TSR display

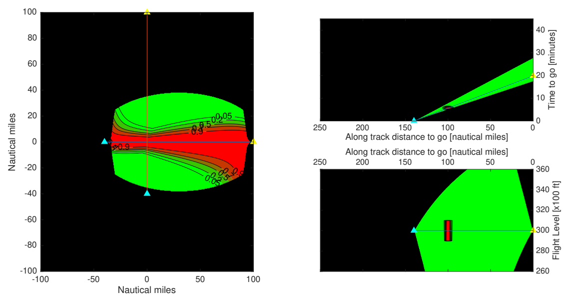

(a) Green - red color map, five contours

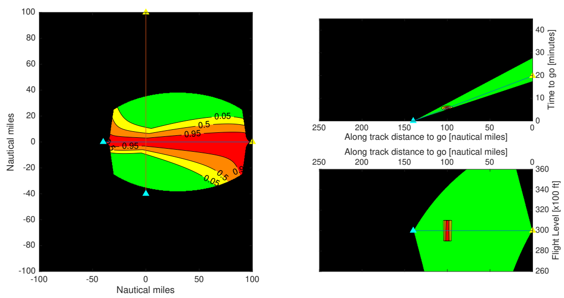

(b) Green - yellow - red color map, three contours

Figure 10-8: Different visualizations of the same traffic scenario

When determining how many different colors should be used and what contours should be drawn, the CD&R control task of the ATCo is inspected. In operation, several conflict indication 'thresholds' are of interest:

- **Safe situation**: This corresponds to a very low conflict probability (e.g., less than 5%).
- **Conflict likely**: Especially with high uncertainty, there will be a 'tipping point', where the ATCo decides to take preventive action. Intuitively, this point will be at 50% conflict probability.
- **Conflict certain**: There should also be a contour indicating (almost) certain conflicts which should trigger the immediate attention of the ATCo. In Figure 10-8b, this is set at 95% conflict probability indication.

This rationale leads to the visualization as presented in Figure 10-8b. The three contours of interest yield four colors to be used in the interface.

Furthermore, the ETA indication delta with respect to the RTA should be displayed. When this delta value exceeds a set threshold, the ATCo should be made aware of this. Because color coding is already used for conflict indication in the display, the delta can be displayed in text next to the already available information. This is similar to the well-received traffic flow management representation by Prevot et al. (2005). The text can be colored if the threshold is exceeded to indicate that user action is required. Examples of this are shown in Figure 10-9.

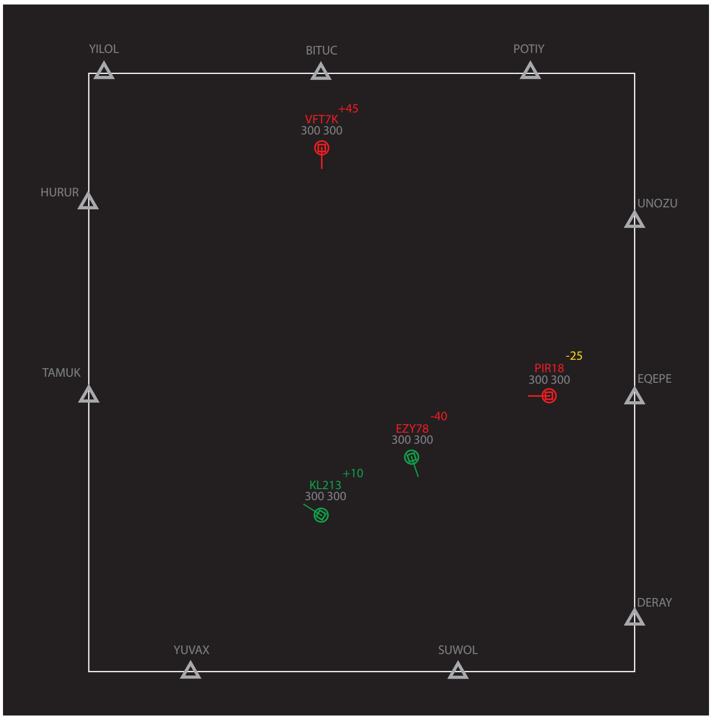

Figure 10-9: ETA delta indication example on PVD

When selecting an aircraft to modify its trajectory to change the ETA, the range of options is presented to the ATCo in terms of the freedom of movement of the TSD label. The TSD label will in this case deviate from the 4D flight plan (i.e., the blue diamond), as shown in Figure 10-10. In this example, the ATCo will have to delay the selected aircraft to ensure it reaches the sector exit at RTA. This is done by lining up the label (ETA) with the blue diamond (RTA) again.

10-3 Final Interface

Following the presented interface concepts in Section 10-2, a final concept to be implemented in the remainder of this thesis can be determined. This selection is done in cooperation with domain experts at LVNL. Feedback to the presented concepts yielded several conclusions on the final interface:

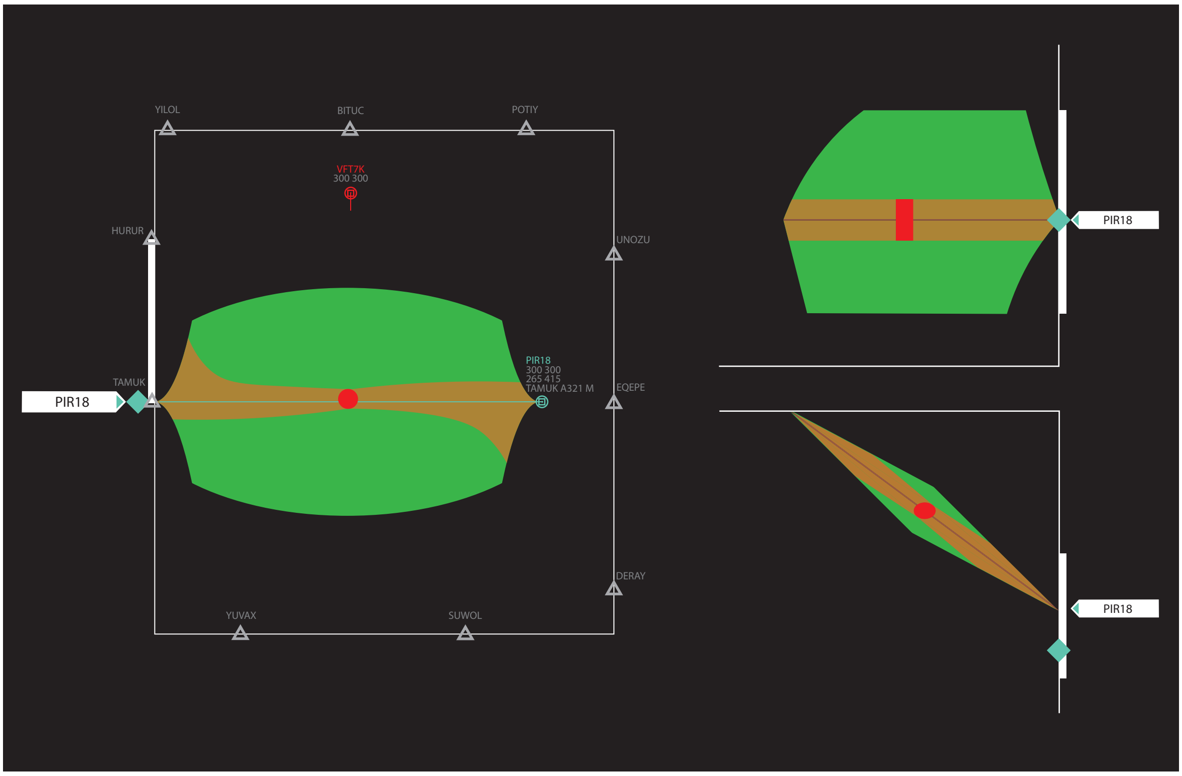

Figure 10-10: Diverted ETA and RTA shown on the TSD

- Wind visualization was considered useful, but should not always be shown. A way to implement this is to include a 'toggle' option. The operator can then turn the wind field visualization on or off for all displays depending on the information wanted.

- Wind visualization should also be available when no aircraft is selected (in the PVD only).

- In the wind visualization, the number of arrows and arrow length should be a flexible setting (per display) in the final interface.

- Wind speeds should somehow also be displayed in addition to just the arrows. An implementation of this could be to display numbers instead of arrows on some points of the screen as shown in Figure 10-11. While only showing the PVD in the figure, the same effect should be implemented in the TSD and VSD.

- With no aircraft selected, the rate of change for both conflict indication and ETA delta should somehow be displayed. This can make the difference between choosing to (already) reroute an aircraft or doing nothing. For instance, if the ETA delta is close to its threshold, the value going up or down will make a large difference for the actions to be taken by the ATCo. An example implementation can be with arrows indicating the sign of the rate of change, as illustrated in Figure 10-12.

- The distinction into four colors (as displayed in Figure 10-8b) was questioned. While the use of each color itself is justified, an ATCo generally prefers a minimalistic interface.

This is something that could be taken into account, for example by coloring only the contour boundaries instead of the complete solution space.

- The contour magnitude to be displayed is a parameter of interest. Especially the 95% conflict probability contour should intuitively be brought down to around 80%. The quantitative influence of these settings should, however, be determined in experimental settings.

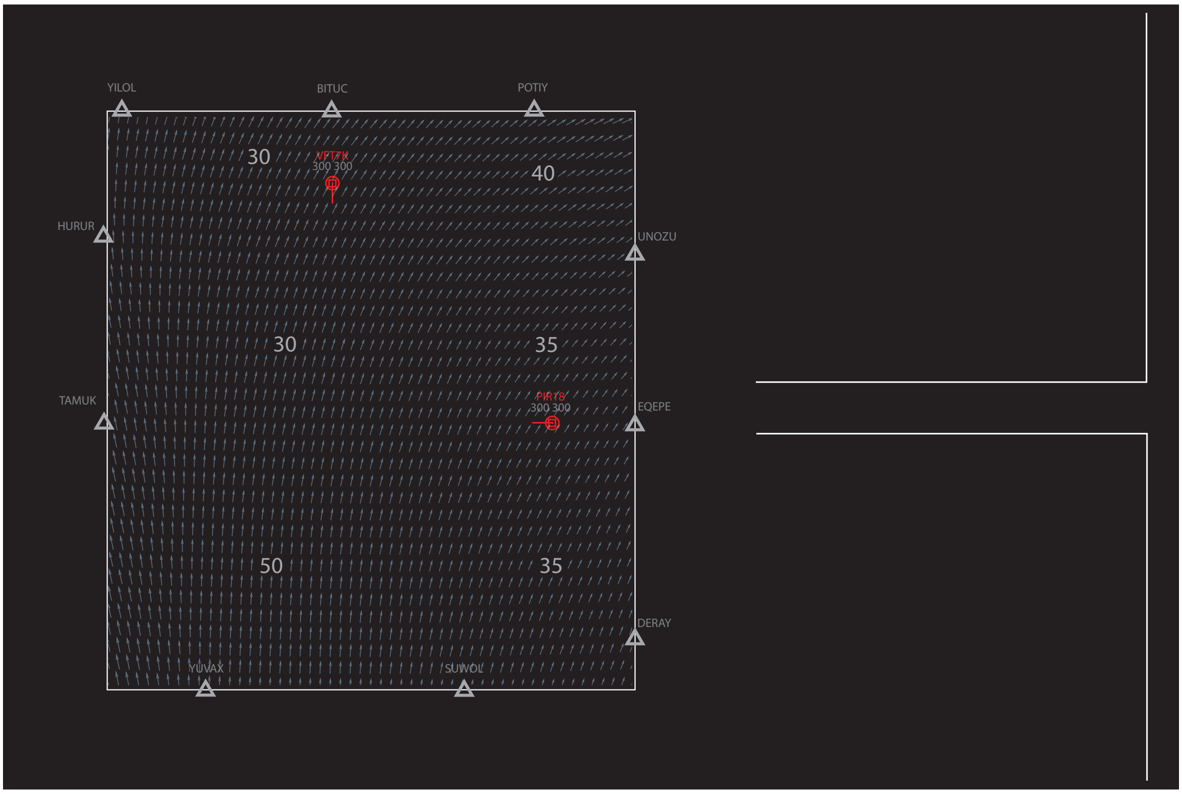

Figure 10-11: Wind field visualization with wind speed information

The final interface will consist of the presented concepts in Section 10-2 with the presented feedback in mind. As it is likely that further changes will be made as development continues, the interface should be programmed with display flexibility in mind. This will facilitate changes in the remainder of this thesis and in any possible future research.

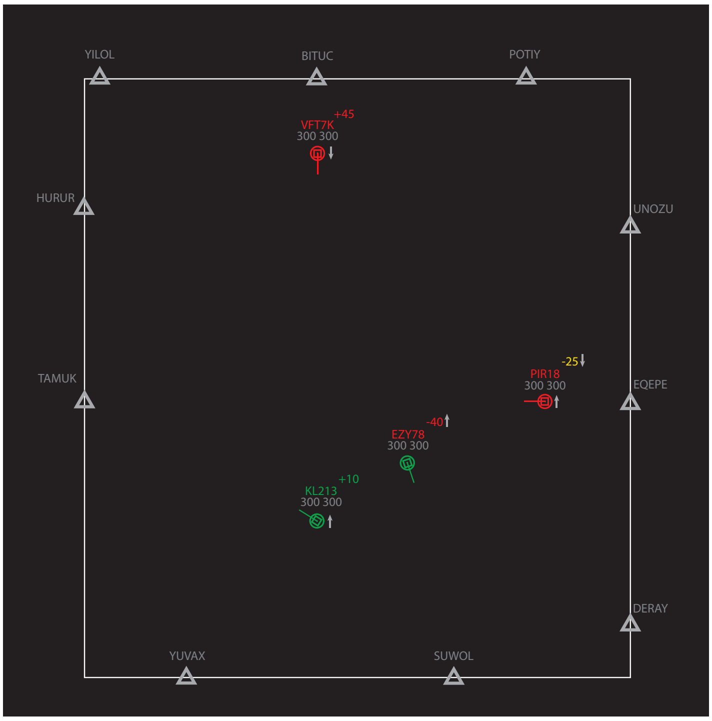

Figure 10-12: Example PVD including sign rate of change for both ETA delta and conflict indication

Chapter 11

Experiment

Following the interface concepts presented in Chapter 10, the interface will be implemented in the existing real-time simulation environment, allowing it to be validated in an experimental setting. The work needed to be done to prepare the real-time simulation interface is outlined in Section 11-1, followed by a high-level description of the validation experiment in Section 11-2.

11-1 Java Simulator

As the current TSR interface has been programmed in a real-time Java simulation environment, this will be used as the basis for the validation experiment. A significant amount of work will need to be done to integrate the presented concepts. The following changelog lists the most important alterations to be made:

- Change screen configuration and flip the TSD vertical axis.
- Update solution space generating algorithms to the new rationale for each screen as presented in Section 10-1.
- Include more realistic climb/descent model (constant M settings).
- Include implementation of wind model as described in Chapter 7.
- Include implementation of trajectory uncertainty model as described in Chapter 8.
- Include front-end visualizations of wind and trajectory uncertainty information as described in Section 10-2.
- Update AMM component to accept (pseudo-random) stochastic inputs.

11-2 Experiment Design

11-2-1 Experiment Goal

As significant changes will be made with respect to the current TSR interface, a direct comparison of experiment results obtained using the old and new interface will not be possible. The aim of the experiment will therefore be to validate the usability of the interface in its entirety. To that end, the following hypotheses will be tested:

- Controller workload will be lowered with the availability of wind and trajectory uncertainty information on the interface.
- The availability of wind and trajectory uncertainty information will increase task performance.
- With trajectory uncertainty information available, the ATCo will solve conflicts at a later point in time when compared to not having this information.

11-2-2 Experimental Set-Up

The experimental set-up consists of a Java package which will be run on a desktop computer to simulate real-world air traffic scenarios with the designed ATC interface. In order to get familiarized with the software, participants will be briefed extensively and given a training run. The traffic scenario will likely be based on a real-life situation with data being provided by LVNL. This is yet to be discussed, however, at the moment of writing.

Control Task

The control task will be to manage air traffic safely while trying to adhere to the 4D time and position constraints. During the experiment, the participants will be asked to rate their workload at fixed intervals. This control task is very similar to the way ATCos do their work in current ATC, with 4D constraints being a key difference.

Participants

Since the interface is designed to be used by real ATCos, the experiment should ideally be executed using real ATCos as well. Because of the busy work schedules of ATCos at LVNL and the amount of time required for a single run, however, this is not a realistic goal. Experiment participants will therefore range from novices and moderately experienced people to real ATCos. To avoid experiment confounds resulting from the availability of wind and trajectory uncertainty information and the skill level of the participants, a Latin Square experiment design will be set up. The amount of participants is still to be determined.

Dependent Variables

- Aircraft states at each point in time (from which to-be-defined task performance measures will be calculated)
- Subjective controller workload, as rated by participants during the experiment
- Observations gained during the experiment on participant behavior to determine control strategy, to be discussed afterwards with the participant to confirm the observed strategy
- Mouse activity

Independent Variables

- Availability of wind and trajectory uncertainty information

Control Variables

The control variables in this experiment are listed below. The exact values given to each variable will be determined at a later stage.

- Sector parameters
- Aircraft type
- Scenario duration
- Experiment environment
- Traffic scenario

11-2-3 Results, Outcome and Relevance

The experiment results will consist of three different data sets, all recorded by the Java simulation platform.

Firstly, all aircraft states at each point in the experiment will be recorded. These will serve as a basis to measure the controller task performance, using the set of determined measures (resulting from one of the research sub-questions) calculated from these states.

Controller workload will primarily be measured using the subjective workload ratings recorded during the experiment. The mouse activity will also be taken into account, since a lot of mouse activity could indicate a higher objective workload.

Lastly, the applied control strategies can be obtained by looking at the given commands on the different interface view-ports in combination with recorded mouse movements on the screen.

It is expected that the availability of wind and trajectory uncertainty information on the interface will lower the subjective workload, while increasing the task performance. Furthermore, the added trajectory uncertainty information is expected to make controllers change their strategy. It is expected that less control activity will be required, because more better estimates on conflict probability and ETA are available to the participants.

This research is relevant because its outcome will indicate if an solution space based DST with additional wind and trajectory uncertainty information will still be helpful to the ATCo. The possibility exists that too much information is presented, resulting in loss of overview and ultimately degraded task performance.

Chapter 12

Concluding Remarks

The aim of this preliminary thesis was to set a framework for the final research goal: to evaluate the effects on measured control strategies, workload and task performance of implementing wind and trajectory uncertainty information in an existing strategic 4D ATC ACC decision support interface. This knowledge will contribute to the further development of this 4D ATC decision support interface. Ultimately, the research should indicate if a solution-space-based interface is still beneficial to the ATCo in a realistic 4D ATC environment, or that it overloads the ATCo with information resulting in a loss of overview and degraded task performance.

This report included a literature review on the current and future states of ATM, existing interface design frameworks, previously designed interfaces, wind and trajectory uncertainty. Following this, a description of the envisioned ATM CONOPS was given.

With the knowledge gained from the literature study, preliminary research was conducted on the influence of both wind and trajectory uncertainty information on the solution spaces in each dimension. Furthermore, a CWA was performed to gain insight into the elements to be integrated into the interface. Lastly, interface concepts were generated and presented to domain experts, after which a final interface concept was discussed. This concept will serve as the basis during the final research phase, as it will be implemented into the simulation environment and used in a validation experiment.

Literature Study

An extensive literature study was performed to gain insight into the research field. Firstly, the current and future states of ATM were investigated. While future airspace structure is unknown, more automation is expected to make its way into the ATCo work domain. This automation should, however, be implemented with caution, as mistrust has historically led to lowered automation acceptance.

Because of its relevance in complex interface design, Rasmussen's EID framework was discussed in detail. Furthermore, various frameworks to aid in display design were summarized.

Especially in multiple-display interfaces, display consistency was found to be very important to increase intuitiveness and therefore operator acceptance. Several previous display design efforts considered relevant to this research were reviewed.

Wind field properties and modeling techniques were discussed. The most important wind field properties in direct ATM context were found to be average wind velocity and direction together with wind shear. Furthermore, the influence of wind on aircraft performance and 4D trajectory management was discussed.

The concept of trajectory uncertainty was discussed in terms of its metrics, sources of uncertainty and modeling techniques to quantify uncertainty. Many different modeling techniques were found to exist, each differing in terms of computational load and accuracy. Visualization techniques on trajectory uncertainty were found to be limited, especially in 4D context.

Preliminary Research

As a first research step, the envisioned ATM CONOPS was discussed. Rather than using the FMS to meet RTA waypoints, this control task was assigned to ATC. This approach contained numerous advantages over the use of the FMS RTA functionality, including the by-passing of 'black-box' proprietary RTA algorithms, lower-level FMS requirements, less complex data link requirements and higher on-ground available computational capacity.

The effects of wind on the existing solution space were researched. Using a verified MATLAB model, a crossing conflict traffic scenario was simulated using a variety of wind scenarios. It was found that the PVD solution space is significantly impacted by the presence of wind, sometimes leading to asymmetrical shapes. The TSD solution space is also impacted, as the ground speed and therefore the possible ETA range changes with the addition of wind. Lastly, the VSD solution space changes considerably with the addition of wind.

To model trajectory uncertainty, a parametric estimation of the position error properties was implemented. This approach was favored over more accurate Monte Carlo and PCE methods due to its relatively low computational load. Various realistic settings for the along-track, cross-track and vertical errors were used to assess the impact of trajectory uncertainty on the existing solution space. It was found that in en-route traffic scenarios, along-track error has a more dominant effect on conflict probability than cross-track error. The same was already concluded in earlier research, thereby validating this conclusion. Furthermore, conflict probability was found to be higher as TTC decreases, potentially delaying ATCo rerouting action to be taken. This was found to be in accordance with current ATCo working practice.

To support the integration of the new information into the display, a CWA was performed. This yielded several display elements to be added to the interface, as well as other workflow modifications to better comply with current ATCo control strategies.

Based on a display consistency analysis and the CWA results, the rationale behind the TSD and VSD solution space was altered. This resulted in a more coherent and intuitive representation of each solution space, where aircraft trajectory can directly be manipulated in each dimension. The different display concepts were reviewed by domain experts, resulting in a proposed display concept to be implemented in the final research phase.

Future Steps

The future research steps needed to complete this research will consist of the implementation of the final interface concept into the existing real-time Java simulation platform, followed by the execution of a validation experiment.

Verification of the implemented wind and trajectory uncertainty models can be performed using the developed MATLAB package used to investigate the effect of wind and trajectory uncertainty information on the current solution spaces.

The implementation into the existing real-time Java simulation platform will not only consist of the visualizations as presented in this report, but also of various back-end changes. The TP will have to handle (pseudo-random) stochastic inputs to create a realistic simulation environment.

In the to-be-performed validation experiment, a realistic traffic and weather scenario in sector three in the Netherlands will be used. Because LVNL currently already sets a target time at the IAF, a quantitative comparison can be made between scenarios with or without wind and trajectory uncertainty information.

Future Research

Once this research has been completed, one of the first next steps would be to further develop the trajectory uncertainty model. Effects such as wind error correlation and non-normally distributed error sources will change the stochastic properties of the position error in all three dimensions. Because the trajectory uncertainty model can accept any form of stochastic input distribution, changes in the parametric position error can easily be implemented and tested experimentally.

Another effect to be included is that of predicted atmospheric parameters other than wind (e.g., temperature, air density, etc.). This will likely alter the solution spaces as velocity calculations are influenced by these parameters.

Furthermore, the visualization of specific uncertainty contours could be explored. In the current model, three contours will be shown to the operator. Reducing the number of contours or changing the contour levels will likely change the applied control strategy and therefore possibly also workload and task performance.

Lastly, a more advanced CONOPS with enhanced data-link capability could be assumed to be in use. This would enable the use of the FMS RTA functionality, thereby closing the RTA control loop in the air instead of on the ground, thereby altering the current ATCo ETA management control sub-task.

Part III

Preliminary Thesis Appendices [1]

[1] The content in this part has been graded as part of the preliminary thesis report under AE4020.

Appendix A

Hirlam Table

Table A-1: Table of $A(n)$ and $B(n)$ values used in GRIB altitude calculation

Level	$A(n)$	$B(n)$
1	1003.03	0
2	3001.41	0
3	4960.22	0.000396
4	6836.06	0.001921
5	8594.78	0.00519
6	10210	0.010709
7	11661.8	0.018878
8	12935.9	0.03
9	14022.3	0.044287
10	14915.2	0.061865
11	15611.9	0.08278
12	16112.8	0.107006
13	16420.6	0.13445
14	16540.3	0.16496
15	16479.1	0.198329
16	16246	0.234302
17	15851.9	0.272583
18	15309.1	0.31284
19	14631.8	0.354714
20	13835.6	0.397821
21	12937.4	0.441764
22	11955.4	0.486131
23	10908.9	0.530511
24	9818	0.574494
25	8703.38	0.617676
26	7586.11	0.659672
27	6487.13	0.700117
28	5426.91	0.738673
29	4424.98	0.775036
30	3499.36	0.808943
31	2665.98	0.840176
32	1938.04	0.868572
33	1325.32	0.894024
34	833.381	0.916493
35	462.82	0.93601
36	208.414	0.952684
37	58.2348	0.96671
38	3.63365	0.97837
39	0	0.988046
40	0	0.996221

Part IV

Master of Science Thesis Appendices

Appendix B

Atmospheric Data Implementation

The wind prediction data used in the case study comes from the KNMI and is specified in GRIB file format. This appendix specifies the operations performed on the raw files to make the wind prediction data useable in the simulation.

GRIB is a common data structure used in meteorology to store historical and forecast weather data. Every hour, the KNMI publishes a high resolution weather forecast made using the HIRLAM footnoteSee `http://hirlam.org/` in GRIB format. Here, atmospheric predictions are provided on a total of 40 pressure layers containing 2D grids with a 0.1 degrees resolution for latitude and longitude. These layers use a so-called 'hybrid level definition': close to the surface, the pressure layers follow the terrain contours, while this transforms to pressure levels at higher altitudes. This is described in Equation (B-1), where $A(n)$ and $B(n)$ are constant values indicating the fixed pressure for level n and fixed fraction of surface pressure for level n, respectively. The values for $A(n)$ and $B(n)$ on each pressure level are given in Table A-1.

$$P(n) = A(n) + B(n)P_s \tag{B-1}$$

To calculate the resulting altitude from these pressure levels, Equation (B-2) and Equation (B-3) are used. Here, level 40 is the level closest to the surface and level 1 is the top level.

$$z(40) = \frac{[(P_s - P(40))]RT(40)}{0.5(P_s + P(40))g} \tag{B-2}$$

$$z(n) = z(n+1) + \frac{(P(n+1) - P(n))R(T(n+1) + T(n))}{(P(n+1) + P(n))g} \tag{B-3}$$

An example of real-life atmospheric weather forecast data is shown in Figure B-1. As can be seen, the lowest layer resembles an altitude profile close to the ground. Upon inspection, the altitude profile in Figure B-1 matches that of the corresponding real-world location, showing altitude peaks in the south-west resembling the Belgian Ardennes.

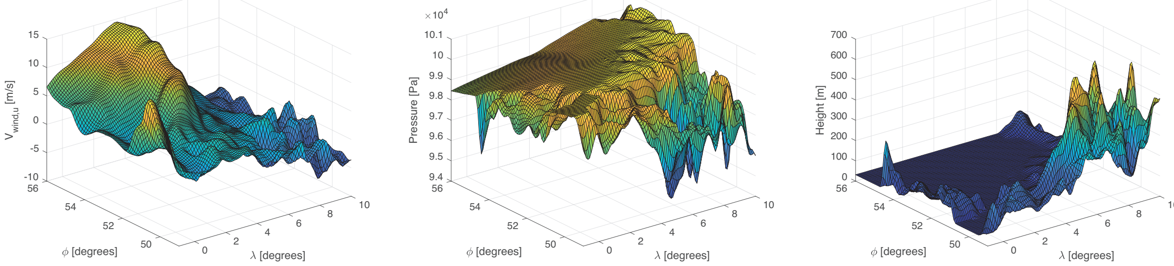

Figure B-1: Visualization of layer 40 (closest to the ground) of a KNMI GRIB weather file of November 29th, 2018

To use the prediction data for TP purposes, the data will be needed on an x, y, z grid. To this end, a stereographic projection has been used to map the decimal coordinates onto x, y coordinates as shown in Equation (B-4) to Equation (B-6) (Snyder, 1983).

$$x = k \cos\phi \sin\lambda - \lambda_0 \tag{B-4}$$

$$y = k \cos\phi_1 \sin(\lambda - \lambda_0) \tag{B-5}$$

$$k = \frac{2R_e}{1 + \sin\phi_1 \sin\phi + \cos\phi_1 \cos\phi \cos(\lambda - \lambda_0)} \tag{B-6}$$

As can be seen in Figure B-2, resolution will decrease when moving further away from the central point. As a result, an irregular grid spacing is obtained in all three dimensions (lateral due to the projection, vertical due to the pressure levels being used). This spacing is mapped onto a regular grid using a trilinear interpolation algorithm, significantly reducing computational load.

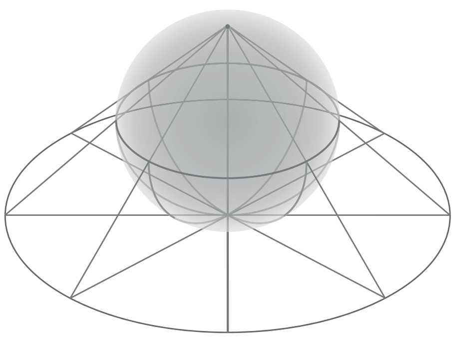

Figure B-2: 3D representation of a stereographic projection (taken from `wikimedia.org`)

Appendix C

Case Study Briefing & Training

Prior to participating in the performed case study, participants were given a short briefing to introduce them to the subject of research and their control task. The contents of this document are shown in Appendix C-1. During the case study itself, participants were provided with a step-by-step interactive training script with accompanying traffic scenarios to allow them to get accustomed with the interface. This contents of this training script are shown in Appendix C-2 [1]. During the training phase, participants were allowed to ask questions.

C-1 Briefing

First of all, thank you for taking part! You will be participating in an experiment, in which a concept 4D trajectory management interface is evaluated. A focus has been put on dealing with changing wind conditions and trajectory uncertainty due to a difference in actual versus predicted wind conditions. This document will provide you with a short introduction on relevant background information, the experiment itself and states what is expected of you as a participant.

C-1-1 Background Information

In the coming years, global air traffic numbers are projected to rise. To facilitate this increase in air traffic, the Air Traffic Management (ATM) system will need to change. Currently, both EUROCONTROL and the FAA envision an Air Traffic Management (ATM) system governed by 4D Trajectory-Based Operations (TBO) (i.e., in time and space). In 4D flight, both the aircraft's position and time are pre-computed, allowing for an airspace in which air traffic flows are optimized and can be de-conflicted before and during operation.

When these pre-planned trajectories are subsequently executed, unforeseen airspace perturbations, such as weather, sequencing and changing airspace constraints, will inevitably require

[1] It should be noted that parts of this training script are similar to that used by Riegman (2018) in his experiment.

small changes in the trajectories to be made by the Air Traffic Controller (ATCo). This perturbation management control task will consist of ensuring a safe operation while adhering to the strict time constraints imposed by the 4D flight plan. This will increase the complexity of the ATCo work domain, as these constraints (and relations between them) will have to be more strictly adhered to than in the current situation.

A concept 4D trajectory management interface has been designed and initially validated at Delft University of Technology. Using the known Required Time of Arrival from the 4D flight plan as a fixed constraint, rerouting possibilities are presented to the ATCo, creating so-called 'solution spaces'. The idea behind this approach is to leave the ATCo in direct control of the actions to take, while supporting him or her in the decision-making process. To enable 4D TBO in a realistic environment, where wind and trajectory uncertainty are taken into account, this interface has been further developed. You will be evaluating this newly designed interface.

C-1-2 Experiment Goal

To evaluate the newly designed interface, you will be asked to control a series of traffic scenarios. These scenarios are based on actual initial radar data as recorded by LVNL, coupled with the corresponding high-resolution meteorological information as provided by the KNMI. The goal of this experiment is to measure your task performance, perceived workload and applied control strategy when interacting with the interface. This will be done in multiple ways:

- By measuring all the aircraft states at each point in time, from which several other parameters can be calculated (such as added track miles, time of arrival deviation and losses of separation).
- By measuring your perceived workload during the experiment at fixed time intervals.
- By gathering you feedback through questionnaires and observations.

C-1-3 Concept of Operations

To effectively operate the interface, some basic knowledge on the effective concept of operations is required. The following information is relevant:

- Airspace rules and restrictions:
  - NORKU: PASS WINDOW FL240-280.
  - EELDE: PASS WINDOW FL200-260.
  - When a DCT command before the entry COP is issued, the FL constraint shown above will still be active.
- All aircraft follow your instructions immediately and without any delay.
- Every aircraft's Flight Management System (FMS) is programmed to do the following:

  - All aircraft follow speed instructions issued by ATC and do not deviate from these unless commanded otherwise.
  - All aircraft fly at a constant track (i.e., the aircraft compensates for the experienced wind).
  - All aircraft descend using a geometric path (i.e., maintain a constant IAS/Mach, varying rate of descent and required thrust setting accordingly). You will not be able to change the glide slope angle calculated by the FMS of an aircraft.
  - All aircraft climb using a FLCH command (i.e. maintain a constant IAS/Mach and thrust setting, varying the rate of climb).

- All aircraft arrive on your radar with an IAS speed schedule set to (try to) reach the EAT at ARTIP.

C-1-4 Experiment Execution Procedure

Before starting with the experiment, you will be asked to fill out a short questionnaire, in which your current thoughts on ATC are questioned. To make you familiar with the concept interface, you will be given an interactive training script that will guide you through its possibilities. After completing this training script, you will be controlling four traffic scenarios .

After the experiment has taken place, you will again be asked to fill out a questionnaire to obtain your detailed feedback on the various interface components. Some last remarks:

- Please try to be well-rested before the experiment.
- Please do not discuss any of the scenarios or the procedure in general with other participants.

Thank you again for participating and do not hesitate to get in touch in case of questions or remarks.

Contact information researcher:	Contact information research supervisor TU Delft:	Contact information research supervisor LVNL:
Matthijs Ottenhoff mmottenhoff@gmail.com +31 6 5499 5049	dr. ir. Clark Borst c.borst@tudelft.nl +31 15 2789099	Ferdinand Dijkstra ferdinand.dijkstra@lvnl.nl +31 6 3957 3800

C-2 Training Script

Purpose of the Training

In order to have a good understanding of how to perform your task in the main experiment, all tools and features that are available to you in the experiment simulator will be described in this training session. The training will be in the form of an interactive step-by-step script that will guide you through a number of scenarios. Each scenario will focus on a specific learning objective. At certain points during the scenario you may be required to answer one or more questions to test your understanding so far.

Your main task in the experiment will be to manage the traffic safely, and to try to adhere as much as possible to the Expected Approach Times. That is, to keep any delays at ARTIP as small as possible. This will be explained in more detail during the training.

Please try to talk out loud and try to motivate your reasoning for the decisions you make during the training scenarios. Read all the instructions carefully and don't hesitate to ask questions if something is unclear. During the training you are free to ask questions or ask for help, but in the main experiment you will be asked to control the traffic without external interference.

Airspace and Traffic

The controlled airspace used in the training scenarios and in the main experiment are a mix of artificial, en-route upper airspace sectors, as well as real-life sectors you are familiar with. All aircraft resemble a generic type of medium-sized commercial airliner and have their own performance characteristics (speed envelope, acceleration, etc.). You will be able to manipulate the route and the speed of the aircraft.

C-2-1 Scenario 1 - En-route

Part 1: System functionality and basic representations

The simulation is paused at this point, so please take the time to carefully read each following step. The experiment simulator is built up by three separate screens:

- **PVD (Plan View Display):** The screen on the left hand side shows the top-down radar view of the sector, the entry and exit waypoints and all aircraft. The controlled sector in the training session has 12 unique entry and exit points, and in this scenario there is one controlled aircraft (callsign: BMS02N). You will use this screen to manipulate the lateral route of the aircraft.
- **TSD (Time-Space Diagram):** The screen on the bottom-right hand side is a so-called Time-Space Diagram and will visualize information about the trajectory of a selected aircraft in terms of distance and time. A more in-depth explanation will follow later on.
- **VSD (Vertical Situation Diagram):** The screen at the top right-hand side is the Vertical Situation Diagram. It visualizes information about the altitude and the distance to go of a selected aircraft. It will be used to manipulate the vertical route of the aircraft.

In the remainder of this script, all **<u>actions will be displayed bold & underlined</u>**, while all information is displayed without extra formatting.

Basic information on the PVD (left)

1. The track of BMS02N is indicated with a speed vector that is currently aligned with its route. The tip of the speed vector indicates the position at which the aircraft will be when following the current heading for 90 seconds at the current speed. A longer speed vector therefore indicates a faster flying aircraft. The aircraft is flying towards exit point TAMUK, shown by its route indicated by a thin line.

2. **Highlight BMS02N and its route by hovering over it with the mouse in the PVD.**

3. **Left-click on the highlighted aircraft to select it.** The selected aircraft and its route will turn cyan.

4. More information on the aircraft is now displayed. You can see, the current IAS (265 kts), current GS (415 kts), current FL (300) and desired FL (300).

5. The waypoints along the route of a selected aircraft are visualized using magenta star symbols. BMS02N has one active waypoint that is located at the sector exit point (TAMUK). The planned speed towards this point is shown below the star symbol (also 265 kts).

6. The label attached to the aircraft at the sector exit waypoint indicates the current exit waypoint. The blue cyan diamond indicates the planned sector exit waypoint. Currently, the two coincide, as the aircraft is flying towards its planned exit waypoint.

7. The shaded area that has appeared along the route of BMS02N is the so-called solution space of the aircraft. The solution space shows the area in which the aircraft can be rerouted and will still be able to arrive at the originally planned time at the sector exit point. Note that any deviation from the current direct route to the exit point will lead to a longer trajectory, and as a result, the aircraft will have to fly faster to reach the original exit time. The solution space is therefore bound by the speed envelope of the aircraft. That is, the solution space is bounded by the maximum or minimum speed that the aircraft can fly.

Basic information on the TSD (bottom-right)

1. The TSD (bottom-right screen) shows the time-space representation of the trajectory. Here, the horizontal axis indicates the distance from the sector exit point along the current trajectory. The vertical axis indicates future time. The cyan line represents the trajectory of the aircraft. Observe that at the current time (00:00), the aircraft has approximately 175 nautical miles to fly until reaching the exit point. The arrival time of the aircraft at the sector exit point is approximately at (00:26), and is indicated by the intersection of the line with the time-axis.

2. The position of the aircraft label along the time axis in the TSD indicates the current exit time of the aircraft. The cyan diamond along the time axis indicates the originally planned exit time of the aircraft. Note that these are now the same, but in case of a delay they will be different.

3. The reachable exit times for this aircraft can be obtained by inspecting the thick white vertical line on the time axis. As can be seen, the aircraft can reach its exit waypoint between approximately (00:22) to (00:32) without altering its lateral path. Note that if the aircraft would fly slower than currently (i.e., arrive at a later time), the time-space line will be steeper. Vice versa, a more shallow line indicates a faster flying aircraft.
4. The time-based solution space of the aircraft is also represented in the TSD by a shaded area. This area currently has the shape of a parallelogram, because an aircraft has to meet the Required Time of Arrival at the next waypoint. Therefore, the aircraft can either accelerate and then decelerate (any point above the current time-space line) or decelerate and then accelerate (any point below the current time-space line). The boundaries of the parallelogram follow from the speed envelope of the aircraft.
5. Furthermore, the white triangle at the left-top of the TSD is a slider that can be used to make a projection of the future aircraft movements. **Drag the slider down to see the expected position of the aircraft in future time on the PVD.**

Basic information on the VSD (top-right)

1. The VSD (top-right screen) shows the altitude-distance representation of the trajectory. Here, the horizontal axis, as in the TSD, indicates the distance from the sector exit point along the current trajectory. The vertical axis indicates the flight level. The cyan line represents the trajectory of the aircraft. The circle represents the current location of the aircraft, currently approximately 175 nautical miles from the sector exit. Note that the Flight Level is 300 throughout the trajectory.
2. The label attached to the aircraft at the end of the cyan line indicates the current exit altitude. The blue cyan diamond indicates the planned sector exit altitude. Currently, the two coincide, as the aircraft is flying towards its planned exit altitude.
3. Any applicable altitude constraints are also represented in the VSD. Currently, the exit waypoint has a PASS AT constraint at FL300, indicated by the two grey triangles at the exit waypoint.
4. The vertical solution space is not shown to you, as you will not be using this during the experiment.
5. You may have noticed the white triangle on the left side of the VSD. This is the altitude slider, which is set at the aircraft's current altitude. Its use will be explained to you in more detail later on.
6. **Deselect the aircraft with a right mouse click on any viewport.** The time-slider in the TSD will also reset to the initial position, while the altitude-slider in the VSD will remain at its current altitude.

Part 2: Route manipulation

The route of an aircraft can be manipulated within the bounds of the 4D contract in each screen.

Route manipulation on the PVD (left)

1. The route of an aircraft can be modified in the PVD by adding or deleting waypoints. **Please select BMS02N in the PVD.**
2. **Hold CTRL to enter route manipulation mode.** A waypoint symbol will be attached to the mouse cursor.
3. **Hold CTRL and left click on a position inside the solution space to insert an intermediate waypoint into the trajectory of the selected aircraft.**
4. You can see that the route has been split-up into two segments and the aircraft route passes through the newly created waypoint. The two new segments will have an equal speed (check that by the speed indication label under the waypoints).
5. Observe in the TSD that the sector exit time of the aircraft has not changed (the label and cyan star coincide), but that the range of available exit times has changed (since the lateral path has been altered).
6. Also notice that the new waypoint is visible in both the TSD and VSD, and that, as for the PVD solution space, the speed/time constraints have been split over the two segments.
7. **Delete the waypoint by pressing CTRL and right clicking on it when it is highlighted.**
8. **Try to insert and delete waypoints at locations both inside and outside the solution space.** Note how placing a waypoint outside the solution space will cause the aircraft to be delayed, since it cannot fly fast enough to reach its exit waypoint on time.

Route manipulation on the TSD (bottom-right)

1. Waypoints can also be added, manipulated and deleted on the TSD. **Press and hold CTRL when the mouse cursor is in the TSD.**
2. **Holding CTRL, left click somewhere in the time-based solution space on the time-space line of BMS02N to insert a waypoint into the trajectory of that aircraft.**
3. Note that placing a waypoint above the current time-space line corresponds to an initial speed increase, followed by a decrease to meet the Required Time of Arrival at the next waypoint.
4. Also note that the waypoint immediately shows op in both the PVD and VSD. Take a moment to recognize the coupling between the screens.
5. Besides placing an intermediate waypoint, you can also edit the timing of current waypoints. You can do this by clicking and dragging an existing waypoint upwards or downwards, depending on your desired action. Upon, dragging, the available ‘dragging range‘ is immediately shown to you in the time-based solution space spanned between the previous and next waypoint. **Try to play around with this feature using the waypoint you added previously.**

6. Note that doing so alters the given speed command towards this waypoint, but also towards the next waypoint to meet its Required Time of Arrival.

7. **Delete the waypoint in the TSD by pressing CTRL and right clicking on it when it is highlighted.**

Route manipulation on the VSD (top-right)

This feature will not be explained, as you will not be using this in the experiment.

1. So far, you have only modified the ‘probe trajectory of the aircraft. Any changes made here have not been sent to the aircraft and the aircraft would continue to fly along its original trajectory if the simulator was running.

2. **Deselect the aircraft by right-clicking on any viewscreen and select BMS02N in the PVD again.** As can be seen any unconfirmed changes made to the trajectory have been reset. Deselecting an aircraft will also cause any changes made to the probe trajectory to be reset. You can use this cancel the probe trajectory.

3. **Manipulate the route of BMS02N in the PVD and press ENTER to send it to the aircraft.** You will notice a message at the top left corner of the PVD that confirms that the trajectory of the selected aircraft has been updated. Manipulated aircraft are shown in a brighter shade of green. You can see this after the aircraft is deselected.

4. **Deselect the aircraft by right-clicking on any viewscreen.**

Part 3: Contract manipulation

Apart from manipulating the routes within the given 4D flight plan as you have done previously, the 4D contract itself can also be manipulated. In case you are wondering, contract manipulation on the PVD will not be possible in the experiment, hence it is not explained to you in this training.

Contract manipulation on the TSD (bottom-right)

1. **Please select BMS02N in the PVD again.**

2. The label on the right side of the TSD can be used to break the time component (i.e., have an aircraft be early or be delayed).

3. **Try to move the label by clicking and dragging it.** You will notice the exit time changing and you will see the planned speeds towards the waypoints increase or decrease correspondingly. This means that all previously given TSD speed commands will be erased when moving the TSD label.

4. Also notice how the solution space on the PVD is directly influenced by speeding up or slowing down the aircraft when releasing the mouse button again. In general, the area of the solution space will increase when the aircraft is delayed.

5. **Reset the probing trajectory again by clicking the aircraft label you just dragged.**

6. If you only want to alter the speed towards the last waypoint, click the last waypoint instead of the label. **Practice doing this, and note the difference between dragging the label versus only the last waypoint.**

7. Also note how the original exit time is still shown by means of the cyan diamond.

8. **Reset the probing trajectory again by clicking the aircraft label you just dragged.**

Contract manipulation on the VSD (top-right)

1. The label on the right side of the VSD can be used to break the altitude component (i.e., change the planned altitude of the aircraft at sector exit).

2. **Try to move the label by clicking and dragging it.** You will notice the exit altitude changing per 10 Flight Levels.

3. You will note that the planned Indicated Airspeed at the new altitude will change with respect to the original Indicated Airspeed. Because True Airspeed varies with altitude, the Indicated Airspeed will need to be compensated to maintain the correct sector exit time.

4. Also notice how the solution spaces on both the PVD and TSD are directly influenced by increasing or decreasing the aircraft's exit altitude.

5. **Set the aircraft's exit altitude to FL270.**

6. **Hover over the descending segment.** You will notice that both the Top of Descent and Bottom of Descent will be highlighted.

7. **Once highlighted, click the segment and drag it to the left.** You will notice a shaded area along the descent segment as you drag it. This area indicates the feasible points to descend.

8. You will note that the planned Indicated Airspeed at the new altitude will change with respect to the original Indicated Airspeed. Because True Airspeed varies with altitude, the Indicated Airspeed will need to be compensated to maintain the correct sector exit time.

9. **Play around with manipulating the climbing or descending segments like this.** Try to get a feel for you actions and their consequences on the velocity commands given.

10. **Reset the probing trajectory again by clicking the aircraft label you just dragged.**

Part 4: Dynamic traffic

1. **Press the fast forward button on the top-right corner of the simulator above the TSD.** The simulator will start running at 4x speed (fast-time).
2. **When the simulator is running, select the aircraft and observe how it maneuvers along the updated trajectory in the PVD.** Also observe how the time-axis moves down as time progresses in the TSD. In accordance, you can see that the along-track distance of the aircraft to the exit point will decrease. **Practice adding, manipulating, deleting and sending updated trajectories for BMS02N.**
3. Every 2nd minute a workload rating scale will appear on the left side of the PVD. **Please indicate your experienced workload at that time (0 to 100, low to high) by clicking in this scale.**
4. You may continue to the next scenario when you feel comfortable with manipulating the route of the aircraft.

C-2-2 Scenario 2 – En-route

Part 1: Predicted conflict resolution

Conflict resolution on the PVD (left)

1. The color of an aircraft indicates the probability of loss of separation with another aircraft (within 5 NM or 1000ft) at some point in the future. There are four colors to be distinguished:
   (a) An red colored aircraft indicates >90% conflict probability
   (b) An orange colored aircraft indicates >50% conflict probability
   (c) A yellow colored aircraft indicates >5% conflict probability
   (d) A green colored aircraft indicates <5% conflict probability
2. The two aircraft are currently orange and thus have a conflict probability between 50-90%. **Use the time slider in the TSD to investigate where and when probable loss of separation will occur (do not yet select an aircraft).**
3. While the circles (indicated the 2,5NM radius around an aircraft) overlap when the two aircraft paths cross, the probability of conflict is still not 100%. This follows from the uncertainty in path prediction taken into account when computing the conflict probability. Because the two aircraft still have around 100NM to cover before the conflict occurs, a conflict cannot be predicted with 100% certainty yet.
4. **Select one of the aircraft on the PVD.**
5. Notice the orange and yellow part of the trajectory of the selected aircraft (not in the solution space, but along the trajectory line itself). The orange section indicates the location of the 50-90% conflict probability. The yellow section indicates the location of the 5-50% conflict probability.

6. Also notice that a large orange zone is present in the solution space of the aircraft. The orange zone shows all the locations that are unsafe to place a waypoint in, as there is a 50-90% probability of conflict. When a waypoint is placed somewhere in this zone, the new trajectory will lead to a likely conflict with other traffic.
7. The yellow boundary around the orange region indicates that if a waypoint is placed in that area, the new trajectory will have a 5-50% probability of conflict.
8. **Hover over the orange region in the solution space on the PVD with the mouse to highlight the aircraft that causes this zone.**
9. **Left click on the zone to select the other aircraft.** You can see how the solution space of both aircraft is affected by the other aircraft.
10. **Add a waypoint somewhere in the orange field of travel for the selected aircraft and check with the time slider in the TSD that the conflict has (likely) not been resolved.**
11. **Add a waypoint somewhere in the green field of travel for the selected aircraft and check with the time slider in the TSD that the conflict has (likely) been resolved.**
12. **Please delete all newly created waypoints for both aircraft before continuing to the next part.**

Conflict resolution on the TSD (bottom-right)

1. Notice the restricted field of travel in the TSD. This restricted area represents the locations in time and distance to go for the selected aircraft that are unsafe to place a waypoint in, as a (likely) conflict will occur when the following trajectory will be executed. The same coloring scheme is applied as in the PVD.
2. Similar to the PVD, the orange and yellow part of the trajectory of the selected aircraft (not in the solution space, but along the trajectory line itself) indicates the locations of conflict probability along the flight path.
3. **Hover over the restricted field of travel in the TSD with the mouse to highlight the aircraft that causes this zone.**
4. **Left click on the highlighted zone to select the other aircraft.** You can also see here how the solution spaces of both aircraft are affected by the other aircraft.
5. **Resolve the conflict by changing the arrival time at the sector exit for one of the aircraft and check the validity of this solution by using the time slider in the TSD.**
6. In this scenario, it is possible to resolve the conflict and to let both aircraft arrive at the sector exit point at their originally planned time by adding an intermediate waypoint in the TSD. **Experiment with such a solution for a given aircraft and check the solution with the time slider.**

7. **Please delete all newly created waypoints for both aircraft before continuing to the next part.**

Conflict resolution on the VSD (top-right)

1. As stated you cannot see the vertical solution space, because you will not be using this during the experiment.
2. Similar to the PVD, the orange and yellow part of the trajectory of the selected aircraft (not in the solution space, but along the trajectory line itself) indicates the locations of conflict probability along the flight path.
3. **Change the planned altitude at sector exit to FL280.** You will note that the conflict has not been solved yet, because the aircraft's FMS will want to keep its current altitude as long as possible.
4. **Drag the descending segment forward.** You will note the corresponding solution space appearing. Resolve the conflict by selecting an appropriate top of descent.
5. **Please reset the current aircraft's trajectory by clicking the altitude label again.**
6. **Deselect the current aircraft.**

Part 2: Pure CPA conflict resolution

1. The conflict prediction can also be switched to 'pure CPA' mode, where the current nominal trajectories will be taken exactly without any uncertainty to calculate the conflict probability. In this mode, the color coding changes slightly:
   (a) A red colored aircraft indicates a predicted loss of separation at some point in the future
   (b) A green colored aircraft indicated a safe trajectory without any conflicts.
2. **Enter this mode by pressing the Z key on your keyboard.**
3. Note how both aircraft in the PVD have turned red. The expected, but not yet certain conflict that was predicted, is now shown directly without taking into account the distance to fly before conflict.
4. **Inspect the solution spaces of both aircraft with and without trajectory uncertainty taken into account.** You can do this by pressing Z again to switch between modes.
5. During the experiment, you are free to use any conflict detection metric (either using probabilities or using the pure CPA display). It is up to you what mode you prefer.
6. You can always check what mode you are in by looking at the top-right of the PVD. It shows whether or not uncertainty is taken into account.
7. **For now, switch to the probabilistic conflict detection by pressing Z again.**

Part 3: Dynamic conflict resolution

1. When the simulator is running, select an aircraft and observe how the restricted fields of travel evolve in the PVD and TSD. Also note that the available control space becomes smaller as the aircraft close in.
2. **Press the fast forward button on the top-right corner of the simulator above the TSD.** The simulator will start running at 4x speed (fast-time).
3. Note that when doing nothing for a while, a red conflict zone will start to emerge. This is because the aircraft are closer together and a conflict can therefore be predicted with more certainty.
4. **Practice conflict resolution with the simulator running.** You could, for instance, try to perform a cooperative resolution in which the conflict is resolved by giving both aircraft a small path deviation (spatial or time), rather than manipulating only one aircraft. This will reduce the relative path deviation for each individual aircraft.
5. You may continue to the next scenario when you feel comfortable with manipulating the route of the aircraft.

C-2-3 Scenario 3 – En-route

Part 1: Wind

The last scenarios were without any wind present. From now on, there will be wind present in each scenario. The wind visuals, and also the effect of wind on each of the solution spaces will be explained in this part.

Wind field visualization

1. Without any aircraft selected, you can visualize the current wind field. **Press SHIFT once to do so show the current wind field. You will note a southern wind present in the current sector.**
2. The wind shown in the PVD is the wind at FL260 and at the current time. You have the option to 'peak' through the current wind field at different flight levels and at different look-ahead times by moving around the sliders in the TSD and VSD.
3. By clicking and dragging the VSD slider, you can change the currently shown wind altitude. **Try to play around with the VSD slider and note the dynamic nature of the wind at different flight levels.**
4. By clicking and dragging the TSD slider, you can change the look ahead-time of the currently shown wind field. For example, when moving the TSD slider to 30 minutes with the VSD slider set at FL300, you will get a peak of the wind field at FL300 in 30 minutes.
5. **Turn off the wind visuals by pressing SHIFT again.**

Wind in the PVD

1. **Select VFT7K in the PVD. Compare its solution space with that of PIR18.**
2. You will notice that PIR18 has more maneuvering room than VFT7K. This is primarily due to wind effects.
3. **Press SHIFT again to see the coupling between visuals and the presented solution spaces of both aircraft.**
4. When an aircraft is selected, the wind field shown in then PVD is no longer fixed at a certain altitude, but becomes path dependent. Therefore, the wind is only visible around the aircraft path and not in the entire sector anymore.

Wind in the TSD & VSD

1. Similar to the PVD solution space, the TSD and VSD solution spaces are also impacted by the presence of wind, as the aircraft's ground speed envelope changes.
2. You will see that, with the wind visuals turned on, the along-track component of the path dependent wind is displayed in both the TSD and the VSD.
   (a) In the VSD, the wind on the current lateral path at different Flight Levels is shown. Note how the along-track wind speed varies a lot with altitude. This will be important to note when handling inbound traffic with large altitude differences later on in the experiment.
   (b) In the TSD, the path dependent wind with increasing look-ahead wind is presented. Any sudden changes in wind direction and/or speed in time will be noticeable here.
3. **Select PIR18 and place a waypoint somewhere in the PVD.** Note how the along-track wind fields in the TSD and VSD are immediately updated.
4. **Take the time to play around with these aircraft until you are comfortable with the interaction between the wind information and the corresponding trajectory / solution spaces in all screens.**
5. Note that you can – at any point – turn off the wind field visualization by pressing SHIFT again.
6. In the actual experiment scenarios, you will always be able to toggle the wind visualization by using SHIFT. It is up to you whether or not to use this visualization.

Part 2: Actual trajectory uncertainty

You will now be running the simulation. To increase the realism of this scenario, the actual wind present in the sector is different to the information used to make the trajectory predictions.

1. **Press the fast forward button on the top-right corner of the simulator above the TSD. The simulator will start running at 4x speed (fast-time).**
2. Observe how:
   (a) After a while, an arrow will appear next to both aircraft. This arrow indicated the RTA delta change. Because there is a different wind than expected, expected arrival times will start changing. This difference will also become visible next to the arrow (rounded to the nearest five seconds).
   (b) The expected conflict predictions will also change. Will the predicted conflict actually happen?

C-2-4 Scenario 4 – Inbound

The previous scenarios have been situated in large en-route airspace sectors. As you will be managing inbound peaks towards ARTIP in the experiment later on, you will now practice using the interface with inbound traffic.

Part 1: Introduction

1. Note that the altitude range available in the VSD is now much larger than in the previous scenarios.
2. **Without selecting any aircraft, turn on the wind visualization by pressing SHIFT.** Take the time to scroll through the current wind at different flight levels and observe the large differences in wind speed and direction.
3. **Select TFL752.**
4. Observe how the along-track wind displayed in the PVD is now altitude dependent. It shows the heavy winds at FL380 near the current radar position, while the wind at FL100 near ARTIP is shown. Take a moment to visualize the coupling between the wind fields shown in the VSD and PVD.
5. Note that TFL752 will currently arrive too early at ARTIP, and that it cannot arrive any later when sticking to its current lateral path. You can quickly see this by inspecting the reachable ETA range in the TSD.
6. Because you will not be able to alter the glide slope angle of the aircraft, you cannot modify the vertical trajectory between NORKU and ARTIP. You can, however, bring forward the initial descent phase towards NORKU. **Do this by dragging the corresponding track segment forward.**
7. Use the TSD label to match the ETO with the EAT (the cyan diamond). With the change in the vertical profile you made, the aircraft will be able to reach its EAT at ARTIP.
8. **Reset the probing trajectory again by clicking the aircraft label you just dragged.**

9. Besides altering the vertical profile of this aircraft, you can also resolve this by adding track miles once the aircraft in within the Dutch FIR. **Try to place an intermediate waypoint with which TFL752 will reach its EAT at ARTIP using the solution space in the PVD.**

10. **Press ENTER to confirm the modified aircraft trajectory and deselect the aircraft.**

11. **Select TRA5680 in the PVD.**

12. Note that TRA5680 will currently arrive too late at ARTIP, and that it cannot arrive any sooner when sticking to its current lateral path. You can quickly see this by inspecting the reachable ETA range in the TSD.

13. **Resolve this by removing the NORKU waypoint in the PVD and sending TRA5680 direct to ARTIP.**

14. Note that after doing so, TRA5680 will be able to arrive on time. Also note that the fixed altitude constraint at NORKU has been relocated on the new path and is still active.

Part 2: Dynamic traffic

1. **Press the fast forward button on the top-right corner of the simulator above the TSD.** The simulator will start running at 4x speed (fast-time).

2. **Practice managing air traffic with the simulator running.**

3. You may continue to the next scenario when you feel comfortable with manipulating the route of the aircraft.

C-2-5 Scenario 5 – Inbound

Part 1: Introduction

1. **Without selecting any aircraft, turn on the wind visualization by pressing SHIFT.** Take the time to scroll through the current wind at different flight levels and observe the large differences in wind speed and direction.

2. **Select CAL073 (the most northern aircraft currently in the PVD).**

3. **Try to place a waypoint in the PVD before CAL073 has entered the Dutch FIR.** Note that this is not possible.

4. Observe how the along-track wind displayed in the PVD is now altitude dependent. It shows the heavy winds at FL360 near the current radar position, while the wind at FL100 near ARTIP is shown. Take a moment to visualize the coupling between the wind fields shown in the VSD and PVD.

5. **Select KLM96F (located just south of CAL073).**

6. By hovering over the orange solution space in the PVD, you can see that is expected to run into conflict with MPH8142. **Select MPH8142 by clicking on the orange zone.**

7. Note that the aircraft will currently arrive too early at ARTIP, and that it cannot arrive any later when sticking to its current lateral path. You can quickly see this by inspecting the reachable ETA range in the TSD.

8. To ensure that MPH8142 is delayed, track miles will have to be added. **Try to place an intermediate waypoint with which MPH8142 will reach its EAT at ARTIP using the solution space in the PVD.**

9. Note that after doing so, the expected conflict with KLM96F has also been resolved.

10. **Resolve the remaining expected conflict using the interface.**

Part 2: Dynamic traffic

1. **Press the fast forward button on the top-right corner of the simulator above the TSD.** The simulator will start running at 4x speed (fast-time).

2. **Practice managing air traffic with the simulator running.**

3. You may continue to the next scenario when you feel comfortable with manipulating the route of the aircraft.

C-2-6 Practice scenarios

1. In the previous scenarios you have been shown all the tools and features that are available to you to in the experiment simulator. The following training scenarios are intended as practice, to increase your experience, and to make you feel comfortable with performing your task in this experiment.

2. In each scenario you are free to manipulate the trajectories of the aircraft to resolve any further conflicts during the remainder of the scenario. Try to minimize any delays at the sector exit point, and please try to avoid any losses of separation.

3. You may continue to the next scenario when all incoming aircraft have left the sector.

4. At the start of each scenario, press the fast forward on the top-right corner of the simulator above the TSD. The simulator will start running at 4x speed (fast-time).

Appendix D

Expert Questionnaires

As part of the case study, participants were asked to fill out two questionnaires. Firstly, a pre-questionnaire was given to obtain information on participants' current attitude towards future ATM and their own ATC preferences. The questions, answers and motivations for all participants are presented in Appendix D-1. To obtain detailed feedback on the designed interface, a post-questionnaire was presented following the runs. These questions, results and motivations are presented in Appendix D-2.

D-1 Pre-Questionnaire

Name: ....
Date: ....
Time: ....

Please indicate how much you agree with the following statements:

1. **Automation will change the way controllers operate within the next 10 years.**
   O Strongly disagree O Disagree O Neither agree nor disagree O Agree O Strongly Agree
   Please explain:..
   ....
   ....

   P1 (Agree): Smarter support functions will change the ATCo role from active to more monitoring. As well as increasing demands from the environment (rules, regulations). It will be with little steps, so not very much change in 10 years but the trend has started.

   P2 (Agree): I like as much relevant data as possible to make decisions. For example, at the moment I can't measure the distance between two aircraft.

   P3 (Strongly Agree): Conflict detection, conflict solution, No RT anymore.

P4 (Strongly Agree): In order to get more predictable traffic streams (and thus higher overall efficiency), automation will be playing a bigger role in the decision making process (supporting tools and partially taking decisions out controller's hands to minimize human interpretation/unpredictability (although 10 years is relatively short in aviation).

P5 (Agree): With traffic volumes increasing, the current way of working is reaching its limits. It will become necessary to add more technical support in order to deliver the required service levels. However, ATC is a conservative world and 10 years is a short time, so 'real' change will take longer.

P6 (Agree): New information to deal with.

2. **Automation can aid me in my control task.**
O Strongly disagree O Disagree O Neither agree nor disagree O Agree O Strongly Agree
Please explain:...
....
....

P1 (Agree): Take away unknown aspects of our work, more control over what aircraft are doing, automatic 'teamwork' between the controller and the pilot.

P2 (Agree): Simple tasks are more easily done by a computer, and save me time.

P3 (Strongly Agree): See question 1.

P4 (Strongly Agree): Machine learning/extrapolation can give great handholds in decision making.

P5 (Agree): A controller spends a lot of time doing things that can easily be automated: making certain inputs for example. Removing those tasks will lower workload, so more time can be spent on actual problem solving. I also believe better and more advanced information and support will help.

P6 (Agree): More info/help should be improved.

3. **It is important that a person (and not a computer) takes control decisions.**
O Strongly disagree O Disagree O Neither agree nor disagree O Agree O Strongly Agree
Please explain:...
....
....

P1 (Neither agree nor disagree): For now a person is the best alternative due to the unpredictable nature of the work. This will change when automation becomes smarter. Still, a human monitoring will always (?) remain.

P2 (Neither agree nor disagree): Both have their advantages and strong and weak points. Complex calculations vs. creativity for example.

P3 (Strongly disagree): In the end, it will be impossible for a human. The chess computer always beats the human nowadays. Caution: the transition period required maximum attention.

P4 (Strongly Agree): A computer is great at standard situations but the non-standard situations are the core of ATC.

P5 (Agree): As long as a controller is responsible for separation, I think it is important that they can at least have a large influence on control decisions.

P6 (Strongly Agree): Due to ethical issues, failures of the system, human brain is more creative.

4. **4D ATM will require new DST's tool ensure orderly traffic management.**
O Strongly disagree O Disagree O Neither agree nor disagree O Agree O Strongly Agree
Please explain:..
....
....

P1 (Agree): Better insight in consequences of actions is needed.

P2 (Agree): For 1 flight 4D ATM is very easy, but during an inbound peak it has to be more advanced.

P3 (Strongly Agree): -

P4 (Strongly Agree): With 4D the 'picture' is getting too big to oversee without additional info etc. In order to process / take into account all the info needed in a timely manner, extra tools are needed.

P5 (Strongly Agree): There currently is very little tooling that helps visualize or support time as the 4th dimension. As time is becoming more important, so does implementing new tools.

P6 (Agree): New tasks will need new tools.

5. **I believe that fixed arrival routes for all aircraft at EHAM from the IAF will be implemented within the next 10 years.**
O Strongly disagree O Disagree O Neither agree nor disagree O Agree O Strongly Agree
Please explain:..
....
....

P1 (Neither agree nor disagree): Yes, trials will be run and in stable situations it will be used for testing. But in any unpredictable (weather) or busy periods it will remain non-fixed.

P2 (Neither agree nor disagree): Depends on the capacity with those transitions.

P3 (Strongly Agree): Although not applicable with adverse weather.

P4 (Agree): The way forward to predictable traffic patterns.

P5 (Disagree): I do believe that fixed arrival routes will be used and implemented more and more, however I don't expect all aircraft to use them in the near future (or maybe the longer future). This is due to performance equipment and also unforeseeable issues such as weather of emergencies.

P6 (Neither agree nor disagree): It will probably take more time.

6. **I believe that the EAT at IAF can be met with a 30-second accuracy within the next 10 years.**

O Strongly disagree O Disagree O Neither agree nor disagree O Agree O Strongly Agree
Please explain:..
....
....

P1 (Agree): Change of mindset is needed (and a better wind-model!).

P2 (Agree): If the wind and descend profile are accurate, this could easily be done (and should be done).

P3 (Strongly Agree): It is already possible now. The next step is to take out the ATCo.

P4 (Strongly Agree): With the proper support and willingness, definitely!

P5 (Strongly Agree): I believe that right now in most cases we can already mee a higher accuracy. It will be a combination of culture, training and system support to further improve.

P6 (Agree): With new tools for sure.

7. **I believe that the EAT at IAF can be met with a 10-second accuracy within the next 10 years.**
O Strongly disagree O Disagree O Neither agree nor disagree O Agree O Strongly Agree
Please explain:..
....
....

P1 (Disagree): The information needed for that kind of accuracy always is not available in this time frame.

P2 (Agree): If the wind and descend profile are accurate, this could easily be done (and should be done).

P3 (Disagree): That will take some more time, especially to improve the FMS.

P4 (Neither agree nor disagree): Unsure, hard to imagine (especially within 10 years), but looking at current developments, automation and accuracy it probably will (only with limited human interaction though...).

P5 (Disagree): Even with very advanced system support, 10 seconds is very hard to achieve because of the dynamic nature of weather, pilot's behavior and aircraft performance.

P6 (Disagree): Too many unpredictabilities.

8. **A clutter-free screen is important to me when controlling air traffic.**
O Strongly disagree O Disagree O Neither agree nor disagree O Agree O Strongly Agree
Please explain:..
....
....

P1 (Agree): To get a clean overview of the traffic is important to keep control. All extra information should be available 'on demand'.

P2 (Strongly Agree): I only want to see relevant information.

P3 (Agree): But only if I have to take the decisions.

P4 (Strongly Agree): Clutter is distracting from the core business and therefore limiting capacity (brain busy filtering out useless info, potentially dangerous workarounds).

P5 (Agree): Clutter to me means non-relevant info, and logically I don't want non-relevant info. Furthermore, too much info in general (even relevant) can make instant decision making difficult and thus has a negative effect on performance.

P6 (Agree): Non-info raises the workload.

D-2 Post-Questionnaire

Name: ....
Date: ....
Time: ....

Please indicate how much you agree with the following statements:

1. **The air traffic control simulation resembles reality.**
   O Strongly disagree O Disagree O Neither agree nor disagree O Agree O Strongly Agree
   Please explain:...
   ....
   ....

   P1 (Agree): Descent paths, speeds are realistic.

   P2 (Neither agree nor disagree): Wind and trajectories are realistic, but descend paths are in reality way more variable.

   P3 (Neither agree nor disagree): Difficult to tell.

   P4 (Strongly Agree): Resembles daily inbound peak.

   P5 (Neither agree nor disagree / Agree): On the one hand, there is a realistic meteorological input. On the other hand, in reality there is much more uncertainty especially regarding a/c performance (ROC/ROD) + the SPD bracket in reality is much smaller.

   P6 (Strongly disagree): Not at all. The presentation is clear, but only in the perfect world.

2. **I was able to derive and execute my preferred strategy without being limited by the interface within the constraints set for the experiment.**
   O Strongly disagree O Disagree O Neither agree nor disagree O Agree O Strongly Agree
   Please explain:...
   ....
   ....

   P1 (Agree): To solve the conflicts with as little lateral movements as possible.

   P2 (Agree): It was easy to make every conflict green.

   P3 (Disagree): My strategy was influenced by the system.

P4 (Neither agree nor disagree): Bit difficult to read labels etc every now and then but overall fine.

P5 (Neither agree nor disagree): My preferred strategy is completely different form this system, but that is not due to faults in the interface, but because of the introduction of a completely different operational concept.

P6 (Agree): -

3. **I was controlling air traffic at a more strategic level than I am currently used to.**
   O Strongly disagree O Disagree O Neither agree nor disagree O Agree O Strongly Agree
   Please explain:..
   ....
   ....

   P1 (Agree): Starting the sequence already in MUAC airspace.

   P2 (Neither agree nor disagree): Usually I am planning ahead as far as I did in the simulation, but I didn't have to give any clearances.

   P3 (Strongly Agree): Very early corrections.

   P4 (Agree): Trying to make the times work, more than the usual sequencing.

   P5 (Strongly Agree): I barely looked at the lateral path or actual position of the aircraft, but managed the traffic almost completely based on times.

   P6 (Strongly disagree): There was no 'control' from my side. Just administration.

4. **It was easy to deliver the aircraft at their EAT.**
   O Strongly disagree O Disagree O Neither agree nor disagree O Agree O Strongly Agree
   Please explain:..
   ....
   ....

   P1 (Agree): The calculation of the EAT is very accurate, and one act was compensated automatically (dog leg $--$ $>$ speed increase).

   P2 (Strongly Agree): The wind had a high resolution, so the calculated time over ARTIP was accurate.

   P3 (Strongly Agree): If you trust the system!

   P4 (Agree): Bit hard to make the times with 5 seconds variation.

   P5 (Strongly Agree): The entire system focusses on aiming on the EAT, so the support makes it very easy.

   P6 (Agree): -

5. **It was easy to monitor and maintain separation between all aircraft.**
   O Strongly disagree O Disagree O Neither agree nor disagree O Agree O Strongly Agree
   Please explain:..
   ....

. . . .

P1 (Disagree): Had to have confidence in the system, no way to tell for myself if it would stay 5NM. Too far zoomed out.

P2 (Agree): I like the conflict calculation based on routing and speed.

P3 (Disagree): Could also be the scale. But I also used the probe/prediction system a lot. But around ARTIP, you have to trust the system.

P4 (Neither agree nor disagree): The green makes it easy but I fully rely on that instead of monitoring groundspeeds for example.

P5 (Neither agree nor disagree): On the one hand, as long as all labels stay green, there is no problem. On the other hand, the SPD behavior was not always as I expected, which resulted in more difficult problem solving. This is also due to experience if working in a different way.

P6 (Strongly disagree): More busy with administration.

6. **Usefulness per element**
For each element, please indicate its usefulness on a scale of 1 (not useful) to 5 (very useful)

   (a) **Wind visualization (across all displays)** Rating:. . . . . .
   Please explain: . . . .
   . . . .
   . . . .

   P1 (5): Much better understanding of the effect of the wind.
   P2 (2): -
   P3 (2): Nice for 1 time.
   P4 (2): Interesting but I tend not to use it often.
   P5 (3): It is nice to have, but I don't need it as long as I know the system will take the wind into account.
   P6 (1): Don't have to do anything with the info. The system is using the info.

   (b) **Solution spaces (across all displays)** Rating:. . . . . .
   Please explain: . . . .
   . . . .
   . . . .

   P1 (4): Could see clearly which solution was viable and how much deviation from the current path was needed.
   P2 (2): -
   P3 (4): Very easy to kee a safe and most efficient handling of traffic.
   P4 (5): Makes it easier to solve.
   P5 (4): On the radar screen, very useful and intuitive. In the time display less intuitive. Could also be because of the low-res screen.
   P6 (3): Not so easy to use.

(c) **Estimated time-over difference** Rating:......
Please explain: ....
....
....

P1 (5): Could easily tell the differences.

P2 (5): -

P3 (5): Necessary to fulfill the target time over control task.

P4 (3): Good info but hard to read.

P5 (5): Perfect for fine-tuning the EAT's.

P6 (5): Clearly presented.

(d) **Aircraft conflict indication** Rating:......
Please explain: ....
....
....

P1 (2): Looked promising, had to trust it to be able to manage traffic. Was surprised by a conflict at ATRIP at the last minute (was all the while green), just red seconds before ARTIP. This takes away faith/trust in the system.

P2 (4): -

P3 (4): Very nice to see it early. Definitely necessary in this concept.

P4 (5): Makes it easy to monitor/tell where conflicts will be.

P5 (5): Indicates where action is needed.

P6 (4): Clearly presented, grabs your attention.

(e) **Available ETO range at IAF (shown in TSD)** Rating:......
Please explain: ....
....
....

P1 (4): Good visualization.

P2 (2): -

P3 (4): Nice to see what is possible.

P4 (3): Good to know, but difficult to see/spot in this interface.

P5 (4): This was more intuitive than the Speed solution space.

P6 (4): Clearly presented.

7. **The estimated conflict probabilities drawn in the solution spaces helped me to estimate the consequence of my control actions.**
O Strongly disagree O Disagree O Neither agree nor disagree O Agree O Strongly Agree
Please explain:...
....
....

P1 (Agree): Used it to solve conflicts with minimal impact on the flights.

P2 (Neither agree nor disagree / Agree): Nice to see, could be helpful. For example, to solve a conflict sometimes a turn of 5 to 10 degrees is sufficient, but not always.

P3 (Agree): It does, but takes more time to keep situational awareness.

P4 (Agree): Easy to use but need a bit more experience to use it to its max potential.

P5 (Agree): Gives a good indication whether immediate action is required or if it's possible to only monitor.

P6 (Agree): It was clearly presented.

8. **The added situational awareness of the new display elements outweigh the added screen clutter.**
   O Strongly disagree O Disagree O Neither agree nor disagree O Agree O Strongly Agree
   Please explain:..
   ....
   ....

P1 (Agree): The clutter when there was no conflict was minimal. With conflicts, it was helpful.

P2 (Neither agree nor disagree): If it was up to me, I don't want to see it when there isn't a conflict. The wind only on request. Time window was nice, better than the stacklist in AAA.

P3 (Disagree): Could also be the scale: but it feels uncomfortable not to be able to se all the information especially around ARTIP where the aircraft are flying close together.

P4 (Neither agree nor disagree): It's good some things can be turned off.

P5 (Agree): I agree, but there are important side notes. The AC need to behave more predictable than today. It should be possible to direct traffic as shown.

P6 (Disagree): But the info was needed.

9. **The proposed visualization elements could make the air traffic control task easier.**
   O Strongly disagree O Disagree O Neither agree nor disagree O Agree O Strongly Agree
   Please explain:..
   ....
   ....

P1 (Agree): Would have to take into account more types of flights and factors, but promising.

P2 (Agree): Conflict alert and solution, and time window (vertical presentation).

P3 (Agree): TSD: I think only the Y-axis is useful.

P4 (Agree): If balanced properly (right info and no clutter).

P5 (Agree): Yes, but the entire way of working will have to change, since the controller will base decisions much more on system predictions.

P6 (Agree): The (integration of) wind info is very useful.

10. **With further research, (part of) this interface should be implemented in the future.**
O Strongly disagree O Disagree O Neither agree nor disagree O Agree O Strongly Agree
Please explain:...
....
....

P1 (Agree): -

P2 (Agree): See above.

P3 (Strongly Agree): But: without an ATCo, or with different responsibilities.

P4 (Agree): Hopefully!

P5 (Agree): In order to increase performance, system support is necessary. I think this system certainly has potential.

P6 (Agree): It's the future. But not all of it :) Wind is very useful. Conflict detection is very useful, but more on the background.

11. **When looking at the pre-questionnaire again, would you want to change any answer or rating given after performing this experiment?**
P1:-

P2:-

P3:-

P4:-

P5:-

P6:-

12. **If you have any further remarks, please state them below.**
P1:-

P2: The cleared and current flight level is just as important as the routing and speed in conflict detection.

P3:-

P4:-

P5:-

P6:-

Appendix E

Case Study Control Strategies

Next to the presented result data in the Master of Science thesis paper, an analysis of every participant's applied strategy throughout the case study was performed. This has been done through observations, direct participant feedback and by tracking mouse activity.

E-1 Participant 1

P1 often removed the entry Change-Over Point (COP) as a way to solve conflicts at the Flight Information Region (FIR) boundary as a first step. Then, speed control was applied to correct for any occurring RTA deviation and small course corrections were applied to minimize conflict probability. If course corrections alone were not sufficient, a different FL over ARTIP was used. The wind information was used only once at the beginning of every run to get a feel for the present wind field. P1 was very quick in noticing the geographic location of present wind prediction errors and proactively adjusted arrival time in response to this.

The mouse heatmaps for all scenarios of this participant are shown in Figures E-1 to E-4. As can be seen, mouse activity focusses around the entry COPs in the PVD and the vertical axis in the TSD. When adjusting trajectories in the TSD, the last waypoint (located *on* the timing axis) was often used instead of the aircraft label (located *to the right of* the timing axis). The reason for this was the difficulty in selecting the aircraft label when aircraft were located close together on the TSD, causing overlapping labels.

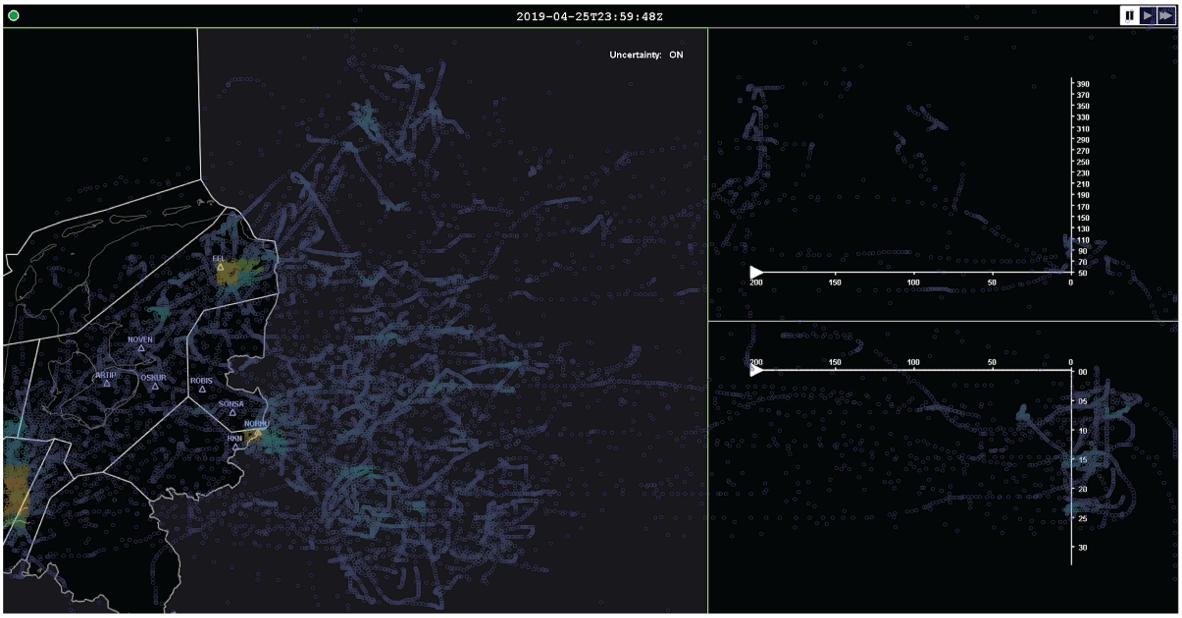

Figure E-1: Heatmap of mouse activity on the interface of P1 in Scenario 1

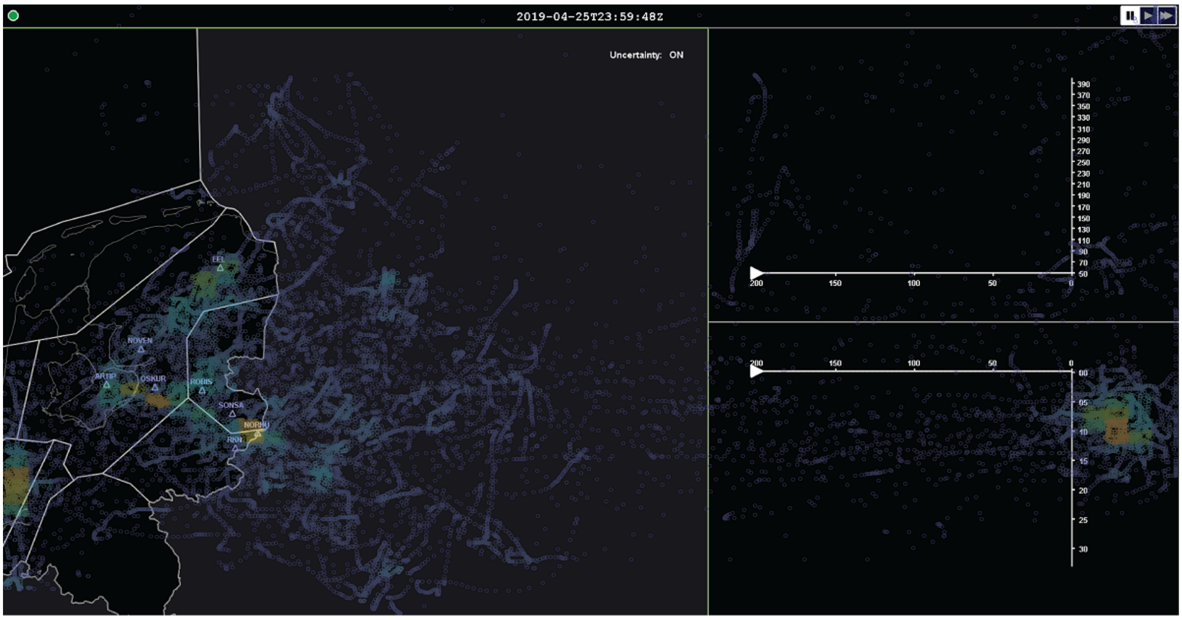

Figure E-2: Heatmap of mouse activity on the interface of P1 in Scenario 2

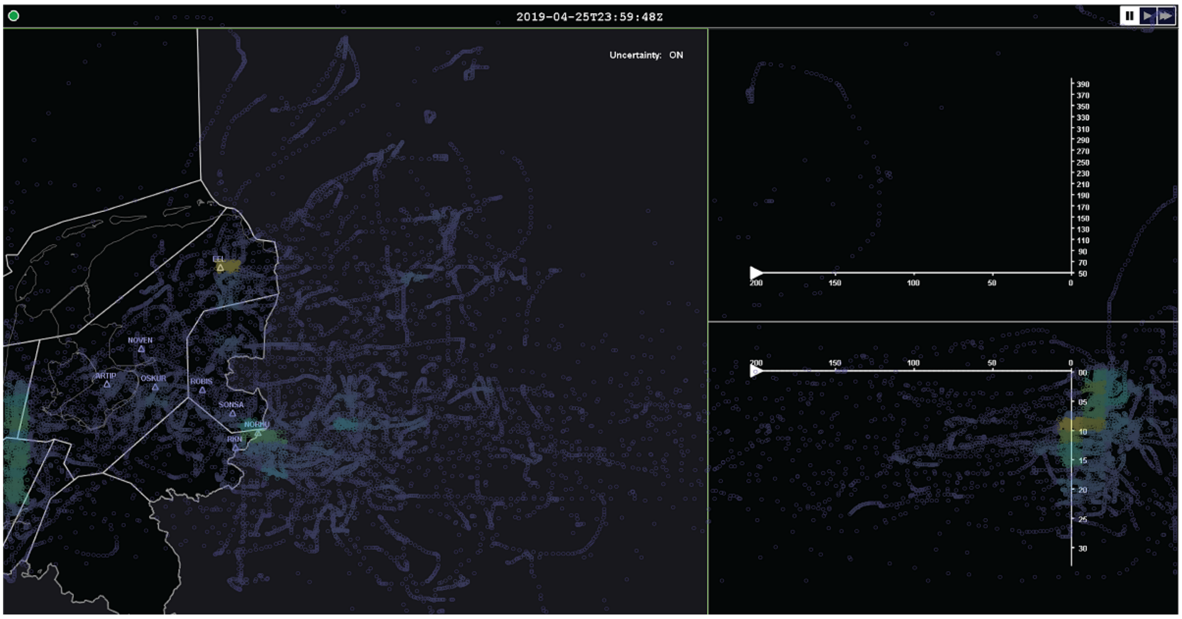

Figure E-3: Heatmap of mouse activity on the interface of P1 in Scenario 3

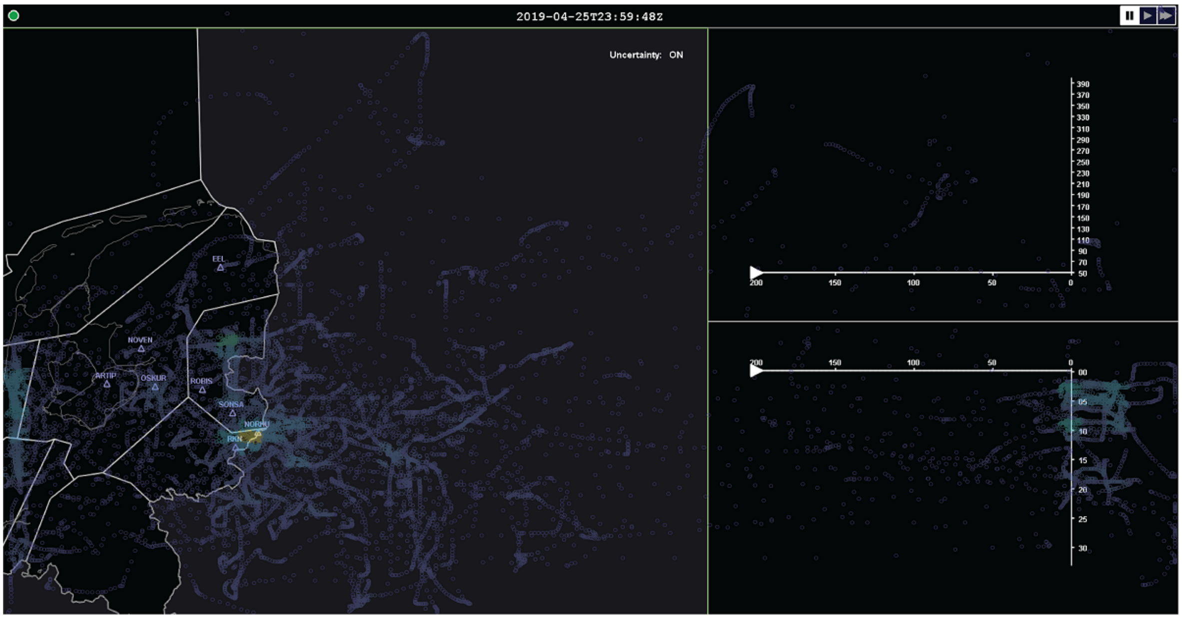

Figure E-4: Heatmap of mouse activity on the interface of P1 in Scenario 4

E-2 Participant 2

In managing air traffic, P2 mentioned the primary strategy was to '*make everything green as early as possible*'. P2 often removed the entry COP to structure the incoming traffic to ARTIP, solving any expected conflicts with more than 5% conflict probability immediately afterwards. After initial structuring, aircraft arrival times were managed on the TSD to minimize the RTA deviation. If any conflict near ARTIP would be predicted, a FL adjustment would be applied to resolve this. To get a prediction on future aircraft positions, the time slider feature (projecting aircraft positions along the nominal predicted path in time) was used frequently.

The mouse heatmaps for all scenarios of this participant are shown in Figures E-5 to E-8. Mouse movements concentrate around the entry COPs and the timing axis in the TSD. Furthermore, the heavy time slider usage can be noticed.

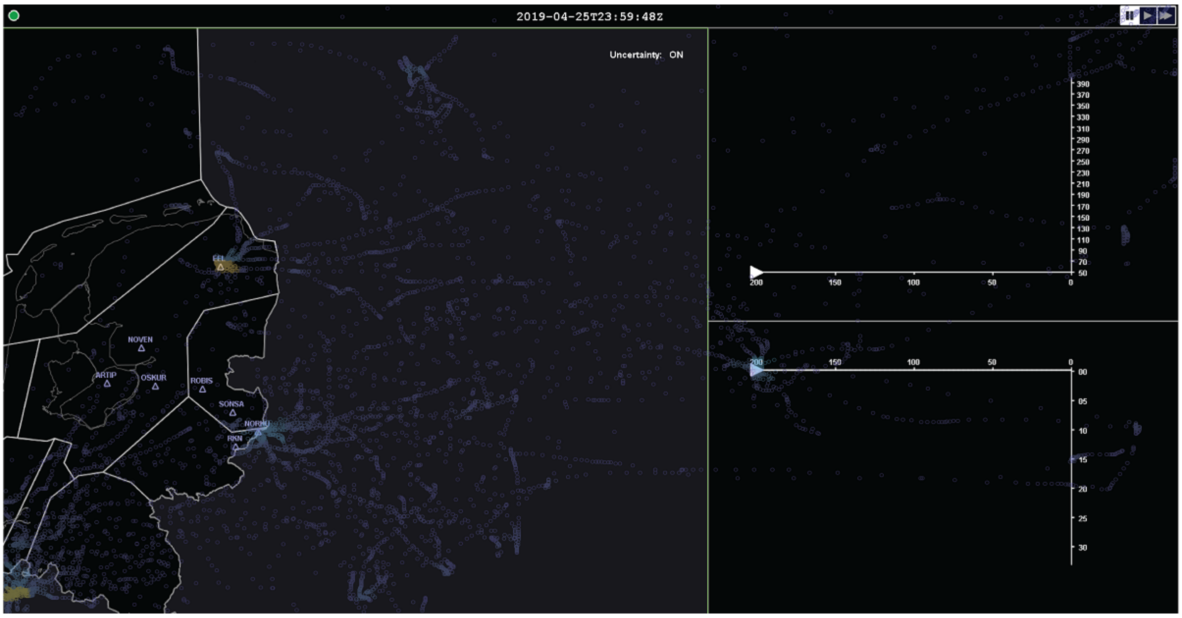

Figure E-5: Heatmap of mouse activity on the interface of P2 in Scenario 1

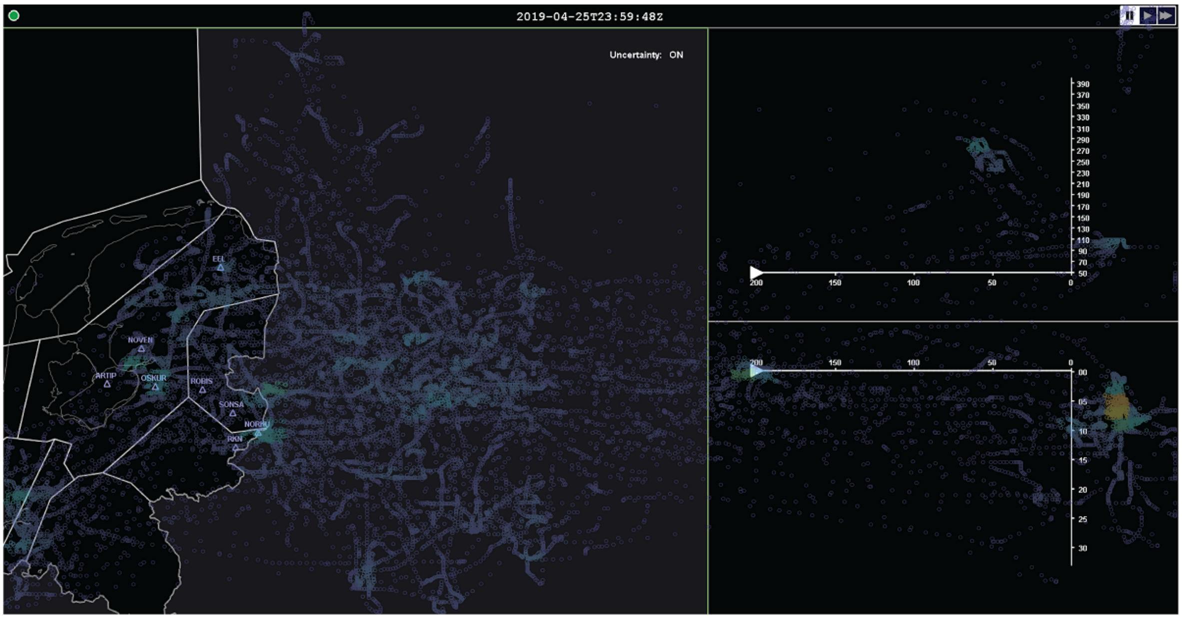

Figure E-6: Heatmap of mouse activity on the interface of P2 in Scenario 2

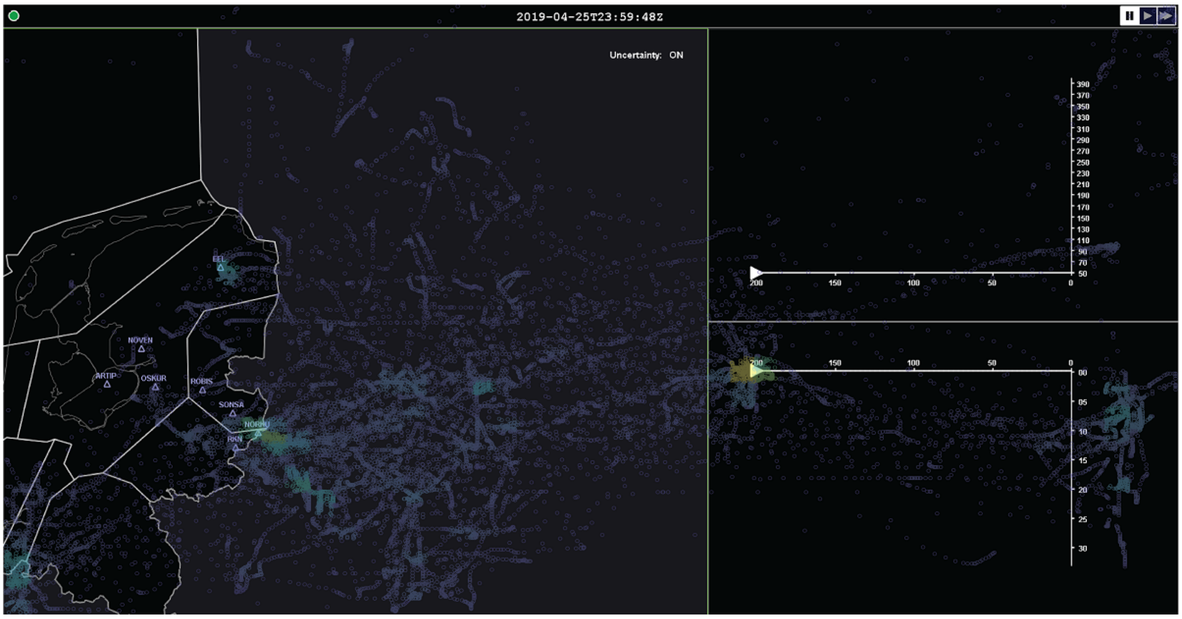

Figure E-7: Heatmap of mouse activity on the interface of P2 in Scenario 3

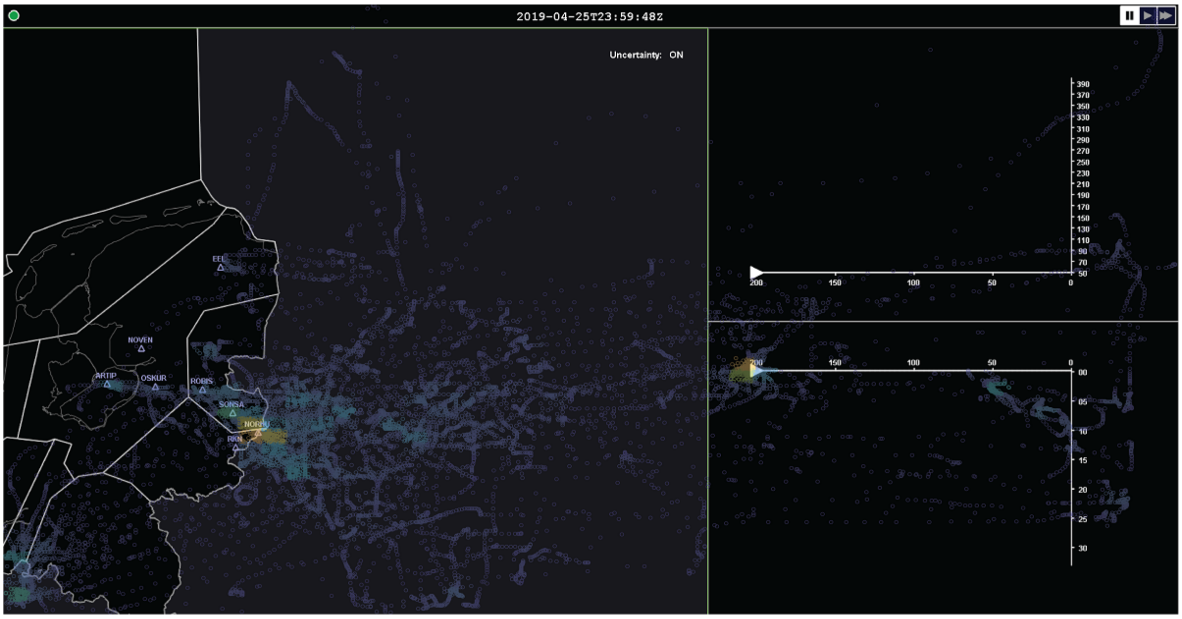

Figure E-8: Heatmap of mouse activity on the interface of P2 in Scenario 4

E-3 Participant 3

In initial air traffic structuring, P3 often removed the entry COP. P3 mentioned that this strategy was seen as 'front loading' to increase the control space around ARTIP. After this, conflicts were managed primarily on the PVD. To do this, the uncertainty toggle was used frequently to assess the nature of the predicted conflict in combination with the time slider feature on the TSD. As a result, predicted conflicts were often not resolved immediately, because P3 wanted to see how the situation would evolve. When workload allowed, aircraft arrival times were managed. P3 would ‘accept’ a 5-second delay, correcting the RTA deviation only if it was 10 seconds or larger. Vertical trajectory modifications were only made when two aircraft had similar times at ARTIP.

The mouse heatmaps for all scenarios of this participant are shown in Figures E-9 to E-12. Frequent entry COP removal and time slider usage can be noticed on all of these, confirming the observations.

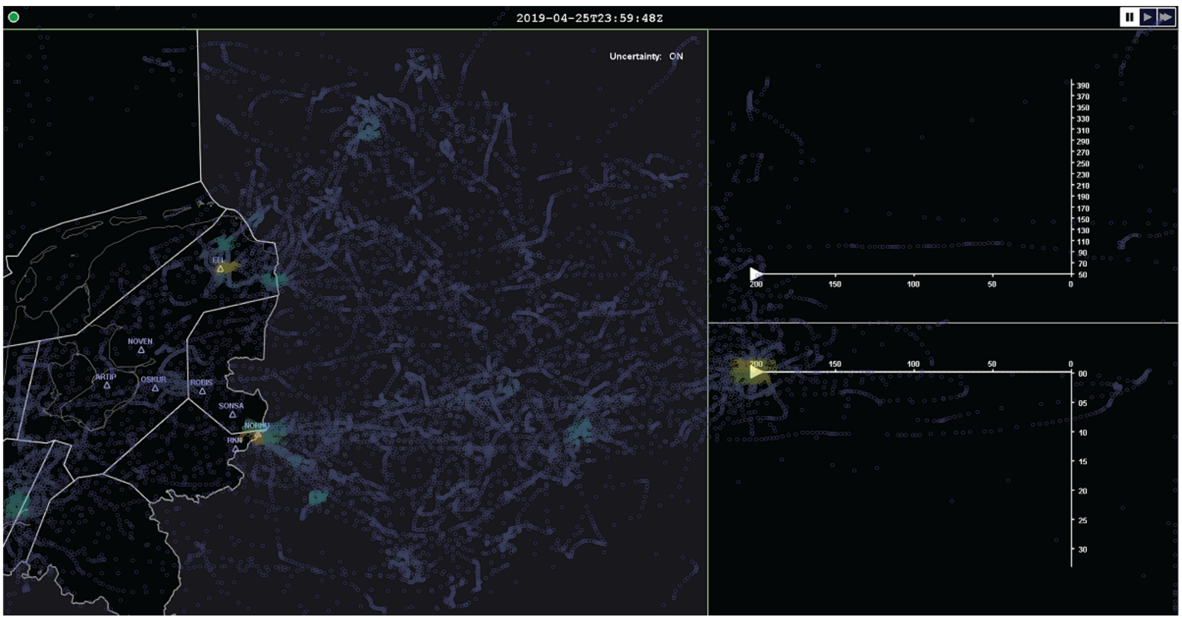

Figure E-9: Heatmap of mouse activity on the interface of P3 in Scenario 1

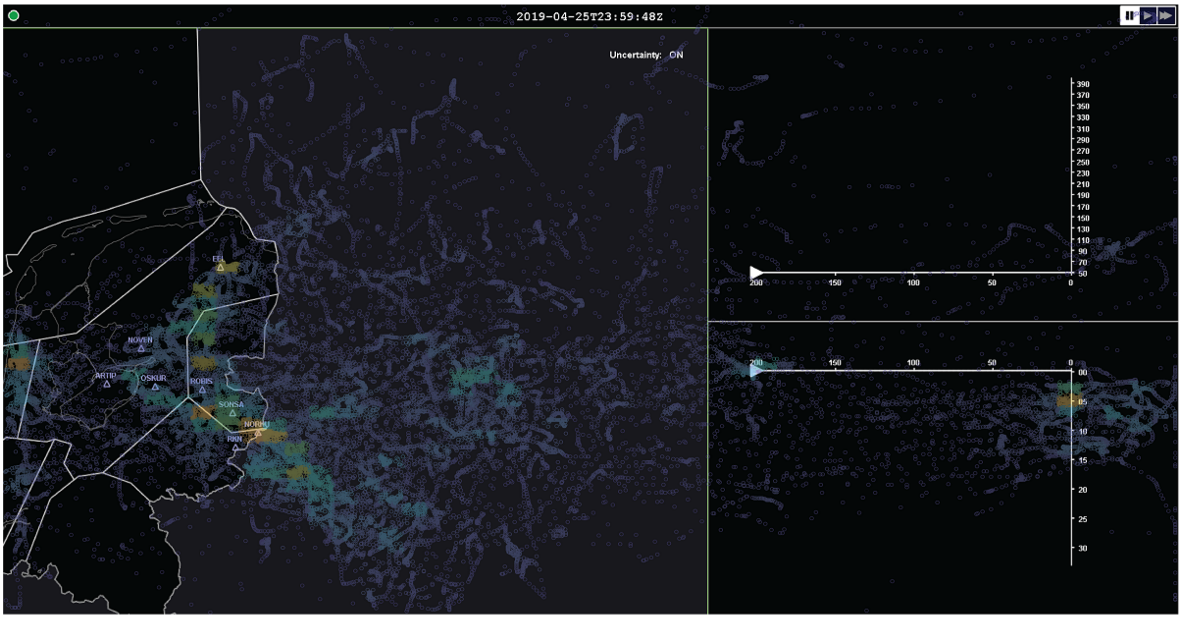

Figure E-10: Heatmap of mouse activity on the interface of P3 in Scenario 2

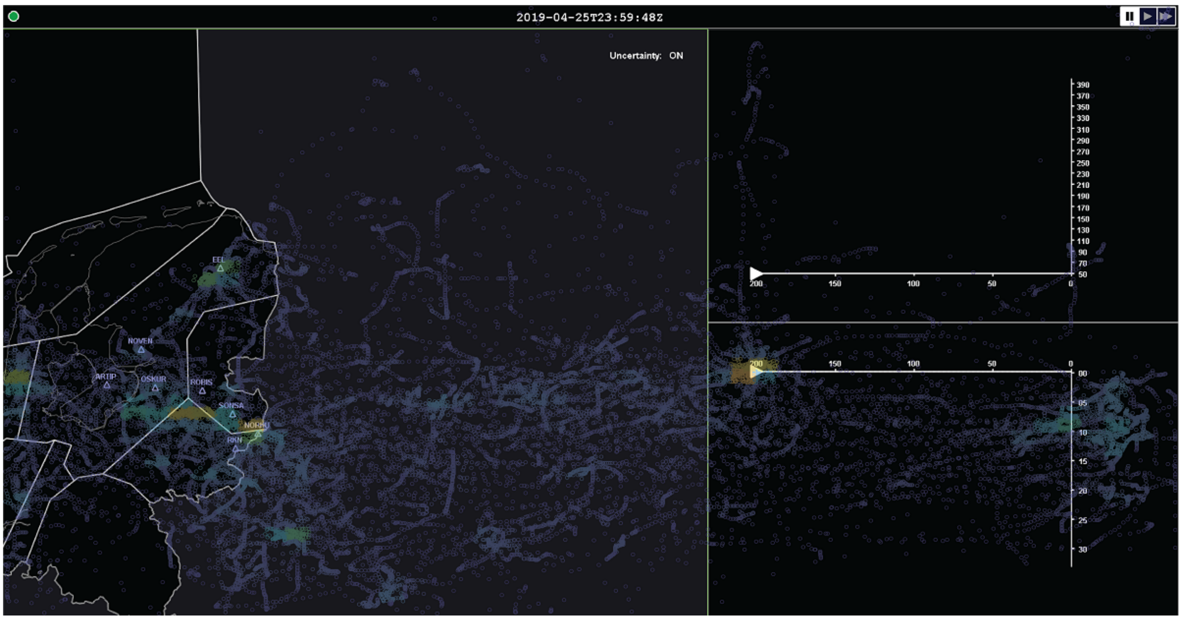

Figure E-11: Heatmap of mouse activity on the interface of P3 in Scenario 3

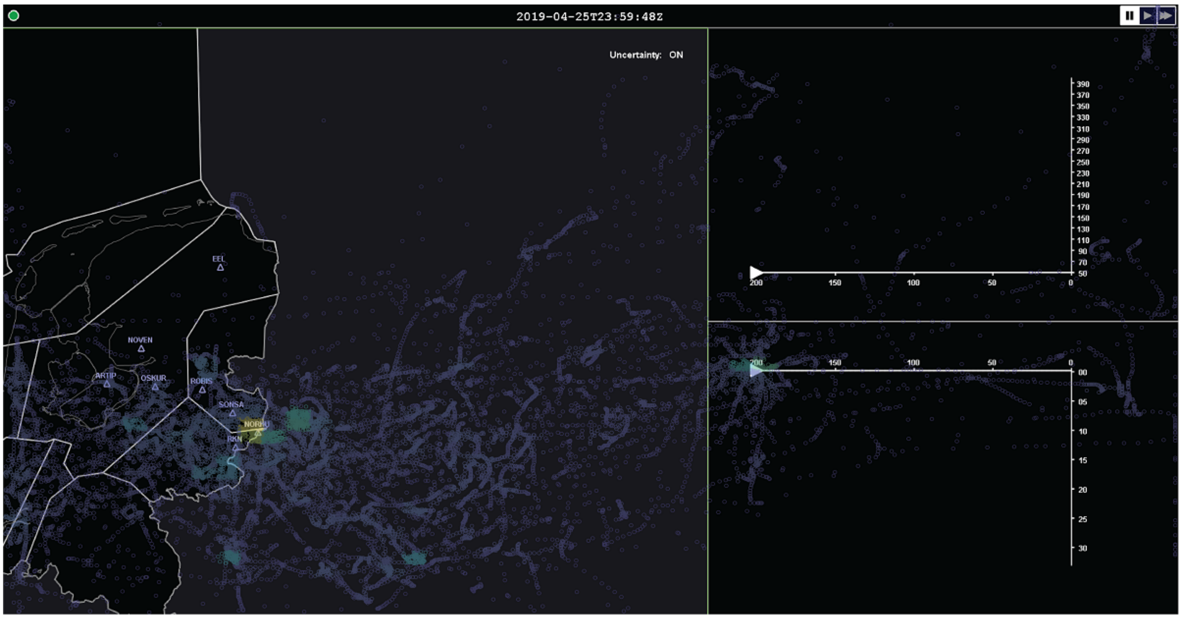

Figure E-12: Heatmap of mouse activity on the interface of P3 in Scenario 4

E-4 Participant 4

In initial air traffic structuring, the entry COP was frequently removed, managing conflicts and arrival times afterwards. Maintaining separation was prioritized over managing arrival times. P4 repeatedly reported difficulties in controlling traffic around ARTIP due to poor readability and the small screen. P4 had some difficulties with the combined speed and route resolutions imposed by the interface, applying common practice lateral sequencing solutions in using the PVD. These solutions did not work, as selecting intermediate waypoint locations in the PVD implied a corresponding velocity increase to meet the RTA, rendering the 'sequencing' action unsuccessful. P4 reported recognizing this 'thinking error' and acted accordingly in subsequent runs by resolving these situations using vertical separation at ARTIP. The TSD was used for ETA management when time allowed. To judge the nature of the predicted conflicts, P4 frequently made use of the uncertainty mode toggle.

The mouse heatmaps for all scenarios of this participant are shown in Figures E-13 to E-16. Frequent COP removal and time slider usage can be noted. Furthermore, the reported tactical conflict management around ARTIP can clearly be seen in Scenario 2, with much mouse activity in this region.

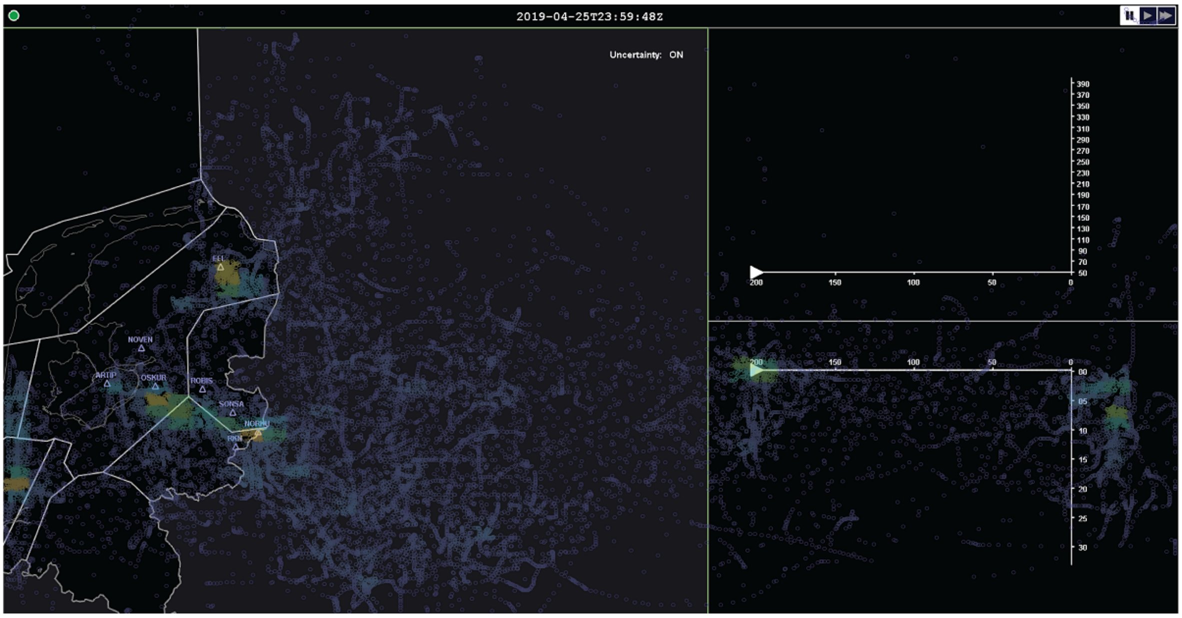

Figure E-13: Heatmap of mouse activity on the interface of P4 in Scenario 1

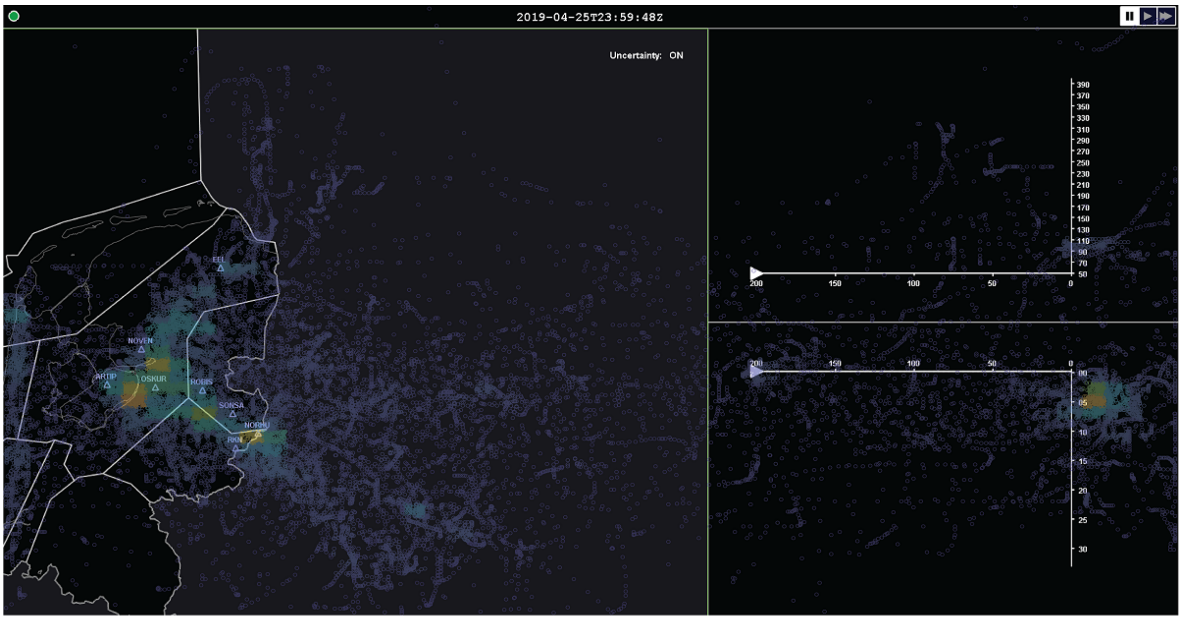

Figure E-14: Heatmap of mouse activity on the interface of P4 in Scenario 2

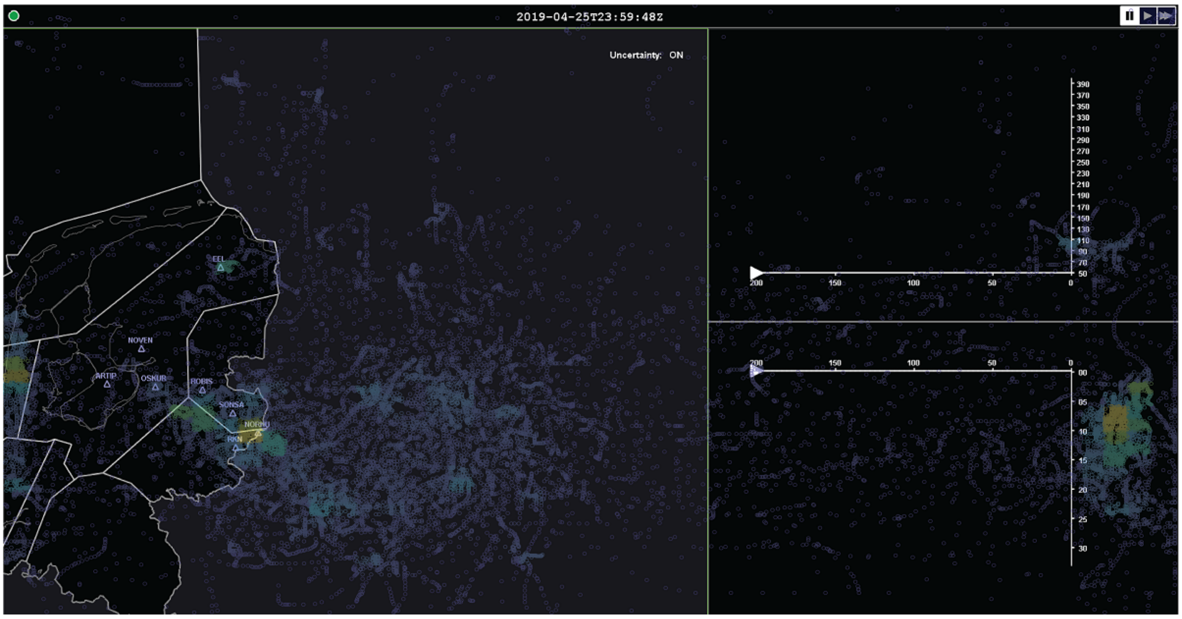

Figure E-15: Heatmap of mouse activity on the interface of P4 in Scenario 3

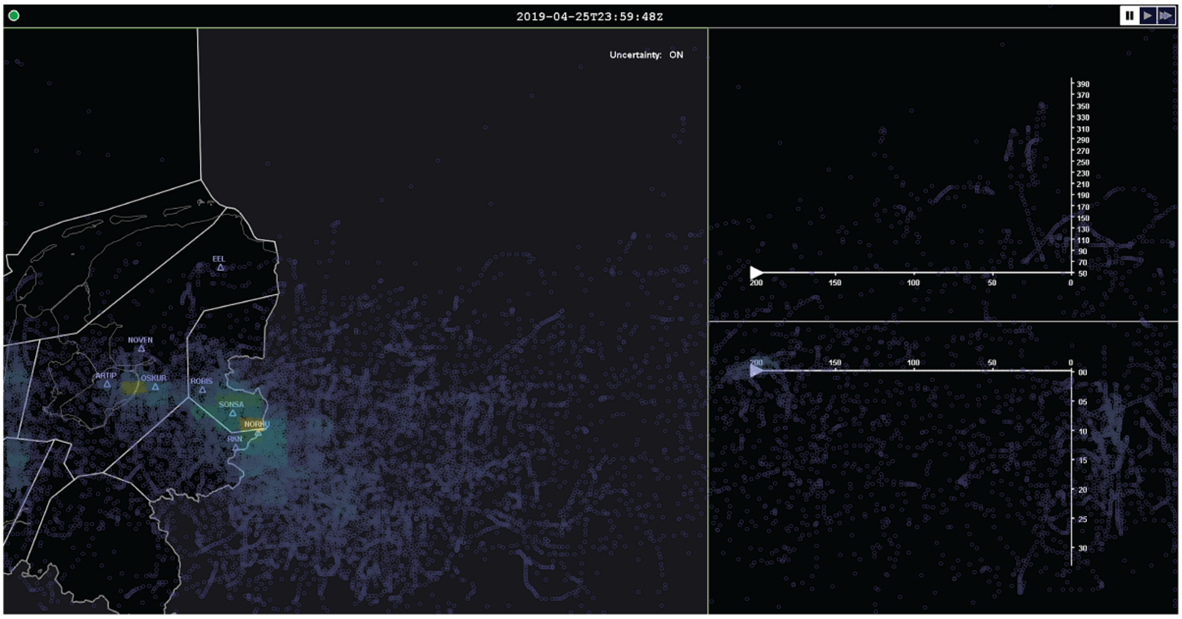

Figure E-16: Heatmap of mouse activity on the interface of P4 in Scenario 4

Appendix F

Interface Code

This appendix contains a comprehensive description of the software used in the case study. This starts with an overview of the JCS Master software package, a collaborative effort of Rolf Klomp, Clark Borst, Rick Riegman and the author, in Appendix F-1. The TP and dynamic wind visualization algorithms are discussed in detail in Appendices F-2 and F-3, respectively. A detailed explanation on the computation of the various solution spaces can be found in Appendix F-4. Lastly, the verification and (where possible) validation of the interface code is discussed in Appendix F-5. It should be noted that, due to the size of the framework, this overview is not all-encompassing. Rather than that, it aims to clarify the software for those unfamiliar with the simulator. A full copy of all relevant software, used scenario and traffic data can be found on `https://gitlab.tudelft.nl/clarkborst/thesis-matthijs`.

F-1 JCS Master Overview

The full integrated software package is built around several modules. In this section, a complete package overview is given in Appendix F-1-1, followed by a description of the rationale behind the top-level software packages in Appendix F-1-2. Lastly, the main workflow of the program is briefly discussed in Appendix F-1-3.

F-1-1 Package Overview

A complete overview of the Java package is given in Figures F-1 and F-2. Edited classes with respect to the baseline are shown in red. For a detailed overview on all made modifications, the reader is referred to the git repository listed in the beginning of this appendix.

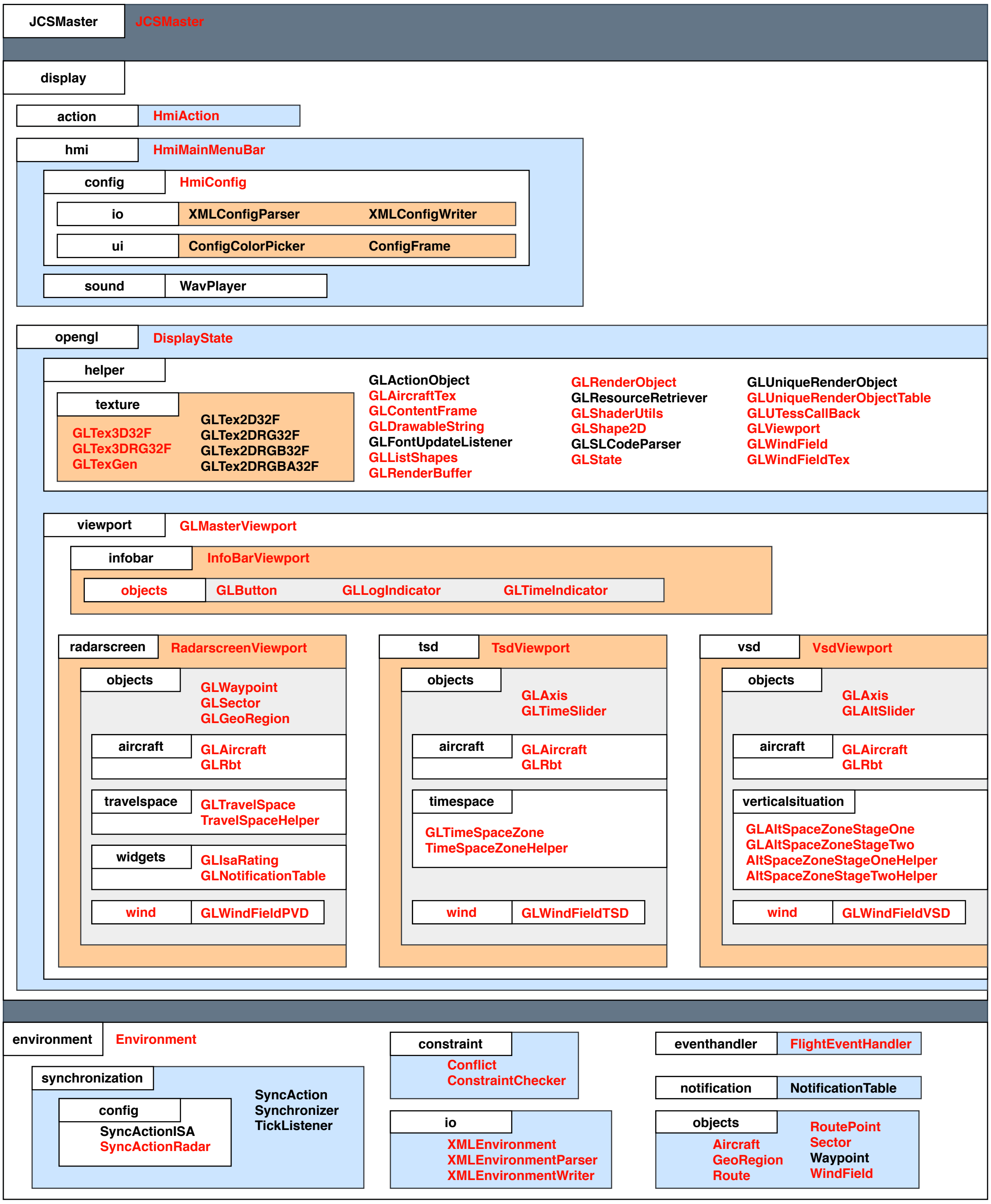

Figure F-1: Java package structure of the interface code (1/2)

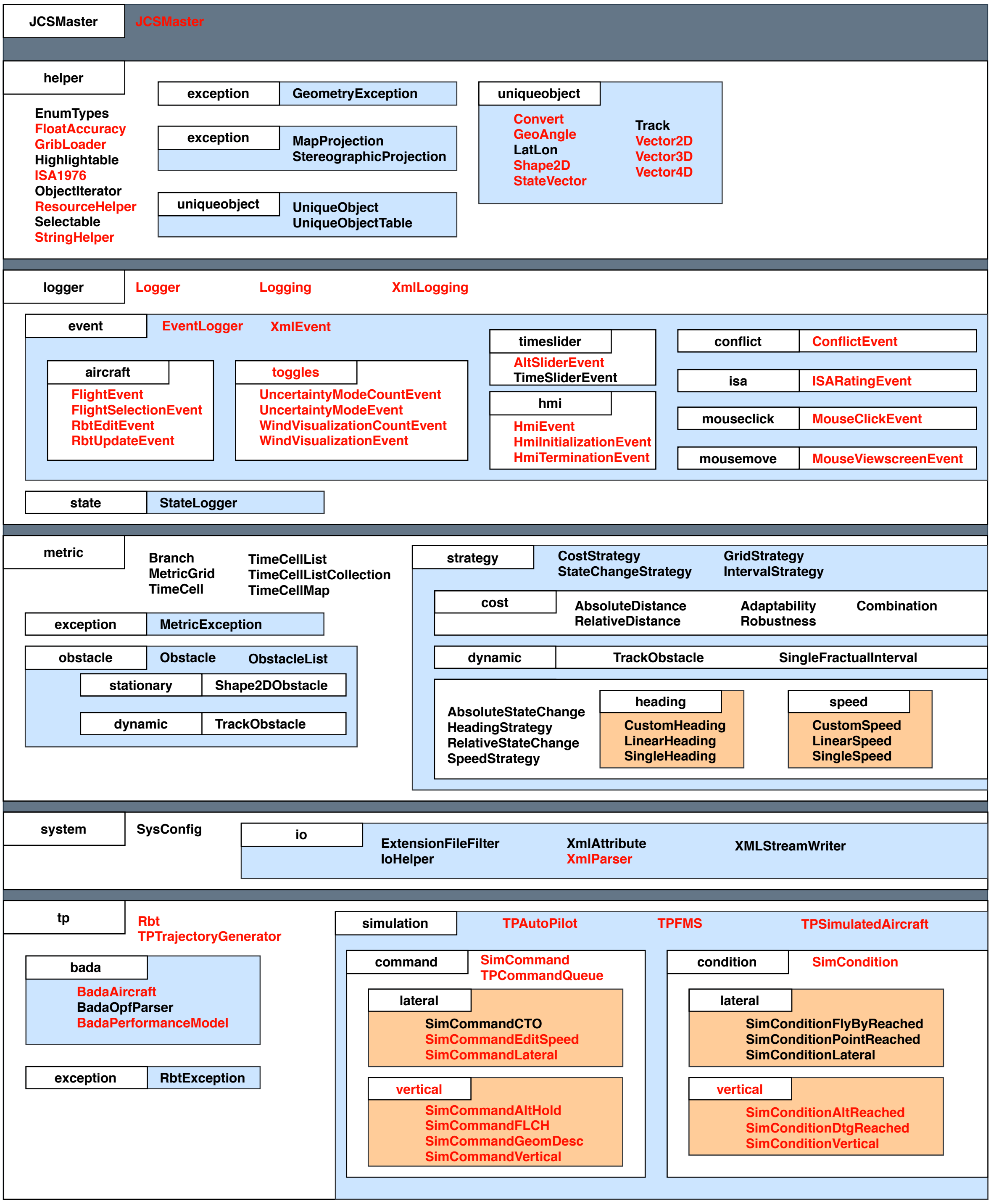

Figure F-2: Java package structure of the interface code (2/2)

F-1-2 Software Package Rationale

- **environment** The software is centered around the environment package. Here, all required items for the simulation are present. These items are initiated when a scenario is loaded. Responsibilities:
  - Storage of all objects in needed for simulation
  - Conflict detection for all aircraft
  - Trajectory modification handling
  - Synchronization of software
- **helper** Support for various parts of the software package:
  - Multi-dimensional vector calculations
  - Map projections
  - Unit conversions
  - Atmospheric calculations (needed in TP process)
  - GRIB file read-in
- **display** Everything that needs to be rendered to the display is located in this package. Some objects here are the 'display' counterparts of already existing objects in the environment package. In this package, all connections to the custom-written graphics shaders are made. Responsibilities:
  - Rendering of all simulation objects to display
  - Display state handling
  - Texture generation and storage
  - Communication of relevant data to custom-written shaders for solution space rendering
- **tp** Support for the trajectory prediction process of all *Aircraft* objects in the environment. Responsibilities:
  - Storage of BADA performance models
  - Autopilot and FMS implementation
  - Generation of trajectory state data
- **logger** All data logging is handled within this package. This includes the collection of relevant data as well as its output to XML file format.
- **system** Low-level support package for system configuration to ensure proper functionality of the simulation across multiple operating systems.
- **metric** This package stores autonomous decision-making algorithms that can be employed as a substitute for the human controller. It has been developed as part of the PhD thesis of Rolf Klomp and has not been modified not used in this MSc thesis project.

F-1-3 Workflow

When initializing the simulation package, several libraries are initialized. All custom written shaders to generate the required on-screen visualizations are compiled, linked and validated. Furthermore, the BADA performance model used for TP processing is initialized, creating an APM for each of the aircraft present in the database.

The simulator configuration is highly flexible in terms of not only appearance, but also functionality. At startup, all relevant parameters are passed using a config file. At any point in time, the configuration of the simulator can be edited using an interactive menu.

Upon loading a scenario, all relevant objects are loaded into the simulator. While most objects are trivial, the *Windfield* and *Aircraft* object are explained here in more detail:

- The type of wind field to be loaded in the scenario is specified in the config file. This ranges from a constant wind field (i.e., wind direction and magnitude only) to a fully dynamic 4D GRIB file structure. Regardless of the wind field type, the *Windfield* object returns the wind vector at the desired 4D location in the simulation by making use of polymorphism.
- When an aircraft is loaded, multiple TP processes are initiated. A ground-based TP is executed using only the information available on the ground (e.g., predicted wind). An FMS-based TP determines the actual trajectory the aircraft will fly if left unattended. When running the simulation, the ground-based TP process is repeated with every radar update to renew predictions on RTA deviation and future conflicts with other aircraft. A third TP process is used to preview the result of a yet to be confirmed trajectory modification.

F-2 Trajectory Predictor

Trajectory prediction forms an essential part of the simulation. Essentially, the TP process consists of estimating the resulting list state vectors, given a set of initial conditions and target route points using a specified APM.

Every simulated aircraft has a lateral and vertical command queue, which is built up and executed to fly the desired trajectory, based on specified route points. Since lateral and vertical motion cannot be fully decoupled, the inner TP algorithm is an iterative process, which is shown in Figure F-3. Roughly, the algorithm works as follows:

1. Estimate the DTG for a given route with constraints
2. Build 4D route point list, based on constraints
3. Build lateral command queue
4. Build vertical command queue
5. Run the simulation and record actual distance flown

6. Converge algorithm until the difference between the estimated DTG and actual distance is below a set threshold.

Wrapped around this is a binary search algorithm to converge the waypoint timing of the trajectory. Because the BADA model is present within the inner TP algorithm only, unreachable constraints will automatically be handled correctly.

In user interaction with an aircraft's trajectory, its route point list or timing constraints are altered and the algorithm shown in Figure F-3 is run. This all happens in real-time without any noticeable delay to the user.

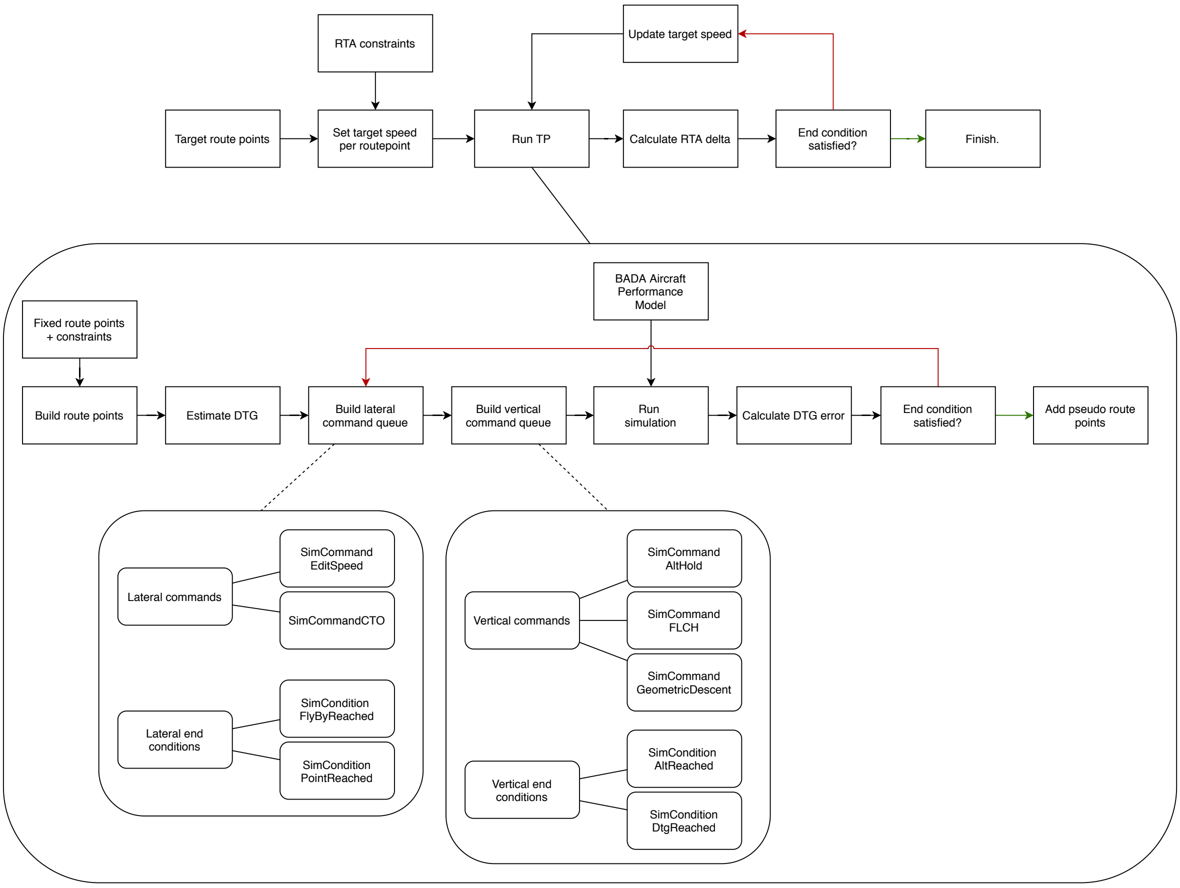

Figure F-3: TP workflow

F-3 Wind Visualization

To enable the dynamic visualization of the wind fields, heavy use is made of the Graphics Processing Unit (GPU). The algorithm used is based on an open-source project [1]. Multiple graphics textures are used to store information at various stages in the visualization loop. The workflow of the algorithm is shown in Figure F-4 and can be roughly summarized as follows:

[1] `https://blog.mapbox.com/how-i-built-a-wind-map-with-webgl-b63022b5537f`

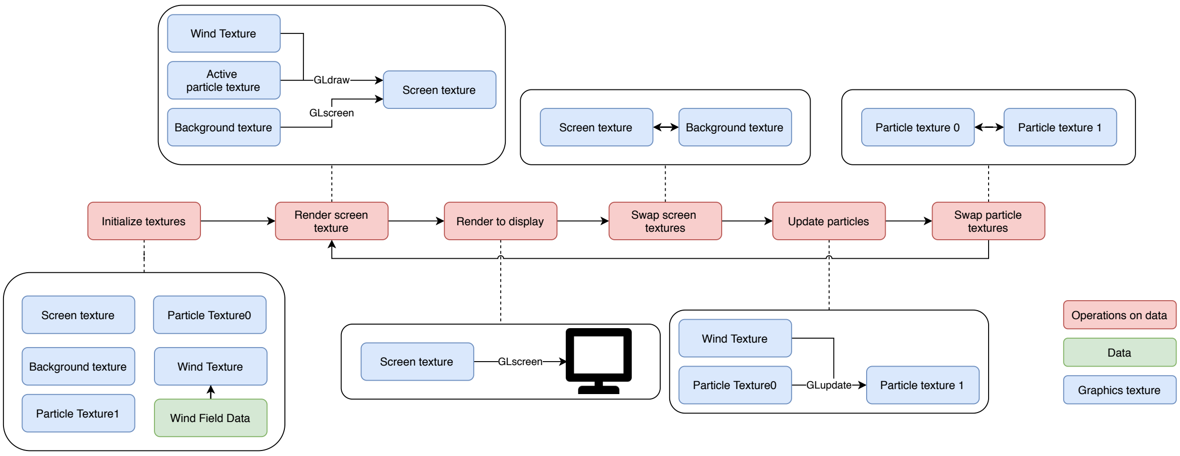

Figure F-4: Dynamic wind visualization workflow

1. Initiate an array of random particle positions on the screen and draw the particles, coloring them based on their velocity.

2. For every particle, obtain the wind velocity vector at that specific position, and move the particle accordingly.

3. Reset a small portion of the particles to a random position (to make sure that areas where the wind blows away from will not become fully empty).

4. Fade the current screen slightly, and draw the next screen on top. This creates the particle trails.

Particle positions are stored in two separate textures that are continuously swapped frame-by-frame to update the particle positions accordingly. To obtain the wind data from a 4D grid, multiple 3D textures are used, where each 3D texture contains the wind information at a moment in time. Linear interpolation in all four dimensions is used to obtain wind information between the 4D grid points.

F-4 Solution Space Computation

To render the solution spaces for every display, the GPU is used. A relatively course TP-process is done on a pixel basis to determine the color of that specific pixel. The colors of all pixels together determine the shape of the rendered solution space. This workflow is displayed in Figure F-5.

To increase computational efficiency, solution spaces itself are rendered to a texture, which is in turn rendered to the screen at 60 frames per second. The contents of this texture are renewed only with a radar update or with user interaction.

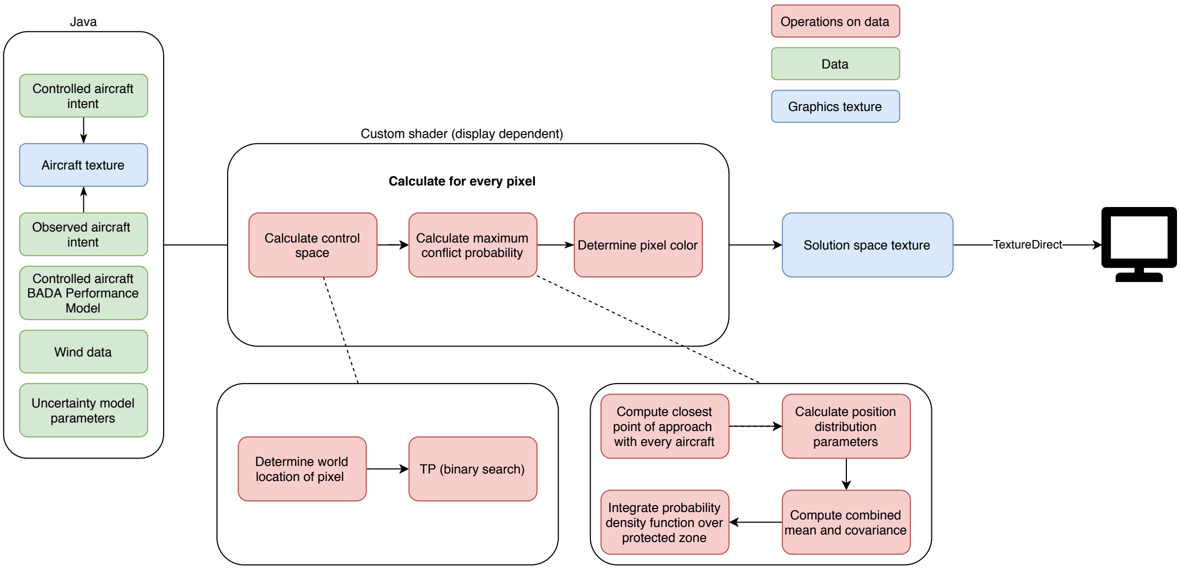

Figure F-5: Simplified workflow of solution space rendering

F-5 Software Verification & Validation

Verification of the software package is done on multiple levels. Besides continuous sanity checks when interacting with the simulator, several low-level packages have been unit-tested extensively using the Junit testing framework with parametrized inputs:

- complete TP package
- complete helper package
- complete environment package

The imported GRIB data and solution spaces for every screen have been verified using a separate software package in MATLAB. Furthermore, several software parts have been verified within the simulation itself. The fact that the TP and solution space calculation processes are completely decoupled allows for one to be used in the verification of the other. To illustrate, clicking outside the PVD solution spaces should form a trajectory where the RTA cannot be reached anymore. Therefore, ‘probing’ the interface shows if the TP process is carried out correctly.

Bibliography

Airbus Customer Services. (2002). *Getting to Grips with Aircraft Performance.* Retrieved from https://www.skybrary.aero/bookshelf/books/2263.pdf

Bainbridge, L. (1983). Ironies of Automation. *Automatica*, *19*(6), 775–779. doi: 10.1016/0005-1098(83)90046-8

Bekier, M., Molesworth, B. R. C., & Williamson, A. (2012, feb). Tipping Point: The Narrow Path Between Automation Acceptance and Rejection in Air Traffic Management. *Safety Science*, *50*(2), 259–265. doi: 10.1016/j.ssci.2011.08.059

Billings, C. E. (1996). *Human-Centered Aviation Automation: Principles and Guidelines* (Technical Memorandum 110381). Moffett Field, California: NASA. Retrieved from https://ntrs.nasa.gov/archive/nasa/casi.ntrs.nasa.gov/19960016374.pdf

Borst, C. (2019). *Supervisory Control & Cognitive Systems: Cognitive Work Analysis AE4318.* Delft, The Netherlands: Delft University of Technology.

Borst, C., Flach, J. M., & Ellerbroek, J. (2015, apr). Beyond Ecological Interface Design: Lessons From Concerns and Misconceptions. *IEEE Transactions on Human-Machine Systems*, *45*(2), 164–175. doi: 10.1109/THMS.2014.2364984

Borst, C., Mulder, M., & Van Paassen, M. M. (2010). A Review of Cognitive Systems Engineering in Aviation. *IFAC Proceedings Volumes*, *43*(13), 221–226. doi: 10.3182/20100831-4-FR-2021.00040

Casado Magaña, E. J. (2016). *Trajectory Prediction Uncertainty Modelling for Air Traffic Management* (Doctoral dissertation, University of Glasgow). Retrieved from http://theses.gla.ac.uk/7700/

Casado Magaña, E. J., Civita, M. L., Vilaplana, M. A., & McGookin, E. W. (2017, sep). Quantification of Aircraft Trajectory Prediction Uncertainty using Polynomial Chaos Expansions. *2017 IEEE/AIAA 36th Digital Avionics Systems Conference (DASC), St. Petersburg, Florida*. doi: 10.1109/DASC.2017.8102052

Casado Magaña, E. J., Goodchild, C., & Vilaplana, M. A. (2012). Identification and Initial Characterization of Sources of Uncertainty Affecting the Performance of Future Trajectory Management Automation Systems. *Proceedings of the 2nd International Conference on Application and Theory of Automation in Command and Control Systems, London, United Kingdom*, 170–175. Retrieved from https://dl.acm.org/citation.cfm?id=2325699

Chaloulos, G., & Lygeros, J. (2007, nov). Effect of Wind Correlation on Aircraft Conflict Probability. *Journal of Guidance, Control, and Dynamics*, *30*(6), 1742–1752. doi: 10.2514/1.28858

Cole, R. E., Green, S. M., Jardin, M., Schwartz, B. E., & Benjamin, S. G. (2000). Wind Prediction Accuracy for Air Traffic Management Decision Support Tools. *3rd USA/Europe Air Traffic Management Research and Development Seminar, Napoli, Italy*. Retrieved from `https://pdfs.semanticscholar.org/3454/dd6757179ffb6296045908321f8bfe1c52f7.pdf?_ga=2.208953937.2105562205.1560504915-774888368.1560504915`

Cui, W., & Lei, X. (2015, may). Modeling and Simulation of Atmospheric Synthetic Wind Field in Flight Simulation. *2015 IEEE 5th International Conference on Electronics Information and Emergency Communication, Beijing, China*, 357–363. doi: 10.1109/ICEIEC.2015.7284558

D'Arcy, J.-F., & Della Rocco, P. S. (2001). *Air Traffic Control Specialist Decision Making and Strategic Planning - A Field Survey* (DOT/FAA/CT-TN01/05). Washington, D.C.: Federal Aviation Administration. Retrieved from `https://hf.tc.faa.gov/publications/2001-air-traffic-control-specialist-decision-making/full_text.pdf`

De Smedt, D., & Berz, G. (2007). Study of the Required Time of Arrival Function of Current FMS in an ATM Context. *AIAA/IEEE Digital Avionics Systems Conference, Dallas, Texas*, 1.D.5–1–1.D.5–10. doi: 10.1109/DASC.2007.4391837

Duong, V., Gawinowski, G., Nicolaon, J.-P., & Smith, D. (2001). Sector-Less Air Traffic Management. *4 th USA / Europe Air Traffic Management R&D Seminar, Santa Fe, New Mexico*. Retrieved from `http://www.atmseminarus.org/seminarContent/seminar4/papers/p_158_NC.pdf`

Endsley, M. R. (1995, mar). Toward a Theory of Situation Awareness in Dynamic Systems. *Human Factors: The Journal of the Human Factors and Ergonomics Society*, *37*(1), 32–64. doi: 10.1518/001872095779049543

Enea, G., & Porretta, M. (2012). A Comparison of 4D-trajectory Operations Envisioned for Nextgen and SESAR, some Preliminary Findings. *28th International Congress of the Aeronautical Sciences (ICAS2012), Brisbane, Australia*. Retrieved from `http://skybrary.aero/bookshelf/books/2377.pdf`

EUROCONTROL. (2009). *EUROCONTROL Specification for Short Term Conflict Alert* (EUROCONTROL-SPEC-122 No. May). Brussels, Belgium: Ben Bakker.

EUROCONTROL. (2012). *More S Elementary Surveillance Moves Up a Gear.* Retrieved 2018-12-04, from `https://www.eurocontrol.int/news/mode-s-elementary-surveillance-moves-gear`

EUROCONTROL. (2017). *Trajectory Based Operations (TBO): Central to the Latest ATM Concepts.* Retrieved 2019-04-16, from `https://www.eurocontrol.int/news/trajectory-based-operations-tbo-central-latest-atm-concepts`

EUROCONTROL Experimental Centre. (2010). *User Manual for the Base of Aircraft Data* (Technical Report No. 2010/003, Rev. 3.8). Brussels, Belgium: EUROCONTROL.

European Commission, & EUROCONTROL. (2015). *SESAR European ATM Master Plan, Edition 2015.* Retrieved from `https://ec.europa.eu/transport/modes/air/sesar/`

Federal Aviation Administration. (2016). *NextGen Implementation Plan.* Retrieved from `https://www.faa.gov/nextgen/media/NextGen_Implementation_Plan-2016.pdf`

Flach, J. M., Tanabe, F., Monta, K., Vicente, K. J., & Rasmussen, J. (1998, oct). An Ecological Approach to Interface Design. *Proceedings of the Human Factors and Ergonomics Society Annual Meeting*, *42*(3), 295–299. doi: 10.1177/154193129804200324

Forkel, I., Schinnenburg, M., & Ang, M. (2004). Generation of Two-Dimensional Correlated Shadowing for Mobile Radio Network Simulation. *7th International Symposium on Wireless Personal Multimedia Communications (WPMC), Abano Terme, Italy.* Retrieved from `https://www.researchgate.net/publication/273318459_Generation_of_Two-Dimensional_Correlated_Shadowing_for_Mobile_Radio_Network_Simulation`

Forrester, D. A., & Davis, K. (1994). *The Improvement of Meteorological Data for Air Traffic Management Purposes* (Stage 2B Report Executive Summary). Toulouse, France: EUROCONTROL. Retrieved from `https://www.eurocontrol.int/phare/gallery/content/public/documents/stage_2b_report.pdf`

Fothergill, S., & Neal, A. (2013, sep). Conflict-Resolution Heuristics for En Route Air Traffic Management. *Proceedings of the Human Factors and Ergonomics Society Annual Meeting*, *57*(1), 71–75. doi: 10.1177/1541931213571018

Gingell, R. M., & Fox, S. A. (1997). *PHARE PD/1 Final report: Lessons Learnt from PD/1* (DOC 96-70-24 Annex F). Brussels, Belgium: EUROCONTROL. Retrieved from `https://www.eurocontrol.int/phare/gallery/content/public/documents/96-70-24pd1_finalreport_vol2_annexf.pdf`

Glina, Y., Reynolds, T. G., Troxel, S. W., & Mcpartland, M. D. (2013). *Wind Information Requirements for NextGen Applications Phase 1: 4D-Trajectory Based Operations (4D-TBO)* (Project Report ATC-399). Lexington, Massachusetts: Massachusetts Institute of Technology. doi: 10.1.1.295.645

Golding, W. (2002). Turbulence and Its Impact on Commercial Aviation. *Journal of Aviation/Aerospace Education & Research*, *11*(2), 19–29. doi: 10.15394/jaaer.2002.1301

Haan, S. D., Haij, M. D., & Sondij, J. (2013). *The Use of a Commercial ADS-B Receiver to Derive Upper Air Wind and Temperature Observations from Mode-S EHS Information in The Netherlands* (TR-336). De Bilt, Netherlands: KNMI. Retrieved from `http://bibliotheek.knmi.nl/knmipubTR/TR336.pdf`

Hilburn, B., Parasuraman, R., Jha, P., & McGarry, K. (2006). *Emerging Human Factors Issues in Future Air Traffic Management* (Tech. Rep.). Center for Human Performance Research. Retrieved from `http://www.chpr.nl/index_htm_files/EMERGE.pdf%5Cnpapers2://publication/uuid/42E27117-C245-4F61-B325-7598E73D9AF1`

Hilburn, B., Westin, C., & Borst, C. (2014, apr). Will Controllers Accept a Machine That Thinks like They Think? The Role of Strategic Conformance in Decision Aiding Automation. *Air Traffic Control Quarterly*, *22*(2), 115–136. doi: 10.2514/atcq.22.2.115

Hu, J., Prandini, M., & Sastry, S. (2003, aug). Aircraft Conflict Detection in Presence of Spatially Correlated Wind Perturbations. *AIAA Guidance, Navigation, and Control Conference and Exhibit, Austin, Texas*, no. AIAA 2003–5339. doi: 10.2514/6.2003-5339

ICAO. (2005). *Global Air Traffic Management Operational Concept* (Tech. Rep.). Retrieved from `https://www.icao.int/Meetings/anconf12/Document%20Archive/9854_cons_en[1].pdf`

ICAO. (2014a). *Managing Unpredictable Evolution in Trajectory Based Operations* (ATMRPP-WG/WHL/4-WP/601). Toulouse, France: International Civil Aviation Organisation.

ICAO. (2014b). *Time Adherence in TBO* (ATMRPP-WG/27-WP/636). Montreal, Canadal: International Civil Aviation Organisation. Retrieved from http://www.sesarju.eu/sites/default/files/documents/reports/WP636_Trajectory_adherence_in_TBO.pdf?issuusl=ignore

Klomp, R. E. (n.d.). *Experiment on the Influence of Traffic Structure and Perturbations on Performance with a TSR Interface* (Unpublished doctoral dissertation). Delft University of Technology.

Klomp, R. E., Borst, C., Mulder, M., & Praetorius, G. (2014, oct). Ecological Interface Design: Control Space Robustness in Future Trajectory-Based Air Traffic Control Decision Support. *2014 IEEE International Conference on Systems, Man, and Cybernetics (SMC), San Diego, California*, 329–334. doi: 10.1109/SMC.2014.6973929

Klomp, R. E., Riegman, E. J. P., Borst, C., Mulder, M., & Van Paassen, M. M. (2019). Solution Space Concept: Human-Machine Interface for 4D Trajectory Management. *Thirteenth USA/Europe Air Traffic Management Research and Development Seminar (ATM2019), Vienna, Austria.*

Klomp, R. E., Van Paassen, M. M., Borst, C., & Mulder, M. (2012). Joint Human-Automation Cognition through a Shared Representation of 4D Trajectory Management. *Second SESAR Innovation Days, Braunschweig, Germany*. Retrieved from https://www.sesarju.eu/sites/default/files/SID_2012-27.pdf

Klomp, R. E., van Paassen, M. M., Borst, C., Mulder, M., Nieuwenhuisen, D., Maij, A., ... van Drunen, A. (2013). Designing for Joint Human-Automation Cognition through a Shared Representation of 4D Trajectory Management. *17th International Symposium on Aviation Psychology*, 518–523. Retrieved from https://corescholar.libraries.wright.edu/cgi/viewcontent.cgi?article=1082&context=isap_2013

Knorr, D., & Walter, L. (2011). Trajectory Uncertainty and the Impact on Sector Complexity and Workload. *First SESAR Innovation Days, Toulouse, France*. Retrieved from https://www.sesarju.eu/sites/default/files/documents/sid/2011/SID%202011-04.pdf

Kopardekar, P., Bilimoria, K., & Sridhar, B. (2007, sep). Initial Concepts for Dynamic Airspace Configuration. *7th AIAA Aviation Technology, Integration and Operations Conference (ATIO), Belfast, Northern Ireland*, no. AIAA 2007–7763. doi: 10.2514/6.2007-7763

Korn, B., Edinger, C., Tittel, S., Kugler, D., Putz, T., Hassa, O., & Mohrhard, B. (2009, oct). Sectorless ATM — A Concept To Increase En-Route Efficiency. *2009 IEEE/AIAA 28th Digital Avionics Systems Conference, Orlando, Florida*, 2.E.1–1–2.E.1–10. doi: 10.1109/DASC.2009.5347535

Kuchar, J. K., & Yang, L. C. (2000). A Review of Conflict Detection and Resolution Modeling Methods. *IEEE Transactions on Intelligent Transportation Systems*, *1*(4), 179–189. doi: 10.1109/6979.898217

Lee, A., Weygandt, S., Schwartz, B. E., & Murphy, J. (2009, aug). Performance of Trajectory Models with Wind Uncertainty. *AIAA Modeling and Simulation Technologies Conference, Chicago, Illinois*, no. AIAA 2009–5834. doi: 10.2514/6.2009-5834

Lee, H., & Milgram, P. (2008, sep). An Integrated Air Traffic Control Display Concept for Conveying Temporal and Probabilistic Conflict Information. *Proceedings of the Human Factors and Ergonomics Society Annual Meeting*, *52*(1), 84–88. doi: 10.1177/154193120805200119

Matsuno, Y., & Tsuchiya, T. (2014). Probabilistic Conflict Detection in the Presence of Uncertainty. In L. Angrisani et al. (Eds.), *Lecture notes in electrical engineering* (Vol. 290, pp. 17–33). Tokyo, Japan: Springer Japan. doi: 10.1007/978-4-431-54475-3

McPartland, M. D., Sandberg, M. J., Edwards, C., Teller, T. L., Troxel, S. W., & Reynolds, T. G. (2014). *Wind Information Requirements for NextGen Applications Phase 3 Final Report* (Project Report ATC-422). Lexington, Massachusetts: Massachusetts Institute of Technology.

Merritt, S. M., & Ilgen, D. R. (2008). Not All Trust Is Created Equal: Dispositional and History-Based Trust in Human-Automation Interactions. *Human Factors: The Journal of the Human Factors and Ergonomics Society*, *50*(2), 194–210. doi: 10.1518/001872008X288574

Metzger, U., & Parasuraman, R. (2001, dec). The Role of the Air Traffic Controller in Future Air Traffic Management: An Empirical Study of Active Control versus Passive Monitoring. *Human Factors: The Journal of the Human Factors and Ergonomics Society*, *43*(4), 519–528. doi: 10.1518/001872001775870421

Metzger, U., & Parasuraman, R. (2005, mar). Automation in Future Air Traffic Management: Effects of Decision Aid Reliability on Controller Performance and Mental Workload. *Human Factors: The Journal of the Human Factors and Ergonomics Society*, *47*(1), 35–49. doi: 10.1518/0018720053653802

Mondoloni, S., & Bayraktutar, I. (2005). Impact of Factors, Conditions and Metrics on Trajectory Prediction Accuracy. *6th USA/Europe ATM R&D Seminar, Baltimore, Maryland*. Retrieved from `http://atm-seminar-97.eurocontrol.fr/past-seminars/6th-seminar-baltimore-md-usa-june-2005/papers/paper_062`

Mondoloni, S., Swierstra, S., & Paglione, M. (2005). Assessing Trajectory Prediction Performance - Metrics Definition. *24th Digital Avionics Systems Conference, Washington, D.C.*, 3.C.1–1–3.C.1–13. doi: 10.1109/DASC.2005.1563347

Paielli, R. A. (1998). Empirical Test of Conflict Probability Estimation. *2nd USA/Europe Air Traffic Management R&D Seminar (ATM-98), Orlando, Florida*. Retrieved from `https://www.aviationsystemsdivision.arc.nasa.gov/publications/enroute/upr/paielli_12_98.pdf`

Paielli, R. A., & Erzberger, H. (1997, may). Conflict Probability for Free Flight. *Journal of Guidance, Control, and Dynamics*, *20*(3), 588–596. doi: 10.2514/2.4081

Parasuraman, R., & Davies, D. R. (1984). *Varieties of Attention.* New York, New York: Academic Press.

Prandini, M., Hu, J., Lygeros, J., & Sastry, S. (2000). A Probabilistic Approach to Aircraft Conflict Detection. *IEEE Transactions on Intelligent Transportation Systems*, *1*(4), 199–220. doi: 10.1109/6979.898224

Prevot, T., Homola, J. R., Martin, L. H., Mercer, J. S., & Cabrall, C. D. (2012, feb). Toward Automated Air Traffic Control - Investigating a Fundamental Paradigm Shift in Human/Systems Interaction. *International Journal of Human-Computer Interaction*, *28*(2), 77–98. doi: 10.1080/10447318.2012.634756

Prevot, T., Lee, P. U., Smith, N., & Palmer, E. (2005, aug). ATC Technologies for Controller-Managed and Autonomous Flight Operations. *AIAA Guidance, Navigation, and Control Conference and Exhibit, San Fransisco, California*, no. AIAA 2005–6043. doi: 10.2514/6.2005-6043

Rantanen, E. M., & Nunes, A. (2005, oct). Hierarchical Conflict Detection in Air Traffic Control. *The International Journal of Aviation Psychology*, *15*(4), 339–362. doi: 10.1207/s15327108ijap1504_3

Rasmussen, J. (1976). Outlines of a Hybrid Model of the Process Plant Operator. In T. B. Sheridan & G. Johannsen (Eds.), *Monitoring behavior and supervisory control* (pp. 371–383). New York, New York: Plenum Publishing Corporation. doi: 10.1007/978-1-4684-2523-9_31

Rasmussen, J. (1983, may). Skills, Rules, and Knowledge; Signals, Signs, and Symbols, and Other Distinctions in Human Performance Models. *IEEE Transactions on Systems, Man, and Cybernetics*, *SMC-13*(3), 257–266. doi: 10.1109/TSMC.1983.6313160

Rasmussen, J. (1986). *Information Processing and Human-Machine Interaction: An Approach to Cognitive Engineering.* New York, New York: Elsevier Science Inc.

Reynolds, T. G., Glina, Y., & Mcpartland, M. D. (2012, sep). Wind Information Requirements to Support Four Dimensional Trajectory-Based Operations. *12th AIAA Aviation Technology, Integration, and Operations (ATIO) Conference and 14th AIAA/ISSMO Multidisciplinary Analysis and Optimization Conference, Indianapolis, Indiana*, no. AIAA 2012–5702. doi: 10.2514/6.2012-5702

Riegman, E. J. P. (2018). *Effects of Vertical Situation Diagram in 4D Trajectory Management Interface* (Master's thesis, Delft University of Technology). Retrieved from `http://resolver.tudelft.nl/uuid:89e072c6-e179-4a17-98ac-3e06909692ff`

Robert, E., & De Smedt, D. (2013). Comparison of Operational Wind Forecasts with Recorded Flight Data. *Tenth USA/Europe Air Traffic Management Research and Development Seminar (ATM2013), Chicago, Illinois*. Retrieved from `http://atmseminar.org/seminarContent/seminar10/papers/211-ROBERT_0125131206-Final-Paper-4-10-13.pdf`

Rovira, E., & Parasuraman, R. (2010, jun). Transitioning to Future Air Traffic Management: Effects of Imperfect Automation on Controller Attention and Performance. *Human Factors: The Journal of the Human Factors and Ergonomics Society*, *52*(3), 411–425. doi: 10.1177/0018720810375692

Ruijgrok, G. J. J. (2009). *Elements of Airplane Performance* (2nd ed.). Delft, The Netherlands: VSSD.

SESAR Consortium. (2007). *The ATM Target Concept* (SESAR Definition Phase D3: DLM-0612-001-02-00). Toulouse, France: SESAR Consortium.

SESAR Consortium. (2019). *ATM Roles.* Retrieved 2019-04-17, from `https://www.atmmasterplan.eu/data/roles`

Snyder, J. P. (1983, feb). *Map Projections - A Working Manual* (U.S. Geological Survey Professional Paper 1395). Washington, D.C.: U.S. Department of the Interior.

STATFOR Team. (2018). *EUROCONTROL Seven-Year Forecast.* Retrieved from `https://www.eurocontrol.int/sites/default/files/content/documents/official-documents/forecasts/seven-year-flights-service-units-forecast-2018-2024-Feb2018.pdf`

Telner, J., Milgram, P., & Williamson, A. R. (2003, oct). Experimental Investigation of Predictive Probabilistic and Temporal Conflict Avoidance Displays. *Proceedings of the Human Factors and Ergonomics Society Annual Meeting*, *47*(1), 207–211. doi: 10.1177/154193120304700144

Torres, S. (2010, oct). Determination and Ranking of Trajectory Accuracy Factors. *29th Digital Avionics Systems Conference, Salt Lake City, Utah*, 1.C.1–1–1.C.1–12. doi: 10.1109/DASC.2010.5655521

Torres, S. (2015, jun). Trajectory Accuracy Sensitivity to Modeling Factors. *15th AIAA Aviation Technology, Integration, and Operations Conference, Dallas, Texas*, no. AIAA 2015–2599. doi: 10.2514/6.2015-2599

Vaddi, V. V., Tandale, M. D., & Lin, S. (2013, aug). Spatio-Temporally Correlated Wind

Uncertainty Model for Simulation of Terminal Airspace Operations. *2013 Aviation Technology, Integration, and Operations Conference, Los Angeles, California*, no. AIAA 2013–4404. doi: 10.2514/6.2013-4404

Van Marwijk, B. J. A., Borst, C., Mulder, M., Mulder, M., & Van Paassen, M. M. (2011, jan). Supporting 4D Trajectory Revisions on the Flight Deck: Design of a Human–Machine Interface. *The International Journal of Aviation Psychology*, *21*(1), 35–61. doi: 10.1080/10508414.2011.537559

Van Paassen, M. M., Borst, C., Mulder, M., Klomp, R. E., Van Leeuwen, P., & Mooij, M. (2013). Designing for Shared Cognition in Air Traffic Management. *Journal of Aerospace Operatiions*, *2*, 39–51. doi: 10.3233/AOP-130030

Vicente, K. J. (1999). *Cognitive Work Analysis: Toward Safe, Productive, and Healthy Computer-Based Work*. Mahwah, New Jersey: L. Erlbaum Associates Inc.

Vicente, K. J., & Rasmussen, J. (1992). Ecological Interface Design: Theoretical Foundations. *IEEE Transactions on Systems, Man, and Cybernetics*, *22*(4), 589–606. doi: 10.1109/21.156574

Warren, A. (2000). Trajectory Prediction Concepts for Next Generation Air Traffic Management. *3rd USA/Europe Air Traffic Management R&D Seminar, Napoli, Italy*. Retrieved from `http://citeseerx.ist.psu.edu/viewdoc/download;jsessionid=CF17AA2DBB4F1A919401AB48AB6547CE?doi=10.1.1.473.9089&rep=rep1&type=pdf`

Weitz, P. (2013, apr). Determination and Visualization of Uncertainties in 4D-Trajectory Prediction. *2013 Integrated Communications, Navigation and Surveillance Conference (ICNS), Herndon, Virginia*. doi: 10.1109/ICNSurv.2013.6548525

Westin, C., Borst, C., & Hilburn, B. (2015). An Empirical Investigation into Three Underlying Factors Affecting Automation Acceptance. *Fifth SESAR Innovation Days, Bologna, Italy*. Retrieved from `https://www.sesarju.eu/sites/default/files/documents/sid/2015/SIDs_2015_paper_29.pdf`

Westin, C., Borst, C., & Hilburn, B. (2016, feb). Strategic Conformance: Overcoming Acceptance Issues of Decision Aiding Automation? *IEEE Transactions on Human-Machine Systems*, *46*(1), 41–52. doi: 10.1109/THMS.2015.2482480

Whitaker, R., & Marsh, D. (1997). *PHARE PD/1 Final Report* (Vol. 1; DOC 96-70-24). Brussels, Belgium: EUROCONTROL. Retrieved from `https://www.eurocontrol.int/phare/gallery/content/public/documents/96-70-24pd1finalreport_vol1.pdf`

Whiteley, M. J., & Wilson, I. (1999). *PHARE Advanced Tools Problem Solver Final Report* (Vol. 8; DOC 98-70-18). Brussels, Belgium: EUROCONTROL. Retrieved from `https://www.eurocontrol.int/phare/gallery/content/public/documents/98-70-18-v8_ps.pdf`

Wickens, C. D., Lee, J., Liu, Y., & Baker, S. G. (2004). *An Introduction to Human Factors Engineering* (2nd ed.). Upper Saddle River, New Jersey: Pearson.

Woods, D. D. (1984, sep). Visual Mmomentum: A Concept to Improve the Cognitive Coupling of Person and Computer. *International Journal of Man-Machine Studies*, *21*(3), 229–244. doi: 10.1016/S0020-7373(84)80043-7

Yang, L. C., & Kuchar, J. K. (1998, aug). Using Intent Information in Probabilistic Conflict Analysis. *Guidance, Navigation, and Control Conference and Exhibit, Boston, Massachusetts*, no. A98–37082. doi: 10.2514/6.1998-4237